Identification of Campylobacter Virulence and Colonisation Factors

A thesis submitted in fulfilment of the requirements for the degree of Doctor of Philosophy

Xiaozheng Mu

Biotechnology and Environmental Biology

School of Applied Science

RMIT University

August 2014

Declaration

I certify that except where due acknowledgement has been made, the work is that of the author alone; the work has not been submitted previously, in whole or in part, to qualify for any other academic award; the content of the thesis is the result of work which has been carried out since the official commencement date of the approved research program; any editorial work, paid or unpaid, carried out by a third party is acknowledged; and, ethics procedures and guidelines have been followed.

Xiaozheng Mu

Date: August 30th, 2014

Acknowledgements

Firstly, I would like to thank my primary supervisor Prof. Peter Smooker, for taking me as a Ph.D student and his constant support, encouragement over the duration of my Ph.D course.

Also to my second supervisor, Dr. Andrew Hung. Thank you for guiding me through the molecular modelling and simulation, of which I was totally lost at the beginning of my research. This project cannot be done without many, many hours you spent and lead me to the right direction.

To Dr. Emily Gan, Dr. Aya Taki, Dr. Natalie Kikidopoulos, Danka Jovetic and Mian Chee Gor, thank you, not just for the use of your considerable expertise, but also for the friendship to support me through the hard days. My project cannot be done without you guys.

To Dr. Grace Liu, whose protein knowledge came in handy. Thank you for the help when I had difficulties in protein expression and purification.

I would also like to thank everybody in the Biotechnology laboratory of RMIT, thank you for providing me a pleasant work environment. Thanks to Dr. Binu John and Dr Thi Thu Hao Van, for making me felt extremely welcome when I just started my project.

Last but definitely not least, thanks to my parents, for their guidance and a lot of support.

Tables of Contents

List of Figures

List of Tables

List of Abbreviations

Ω	Ohms
λ	Lambda DNA
µF	Capacitance
µg	Microgram
µL	Microlitre
µM	Micromole
Å	Angstrom
APS	Ammonium persulphate
BLAST	Basic Local Alignment Search Tool
bp	Base pairs
BSA	Bovine serum albumin
ºC	Degrees Celsius
CDS	Coding DNA sequences
CDT	Cytolethal-distending toxin
cfu	Colony forming units
CO_2	Carbon dioxide
CPS	Capsular polysaccharide
CSP	Classically secreted protein
Da	Dalton
DNA	Deoxyribonucleic acid
Dnase	Deoxyribonuclease
DTT	Dithiothreitol
EDTA	Ethylene-diamine-tetra-acetic acid
e.g.	Exempli gratia (for example)
et al.	Et alia (and others)
g	Gram
GBS	Guillain-Barré syndrome

GFP	Green fluorescent protein
GI	Gastrointestinal
GlnA	Glutamine synthetase
GROMACS	GROningen Machine for Chemical Simulations
h	Hour
H_2O	Water
H_2O_2	Hydrogen peroxide
HBA	Horse blood agar
HEPES	N-2-hydroxyethylpiperazine-N-2-ethane sulfonic acid
HMM	Hidden markov model
HRP	Horseradish peroxidase
IL	Interleukin
IMAC	Immobilised metal affinity chromatography
IPTG	Isopropyl-β-D-galactopyranoside
kb	Kilobase
kDa	Kilodalton
LOS	Lipooligosaccharide
LPS	Lipopolysaccharide
M	Molarity
MBP	Maltose-binding protein
MD	Molecular dynamics
MFS	Miller-Fisher syndrome
mg	Milligram
MG H_2O	Molecular grade water
$MgCl_2$	Magnesium chloride
$MgSO_4$	Magnesium sulfate
min	Minutes
mL	Millilitre

mM	Millimole
MOMP	Major outer membrane protein
MTT	3-(4,5-dimethylthiazolyl-2-yl)-2,5-diphenyltetrazolium bromide
MW	Molecular weight
NaCl	Sodium chloride
Na_2CO_3	Sodium carbonate
NaOH	Sodium hydroxide
NCS	New born calf serum
NCSP	Non-classically secreted protein
NF-κB	Nuclear transcription factor kappaB
ng	Nanogram
NK	Natural killer
NN	Neural networks
NO	Nitric oxide
OMP	Outer membrane protein
ORF	Open reading frame
O_2	Oxygen
PBS	Phosphate buffered saline
PCR	Polymerase chain reaction
PFT	Pore forming toxin
PI	Propidium Iodide
POPE	Phosphatidylethanolamine-phosphatidylglycerol
PS	Polysaccharide
pH	Potential of hydrogen
RNA	Ribonucleic acid
RNase	Ribonuclease
rpm	Revolutions per min
RT	Room temperature

SDS	Sodium dodecyl sulphate
SDS-PAGE	Sodium dodecyl sulphate polyacrylamide gel electrophoresis
T2SS	Type II secretion system
T3SS	Type III secretion system
T4SS	Type IV secretion system
T5SS	Type V secretion system
TAE	Tris acetate EDTA buffer
Tat	Twin-arginine translocation
TBE	Tris borate EDTA buffer
TE	Tris EDTA buffer
TEMED	NNN'N'-tetramethylethyleidiamine
TLR	Toll-like receptor
TMH	Transmembrane helices
Tris	Tris (hydroxymethyl) amino methane
U	Units
UV	Ultraviolet
V	Volts
v/v	Volume per volume
VMD	Visual molecular dynamics
w/v	Weight per volume
WCL	Whole cell lysates

Abstract

Campylobacter jejuni, which is a commensal bacteria of birds and some mammals, is the most common *Campylobacter* species associated with campylobacteriosis. It can colonise the intestinal tract of many birds, including poultry, at very high numbers without eliciting a pathological immune response or causing symptoms in the animals. Contamination of poultry with *C. jejuni* during processing and subsequent poor food handling is the major cause of infection in humans.

Effective strategies to control *Campylobacter* contamination and to prevent campylobacteriosis are still lacking, as current knowledge about the pathogenic mechanisms, virulence and pathogen-host interaction mechanisms of *Campylobacter* in poultry is relatively poor. Since contaminated poultry is the major source of campylobacteriosis in industrialised countries, identification of virulence and colonisation factors will without doubt lead to new strategies for minimising colonisation of *C. jejuni* in poultry intestines. A starting point for identifying potential virulence factors is to identify proteins that are secreted from *Campylobacter* and therefore can interact with host molecules/cells.

In 2000, the complete genome sequence of *C. jejuni* subsp. *jejuni* NCTC 11168 was completed, which contains 1,654 coding DNA sequences (CDS). In 2007, the genome sequence was re-annotated and re-analysed. The number of predicted CDS was reduced to 1643 and 18.2% of CDS having their product functions updated. A range of bioinformatics techniques have been employed in this study to identify secreted and surface-exposed proteins, which may have the ability to interact with chicken immune cells. Results indicate that 6.96% of *C. jejuni* proteins have been predicted to contain a signal peptide, and 8.63% are predicted to be non-classically secreted using the web servers SignalP4.0 and Secretome2.0. Among them, a subset of 70 putative non-classically secreted proteins have been selected for further analysis, as they were predicted to be located on the cell surface or

extracellularly using Gneg-PLoc and Gneg-mPLoc. They have been analysed further for the presence of transmembrane helices, transmembrane beta-barrels, putative proteases, enzymes, and virulence. Finally 28 hypothetical putative non-classically secreted virulent proteins were identified as candidates for further analysis.

One of the proteins from the list, Cj0391c, was selected to be expressed as a recombinant protein in an *E. coli* BL21(DE3) pRSET-A expression system. This purified recombinant protein was shown to induce a reduction in viability of chicken macrophage HD11 cells, and induced apoptosis, suggestive of possible roles of this protein in immune system evasion or suppression of immune responses in poultry.

Furthermore, this protein was computationally modelled and molecular dynamics simulations performed at different conditions. The protein Cj0391c was predicted to be alpha-helical. It was modelled based on the structure of an alpha-helical pore-forming toxin, dermcidin. The constructed Cj0391c hexameric structural model was then inserted and simulated in a phosphatidylethanolamine-phosphatidylglycerol bilayer. Under simulated conditions, the model maintained structural integrity at low temperature (300 K) without the presence of zinc, but not at higher temperatures, 310 K and 314 K. The helical bundle was maintained with the presence of zinc from low temperature 300 K to higher temperature 314 K. Simulations also suggest a wider pore in the presence of zinc, suggestive of higher channel conductance. Thus, similar to human dermcidin, zinc may play a role in enabling formation of a stable hexameric channel with a pore of sufficient size to cause pathological membrane permeability, leading to cell death.

Results from this study will help to improve our understanding of pathogenic mechanisms, more specifically, the virulence factors involved in *C. jejuni* pathogenicity. The molecular modelling and simulation revealed one possible mechanism of a protein toxic to chicken macrophage cells. These potential extracellular virulence factors can be used as virulence

candidates for anti-*Campylobacter* strategies. By modelling identified proteins, antigenic determinants and/or functional regions/mechanisms may be found, which can then be used to design vaccines aimed at immunising poultry against *Campylobacter* colonisation.

CHAPTER 1. LITERATURE REVIEW

1.1 Introduction

Campylobacter species are motile, Gram-negative, microaerophilic, spiral-shaped rods belonging to the family Campylobacteraceae (Montville & Matthews, 2008). These organisms have been accepted as one of the most common causes of campylobacteriosis worldwide (Nachamkin & Blaser, 2000). *C. jejuni* and *C. coli* colonise the intestinal tract of poultry at very high numbers without eliciting any pathological immune response (Hendrixson & DiRita, 2004; Newell & Fearnley, 2003). Under experimental conditions, the dose of viable *C. jejuni* required to colonise chicks and chickens can be as low as 40 colony forming units (CFU) (Cawthraw *et al*, 1996). After passage through the poultry system, the colonisation potential of *C. jejuni* can exhibit an enhancement of at least 1,000-fold in most strains and up to 10,000-fold in some strains experimentally (Cawthraw *et al*, 1996), which means that entire flocks can be rapidly infected by horizontal transfer.

C. jejuni and *C. coli* are the most common *Campylobacter* species associated with campylobacteriosis (Montville & Matthews, 2008). In addition, *C. jejuni* is linked with Guillain-Barré syndrome (GBS) which is an autoimmune syndrome that can result in respiratory and severe neurological dysfunction and death (Haddad *et al*, 2010). Campylobacteriosis is responsible for about 30% to 40% of severe GBS cases (Nachamkin & Blaser, 2000).

C. jejuni is now recognised as the most common agent of enteritis in the world, with almost 400 million cases reported each year (Walker, 2005). Campylobacteriosis is the most frequently reported zoonosis in industrialised countries, with incidence varying from 21.9/100,000 in the United States to 396/100,000 in New Zealand (de Zoete *et al*, 2007; Haddad *et al*, 2010). In Europe, the annual number of campylobacteriosis cases exceeds the number of salmonellosis cases, with 62.98 campylobacteriosis cases per 100,000 population (Fosse *et al*, 2008).

Travel-associated campylobacteriosis is also an important issue. There are approximately 80 million travellers per annum from industrialised countries to campylobacteriosis endemic regions (Tribble *et al*, 2008b). A study performed among Swedish travellers revealed that the risk for a traveller to acquire campylobacter-associated diarrhoea in India is 1,253 per 100,000 persons (Ekdahl & Andersson, 2004).

Campylobacteriosis has a major health impact in industrialised countries (Haddad *et al*, 2010). In Fosse *et al*.'s study, the incidence and severity of foodborne human zoonoses cases in Europe have been calculated as risk scores (Fosse *et al*, 2008). *Campylobacter species* have the highest non-control ratio, due to the non-detection of hazards during meat inspection and potential secondary contamination (Fosse *et al*, 2008).

Reducing the level of *Campylobacter* in poultry will limit the number of campylobacteriosis cases. Several strategies to help achieve this aim have been studied. Firstly, high hygiene levels during poultry breeding and prevention of chicken carcass contamination has been considered the most efficient method (Katarzyna *et al*, 2009). Nevertheless, it is difficult to introduce this strategy globally due to the relatively high cost related to the implementation of various interventions (Katarzyna *et al*, 2009). The method of upgrading biosecurity at the farm level and hygiene practices in processing poultry may also vary between countries (Katarzyna *et al*, 2009). Alternatively, genus/species-specific bacteriophage treatment of chickens before butchering or directly onto the chicken carcasses is also under consideration (Atterbury *et al*, 2003; El-Shibiny *et al*, 2005). However, there are many drawbacks to this method, such as the acquisition of resistance to bacteriophage control, and also campylobacter and bacteriophage genetic microbial diversity via recombination events (Scott *et al*, 2007). The most efficient strategy for decreasing campylobacteriosis is still immunoprophylactic methods. However, despite more than 10 years of research, as yet no effective anti-campylobacter vaccine has been developed.

1.2 Campylobacter

1.2.1 Characteristics

Campylobacter were first isolated from sheep and cattle with infectious abortion in the 1900s (Smith & Taylor, 1919). They were originally classified as *Vibrio fetus* until reclassified as *Campylobacter* in 1963 (Sebald & Veron, 1963). So far 25 species and 8 sub-species have been described (Man, 2011). *C. jejuni* and *C. coli* are the most common species involved in human acute bacterial diarrhoea worldwide (Nachamkin and Blaser, 2000). *C. jejuni* is most commonly detected specifically in poultry, while *C. coli* and *C. lari* are also detected regularly in birds (Pielsticker *et al*, 2012). Particularly, *C. coli* shows a prevalence of almost 50% in turkeys (Humphrey *et al*, 2007).

Campylobacters are characterised as non-spore-forming, oxidase-positive, Gram-negative rods that are slender, spirally curved with tapering ends at the early stage of growth. The shapes become round as the culture ages. The cell size ranges from 1.5-6.0 μm in length and 0.2-0.5 μm in width and they have a polar flagellum at one or both ends (Ketley, 1997b; Young *et al*, 2007). Campylobacters cannot ferment or oxidase sugars, and are normally microaerophilic. They can change biosynthetic processes in response to lower oxygen levels in the environment (Gaynor *et al*, 2004). In the laboratory, *C. jejuni* is identified as a catalase positive, urease negative bacterium that can reduce nitrate. It is susceptible to nalidixic acid but resistant to cephalothin.

Campylobacter can be divided into two groups, non-thermophiles (<37ºC) and thermophiles (37-42ºC), based on their temperature preference (Griffiths & Park, 1990). *C. jejuni* belongs to the latter group, since it has an optimal growth temperature at 42ºC, with the ability to grow slowly at 37ºC. Unlike any other intestinal bacteria such as *Salmonella*, *Campylobacter* grows only under microaerophilic conditions in an atmosphere with 10% CO_2, 5% O_2 and

85% N_2 (Skirrow, 1977). It is commonly found in the intestine of warm-blooded animals and birds (Wallis, 1994).

1.2.2 Pathogenesis

There are clearly different mechanisms of virulence in humans, where disease is caused, and poultry, where the bacterium is a commensal. In humans, despite of the high incidence of campylobacteriosis, the bacterial factors involved in *C. jejuni* intestinal colonisation and pathogenesis are comparatively poorly understood compared to the other enteric pathogens (Oldfield & Wooldridge, 2009). In the review of Dasti *et al*. (2010), the list of bacterial factors involved in the human pathogenesis is shown (Table 1.1). Motility is known to be essential for *C. jejuni* pathogenesis mechanisms in humans (Oldfield & Wooldridge, 2009). In addition, cellular invasion and toxin production are also important *C. jejuni* pathogenesis mechanisms in humans (Oldfield & Wooldridge, 2009). Many investigations of the *C. jejuni* adhesive properties to different host epithelial-cell lines have been studied *in vitro* (Wooldridge & Ketley, 1997). Several *C. jejuni* adhesins have been revealed including lipooligosaccharide, flagellin, P95, Peb1 (CBF1) and Peb4 (CBF2) (Fry *et al*, 2000b; Grant *et al*, 1993; Kelle *et al*, 1998; McSweegan & Walker, 1986; Pei *et al*, 1991). The pathogenesis of *C. jejuni* is further discussed in the Section 1.7.

1.2.3 Reservoirs for C. jejuni

C. jejuni is a commensal bacteria of birds and some mammals, such as pigs, dogs, cattle and sheep (Chansiripornchai & Sasipreeyajan, 2009). Natural reservoirs for *C. jejuni* are wild birds, whose intestines offer a suitable biological niche for their survival and dissemination.

Table 1.1: Representative bacterial factors involved in the human pathogenesis of campylobacteriosis (reproduced from Dasti *et al*, 2010).

	Bacterial factor	Remark	Reference
Responses to stress	GroESL	Heat shock response	(Thies *et al*, 1999)
	DnaJ	Heat shock response	(Konkel *et al*, 1998)
	Lon protease	Heat shock response	(Thies *et al*, 1999)
	RacR-RacS	Regulator of temperature-dependent signalling	(Bras *et al*, 1999)
	γ-glutamyltranspeptidase	Utilization of glutamine and glutathione	(Hofreuter *et al*, 2008)
Motility and chemotaxis	Flagellum	*O*-linked glycosylation	(Guerry, 1992)
	Flagellum FlgR-FlgS	Regulator for flagellum protein biosynthesis	(Hendrixson, 2006)
	Flagellum fliA (sigma28)	Transcription of flagellar genes	(Carrillo *et al*, 2004)
	Flagellum rpoN (sigma54)	Transcription of flagellar genes	(Hendrixson & DiRita, 2003)
	FlgP, FlgQ	Flagellar motility	(Sommerlad & Hendrixson, 2007)
	CheY	Response regulator needed for flagellar rotation	(Yao *et al*, 1997)
Binding and adhesion	Flagellum	Non-motile mutants show less adherence	(Yao *et al*, 1994)
	LOS	Mimicry with GM1 and GD1a gangliosides - GBS	(Young *et al*, 2007)
	GadF	Fibronectin-binging outer membrane protein	(Konkel *et al*, 1997)
	PEB1	Periplasmic binding protein	(Pei & Blaser, 1993)
	JlpA	Surface-exposed lipoprotein	(Jin *et al*, 2001)
Invasion	Flagellum	Aflagellated mutants are less invasive	(Wassenaar & Blaser, 1999)
	LOS	Lipooligosaccharide	(Louwen *et al*, 2008)
	Cia	*Campylobacter*-invasive antigens, especially CiaB = Secreted through the flagella export apparatus	(Konkel *et al*, 2004; Rivera-Amill *et al*, 2001)
	CadF	Activation of Rac1 and Cdc42	(Krause-Gruszczynska *et al*, 2007a; Krause-Gruszczynska *et al*, 2007b)
	CPS	Capsular polysaccharide	(Karlyshev & Wren, 2001)
Toxins	CdtA,B,C	Cytolethal distending toxin CdtB causes • cell cycle arrest and apoptosis • IL-8 secretion	(Pickett & Whitehouse, 1999) (Hickey *et al*, 1999)
Crossing polarized epithelia	Unknown	Disruption of tight junctions Translocation of intestinal commensal bacteria	(MacCallum *et al*, 2005b) (Kalischuk *et al*, 2009)

C. jejuni normally colonise chickens shortly after birth and are the most important source for human infection (Dasti *et al*., 2009). *C. jejuni* can colonise the intestinal tract of many birds including poultry at very high number (up to 10^9 colony-forming units per gram in caecal contents) without eliciting any pathological immune response or causing symptoms (Hendrixson & DiRita, 2004; Newell & Fearnley, 2003). *C. jejuni* is the strain most prevalent in poultry (65-95% vs. *C. coli* 5-35%) (de Zoete *et al*, 2007), while *C. coli* predominates in swine (Kist & Bereswill, 2001). As chickens are considered as the natural host of *C. jejuni*, data on the source arribution in some of the European countries have been collected (Table 1.2). *C. jejuni* can also colonise turkeys and ducks less frequently. Beside poultry, other sources for *C. jejuni* have been described, such as sheep, pigs, cats, dogs, water, raw milk, while rodents and insects are also considered as possible vectors (Bates *et al*, 2004; Guerin *et al*, 2007; Hald *et al*, 2004; Hastings *et al*, 2011; Sahin *et al*, 2002).

Several surveys have indicated a seasonal variation in the prevalence of poultry flock colonisation, which demonstrates a higher rate of infection in summer than in winter (Berndtson *et al*, 1996; Hald, 1999; Jacobs-Reitsma *et al*, 1994). The reason for this seasonal variation is unknown, but this may reflect levels of environmental contamination. Some poultry farms have more ventilation during the summers, which may increase the contact of the chickens with the outside environment (Nachamkin, 2008).

Table 1.2: Source Attribution of *C. jejuni* and *C. coli* in Europe using Multi-Locus Sequence Typing (reproduced from EFSA, 2010).

Attribution Model	Source Animal Dataset	Clinical Dataset	Species	% Attribution to Chicken	% Attribution to Other Sources	Comments	Reference
Asymmetric Island	1145 isolates from 10 previous studies	1255 from NW England; Jan 2000 till Dec 2002	*C. jejuni*	56.5	35.0 (cattle) 4.3 (sheep) 2.3 (wild animals) 1.1 (environment)		(Wilson *et al,* 2008)
Population structure	5247 from Scotland July 2005 to Sep 2006 (9.6% *C. coli*)	999 from Scotland and 3419 from PubMLST	*C. jejuni*	58	38 (ruminants) 4 (wild bird & environment)		(Sheppard *et al*, 2009)
Asymmetric Island	As above	As above	*C. jejuni*	78	38 (ruminants) 4 (wild bird & environment)		(Sheppard *et al*, 2009)
Population structure	As above	As above	*C. coli*	40	40 (sheep) 14 (cattle) 6 (pigs) 1 (turkey)		(Sheppard *et al*, 2009)
Asymmetric Island	As above	As above	*C. coli*	56	40 (sheep) 14 (cattle) <1 (pig) <1 (turkey)		(Sheppard *et al*, 2009)
Population structure	680 contemporaneous isolates from Scotland	225 from rural children in Grampian 2000-06	*C. jejuni* and *C. coli*	19	42 (cattle) 24 (wild birds) 12 (sheep) 3 (pigs)	Rural children < 5 years	(Strachan *et al*, 2009)

Table 1.2: Source Attribution of *C. jejuni* and *C. coli* in Europe using Multi-Locus Sequence Typing (reproduced from EFSA, 2010) (cont.).

Attribution Model	Source Animal Dataset	Clinical Dataset	Species	% Attribution to Chicken	% Attribution to Other Sources	Comments	Reference
Population structure	680 contemporaneous isolates from Scotland	85 from rural children in Grampian 2000-06	*C. jejuni* and *C. coli*	43	35 (cattle) 6 (wild birds) 15 (sheep) 1 (pig)	Rural children < 5 years	(Strachan *et al*, 2009)
Modified Hald	793 isolates	481 from Manawatu, New Zealand	*C. jejuni*	80	10 (cattle) 9 (sheep) 4 (environment)		(Mullner *et al*, 2009)
Dutch Model	521 isolates	As above	*C. jejuni*	52	17 (cattle) 10 (sheep) 5 (wild bird) 11 (water)		(French and the Molecular Epidemiology and Veterinary Public Health Group, 2008)
Modified Hald Model	521 isolates	As above	*C. jejuni*	67	23 (cattle) 8 (sheep) 1 (wild bird) <1 (water)		(French and the Molecular Epidemiology and Veterinary Public Health Group, 2008)
Island Model	521 isolates	As above	*C. jejuni*	75	17 (cattle) 4 (sheep) 2 (wild bird) <1 (water)		(French and the Molecular Epidemiology and Veterinary Public Health Group, 2008)

1.3 Epidemiology

In the developing world, It is estimated that 40-60% of children under 5 years old will develop at least one symptomatic *Campylobacter* infection (Coker *et al*, 2002). A passive clinical surveillance study in Karachi, Pakistan shows that annual incidence of *C. jejuni* infection is 29 per 1,000 person-years, with peak incidence in 2 year-old children (Soofi *et al*, 2011). Additionally, the attention on association between *Campylobacter* and HIV infection may be increased as morbidity and mortality have been discovered among HIV positive patients (Molina *et al*, 1995; Sorvillo *et al*, 1991; Tee & Mijch, 1998). Long-term carriage of *Campylobacter* can occur among HIV infected patients, which sometimes associated with recurrent attacks of enteritis and bacteremia (Guerry *et al*, 2012). With the growing HIV pandemic, it is suggested that the burden of campylobacteriosis in developing world may be listed in the top 10 in 2020 (Guerry *et al*, 2012).

In developed countries, estimates of the level of campylobacteriosis in the general population vary between geography and over time (Guerry *et al*, 2012). The incidences in the USA are around 15/100,000 with a slight decline over the past decade, and rates in Europe are 50-90/100,000 with an increasing trend (Janssen *et al*, 2008). Some Eastern European countries and New Zealand have comparatively high incidence rates, which are about 300-400/100,000 per annum (Guerry *et al*, 2012). It is believed that the true incidence rates are 10-100 times higher than those reported historically as a lot of campylobacteriosis cases have been miss an/or not reported (Guerry *et al*, 2012). The results of population-based estimates of campylobacteriosis studies in a number of western countries are listed in the Table 1.3. These results support that the incidence rates in developed countries ranges from 3 to 15 cases per 1,000 person-years.

Finally, travellers-associated campylobacteriosis cases are high with 5-15% of diarrheal

Table 1.3: Global estimates of *Campylobacter* incidence in developed countries (reproduced from Guerry *et al*, 2012).

Reference	**Kubota *et al*. (2008)**	**Tam *et al*. (2012)**	**De Wit *et al*. (2001)**	**Hall *et al*. (2008)**	**Scallan *et al*. (2011)**
Country	Japan	UK	Netherlands	Australia	US
Year of study	2006-2007	2008-2009	1998-1999	2000-2004	2006
Study design	Two 2-week cross-sectional, population-based telephone surveys combined with catchment area surveillance	Prospective, community cohort study and prospective study of general practice presentation in national surveillance system	Prospective population-based study with nested case-control study in general population	Empirical model based on published and unpublished data from multiple active /passive surveillance source	Empirical model based on published and unpublished data from multiple active/passive surveillance sources
Numbers	4,247 Household interviews, 8,462 laboratory confirmed cases ascertained in active surveillance	6,836 Cohort participants, 800,000 catchment area for national surveillance	4,860 Patients enrolled in cohort	Not applicable	Not applicable
Incidence estimate (95% CI), per 1,000 person-years	15.1 (7.4-28.6)	10.9 (7.4-15.9)	4.8 (1.7-10.4)	11.8(7.6-26.7)	2.8 (not given)
Foodborne illness rank	1 of 3 overall	4 of 12 overall; 1 of 5 bacterial	1 of 5 bacterial	1of 3 overall	4 of 31 overall; 3 of 21 bacterial

cases globally (Riddle *et al*, 2006; Shah *et al*, 2009), with more frequency in some SE Asia areas (Guerry *et al*, 2012). Data from a Canadian community from June 2005 to May 2009 revealed that of the 446 cases of travel-related disease due to enteropathogens reported, campylobacteriosis was the most frequently identified (n = 123,28%) (Ravel *et al*, 2011). Similarly, surveillance data collected by GeoSentinel Travel Network showed that for 17,353 ill returned travellers, the incidence of *Campylobacter* infection was identified in 8.5 per 100 diarrheal cases, which was the leading bacterial etiology (Freedman *et al*, 2006).

1.3.1 Transmission

Several environmental reservoirs can lead to human infections by *C. jejuni*. *C. jejuni* colonises the gastrointestinal tract of its natural host chicken in high numbers, and is rapidly spread throughout the entire flock via the faecal-oral route (Young *et al*, 2007). The main route of *C. jejuni* human infection is through undercooked poultry, processed retail poultry meats, or improperly handling other food types that are cross-contaminated during food preparation and handling (Altekruse *et al*, 1999). In some European countries, 70% of the chickens were colonised with *Campylobacter* at the time of slaughter (Bywater, 2004). As much as 70% of raw poultry meat products sold in the USA in 1999/2000 were found to carry *Campylobacter* (Zhao *et al*, 2001). When the chicken is slaughtered, the bacteria within the digestive tract comes into the contact with the meat, and it can survive processing procedures. When the meat is not correctly cooked or prepared, the bacteria is then ingested and may cause campylobacteriosis. Consumption of contaminated poultry, beef and unpasteurised milk are responsible for approximately 90% of human infection cases (Figure 1.1). Sheep, contaminated water and pet animals are responsible for the remaining 10% of cases (Wilson *et al.,* 2008). Large scale outbreaks of campylobacteriosis are rare, and are usually linked to the consumption of polluted water or raw milk (Oldfield & Wooldridge, 2009). In the USA, campylobacteriosis cases are estimated to be about 2.4 million per year

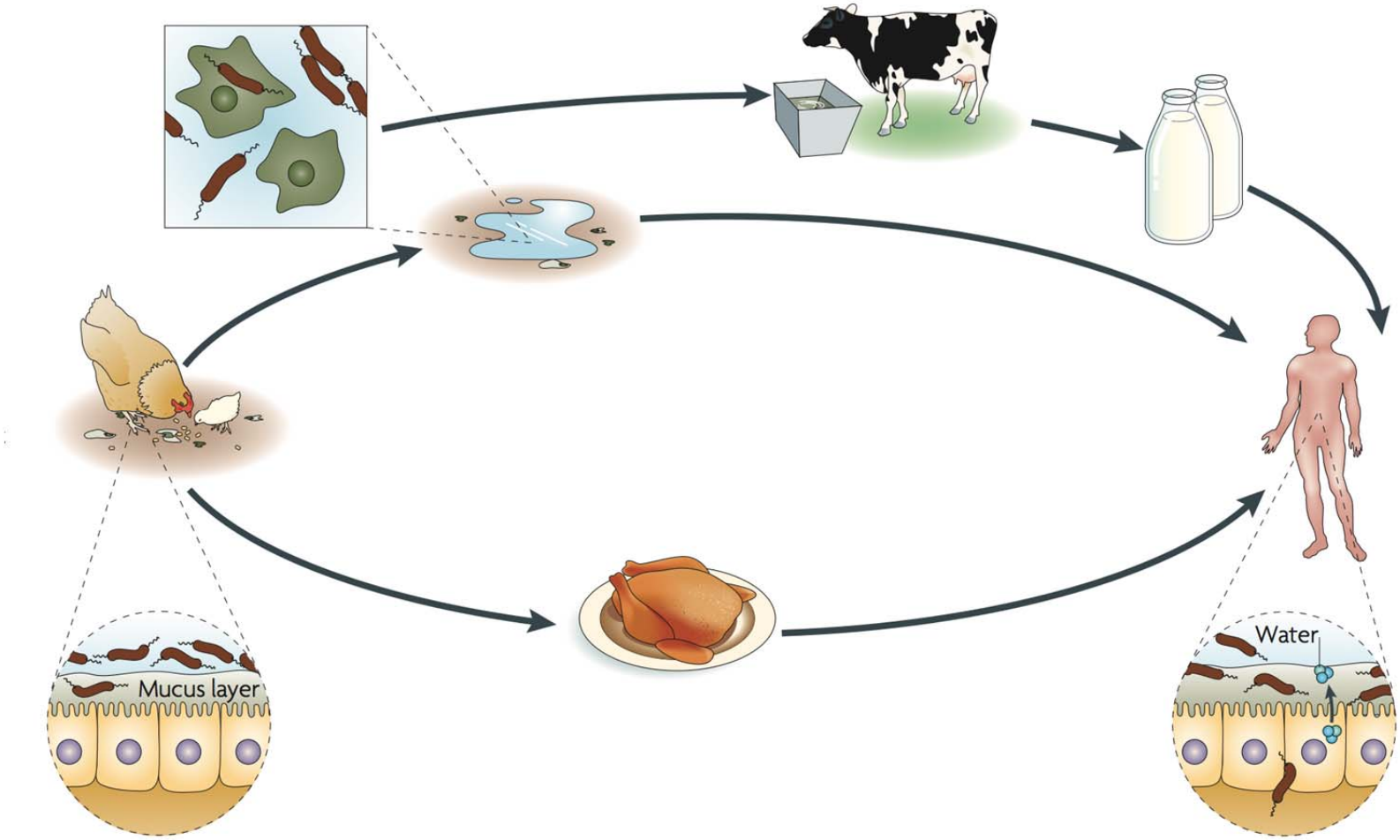

Figure 1.1: Most important routes for human infection by *Campylobacter jejuni* (reproduced from Young *et al,* 2007).

(Friedman, 2000), with up to 70% of sporadic infections related to *Campylobacter*-contaminated poultry (Harris *et al*, 1986). Finally, although direct infection from human to human might occur, it is of no large epidemiological relevance (Nachamkin & Blaser, 2000).

1.3.2 Trends

In the western countries, the people most at risk of infection are young children, immunocompromised patients and young adults (Friedman, 2000). In developing nations, children and immunocompromised patients are the populations who are most at risk and the mortality rates are much greater compared to the developed countries for many economic associated reasons (O'Ryan *et al*, 2005). Children at weaning age are of particular concern in developing countries as they are not receiving maternal antibodies against *Campylobacter* and they are immunologically immature (Coker *et al*, 2002; Nachamkin *et al*, 1994). Furthermore, children in developing nations have more access to farm animals, untreated drinking water and milk (O'Ryan *et al*, 2005). In developing countries, such as Thailand, Mexico and Peru, the incidence rates for children under 5 years old were as high as 40,000-60,000 per 100,000 population (Calva *et al*, 1988; Oberhelman *et al*, 1999; Taylor *et al*, 1988). In contrast, the estimated incidence rate for the same age group in industrialised countries was less then 300/100,000 during the same period (Skirrow, 1987).

Males present with campylobacteriosis 1.2-1.5 times more often than females, which is most apparent in young adults (Friedman, 2000; Kapperud & Aasen, 1992; Skirrow, 1987). The reason for this observation is unclear, but it might be that males are more at risk of *C. jejuni* infection due to their different food handling and consumption practices than females (Ekdahl & Andersson, 2004; Samuel *et al*, 2004).

A seasonal trend has also been discovered as there are more campylobacteriosis cases in summer compared to the winter season (Louis *et al*, 2005; Meldrum *et al*, 2005; Miller *et al*, 2004; Nylen *et al*, 2002). There are several possible reasons for this trend: (1) more

barbecues occur in summer, giving rise to a higher chance for people to ingest undercooked poultry or contaminated food; (2) high temperatures encourage the growth of *C. jejuni* in environmental waters; (3) children have more chance to come into contact with farm animals during the school holidays; (4) flies can act as vectors by carrying the bacteria from uncooked meat or animals faeces and contaminating food sources (Ekdahl *et al*, 2005; Kemp *et al*, 2005; Louis *et al*, 2005; Stanley *et al*, 1998).

1.3.3 Economic Impact

Foodborne zoonoses, such as campylobacteriosis, have a major health impact in industrialized countries (Haddad *et al*, 2010). Lethality and hospitalization rates were combined to assess severity, using a term (λ) to increase the weighting of lethality. The score for the clinical severity of campylobacteriosis using this method was 11.2, compared with 32.3 for *Salmonella* enteric infection (Fosse *et al*, 2008). *Campylobacter* spp. are responsible for approximately 17% of food-borne infection associated hospitalisation in Europe (Mead *et al*., 1999).

In Australia, the economic burden of foodborne disease is AUD$2.6 billion per year (www.foodstandards.gov.au). This website also reported *Campylobacter* being responsible for 51.3% of the total number of foodborne illness in Australia, which means that the cost of campylobacteriosis in Australia is about AUD$1.3 billion/year. The cost includes cost of salary due to illness, medication, product recall, hospitalisation and others. In New Zealand, a study showed that the cost of *Campylobacter* associated disease was NZD$4.48 billion in the year of 1995 (Withington & Chambers, 1997). In the USA, the cost of Campylobacteriosis is about $1.3-6.2 billion per annum, and $1.5-8 billion per annum if the associated complications were included(Buzby *et al*, 1997). In addition, *C. jejuni* is an important factor in the development of GBS, which remains a public health burden (Fujimura, 2013).

1.4 Clinical Aspects of *C. jejuni* Infection

Infection in humans occurs via oral ingestion of *C. jejuni* contaminated food or water, bacterial colonisation of the colonic mucosal layer, adherence to the underlying epithelial cells, secretion of virulence proteins and internalisation of *C. jejuni* by epithelial cells (Raphael *et al*, 2005; Young *et al*, 2007). *Campylobacter* infection is commonly characterised as an acute gastroenteritis with inflammation, abdominal pain, fever and diarrhoea (Black *et al*, 1988). The infection dose can be as low as 500-800 CFU (Robinson, 1981). The incubation period prior to the onset of symptoms arising from campylobacteriosis is usually between 1 to 7 days (Ketley, 1997b). Although campylobacteriosis generally lasts one week, symptoms can last up to 2 weeks (Young *et al*, 2007). Generally, it is self-limiting with the presence of a couple of days of prodromal symptoms i.e. fever, vomiting, headaches and abdominal pain. For more severe cases, these symptoms are followed with 3-7 days of diarrhoea with/without blood. In general, the illness can range from mild to severe with dehydration that might require hospitalization (Dasti, *et al*., 2009). Differences in virulence potential in *C. jejuni* strains and differences between patient immune statuses may contribute to the wide range of clinical symptoms (Poly *et al*, 2007). There are two disease manifestations involved with campylobacteriosis, which are associated with socio-economic status (Blaser *et al*, 1980). In industrialised countries, it manifests as bloody diarrhoea with mucus. In the developing countries, watery diarrhoea predominates, and infection is more frequent in children. The milder cases are predominant in young children from developing countries, while the severe symptoms predominate in patients from industrialised countries.

Patients with full protective immunity, partial immunity or with/without previous *Campylobacter* infection may elicit different immune response and clinical outcomes (i.e. asymptomatic infection, watery diarrhoea, inflammatory diarrhoea with/without blood) (Ketley, 1997a). Infections occur at all ages, although peaks are described for children younger than 4-years-old and for patients aged between 15 and 39 years old (Dasti, *et al*., 2009).

1.4.1 Complications of C. jejuni Infection

Campylobacteriosis has been recognised as an important risk factor for the development of inflammatory bowel disease and extra-intestinal manifestations such as polyarthralgia (i.e., reactive arthritis) or GBS (Haddad *et al*, 2010). The incidence of GBS in humans is < 0.1% of all *Campylobacter* infections (Allos, 2001). The immune system involvement in the progression of GBS involves the accumulation of T-cells and immunoglobulin-mediated, macrophage-orchestrated attacks on the peripheral nerves. The disease is self-limiting, with muscle strength usually reaching a nadir within 2 to 3 weeks, followed by partial or complete recovery over a period of weeks to months. This attack damages the axons or nerve fibres and leads to the inability to conduct electrical impulses stimulating the senses and movement of the extremities (Goodman & Sladky, 2005). Even with treatment, GBS can still cause respiratory distress.

Other complications, such as Miller-Fisher syndrome (MFS) and acute post-infectious polyneuritis are also usually associated with serological evidence of recent previous infection with *Campylobacter* species (Mishu & Blaser, 1993). MFS is a variant of GBS and is known to be involved in peripheral nerve demyelination. Symptoms include areflexia, ataxia and paralysis of one or more of the eye muscles. Some evidence of post-*Campylobacter* infection risk of select chronic disease is listed in Table 1.4.

1.4.2 Treatment and Preventions

Infections caused by *C. jejuni* or *C. coli* are characterised by fever, abdominal cramping, and diarrhoea (with or without blood). Infection is normally self-limiting and lasts several days to > 1 week (Nachamkin and Blaser, 2000, Montville and Matthews, 2008). Normal treatment

Table 1.4: Summary evidence of post-*Campylobacter* infection risk of select chronic health consequences (reproduced from Guerry *et al*., 2012).

Sequelae	Post-infective attributable risk*	Comment	Reference
Guillain Barré syndrome	1 per 1,000	14-32% of GBS cases can be attributed to *C. jejuni*	(Nachamkin & Blaser, 2000)
Reactive arthritis	1-5%	5% of *C. jejuni* ReA may be chronic or relapsing	(Pope *et al*, 2007)
Inflammatory bowel	3-4 per 1,000	Recent evidence suggests that *C. jejuni* can breach the intestinal barrier and may prime the intestine for chronic inflammatory responses in susceptible individuals (Kalischuk and Buret, 2010)	(Gradel *et al*, 2009; Jess *et al*, 2011; Rodriguez *et al*, 2006)
Irritable bowel syndrome	1-10%	IBS developed in 36% of patients associated with a large waterborne outbreak of mixed *Campylobacter* and STEC in Walkerton, Canada. Symptoms persist in approximately 40-50% at 5-7 years	(Dunlop *et al*, 2003; Marshall *et al*, 2006; Rodriguez & Ruigomez, 1999; Thornley *et al*, 2001)

*Post-infective attributable risk considers the absolute difference of the rate of sequelae after *C. jejuni* compared to the rate of the sequelae in an unexposed population.

STEC=Shiga Toxin-producing *Escherichia coli*

involves rehydration to replace the electrolytes and fluid loss as a result of diarrhoea and/or vomiting (Faruque *et al*, 1993; Mackenzie & Barnes, 1988; Skirrow, 2000). In severe cases or when the patient is immunocompromised or pregnant, macrolides (e.g. erythromycin) are usually prescribed (Mamelli *et al*, 2003).

Campylobacteriosis confirmation can take up to 4 days, as time is needed to isolate and culture the bacteria from patient stool samples (Allos, 2001). Sometimes fluoroquinolones are given, as they are the antimicrobial drugs of choice in the treatment of other enteric pathogens, e.g., *Salmonella* or *Shigela* species are also susceptible to them. Thus, the patient could be treated without the need for laboratory testing results (Allos, 2001). Tetracylines have been suggested to replace erythromycin in the case that *Campylobacter* develops erythromycin resistance (Funke *et al*, 1994; Moore *et al*, 2005). The newer macrolides, azithromycin and clarithromycin, are effective with campylobacteriosis treatment, but they are more expensive and without added therapeutic advantage (Allos, 2001).

There are several ways of thinking to prevent campylobacteriosis. Firstly, the improvement of strategies to help reduce cross-contamination during food processing and slaughter. Secondly, treatment of the meat before retail sale in order to reduce the number of live *Campylobacter* on the carcass. Third, public education of food handling and cooking, and awareness of potential cross contamination in the kitchen (Humphrey *et al*, 2001). However, development of a vaccine to protect chicks from colonisation would be the most efficient way to prevent the disease (discussed in the Section 1.11).

1.5 Genetic Features of *C. jejuni*

The complete genome sequence of *C. jejuni* NCTC11168 was completed in 2000, which reveals that *C. jejuni* has the densest bacterial genome sequenced to date, with 94.3% of the genome encoding proteins (Parkhill *et al.* 2000). The entire genome contains 1,641,481 base pairs (bp) with a low G+C content (30.6%), and 1,654 predicted CDS (Parkhill *et al*, 2000). The genome is unusual as there are virtually no insertion sequences, no phage-associated sequences, few repeat sequences, and with the presence of hypervariable sequences (Parkhill *et al*, 2000).

In 2007, the genome sequence from *C. jejuni* NCTC 11168 was re-annotated and re-analysed by more advanced genomic screening techniques (Gundogdu *et al*, 2007). The number of predicted CDS was reduced to 1643, and 18.2% of CDS had their product functions updated (Gundogdu *et al*, 2007). Importantly, major updates in this analysis involved the genes for biosynthesis of important surface structures, which include lipooligosaccharide, capsule and both *O*- and *N*-linked glycosylation (Gundogdu *et al*, 2007). It was shown that 55.4% of *C. jejuni* genes are similar to *Helicobacter pylori,* 28.0% are similar to *Escherichia coli (E. coli)* and 27.0% are similar to *Bacillus subtilis*.

The intragenomic mechanisms and genetic exchanges between strains results in *C. jejuni* displays extensive genetic variation. *C. jejuni* is naturally competent, enabling it to import macromolecular DNA from the environment and incorporate it into its genome (Wiesner *et al*, 2003). Natural transformation enables horizontal gene transfer to occur, generating genetic diversity among *C. jejuni* strains (Dingle *et al*, 2001). The horizontal transfer of *C. jejuni* plasmid and chromosomal DNA happens *in vitro* and during chicken colonisation without any selective pressure, which may contribute to its genome plasticity and antibiotic resistance (Avrain *et al*, 2004; de Boer *et al*, 2002; Wilson *et al*, 2003). However, the frequency of natural transformation is affected by carbon dioxide and the bacterial cell density, which reveals that horizontal exchange may be environmentally regulated *in vivo* (Wilson *et al*.,

2003). Several genes that have been identified are required for natural transformation, which include some components of the type II secretion system (T2SS) (Wiesner *et al*, 2003) (discussed in Section 1.9.3). In addition, genes with implicated elements of a plasmid-encoded type IV secretion system (T4SS) (discussed in Section 1.9.4), genes for *N*-linked glycosylation, genes for lipooligosaccharide (LOS) biosynthesis and a putative DNA-processing enzyme encoding gene, were also found to be necessary for wild-type levels of natural transformation (Bacon *et al*, 2000; Fry *et al*, 2000a; Larsen *et al*, 2004; Takata *et al*, 2005). However, no specific mechanism has been identified to explain how extracellular DNA is recognized and accepted by *C. jejuni* (Young *et al*, 2007).

Genome sequencing of *C. jejuni* reveals the presence of hypervariable sequences that consist of homopolymeric tracts, and also the high frequency of variation within these sequences (Parkhill *et al*, 2000). Most of the hypervariable sequences are in the regions where encoded proteins are involved in the biosynthesis or modification of surface – accessible carbohydrate structure, which consists of the capsule, LOS and flagellum (Parkhill *et al*, 2000). Mechanisms such as phase variation, gene duplication and deletion, frameshifts and point mutations, are the main factors responsible for the variation in these structures (Gilbert *et al*, 2002; Guerry *et al*, 2002; Karlyshev *et al*, 2005b; Karlyshev *et al*, 2002; Linton *et al*, 2000; Parkhill *et al*, 2000).

1.6 Immune Responses

1.6.1 Human Immune Response

Adherence of the bacteria to underlying epithelial cells brings about the production of interleukin (IL)-8, a chemokine that is able to recruit professional phagocytes such as macrophages, dendritic cells, monocytes and neutrophils, which then encounter and rapidly interact with *C. jejuni* (Hu *et al*, 2006a; Young *et al*, 2007). Such an interaction will trigger a massive innate pro-inflammatory response through the activation of nuclear transcription factor kappaB (NF-κB), the cytokines IL-1ß, IL-6, IL-10, IL-12 and TNF-α, and also induction of T_H-1-specific adaptive cell-mediated immunity (Hu *et al*, 2006a; Young *et al*, 2007) (Figure 1.2). The cytolethal-distending toxin (CDT) and the surface-exposed heat-shock protein adhesion factor Jlp, are responsible for the IL-8 production from the human epithelial cells (Hickey *et al*, 2000; Jin *et al*, 2003). Anti-*Campylobacter* specific immunoglobulins IgA, IgG, and IgM have been identified from patients' serum samples (Kaldor *et al*, 1983). *C. jejuni* infection of two polarised intestinal epithelial lines, Caco-2 and T84, exhibits the activation of mitogen-activated protein kinase family proteins extracellular signal-regulated kinases and p38 (MacCallum *et al*, 2005a; Watson & Galan, 2005). For the T84 cell line, extracellular signal-regulated kinases activation is essential for the stimulation of IL-8 (Watson & Galan, 2005). For an intestinal cell line as INT 407, CDT contributes to IL-8 secretion. Therefore, *C. jejuni* can breach the physical barrier of intestinal epithelium, and these cells can in turn signal for the recruitment of inflammatory cells to the site of infection (Figure 1.2).

Human innate immune responses against pathogen microbes are mainly mediated by the activation of Toll-like receptors (TLRs) (Kopp & Medzhitov, 2003). The main TLRs involved in bacterial infections are TLR2/1/6 (detects lipoproteins), TLR4/myeloid differentiation protein-2 (detects lipopolysaccharide/LPS), TLR5 (detects flagellin) and TLR9 (detects DNA)

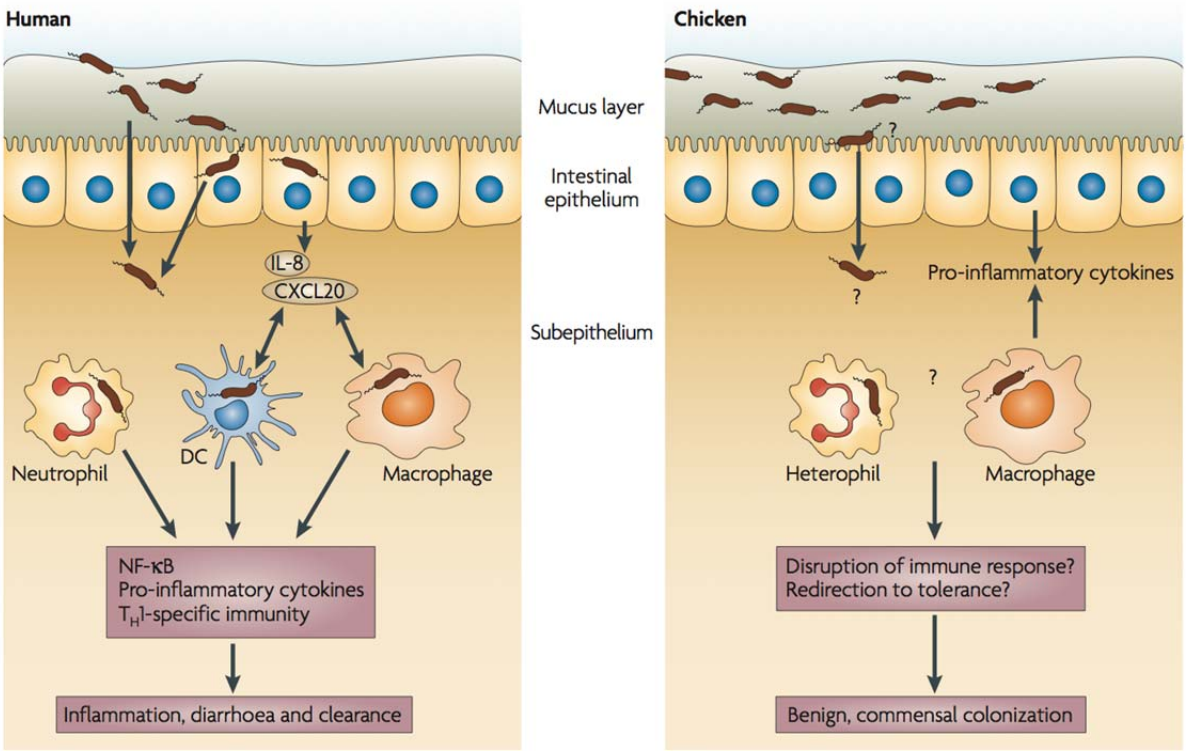

Figure 1.2: Molecular and cellular feature of the humans and chickens innate immune response to *Campylobacter jejuni* (reproduced from Young *et al*, 2007).

(de Zoete *et al*, 2010). After TLR activation, a signal cascade involving the adapter protein MyD88 (all TLRs except TLR3) or TRIF (TLR3 and TLR4 only) results in the activation and translocation of nuclear transcription factors that in turn induce the transcription of cytokines and other immune genes (Akira, 2006). TLR signalling also involves a TLR4-mediated, MyD88-independent pathway associated with the induction of late phase NF-κB and interferon (IFN)-inducible genes, such as IFN-ß, which is involved in natural killer (NK) cell activation and maturation of dendritic cells (Yamamoto *et al*, 2003). *Campylobacter* flagellin is not recognised by the human TLR-5 due to a complex series of mutations in the flagellin TLR-5 recognition site and compensatory amino acid changes in flagellin (Andersen-Nissen *et al*, 2005). *C. jejuni* is not recognised by human TLR-9 as well, because of the AT-rich nature of the *C. jejuni* genome (Dalpke *et al*, 2006). However, the intracellular pathogen-recognition receptor NOD1 plays a crucial role in immune stimulation by *C. jejuni* (Zilbauer *et al*, 2007).

The role of monocytes and macrophages in *C. jejuni* infection various between different cell lines or primary cells (Young *et al*, 2007). Evidence shows that the monocyte cell line THP-1 stimulated with *C. jejuni* induces NF-κB and the pro-inflammatory cytokine IL-1β production (Siegesmund *et al*, 2004; Wassenaar *et al*, 1997). However, a signification proportion of *C. jejuni* infected monocytic cells also undergo apoptosis (Hickey *et al*, 2005; Wassenaar *et al*, 1997). There are a few studies showing that clinical isolates of *C. jejuni* survived for several days in murine peritoneal macrophages and the macrophage cell line J774A.1 (Day *et al*, 2000; Hickey *et al*, 2005; Nachamkin & Yang, 1989). Interestingly, one group (Kiehlbauch *et al,* 1985) found that *C. jejuni* is killed immediately by macrophages derived from human monocytes. The possible reasons for the different observation might be the use of different *C. jejuni* strains and/or the different macrophage-like cell lines.

An adaptive human immune response has been observed during *C. jejuni* infection, although the bacteria has multiple levels of variation in its surface structure, which would help it to evade antibody responses (Young *et al*, 2007). Antibodies from human sera have been

identified during *C. jejuni* infection, which include antibodies to flagella, major outer membrane protein (MOMP), outer membrane protein (OMP), LOS and CDT (Abuoun *et al*, 2005; Guerry *et al*, 2000; Panigrahi *et al*, 1992). CDT has been recognised as a major antigen for antibody production, and neutralizing antibodies that are directed against CDT are observed during human infection (Abuoun *et al*, 2005). CDT will be further discussed in Section 1.8.7.

Children with campylobacteriosis under 6 months old show low levels of specific IgA, IgG and IgM, which may due to the presence of maternal antibodies (Kaldor *et al*, 1983). About 80%-90% patients who were infected with culturable *C. jejuni* produced *C. jejuni* specific serum immunoglobulins (Lee & Newell, 2006). Elevated levels of IgA were only detectable from the onset of symptoms until the clearance of *C. jejuni* (Lee & Newell, 2006). However, elevated IgG persisted after the clearance (Lee & Newell, 2006).

1.6.2 Chicken Immune Response

As with all vertebrates, the immune system of all avian species including chickens is comprised of two arms, an innate (non-specific) immunity and adaptive (specific) immunity (Erf, 1997; Sharma, 1991). Humoral immunity is characterized by B lymphocyte secreted antibodies under the control of the bursa of Fabricius, while the cellular immune system is under the control of the thymus (Sharma, 1991). Other important chicken cellular immune response cells include macrophages, dendritic cells, NK cells and effector cells of antibody dependent cellular cytotoxicity (Sharma, 1991).

The chicken intestinal innate immune system comprises several tissues, cells (i.e. epithelial cells, monocytes/macrophages, dendritic cells, NK cells and neutrophils), and germline-encoded molecules (i.e. chemokines, cytokines, antimicrobial peptides and nitric oxide) that can limit commensal and pathogenic bacteria (Brisbin *et al*., 2008). The primary site of *C. jejuni* ~~infection~~ colonisation in chickens occurs in the deep crypts of ceacum, in the mucous

layer located close to the epithelial cells (Lee & Newell, 2006). *C. jejuni* ~~infection~~ colonisation produces both systemic and secretory IgA antibody responses to a range of antigens including flagellin (Cawthraw *et al*, 1994; Widders *et al*, 1996). *C. jejuni* has been shown to be able to adhere to, invade in and stimulate inflammatory responses from chicken macrophages and epithelial cells *in vitro* (Smith *et al*., 2005; Byrne *et al*., 2007; Larson *et al*., 2008; Van Deun *et al*., 2008). An elevated production of IL-1β, IL-6 and inducible nitric oxide synthase was identified from both cell types, which indicates that *C. jejuni* can stimulate chicken innate immune responses (Young *et al*, 2007) (Figure 1.2).

A crucial step in the host innate immune response to bacterial entrance in the gastrointestinal (GI) tract is the activation of TLRs. TLRs are expressed on a variety of GI mucosa cells, including macrophages and epithelial cells (He *et al*., 2006; Linde *et al*., 2008) and are recognised by specific bacterial ligands. Once TLRs are activated, they promote the expression of effector molecules such as antimicrobial peptides, nitric oxide (NO), and inflammatory cytokines (Hermans *et al*, 2012). Several TLRs have been identified to play a role in *C. jejuni* recognition, such as the chicken cell-surface-expressed chTLR2, chicken TLR4/myeloid differentiation protein-2 complex, and TLR21. TLR2, TLR4 and TLR21 recognise lipopeptides, LOS and unmethylated single-stranded microbial 2′-deoxyribo DNA motifs, respectively (Hermans *et al*, 2012). Activation of chTCR2, chTLR4 and chTLR21 results in a chicken innate immune response involving myeloid differentiation primary response gene 88 (MyD88)-dependent activation of NF-κB and subsequent production of inflammatory cytokines and chemokines (Brownlie *et al*, 2009; de Zoete *et al*, 2010; Keestra *et al*, 2010). Furthermore, chTLR4 and chTLR21 ligands can induce the production of inducible nitric oxide synthase-mediated NO from chicken monocytes (He *et al*, 2006).

In the first two weeks of a chicken's life, when the innate intestinal immune system is still under development, maternal antibodies are still present, which protects the newborn chicks against *C. jejuni* colonisation (Cawthraw *et al*, 1994; Sahin *et al*, 2001). Exposure to *C. jejuni* at this stage can stimulate a slow progressive humoral immune response, the recruitment of

heterophils and lymphocytes, and proinflammatory cytokines IL-1β, IL-8 and K203 (Cawthraw *et al*, 1994; Ge *et al*, 2006; Sahin *et al*, 2003). Some immunoblotting results revealed that the maternal antibodies reacted strongly with outer membrane surface components (flagellin, LOS, and MOMPs) of *C. jejuni* (Cawthraw *et al*, 1994; Sahin *et al*, 2001; Shoaf-Sweeney *et al*, 2008). A study showed that chicken maternal antibodies conferred partial protection against *C. jejuni* and delayed colonisation in young chicks (Sahin *et al*, 2003). After the first 2 weeks of age, as the maternal antibodies decline, *Campylobacter* can be detected in 2-3 weeks old chicks (S. Cawthraw *et al*., 1994). Other factors such as changes in the microbiota and management practices may also have an impact (Wigley, 2013). It is revealed that by 3 weeks of age the chicks produce their own antibodies in response to *C. jejuni*, primarily to flagellin (Cawthraw *et al*, 1994; Jeurissen *et al*, 1998). *C. jejuni* produces CDT in chicks, as in humans, but neutralizing antibodies against CDT are not found in chicks, which is opposite to humans (Abuoun *et al*, 2005).

The capsule expressed by many pathogens normally induces a strong antigenic response, but the chicken humoral response to polysaccharides is weak (Jeurissen *et al*, 1998). It may be associated with incomplete response by chicken to T-cell independent type 2 (TI-2) antigens (e.g. polysaccharides) (Jeurissen *et al*, 1998). TI-2 antigens active chicken B cells independently of T cells, which may associated with their ability to crosslink cell-surface immunoglobins, thereby contributes to *C. jejuni* colonisation in chicken (Young *et al*, 2007).

1.7 Campylobacter Virulence Mechanisms

Virulence is the sum of mechanisms that permits an organism to adhere to and colonise host tissue, the occurrence of cytopathogenic effects, and the host characteristics involved (Haddad *et al*, 2010). It is the measure of the degree of pathogenicity of an organism. The mechanism of pathogenesis of *C. jejuni* comprises of four main stages: adhesion to intestinal cells, colonization of the digestive tract, invasion of targeted cells, and toxin production (Haddad *et al*, 2010).

In response to the high number of cases of human campylobacteriosis, various virulence study models are available depending on the virulence stage being analysed. Despite the high cost and limited availability, animal models are frequently used to study digestive disease, in particular to analyse the colonization stage. Eukaryotic cell cultures have been developed because of fewer restrictions on their use and the lower cost of these cultures studies compared with animal models, and this *ex vivo* approach makes it possible to mimic the bacterial cell–host interactions observed in natural disease cases. Models are complemented by molecular biology tools, especially mutagenesis and DNA microarray methods to identify putative virulence genes or proteins and permit their characterisation. No current model seems to be ideal for studying the complete range of *C. jejuni* virulence. However, the models available deal with different aspects of the complex pathogenic mechanisms particular to this bacterium (Haddad *et al.*).

1.7.1 Adherence Mechanisms

Adhesins belong to an important class of bacterial proteins, which play an important role in the processing of bacterial adherence to the host cells (Garg & Gupta, 2008). This class of proteins include fimbria and pili, which are found in a variety of bacteria including *E. coli, Virbio cholera, Neisseria* species *et al.* (Garg & Gupta, 2008). Adhesins have been

considered as important vaccine candidates as they are often surface exposed (Garg & Gupta, 2008).

Several proteins that are related to *C. jejuni* adherence to eukaryotic cells have been identified. *C. jejuni* CadF is a protein similar to the *E. coli* OmpA and it functions by forming membrane channels (Mamelli *et al*, 2006). It binds specifically to fibronectin, which is located basolaterally on epithelial cells *in* situ (Konkel *et al*, 1997; Monteville & Konkel, 2002; Monteville *et al*, 2003). The CadF fibronectin-binding domain contains a novel fibronectin-binding motif, which consists of amino acids 134-137 (FRLS) (Konkel *et al*, 2005). CadF is required for *C. jejuni* binding and invasion *in vitro*, and *cadF* mutants show reduced colonisation ability compared to the wild type (Monteville *et al*, 2003; Ziprin *et al*, 1999). In addition, CadF appears to have multiple functions, as it is also required for signalling to the host cell leading to the activation of the small GTPases Rac and CDC42, and subsequence uptake of bacteria into the host cell (Krause-Gruszczynska *et al*, 2007a).

JlpA is another characterized adhesin, which is a surface-exposed lipoprotein that is crucial for Hep-2 cell binding (Jin *et al*, 2001). It binds to heat shock protein (Hsp) 90α, and activates the NF-κB and p38 mitogen-activated protein kinase (Jin *et al*, 2003). NF-κB and mitogen-activated protein kinase both contribute to proinflammatory responses (Jin *et al*, 2003). It has been suggested that some of the inflammation during *C. jejuni* pathogenesis may be related to JlpA-dependent adherence (Young *et al*, 2007).

Another lipoprotein, autotransporter CapA, is also implicated as an adhesin (Ashgar *et al*, 2007). *C. jejuni* mutants with *capA* gene deficiency have decreased adherence to Caco-2 cells *in vitro* (Ashgar *et al*, 2007). The mutants also display decreased colonization and persistence in a chicken model (Ashgar *et al*, 2007). The *capA* mutants were severely impaired in their ability to colonise chickens, and was rapidly cleared from infected birds, in contrast to the wide-type strain, which persisted in high numbers during the 6-week experimental time (Ashgar *et al*, 2007).

Interestingly, some putative *C. jejuni* adhesins are located in the periplasm. For instance, the Peb1 adhesin (also known as CBF1), is a periplasmic-binding protein, and shares similarity with the periplasmic-binding proteins of amino acid ATP-binding cassette (ABC) transporters (Leon-Kempis Mdel *et al*, 2006; Pei & Blaser, 1993). Antibodies induced against the Peb1 protein block the adherence of *C. jejuni* to intestinal cells (Kervella *et al*, 1993; Pei *et al*, 1998). Peb1 binds tightly to both aspartate and glutamate and mutants lacking *peb1* cannot grow if amino acids aspartate and glutamate are the major carbon source (Leon-Kempis Mdel *et al*, 2006). Although Peb1 has not been localized to the inner or outer membrane, it has been detected in the culture supernatant (Leon-Kempis Mdel *et al*, 2006). In addition, Peb1 contains a predicted peptidase II signal recognition site, which indicates that it is possible that some Peb1 is surface accessible (Leon-Kempis Mdel *et al*, 2006; Pei & Blaser, 1993). *Peb1*-deficient mutants have decreased colonisation ability in mice, which could be attributed to the loss of either the adhesion or the amino acid transportation, or both (Leon-Kempis Mdel *et al*, 2006; Pei *et al*, 1998).

Protein Peb4 was first classified as a cell-binding factor, which is homologous to a petidyl-prolyl *cis/trans* isomerise of *E. coli*. The petidyl-prolyl *cis/trans* isomerise has multiple roles in *E. coli*, for example, being involved in outer membrane protein biogenesis, in pilus assembly, and for *in vivo* persistence (Justice *et al*, 2006; Oldfield & Wooldridge, 2009). Later it was found that Peb4 is required for optimal cell adhesion and biofilm formation (Asakura *et al*, 2007).

Another periplasmic proteins, Cj1496c, is a glycoprotein that has sequence similarity to a magnesium transporter. Cj1496c is also required for wild type levels of adherence(Kakuda & DiRita, 2006). The mechanisms of periplasmic proteins affecting host-cell adherence is still unclear.

1.7.2 Colonisation

C. jejuni can colonise chickens at very high numbers (up to 10^{10} CFU per gram of infected intestine) (Young *et al*, 2007). Deep crypts of the caecum is the primary site of colonisation (Young *et al*, 2007). *C. jejuni* is commonly found in the mucus layer close to epithelial cells (Young *et al*, 2007). Chicken caeca are large closed pouches, found off the colon (Young *et al*, 2007). They are located just past the ileal junction (Young *et al*, 2007). Experiments where chicken intestinal mucus was added to human epithelial cells show that less *C. jejuni* invasion is observed, which indicates that the chicken intestinal mucus might play a important role in the asymptomatic nature of chicken colonisation (Nachamkin *et al*, 1993).

Colonisation factors are a class of proteins that enable bacteria to colonise the host. *Campylobacter* posses a single polar flagella which has been shown to be critical for intestinal colonization and invasion (Yao *et al*, 1994). Flagellin has been shown to be the immunodominant antigen during human and animal colonisation, and it is also required for colonization *in vivo* (Guerry *et al*, 2000). Flagellar biosynthesis is regulated in a hierarchical fashion with genes expressed in the order in which they are required for the assembly of the flagellum. The production of flagella, however, requires a significant expenditure of energy. Therefore, the regulation of these genes is of critical importance to the organism. However, unlike other bacterial species, only three sigma factors have been identified in *C. jejuni* (σ^{70}, σ^{54} and σ^{28}) (Parkhill *et al*, 2000). These observations suggest that a number of *Campylobacter* genes are coordinately regulated.

Among members of the family Enterobacteriaceae, the genes *flhC* and *flhD* are the initial regulators of the flagellar regulatory cascade (Macnab, 2003). Within this scheme, a feedback mechanism ensures the correct order of flagellar gene expression. In *C. jejuni* that lacks the *flhC* and *flhD* regulators, the genes in the flagella regulon expressed intermediate and late in the flagella regulatory cascade are controlled by the sigma factors σ^{54} and σ^{28}, respectively. Gene *flhA* and *fliA* are also involved with *C. jejuni* colonisation. Based on

studies on the *flhA* gene and the gene *fliA* in *C. jejuni* strain NCTC 11168, it has been observed that a number of genes with unknown functions, but not appearing to be directly involved in flagella function, were also co-regulated along with those genes associated with flagella function (Carrillo *et al*, 2004; Parkhill *et al*, 2000). The *flhA* gene is expressed early in the cascade and is involved in the export of flagella proteins, while the gene *fliA* encodes σ^{28}. Additionally, mutants in the gene that encodes the flagellin FlgR also display defects in chicken colonisation (Hendrixson, 2006).

Other regulators that are not related to flagellar motility are also associated with efficient chicken colonisation, and include CbrR (Stintzi, 2003). CbrR regulates deoxycholate resistance, and contains two response-regulator domains and a GGDEF domain (Stintzi, 2003).

Another wide-type chicken colonisation system required by *C. jejuni* is RacRS, which is a two-component system (Purdy *et al*, 1999). Mutants lacking RacRS expression have a growth defect at 42ºC (Purdy *et al*, 1999). The RacRS system is involved in a temperature-dependent manner, which can act as both as an activator and repressor (Purdy *et al*, 1999).

C. jejuni mutants in DccRS, a two-component system, also have defective in chicken colonisation compared with the wild type (Purdy *et al*, 1999). No known predicted functions have been identified within DccRS-regulated genes (Purdy *et al*, 1999). However, one of genes seems to be essential for bacteria growth, while two genes mutants lead to colonisation defects in chicken (Purdy *et al*, 1999).

Several other genes not involved in motility or gene regulation were also found to be essential for chicken colonisation. These genes include genes that encode the protein *N*-linked glycosylation related enzymes (Hendrixson & DiRita, 2004; Kakuda & DiRita, 2006; Karlyshev *et al*, 2004), and various adherence and invasion factors, such as *cadF* and *ciaB* (Ziprin *et al*, 2001; Ziprin *et al*, 1999). In addition, *Campylobacter* invasive antigen/Cia

proteins, which are normally involved in host invasion, have been shown to play an important role in the colonisation process since Cia negative strains colonised chickens at approximately 1000-fold lower levels than wild-type strains (Biswas *et al*, 2007).

Finally, other factors such as antimicrobial resistance mechanisms, and metabolism mechanisms that are related to low iron, low oxygen and high serine or other amino acids environment, may also have an impact on chicken colonisation (Lin *et al*, 2003; Luo *et al*, 2003; Palyada *et al*, 2004; Smith *et al*, 2005; Velayudhan *et al*, 2004; Woodall *et al*, 2005).

1.7.3 Invasion

To establish an infection, *C. jejuni* must cross the mechanical and immunological barriers of the GI tract (Young *et al*, 2007). The mucus layer of the GI epithelium is the first of line of defence, but *C. jejuni* penetrates this barrier by several mechanisms, which include its motility and corkscrew morphology, and its relatively short LOS *O*-sidechain (Young *et al*, 2007). The short *O*-sidechain of the LOS is proposed to reduce nonspecific binding to mucin glycoproteins (McSweegan & Walker, 1986). After *C. jejuni* passes the mucus layer, it interacts with the underlying epithelial cells using various mechanisms.

Campylobacter invades the human intestinal epithelial cell layer (van Spreeuwel *et al*, 1985), but complete understanding of the exact mechanism that controls the invasion is complicated, as it varies between strains (Young *et al*, 2007). It is shown that microtubule polymerisation is required by all strains for maximal invasion (Hu & Kopecko, 1999; Monteville *et al*, 2003). Some strains also require microfilament polymerisation (Biswas *et al*, 2003; Oelschlaeger *et al*, 1993). Microtubule polymerisation mechanism for invasion makes *Campylobacter* different from other invasive organisms that use a microfilament-dependent mechanism of entry. Human epithelial cell membrane pseudopods that extend towards and envelop *C. jejuni*, have been visualised by scanning electron microscopy (Biswas *et al*, 2003). Immunofluorescence experiments have also shown that these pseudopods contain

microtubules (Hu & Kopecko, 1999). Once internalised within cells, *C. jejuni*-containing vacuoles seem to move along microtubules to the perinuclear region of the cell by interactions with dynein (Hu & Kopecko, 1999).

The invasion factors normally disrupt the host cell membranes and stimulate endocytosis, which facilitates the entry of bacteria into the host body across protective epithelial tissue layers (Garg & Gupta, 2008). Biopsies of humans diagnosed with *C. jejuni* exhibit the presence of intercellular bacteria revealing that host cell invasion may be important in *C. jejuni* infection and subsequent tissue damage (van Spreeuwel *et al*, 1985). Some isolates of *C. jejuni* are highly invasive in cell-based models, such as in the human enterocyte-derived Caoco-2 cell line. However, many isolates show low levels of invasion *in vitro* (Biswas *et al*, 2003). The method of *C. jejuni* entry into host cells needs to be better investigated and may be strain-dependent (Oldfield & Wooldridge, 2009). The highly invasive strain *C. jejuni* 81-176 displays microtubule-dependent invasion, and is also likely to rely on microtubule motors for uptake and intracellular motility (Hu & Kopecko, 1999). This strain contains a virulence plasmid pVir that encodes a T4SS (discussed in Section 1.9). Most other strains of *C. jejuni* that do not carry this plasmid appear to invade human epithelial cells via a microfilament-dependent (Konkel & Cieplak, 1992) or microfilament/microtubule-dependent mechanisms (Biswas *et al*, 2003). It was reported that *C. jejuni* invasion requires tyrosine phosphorylation of host proteins, and also the presence of lipid rafts in the host membrane (Hu *et al*, 2006b; Konkel *et al*, 2004; Wooldridge *et al*). There is also evidence that small guanosine triphosphate (GTP)-binding proteins, such as Rac1 and Cdc42, and membrane ruffling are required for *C. jejuni* host invasion (Krause-Gruszczynska *et al*, 2007a). It is possible that all of the mechanisms are important *in vivo*, while different strains and the presence and/or abundance of certain host receptors may have an impact on which invasion pathway predominates (Oldfield & Wooldridge, 2009).

Host invasion seems to involve the mobilisation of bacterial effector proteins into host cells, which stimulates host cell signalling and triggers bacterial internalisation (Oldfield &

Wooldridge, 2009). It is reported that *C. jejuni* F3800 produces at least 14 proteins during co-culture with epithelial cells, and a subset of these proteins are secreted in the presence of eukaryotic cells or cell culture-conditioned medium (Konkel & Cieplak, 1992; Konkel *et al*, 1999). The functions of these proteins are unknown. However, confocal microscopy results indicates that one protein, CiaB, enters host cells during invasion (Konkel *et al*, 1999). Isogenic mutants lacking-*ciaB* are deficient in Cia protein secretion and impaired in their ability to invade host cells. Cia protein synthesis is stimulated by the bile component deoxycholate, serum and heat-stable eukaryotic host cell components, but the secretion is not (Rivera-Amill *et al*, 2001). It is suggested that Cia production might be stimulated at the early stage of colonisation, in the small intestine (Rivera-Amill *et al*, 2001). Then secretion happens only after adherence at the site of long-term colonisation (Rivera-Amill *et al*, 2001). The secretion of CiaB is further discussed in Section 1.9.2.

Another flagella exporting protein, FlaC is also related to host cell invasion. Unlike the Cia proteins, synthesis of FlaC in the strain TGH9011 does not require contact with epithelial cells or culturing in conditioned medium (Song *et al*, 2004). After secretion, FlaC binds to the surface of human epithelial cells and plays a role in invasion, as mutants lacking *flaC* have invasion levels that were reduced to 14% compared with wild type cells (Song *et al*, 2004).

1.7.4 Defensive Virulence Factors

Cell surface carbohydrates and proteins that protect pathogens from host defence mechanisms belong to the class of defensive virulence factors, and include capsular polysaccharides, lipopolysaccharides and outer membrane proteins (discussed in Section 1.8.2).

1.8 Virulence Determinants of *C. jejuni*

Five classes of virulence factors have been widely discussed: adhesions, colonisation factors, invasion factors, toxins and defensive virulence factors. Apart from these, there are also other virulence traits that are indirectly involved in bacteria virulence, such as secretory machinery, sideophores, catalases and regulators, and these are also essential for pathogens to manifest infection (Brogden, 2000). Molecular mechanisms of *C. jejuni* virulence show *C. jejuni* is able to execute the *N*-linked glycosylation of more than 30 colonisation, adherence and invasion related proteins (Dasti *et al*., 2009). Unlike other diarrhoea-causing bacteria, no other classical virulence factors have yet to be identified in *C. jejuni* except CDTs (Dasti *et al*., 2009). CDT holotoxin, which consists of three subunits CdtA, CdtB and CdtC, is the only virulence factors in *C. jejuni* shared with other enteric pathogens (Poly *et al*, 2007).

1.8.1 Flagella

The bipolar flagellum of *C. jejuni* is considered as one of its most important virulence factors (Guerry *et al*, 2000). The flagellum is not only depicted to facilitate motility but is also associated with processes such as chemotaxis, the secretion of virulence proteins (such as *Campylobacter* invasive antigens/Cia), auto-agglutination, micro-colony formation and avoidance of the innate immune response. All of these processes are found to be dependent on a fully functional flagellum (Dasti *et al*., 2009; Baker *et al*, 2006; Guerry, 2007; Wadhams & Armitage, 2004). Flagellar regulatory hierarchy that includes σ^{54} (encoded by *rpoN*) and σ^{28} (encoded by *fliA*) as the flagellar σ-factors, and the phase variable two-component system FlgRS have been elucidated by various studies (Carrillo *et al*, 2004; Colegio *et al*, 2001; Hendrixson, 2006; Hendrixson & DiRita, 2003; Jagannathan *et al*, 2001; Wosten *et al*, 2004).

The flagellum allows the organism to move quickly (up to 75 μm/s) through a viscous environment and increases its ability to adhere and invade intestinal epithelial cells (Szymanski *et al*, 1995). Flagellin is the immunodominant antigen in both human and animal infections. The flagellum is essential for *in vivo* colonisation of *C. jejuni* in host organisms, and it is needed as the export apparatus for invasion antigen Cia and FlaC proteins secretion during the host invasion process (Guerry *et al*, 2000). Flagellin is modified by *O*-linked glycosylation, which is required for flagellar assembly and motility, virulence and epithelial cell adherence and invasion (Young *et al*, 2007).

One of the most important proteins in the formation of flagella is FlaA. A mutation of the *flaA* gene results in a very short non-functional flagellum. This leads to a dramatic decline of *C. jejuni* colonisation ability in chickens (Nuijten *et al*, 2000). *C. jejuni* FlaB is involved in the flagella export apparatus. It is shown that in the absence of FlaB, *C. jejuni* is non-motile. Homologues of the flagellar master regulators FlhC and FlhD have not been identified in the *C. jejuni* genome (Parkhill *et al*, 2000). Another two flagella proteins, FlgP (encoded by *cj1026c)* and FlgQ (encoded by *cj1025c*), have been identified as required for the motility of *C. jejuni*, but not for flagellar biosynthesis (Sommerlad & Hendrixson, 2007). FlgP and FlgQ are not components of the transcriptional regulatory cascades to activate σ^{28} or σ^{54}-dependent expression of flagellar genes (Sommerlad & Hendrixson, 2007). Immunoblot analyses suggests that the majority of FlgP is associated with the *C. jejuni* OM, and the amount of it in the outer membrane is dependent on the presence of FlgQ, which suggests that FlgQ may be required for localization or stability of FlgP (Sommerlad & Hendrixson, 2007).

1.8.2 Lipopolysaccharide, Lipooligosaccharide and Capsule

Lipopolysaccharides (LPSs) are also termed as endotoxins, which form a family of toxic phosphorylated glycolipids found in the outer membrane of Gram-negative organisms (Rietschel *et al*, 1990). LPSs are essential for the physical integrity and also functioning of

these Gram-negative bacteria outer membrane, including *Campylobacter* spp. (Rietschel *et al*, 1990). LPSs play an essential role for these bacteria, as they are involved in the interaction between the organisms with their environment and their hosts (Moran *et al*, 2000). LPS possesses potent immunomodulating and immunostimulating activity (due principally to their lipid component, lipid A), harbours binding sites for antibodies and non-immunoglobulin serum factors, and contributes to bacterial virulence (Rietschel *et al*, 1990).

Interest in determining *Campylobacter* LPSs role in serotyping and pathogenesis has been raised for a number of reasons. First, a sero-typing typing system for *C. jejuni* and *C. coli* based on thermostable antigens, which is of the LPS class of molecules, was firstly described in the 1980s (Penner & Hennessy, 1980; Penner *et al*, 1983). Serotyping of clinical isolates has confirmed an association between antecedent infections with certain serotypes of *C. jejuni* and subsequent development of GBS and MFS (Kuroki *et al*, 1993; Moran *et al*, 1996; Moran *et al*, 1991). Second, the application of serotyping of *C. jejuni* and *C. coli* based on thermostable antigens has led to the interest in its application to other species of *Campylobacter* (Aspinall *et al*, 1995; Kosunen, 1986; Perez-Perez *et al*, 1986). Third, the molecular basis for some LPS activities was unclear.

The LOS is closed related to the LPS molecule. The LOS of *C. jejuni* is highly variable and their structure resembles human neuronal gangliosides, which is thought to lead to autoimmune disorders, which include GBS and MFS (Young *et al*, 2007). Mutations in LOS biosynthesis genes affect serum resistance, and the adherence and invasion of INT 407 cells (Fry *et al*, 2000a). The lack of *N*-acetylneuraminic acid from the LOS core decreases the bacterial immunogenicity in humans (Coker *et al*, 2002).

The capsule structure of *C. jejuni* NCTC 11168 has been determined and it incudes 6-methyl-D-glycero- α-L-glucoheptose, β-D-glucouronic acid modified with 2-amino-2-deoxyglycerol, β-D-Gal*f*NAc and β-D-ribose (St Michael *et al*, 2002), with a novel modification on Gal*f*NAc (Szymanski *et al*, 2003). The structure variation of the *C. jejuni*

capsule can be attributed to multiple mechanisms, which include phase variation of structural genes and *O*-methyl phosphoramidate modification (Karlyshev *et al*, 2005a; Karlyshev *et al*, 2000; St Michael *et al*, 2002; Szymanski *et al*, 2003). The capsule plays an important role in *C. jejuni* serum resistance, the adherence and invasion of epithelial cells, and chicken colonisation and virulence in a ferret model (Bachtiar *et al*, 2007; Bacon *et al*, 2001; Jones *et al*, 2004). It has been shown that the capsule polysaccharide is accessible to the immune system and structure variation is probably important in host immune response evasion (Young *et al*, 2007).

1.8.3 Glycosylation

Glycosylation is the most abundant polypeptide chain modification in nature. *C. jejuni* expresses two protein-glycosylation systems, the *O*-linked glycosylation system and the *N*-linked glycosylation system (Young *et al*, 2007). The *C. jejuni* glycome and surface structures are shown in Figure 1.3.

The *O*-linked glycosylation system in *C. jejuni* modifies flagellin, and the glycan is linked to the flagellin through a serine or threonine residue, which is required for flagella assembly (Young *et al*, 2007). Proteins of the *O*-linked-glycosylation systems together with their biochemical functions and a hypothetical biosynthetic pathway have been investigated by a range of sequence analysis studies, targeting mutation and chemical analysis (Chou *et al*, 2005; Guerry *et al*, 2006; McNally *et al*, 2006; Thibault *et al*, 2001). A specific recognition sequence for *O*-linked glycosylation has not been identified yet, and the addition of the glycan is believed to require surface exposure and hydrophobicity (Thibault *et al*, 2001). It is suspected that the *O*-glycan might have a role in the interactions of flagellin subunits with one another or with other elements of the flagellar apparatus, as *O*-linked glycosylation of flagellin is required for the proper assembly of the flagellar filament (Goon *et al*, 2003). It was shown that *O*-link glycosylation defects caused a loss of motility, a decrease in the

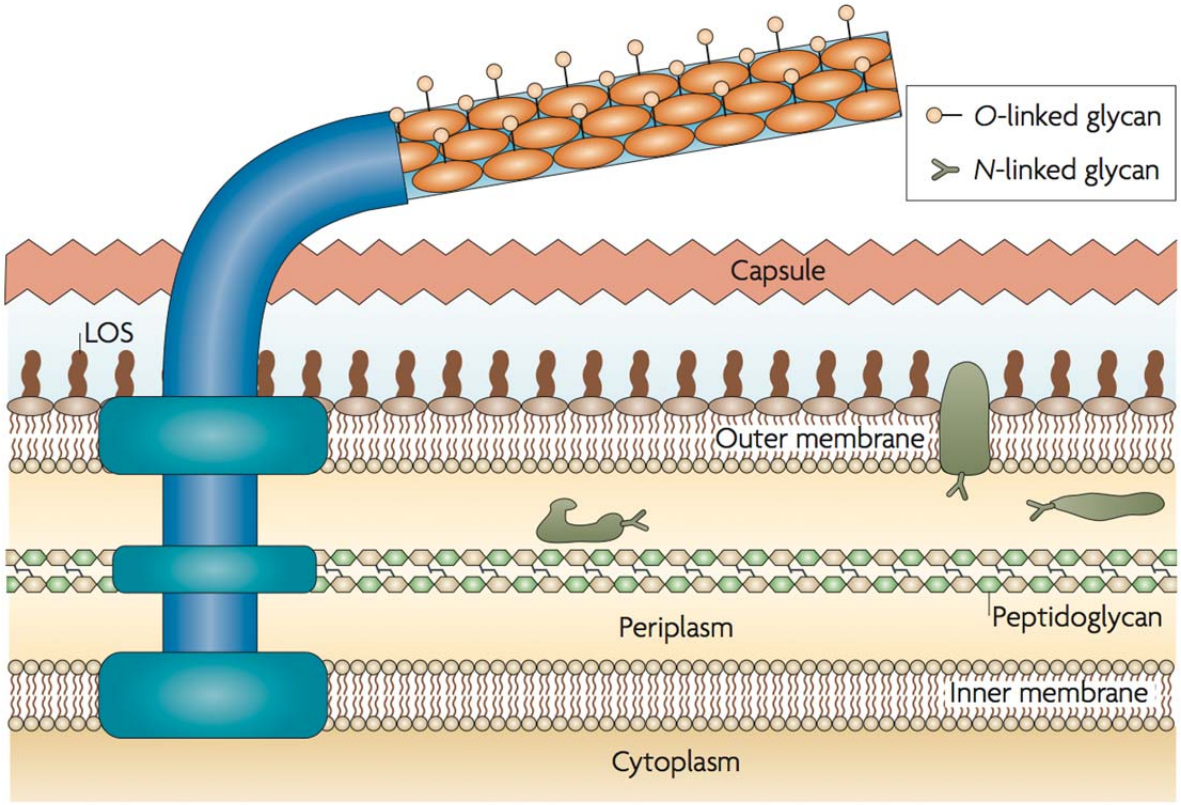

Figure 1.3: The *Campylobacter jejuni* glycome and surface structures (reproduced from Young *et al*, 2007).

adherence to and invasion of host cells and decreased virulence in ferrets (Guerry *et al*, 2006). As the flagellar apparatus of *C. jejuni* spans the inner and outer membranes, *O*-linked glycosylation of the flagellin monomer is believed to occur at the cytoplasm-inner membrane interface (Nothaft & Szymanski, 2010). Cytosine monophosphate-activated sugars are individually added to surface-exposed Ser or Thr residues in the flagellin subunit FlaA by a glycosyltransferase (Young *et al*, 2007).

The *N*-linked-glycosylation of *C. jejuni* is a general glycosylation system, which modifies asparagine residues on many proteins (Young *et al*, 2007). It occurs at the cytoplasmic face of the inner membrane and the system is assembled by the Pgl system, which consists of a heptasaccharide, unlike the tetradecasaccharide that is transferred by the eukaryotic *N*-linked-glycosylation machinery (Wacker *et al*, 2002; Young *et al*, 2002). The *N*-glycan heptasaccharide is flipped across the membrane and added as a block to target proteins in the periplasm (Young *et al*, 2007). Different from the *O*-linked glycosylation machinery, a consensus sequence element (sequon) is present in *N*-linked glycosylation, D/E-X_1-N-X_2-S/T (X_1 and X_2 can be any amino acids except proline) (Kowarik *et al*, 2006; Nita-Lazar *et al*, 2005). The sequon is essential for glycosylation, but not sufficient, other sequences or factors, such as tertiary or quaternary structure may be also be required (Kowarik *et al*, 2006). The *N*-linked glycan is conserved in all *C. jejuni* strains that have been examined (Young *et al*). After comparing the conserved *N*-linked glycosylation with the variability of the other surface carbohydrate traits, it has been suggested that *N*-linked glycosylation may play a more fundamental role in the biology of *C. jejuni* (Young *et al*, 2007). In *C. jejuni*, a heptasaccharide is built on the cytoplasmic side of the inner membrane on a lipid-linked precursor, undecaprenyl phosphate (Linton *et al*, 2005; Reid *et al*, 2008; Reid *et al*, 2009), and then the resulting lipid-linked oligosaccharide is translocated across the inner membrane into the periplasmic space by PglK, which is an ATP-dependent flippase (Alaimo *et al*, 2006; Kelly *et al*, 2006). Lipid-linked oligosaccharide is then transferred to Asn residues in target proteins by PlgIB, which is a bacterial oligosaccharyltransferase.

The role of *N*-linked glycosylation in the biology of *C. jejuni* is not clear, even though the mechanisms of *N*-linked glycosylation are well understood. Conversely, although less is known about the *O*-linked glycosylation mechanisms, its role in *C. jejuni* biology, especially the part it plays in flagella assembly and host-cell interaction, is clear (Young *et al*, 2007). *C. jejuni* strains with *pgl* mutations show decreased adherence and invasion in the INT 407 cell line, as well as defects in natural competence (Larsen *et al*, 2004) and colonisation in the mouse and chicken models (Hendrixson & DiRita, 2004; Kakuda & DiRita, 2006; Karlyshev *et al*, 2004; Kelly *et al*, 2006; Szymanski *et al*, 2002). It is suggested that *N*-linked glycosylation might be involved in the evasion of the immune system, as *N*-linked glycosylation changes the immunoreactivity of at least some glycosylated proteins (Szymanski *et al*, 1999). However, most of the Pgl system modified proteins predicted are located in the periplasmic, rather than surface exposed (Young *et al*, 2002), therefore it is unclear how modifying these proteins would increase immune avoidance.

1.8.4 Chemotaxis

Chemotaxis can be characterised as flagellated bacteria that swim towards the preferred environment and away from a non-preferred environment and it plays an important role in both the commensal and pathogenic lifestyles of *C. jejuni* (Young *et al*, 2007). The general chemotaxis prerequisites are chemoreceptors, a chemosensory signal-transduction system and the flagellar apparatus (Li *et al*, 2014).

A total of 10 methy-accepting chemotaxis receptors have been found in *C. jejuni* and these have been designated as ‘Tlps’ for transducer-like proteins (Li *et al*, 2014). The chemoreceptors from *Campylobacter* can be classified into three groups A, B, and C (Table 1.5). Group A includes membrane-anchored chemoreceptors that have membrane-spanning regions through the inner and outer membrane. They sense periplasmic signals with a periplasmic sensory and a cytoplasmic signalling domain. The *C. jejuni* Group A receptors possesses a similar composition as the *E. coli* methy-accepting chemotaxis proteins and the

Halobacterium salinarium family A transducers (Zhang *et al*, 1996). In general, the structure can be described as two amino-terminal located transmembrane domains and a periplasmic ligand-binding domain, and then a highly conserved carboxy-terminal signalling domain (Morgan *et al*, 1993). Furthermore, a structurally conserved HAMP-domain (a linker domain present in Histidine-kinases, Adeny-cy-clases, Methyl-accepting-proteins and Phosphatases) connects the transmembrane helices (TMH) with the signalling domain (Zautner *et al*, 2012). The signal domains of Tlp2, 3 and 4 are identical (Parkhill *et al*, 2000). The receptor Tlp7 only belongs to group A when it is encoded by one single gene (*cjj81176-0975*) as in the *C. jejuni* strains 81-176 and 81116. In the strains NCTC 11168 and B2, there are two genes involved in Tlp7 coding: the sections for periplasmic binding and transmembrane localisation are encoded on gene *cj0952c*; while the signalling domain is encoded by the adjacent gene *cj0951c (*Marchant *et al,* 2002*;* Tareen *et al,* 2010*).* Group B contains only one receptor, Tlp9 (CetA), which is anchored in the inner membrane and interacts with CetB triggering pyruvate and fumarate signals (Hendrixson *et al*, 2001). CetA serves as an electron donor and CetB is known to be a respiratory electron acceptor (Hendrixson *et al*, 2001). CetA includes two TMH, a HAMP-domain and a highly conserved domain (HCD), and CetB has a PAS (Per, ARNT and Sim) domain. Both proteins together represent a bipartite energy taxis system (Zautner *et al*, 2012). Experiments reveal CetB is a signal sensing protein that conveys the signal to CetA, and then CetA transmits the energy taxis signals to core signal transduction proteins of the chemotactic system CheW/CheV, CheA(Y) and CheY (Elliott & Dirita, 2008; Hendrixson *et al*, 2001). Group C contains four chemoreceptors (Tlp5, 6, 7c and 8), which contain neither a periplasmic binding domain nor transmembrane regions, but only a single cytoplasmic signalling domain (Li *et al*, 2014). They are believed to reside only in the cytosol (Zautner *et al*, 2012).

C. jejuni displays chemotactic motility towards amino acids that are found in high levels in the chicken gastrointestinal (GI) tract, and towards components of mucus (Hugdahl *et al*, 1988). Some Tlp corresponding genes knockout mutants, such as the ones that lack *cj0019c*

Table 1.5: Three different *Campylobacter jejuni* Tlp-chemoreceptor groups (reproduced from Zautner *et al*, 2012).

Group types	Tlp name	Name	Encoded gene
Group A	Tlp1		*cj1506*
	Tlp2		*cj0144*
	Tlp3		*cj1564*
	Tlp4	docC	*cj0262*
	$Tlp7_{mc}$ *		*cjj81176-0975*
	$Tlp7_{m}$ *		*cj0952c*
	Tlp10	docB	*cj0019*
Group B	Tlp9	CetA	*cj1190*
Group C	Tlp5		*cj0019*
	Tlp6		*cj0019*
	$Tlp7_{c}$ *		*cj0951c*
	Tlp8		*cj0019*

*$Tlp7_{mc}$: Membrane-associated and cytoplasmic domains encoded by *cjj81176-0975* in the *C. jejuni* strains 81-176 and 81116

$Tlp7_{m}$: Membrane-associated partial receptor encoded by *cj0952* in the *C. jejuni* strains NCTC 11168 and B2

$Tlp7_{c}$: Cytoplasmic partial receptor encoded by *cj0951c* in the *C. jejuni* strains NCTC 11168 and B2

(Tlp10) or *cj0262c*(Tlp4) *or cj1506c*(Tlp1), displayed decreased chicken colonisation ability (Hendrixson & DiRita, 2004; Zautner *et al*, 2012). However, a transposon insertion in gene Tlp10(*cj0019*) did not affect the *in vitro* motility of the bacteria. Strains that lack of CheY expression (encoded by *cj1118c*), which is the chemotaxis regulatory protein that controls flagellar rotation, exhibit decreased virulence in the ferret model (Yao *et al*, 1997). Tlp7 (*cj0952c/cj0951c, cjj81176-0975*) could be linked to the sensing of electron donor formate, and Tlp1 was identified to represent the chemoreceptor for aspartate (Hartley-Tassell *et al*, 2010; Tareen *et al*, 2010).

The chemotaxis system also affects the bacterial motility of *C. jejuni*. Motility in turn is an essential factor for the pathogenicity of *C. jejuni* as the non-motile strains show a decreased capacity of infection (Morooka *et al*, 1985; Nachamkin *et al*, 1993; Pavlovskis *et al*, 1991). Therefore, the loss of chemoreceptor functions would reduce bacterial motility and, thus, reduce infectivity. It has been shown that a transposon insertion in Tlp3, Tlp4, Tlp7 and Tlp9 is accompanied by reduced motility in *C. jejuni* (Golden & Acheson, 2002; Hendrixson *et al*, 2001; Tareen *et al*, 2010; Vegge *et al*, 2009). Finally, since all chemotaxis sensed signals are transmitted to the flagellum via the chemotaxis core proteins, it is unsurprising that the loss of proteins, such as CheA and CheY, results in *C. jejuni* with reduced motility (Golden & Acheson, 2002). Despite the progress that has been achieved, the overall understanding of chemoreceptors roles and chemotaxis mechanisms is still incomplete and awaits further investigation.

1.8.5 Toxins

The most commonly known bacterial virulence factors are the bacterial toxins that poison the host cells and cause tissue damage (Garg & Gupta, 2008). They have been recognised as a major pathogenicity-associated factor.

C. jejuni Cytolethal distending toxin (CdtA,B,C) causes arrest at the G_1/S or G_2/M transition of the cell cycle, depending on the cell type (Hassane *et al*, 2001; Hassane *et al*, 2003; Lara-Tejero & Galan, 2000; Lara-Tejero & Galan, 2001; Whitehouse *et al*, 1998). The active holotoxin is a complex that includes CdtA, CdtB and CdtC (Lara-Tejero & Galan, 2001) (Figure 1.4), and one study has even shown that the combined CdtB and CdtC still has some cytotoxicity in the absence of CdtA (Lee *et al*, 2003).

CdtB is recognised as the toxic component, as microinjection or transfection of this subunit alone into host cells exhibits the effects that are obtained with the whole holotoxin complex (Lara-Tejero & Galan, 2000). CdtB is thought to act as a DNase as it is homologous with a family of DNase I-like proteins (Young *et al*, 2007). However, CdtB has weak DNase activity *in vitro* (Lara-Tejero & Galan, 2000), and studies that have attempted to determine if the DNA damage *in vivo* is caused by CdtB have produced conflicting results (Hassane *et al*, 2001; Li *et al*, 2002; Mao & DiRienzo, 2002; Sert *et al*, 1999; Whitehouse *et al*, 1998).

CdtB is nuclear localised, and the CdtB sequences from several species reveal the presence of a putative bipartite nuclear-localisation signals located mostly in the carboxy half of the protein (McSweeney & Dreyfus, 2004). One of the putative nuclear-localisation signals from *E. coli* has been identified as essential for CdtB-II nuclear localisation and cytotoxicity (McSweeney & Dreyfus, 2004). Another CdtB from *A. actinomycetemcomitans* also contain a bipartite nuclear-localisation signal domain, which is also required for CdtB nuclear localisation (Nishikubo *et al*, 2003).

The understanding of the exact roles of CdtA and CdtC in this family of toxins is still limited. CdtA and CdtC share some similarity with the B chain of the ricin toxin, which is responsible for receptor-mediated endocytosis of ricin (Lara-Tejero & Galan, 2001). CdtA and CdtC bind to HeLa cells with specificity, which is likely by the same receptor (Lee *et al*, 2003). CdtA and CdtC may mediate binding and subsequent internalisation through the same pathway as

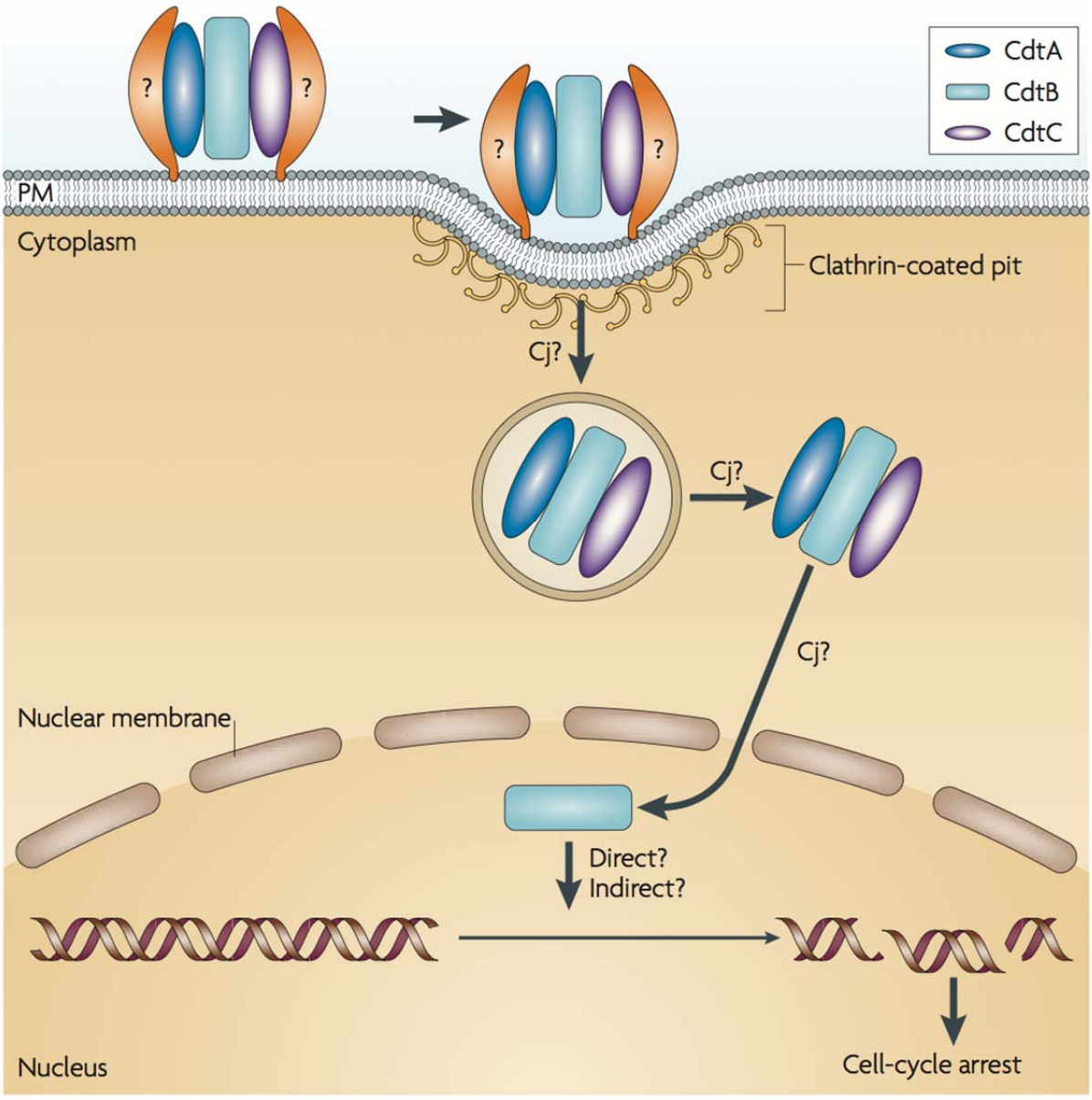

Figure 1.4: *Campylobacter jejuni* cytolethal distending toxin CdtA, CdtB and CdtC (reproduced from Young *et* al, 2007).

H. ducreyi CDT, which is taken up into cells by clathrin-coated pits (Cortes-Bratti *et al*, 2000). CDT may be involved in *C. jejuni* asymptomatic, commensal infections by providing a way to either avoid host immune-response mechanisms, or redirect them towards tolerance (Young *et al*, 2007). CDT is responsible for some of the secretion of IL-8 and there is also a CDT-independent IL-8 stimulation pathway (Hickey *et al*, 2000). In experiments, *C. jejuni* CDT induces apoptosis in monocytic cell lines *in vitro* (Hickey *et al*, 2005). Furthermore, the persistent *C. jejuni* colonisation of wild-type mice, but not NF-κB deficient mice, indicates that CDT might allow *C. jejuni* to escape immune surveillance by inducing NF-κB by CdtB (Fox *et al*, 2004). In chicks, CDT is expressed by bacteria in the caeca, although CDT-neutralising antibodies are not detected in the colonised chicks (Abuoun *et al*, 2005). In addition, *C. jejuni* mutants that lack CDT, colonise chickens with wild-type efficiency (Biswas *et al*, 2006). Therefore, it would seem that CDT is not an important factor in the colonisation of chickens.

A number of putative haemolysins have also been identified from the *C. jejuni* NCTC 11168 genome, including Cj0588 (TlyA) and Cj1351 (PldA) (Parkhill *et al*, 2000). PldA from *E. coli* is an OM-associated phospholipase A with haemolytic activity (Grant *et al*, 1997). A *C. jejuni* mutant lacking-*pldA* was observed to be impaired in its colonisation ability in the chicken caecum (Ziprin *et al*, 2001). The PldA protein does not appear to be secreted as *C. jejuni* can shed large numbers of OM-derived vesicles (Logan & Trust, 1982). Therefore, it is likely that haemolysin PldA and other OM-associated toxins may be shed from the cell by the process of vesicle shedding, which is similar to the pore-forming cytotoxin ClyA in *E. coli* (Wai *et al*, 2003).

1.9 *C. jejuni* Protein Secretions

To overcome the two lipidaceous barriers and allow some proteins to get to their extracellular target locations, Gram-negative bacteria have employed several secretion systems, which include types I-VI and the Chaperone/Usher pathway (Scott-Tucher & Henderson, 2009). Many of these systems are composed of a complex number of macromolecules (Scott-Tucher & Henderson, 2009).

The secretion mechanisms of *Campylobacter* are relative poorly understood compared to other bacterial pathogens. Both Sec-dependent secretion system and the Sec-independent twin-arginine translocation (Tat) export pathways have been identified from genome sequencing of *Campylobacter* (Fouts *et al,* 2005; Parkhill *et al,* 2000). In addition, genes for the signal recognition particle variant of the Sec pathway have also been revealed from the *C. jejuni* genome (Parkhill *et al*, 2000). The Sec system is generally required for periplasmic and outer membrane protein secretion in other Gram-negative organisms (Oldfield & Wooldridge, 2009). Four putative Tat components and 11 putative Tat substrates have been identified from *Campylobacter* genome analysis, which include an unusual alkaline phosphatase protein ($PhoA^{Cj}$) and the nitrate reductase protein NapA (Oldfield & Wooldridge, 2009). Inactivation of *tatC* results in the abolishment of protein $PhoA^{Cj}$ and NapA (van Mourik *et al*, 2008). No type I, III or type IV secretion systems encoding genes have been identified from the *C. jejuni* NCTC 11168 genome (Fouts *et al*, 2005). However, T4SS has been discovered from the *C. jejuni* strain 81-176 and pVir containing strains (Oldfield & Wooldridge, 2009).

1.9.1 Autotransporter Proteins

Autotransporter proteins are secreted proteins that direct their own secretion to the cell surface or extracellular location (Henderson *et al*, 2004). They belong to the type V secretion

system (T5SS) (Scott-Tucher & Henderson, 2009). Even sharing a common code of secretion, autotransporter proteins have highly diverse N-terminal functional domains that are often involved in a range of pathogenic processes (Henderson *et al*, 2004). The pathogenic mechanisms autotransporter protein are involved in include adhesion, toxigenicity and intracellular spread (Henderson *et al*, 2004). Two highly similar autotransporter protein related genes, *capA* and *capB,* have been identified from the *C. jejuni* NCTC 11168 genome (Ashgar *et al*, 2007).

CapA (discussed in Section 1.7.1) and CapB possess characteristic molecular features of autotransporter proteins, which include an N-terminal signal peptide, relatively low cysteine content, a β-sheet rich C-terminal domain and a C-terminal autotransporter protein motif (Y/V/I/F/W)-X-(F/W) (Oldfield & Wooldridge, 2009). It has been confirmed to be an outer membrane protein found on the cell surface (Oldfield & Wooldridge, 2009). However, unlike other autotransporter proteins, CapA is not released into the extracellular environment (Oldfield & Wooldridge, 2009). CapA has been identified as a lipoprotein, due to the reduced amount of CapA in the outer membrane fraction of *C. jejuni* cells grown in the present of globomysin, a specific lipoprotein signal peptidase II inhibitor (Dev *et al*, 1985). It is also an adhesin (discussed in Section 1.7.1). There is no evidence of expression of CapB, or transcription of the *capB* locus *in vitro*, or it may only be expressed under certain unknown conditions (Oldfield & Wooldridge, 2009).

1.9.2 Flagella Exporting Related Secretion

The *C. jejuni* CiaB protein shares similarity with other invasion-related proteins, such as *Salmonella* SipB (Kaniga *et al*, 1995) and *Yersinia* YopB (Hakansson *et al*, 1996). CiaB also lacks an identifiable signal sequence (Konkel *et al*, 1999). Based on the evidence as above, this initially led to suggestions that Cia proteins are secreted via a type III secretion system (T3SS) (Oldfield & Wooldridge, 2009). However, analysis of the *C. jejuni* genome suggests that the only genes with significant similarity to those encoding T3SSs are those encoding

the flagellar export apparatus (Oldfield & Wooldridge, 2009). No known bacterial system has a dual role as a flagellum and as a portal for the secretion of proteins that are unrelated to the primary function of the flagellum (Oldfield & Wooldridge, 2009). This makes Cia secretion so unique as it has been shown to be dependent on the flagella apparatus in *C. jejuni* (Konkel *et al*, 2004; Song *et al*, 2004). Mutational experiments show that secretion of the Cia proteins need a functional flagellar basal body and hook and at least one of the filament proteins, FlaA or FlaB (Konkel *et al*, 2004).

Another flagella exporting related protein is FlaC, which has sequence identity with the N- and C-terminal regions of proteins FlaA and FlaB (Song *et al*, 2004). It is not required for the flagellum formation or motility, but it is secreted via the flagellum, as mutations in the flagellar basal rod gene *flgF* and hook gene *flgE* abolishes the FlaC secretion (Song *et al*, 2004). The FlaC protein seems to be involved in host cell invasion (discussed in Section1.7.3). The small acidic protein FspA is also secreted via the flagella export system (Poly *et al*, 2007). Two variants of this protein are present, FspA1 and FspA2. FspA2 has been identified to rapidly induce apoptosis in INT407 cells, and thus likely to play a role in pathogenesis (Poly *et al*, 2007).

Proteins such as CiaB and FspA are not secreted via typical secretion systems (secreted without any apparent signal peptide or other signal governing their secretion) are often termed non-classically secreted proteins (NCSPs) (Bendtsen & Wooldridge, 2009). Proteins secreted via those alternative routes are likely involved in pathogenesis (Bendtsen & Wooldridge, 2009).

1.9.3 Type II-like Secretion System

As mentioned in Section 1.5, natural transformation in *C. jejuni* requires homologues of proteins that are involved in type II protein secretion in other bacteria (Wiesner *et al*, 2003). T2SSs are involved in proteins secreted across the outer membrane and targeted delivery of

a variety of molecules including toxins, proteases, cellulases and lipases (Oldfield & Wooldridge, 2009). *In silico* analysis and transposon library screening identified genes that when mutated, caused transformation defects with 1000 times lower levels compared to the wide types (Wiesner *et al*, 2003). Five out of the 11 proteins identified in this study are similar to proteins that are also secreted by T2SSs of other bacteria (Wiesner *et al*, 2003). CtsD shares similarity to the outer membrane secretins of T2SS (a T2SS D homologue), CtsE to cytoplasmic ATPases (a T2SS E homologue), CtsF to inner membrane-spanning proteins (a T2SS F homologue), CtsG to major pseudopilins (a T2SS G homologue) and CtsT to minor pseudopilins (a T2SS H, I, J or K homologue) (Oldfield & Wooldridge, 2009). With the usage of the Protein Basic Local Alignment Search Tool (BLASTP) algorithm, a putative pre-pilin peptidase (a T2SS O homologue) was also identified (Wiesner *et al*, 2003). To be a fully functional type II secretion apparatus, it requires 12 core proteins (T2SS CDEFGHIJKLMO), with some species requiring additional proteins (Oldfield & Wooldridge, 2009). The incomplete nature of the T2SS-like system in *C. jejuni* reveals that these proteins may not constitute a functioning protein secretion system (Oldfield & Wooldridge, 2009).

1.9.4 Type IV (pVir-encoded) Secretion System

Plasmid pVir was first discovered in *C. jejuni* 81-176 in 2000 (Bacon *et al*, 2000). It is a 35-kb plasmid containing 54 predicted opening reading frames (ORFs) (Bacon *et al*, 2000), eight of which have similarity to a T4SS in the ruminant commensal *Wolinella succinogenes* (Baar *et al*, 2003). T4SSs are commonly involved in horizontal DNA transfer, in DNA uptake from or release into the extracellular milieu, in toxin secretion and in the injection of bacterial products into the target cell cytosol (Backert & Meyer, 2006). Seven type IV-like genes on pVir, gene *cjp1, cjp2, cjp5, cjp6, cjp31, cjp53* and *cjp54*, have been proposed to encode proteins that form a secretion channel (Bacon *et al*, 2002). Protein Cjp1, Cjp2 and Cjp3 homologues have been found in other bacterial systems as pore-forming proteins (Oldfield & Wooldridge, 2009). Homologues of Cjp5, Cjp6 and Cjp53 have been shown to be an ATPase (Backert & Meyer, 2006). Gene *cjp54* encodes a 5-kDa protein that probably stabilises the

complex of type IV transmembrane channels (Bacon *et al*, 2002). Gene *cjp31* encodes a putative protein with identity to TrbM of plasmid RP4, which is involved in the conjugal transfer of this plasmid (Oldfield & Wooldridge, 2009). Mutants lacking-Cjp2, Cjp3 or Cjp5 showed reduced invasion abilities towards INT407 cell monolayers (Bacon *et al*, 2000; Bacon *et al*, 2002). However, mutants without Cjp1, Cjp6 or Cjp53 displayed wild-type levels of invasion (Bacon *et al*, 2002). Plasmid pVir contributes to the invasion ability of *C. jejuni* strain 81-176 towards INT 407 cells *in vitro* (Bacon *et al*, 2002). However, introduction of pVir to a pVir-absent strain NCTC 11168 did not increase its ability for invasion (Bacon *et al*, 2002). Furthermore, only a limited number of *C. jejuni* clinical isolates contain pVir (Louwen *et al*, 2006; Schmidt-Ott *et al*, 2005; Tracz *et al*, 2005), which indicates that pVir may play a role in pathogenesis, including invasion, but only of a subset of *C. jejuni* strains (Oldfield & Wooldridge, 2009).

Since some of the pVir T4SS proteins share similarity to *Helicobacter pylori* proteins that are involved in natural transformation, the transformation efficiencies of some of the Cjp mutants have also been investigated. Mutations in *cjp1, cjp5* or *cjp6* showed no difference in transformation levels compared to the wild-type strains (Oldfield & Wooldridge, 2009). However, mutants lacking *cjp3* exhibited a modest defect in transformation efficiency (Bacon *et al*, 2000; Wiesner *et al*, 2003).

1.10 Control Strategies for *Campylobacter*

Reducing the level of *Campylobacter* in poultry will limit the number of campylobacteriosis cases. There are several strategies that have been studied. Firstly, high hygiene levels during poultry breeding and prevention of chicken carcass contamination has been considered as the most efficient method (Katarzyna *et al*, 2009). Nevertheless, it is difficult to introduce this strategy globally due to the relatively high cost related to the implementation of various interventions (Katarzyna *et al*, 2009). The method of upgrading biosecurity at the farm level and the hygiene practices in processing poultry may also vary between countries (Katarzyna *et al*, 2009).

Alternatively, genus/species-specific bacteriophage treatment to chickens before butchering or directly onto the chicken carcasses is also under consideration (Atterbury *et al*, 2003; El-Shibiny *et al*, 2005). However, there are many drawbacks to this method, such as the acquisition of resistance to bacteriophage control, and also campylobacter and bacteriophage genetic microbial diversity via recombination events (Scott *et al*, 2007).

The most efficient strategy for decreasing campylobacteriosis is still immunoprophylactic methods (discussed in the next Section). Despite the high incidence of campylobacteriosis in industrialised countries, effective strategies to control *Campylobacter* contamination and to prevent campylobacteriosis are still hindered, as current knowledge about the pathogenic mechanisms, virulence and pathogen-host interaction mechanisms of *Campylobacter* is still limited.

1.11 Campylobacter Vaccines

The most efficient strategy to prevent *Campylobacter* associated disease would be by implementing immunoprophylactic methods, which are protective vaccinations for humans and/or chickens (Jagusztyn-Krynicka *et al*, 2009). Many research groups have investigated an anti-*Campylobacter* human vaccine. For instance, the University of Maryland and the USA Naval Medical Research Centre showed that infection-induced immunity furnishes complete protection against the illness, but does not always prevent the colonisation (Tribble *et al*, 2008a). In addition, the protection was only lasted for 1-2 months (Tribble *et al*, 2008a). In industrialised countries, the anti-*Campylobacter* vaccine for humans will be reserved for persons from high-risk groups, such as travellers to regions where the disease is endemic and immunosuppressed patients (Jagusztyn-Krynicka *et al*, 2009). The introduction of anti-*Campylobacter* vaccines for children in developing countries is still under debate, as several important issues still need to be clarified, which include the necessity of immunisation during the first 6 months of life, the necessity of repeated booster vaccinations and the development of an efficient method of immunization (Tribble *et al*, 2008a).

Anti-*Campylobacter* vaccine studies have mainly analysed the efficiency of vaccines containing killed bacteria and also subunit vaccines of different types (Jagusztyn-Krynicka *et al*, 2009). In recent years, significant progress has been made in anti-*Salmonella* or anti-*Shigella* live-attenuated vaccines (Garmory *et al*, 2002; Levine *et al*, 2007; Phalipon *et al*, 2008; Venkatesan & Ranallo, 2006). However, an attenuated *Campylobacter* strain that transiently colonises the hosts for long enough to induce a protective immune response has not been identified (Jagusztyn-Krynicka *et al*, 2009). In the development of human anti-*Campylobacter* live-attenuated vaccines, eliminating the onset of GBS is still under investigation (Jagusztyn-Krynicka *et al*, 2009). In addition, the naturally transformable property of *Campylobacter* spp. makes vaccine design more complicated (Jagusztyn-Krynicka *et al*, 2009). A *Campylobacter recA* mutant was constructed to prevent genetic

recombination, but it was never used for vaccination (Guerry *et al*, 1994). A selection of tested vaccines are listed in the Table 1.6, which includes different vaccine types and delivery methods. As noted there, several types of chicken anti-*Campylobacter* vaccines have also been created and investigated. As designing a successful vaccine depends on both the delivery mode and the antigen selected, further research is needed to work towards a commercial vaccine.

Table 1.6: List of tested anti-*Campylobacter* vaccines (reproduced from Jagusztyn-Krynicka, 2009).

Type of vaccine	Animal	Route of vaccination/vaccination schedule	Challenge	Effect	Ref.
CWC vaccines					
C. jejuni $_{81\text{-}176}$ (formalin-inactivated)	Ferrets	Orally, two or four does with/without LTR192G	Orally, homologous or heterologous strain (10^9-10^{10} CFU)	40-89% of protection, depending on the vaccination regimen	(Burr *et al*, 2005)
Campyvax® (cells prepared according to the Nutriment Signal Technology)-Antex/NMRC	Human volunteers	Orally, two or four doses	Phase II cinical trial (2002), Phase III clinical trial (results not available)	Immunogenic	(Tribble *et al*, 2008a)
Recombinant protein purified from Escherichia coli cells					
Fused MBP-FlaA (*C. jejuni* VC167)	BALB/c mice	Intranasally, two doses 50 µg MBP-FlaA with LTR192G	Intranasally, *C. jejuni* 81-176 (10^9 CFU)	84% protection efficacy against colonisation	(Lee *et al*, 1999)
			Orally, *C. jejuni* 81-176 (10^8-10^9 CFU)	71-100% protective efficacy against colonisation, depending on the challenge does	

CFU: Colony-forming unit; $CPS_{81\text{-}176}$ -CRM_{197} : Capsular polysaccharide of *Campylobacter jejuni* 81-176 strain conjugated to diphtheria toxin mutant CRM_{197} ; CRM: Cross-reacting molecule; CWC: *Campylobacter* whole-cell; MBP: Maltose-binding protein; MSP: Mouse-specific pathogen-free; NMRC: Naval Medical Research Center.

Table 1.6: List of tested anti-*Campylobacter* vaccines (reproduced from Jagusztyn-Krynicka, 2009) (cont.).

Type of vaccine	Animal	Route of vaccination/vaccination schedule	Challenge	Effect	Ref.
Recombinant protein purified from Escherichia coli cells					
ACE961 – branched-chain amino acid ABC transport system periplasmic-binding protein (*C. jejuni* ML53)	Mice	Subcutaneously, three doses with alum	Orally, *C. jejuni* ML1/ML53 (10^8 CFU)	Reduction of colonisation	(Prokhorova *et al*, 2006)
ACE1569 – putative periplasmic protein (*C. jejuni* ML53)	Mice	Subcutaneously, three doses with alum	Orally, *C. jejuni* ML1/ML53 (10^8 CFU)	Reduction of colonisation	(Prokhorova *et al*, 2006)
Flagellum-secreted proteins					
FlaC (*C. jejuni* 81-176)	BALB/c mice	Intranasally with/without LTR192G; three doses delivered at 2-week intervals	Intranasally, *C. jejuni* 81-176 or CG8486 (10^9 CFU)	18% protection against disease from *C. jejuni* 81-176	(Baqar *et al*, 2008)
FspA1 (*C. jejuni* 81-176)	BALB/c mice	Intranasally with/without LTR192G; three doses delivered at 2-week intervals	Intranasally, *C. jejuni* 81-176 or CG8486 (10^9 CFU)	Protection (with adjuvant) against disease: homologous challenge: 63.8%; heterologous challenge: 44.8%	(Baqar *et al*, 2008)

CFU: Colony-forming unit; $CPS_{81\text{-}176}$ -CRM_{197} : Capsular polysaccharide of *Campylobacter jejuni* 81-176 strain conjugated to diphtheria toxin mutant CRM_{197} ; CRM: Cross-reacting molecule; CWC: *Campylobacter* whole-cell; MBP: Maltose-binding protein; MSP: Mouse-specific pathogen-free; NMRC: Naval Medical Research Center.

Table 1.6: List of tested anti-*Campylobacter* vaccines (reproduced from Jagusztyn-Krynicka, 2009) (cont.).

Type of vaccine	Animal	Route of vaccination/vaccination schedule	Challenge	Effect	Ref.
Flagellum-secreted proteins					
FspA2 (*C. jejuni* CG8486)	BALB/c mice	Intranasally with/without LTR192G; three doses delivered at 2-week intervals	Intranasally, *C. jejuni* 81-176 or CG8484 (10^9 CFU)	47.2% protection (with adjuvant) against disease: homologous challenge	(Baqar *et al*, 2008)
Conjugated capsule polysaccharide vaccines					
$CPS_{81\text{-}176}$ -CRM_{197}	BALB/c mice	Subcutaneously, 5 or 25 µg of $CPS_{81\text{-}176}$ -CRM_{197}	Intranasally (3 X 10^9 CFU)	Immunogenic (IgM, IgA and IgG), significant dose-dependent reduction of illness – homologous strain challenge	(Monteiro *et al*, 2009)
$CPS_{81\text{-}176}$ - CRM_{197} adjuvant with alum	Aotus nancymae (nonhuman primates)	Subcutaneously, three doses (25 µg) at 6-week intervals	Intranasally (5 X 10^{11} CFU)	Dose-related serum IgG and IgM response, no increase in serum IgA response, protection against diarrhoea but not colonisation	(Monteiro *et al*, 2009)

CFU: Colony-forming unit; $CPS_{81\text{-}176}$ -CRM_{197} : Capsular polysaccharide of *Campylobacter jejuni* 81-176 strain conjugated to diphtheria toxin mutant CRM_{197} ; CRM: Cross-reacting molecule; CWC: *Campylobacter* whole-cell; MBP: Maltose-binding protein; MSP: Mouse-specific pathogen-free; NMRC: Naval Medical Research Center.

Table 1.6: List of tested anti-*Campylobacter* vaccines (reproduced from Jagusztyn-Krynicka, 2009) (cont.).

Type of vaccine	Animal	Route of vaccination/vaccination schedule	Challenge	Effect	Ref.
C. jejuni antigens delivered by attenuated Salmonella enterica sv. Typhimurium strains					
S. enterica sv.Typhimurium & Delta;*phoP/Q* peb1 protein expressed from three plasmids (pYA3342, pMEG-1399 and pMEG-1415)	BALB/c mice, MSP	Orally, two doses (10^8 CFU)	Orally, *C. jejuni* 81-176, *C. jejuni* MGN 4735	Induction of specific serum IgG, measured by western blot; no protection	(Sizemore *et al*, 2006)
S. enterica sv. Typhimurium χ3987 CjaA cloned into pYA3341	Chicken	Orally, two doses (10^8 CFU)	Orally, heterologous *Campylobacter* strains (10^8 CFU)	[proportional to]6logs reduction of colonisation	(Wyszynska *et al*, 2004)
S. enterica sv. Typhimurium χ3987 CjaD cloned into pYA3341	Chicken	Orally, two doses (10^8 CFU)	Orally, heterologous *Campylobacter* strains (10^8 CFU)	Induction of specific intestinal sIgA and serum IgG; protection – not tested	(Jagusztyn-Krynicka *et al.,* Unpublished data)

CFU: Colony-forming unit; $CPS_{81\text{-}176}$ -CRM_{197} : Capsular polysaccharide of *Campylobacter jejuni* 81-176 strain conjugated to diphtheria toxin mutant CRM_{197} ; CRM: Cross-reacting molecule; CWC: *Campylobacter* whole-cell; MBP: Maltose-binding protein; MSP: Mouse-specific pathogen-free; NMRC: Naval Medical Research Center.

1.12 Aims of Project

Despite the high incidence of *C. jejuni* and many years of research, the virulence factors of *C. jejuni* are still poorly understood compared with other enteric bacteria. Although the identification of the virulence factors needs various chemical and biological experiments, the approach of purely lab-based experiments is time-consuming, labour-intensive, and, requires used of expensive reagents. As the genome sequence of *Campylobacter* is known, bioinformatics methods can be used to narrow down the list of possible virulence factors, which may be exploited as vaccine candidates. In this work, it is proposed that proteins that aid *Campylobacter* to evade the chicken immune system are either secreted, or in the bacterial outer membrane, so as to directly interact with host components. In this study, we analysed 1623 predicted proteins based on their sequences through various bioinformatics analysis methods, in order to identify the number of *C. jejuni* proteins predicted to be located in the outer membrane or extracellularly. These may be involved in the virulence mechanisms of the pathogen.

Most of the surface-exposed proteins are secreted with signal peptides, which localise them into the outer membrane or extracellular space. However, there is also a subset of proteins locates at these positions without a signal peptide. They are the proteins so called NCSPs. It is believed that these proteins secreted via alternative routes are involved in pathogenesis. The aims of this study are to select, express and purify some of the NCSPs encoded by the *C. jejuni* NCTC 11168 genome. The recombinant protein was assayed for its function.

Results from this study will help to improve our understanding of pathogenic mechanisms, more specifically, the virulence factors involved in *C. jejuni* pathogenicity. A starting point for identifying potential virulence factors is to identify proteins that are secreted from campylobacter, and therefore can interact with host molecules/cells. However, many of these proteins are of unknown structure and function. This thesis describes the prediction and

modelling of a NCSP that we have demonstrated to cause chicken macrophage cell apoptosis. By modelling this and other NCSPs, the structures of potentially antigenic and/or functional regions may be examined, and lead to design of vaccines aimed at immunising poultry against *Campylobacter* colonisation. A vaccine would dramatically reduce the contamination of poultry. Consequentially it will help to reduce the incidence of campylobacteriosis in human populations and therefore ultimately reduce the cost of public health care service.

CHAPTER 2. BIOINFORMATICS ANALYSIS OF THE *C. JEJUNI* SECRETOME

2.1 Introduction

The number of sequences entering into databanks has been rapidly increasing. For instance, the number of total protein sequences entries in Swiss-Prot was only 3,939 in 1986. A recent search on 9 July 2014 showed that the number has jumped to 546,000, meaning that the number of the entries now is more than 100 times the number in 1986. With the explosion of protein sequences entering into databanks, it is a fact that experimentally testing every single protein is both too time-consuming and costly. Therefore, bioinformatics tools would be helpful as a fast and effective way of identifying a newly found / hypothetical protein for its possible function / subcellular location.

C. jejuni has the densest bacterial genome analysed to date, with 94.3% of the genome encoding proteins (Parkhill *et al*, 2000). In 2000, the complete genome sequence of *C. jejuni* subsp. *jejuni* NCTC 11168 was completed (in this study, where *C. jejuni* is mentioned we refer to *C. jejuni* subsp. *jejuni*). The entire genome contains 1,641,481 base pairs (bp) with a low G+C content (30.6%), and 1,654 CDS (Parkhill *et al*, 2000). In 2007, the genome sequence from *C. jejuni* NTCT 11168 was re-annotated and re-analysed (Gundogdu *et al*, 2007). The number of predicted CDS was reduced to 1643, and 18.2% of CDS had their product functions updated (Gundogdu *et al*, 2007). As of February 2012, there were 1623 *C. jejuni* NCTC 11168 protein sequences accessible from NCBI (Accession: PRJNA57587, ID: 57587).

Elucidating *Campylobacter* proteins that have the potential to interact with the chicken immune system (i.e. secreted proteins) may lead to new approaches for eliminating *Campylobacter* from chickens and hence reduce the incidence of human infection. A range of bioinformatics techniques have been employed to identify secreted and surface-exposed proteins, which may have propensities for direct interactions with the chicken immune system. Of the approximately 1600 proteins encoded by the *C. jejuni* NCTC 11168 genome,

up to 400 are predicted to be secreted from the bacterium, or inserted into the outer membrane, as identified using a set of bioinformatics tools (Figure 2.1). This includes proteins predicted to contain a signal peptide, and a subset of proteins predicted to be non-classically secreted. Secreted proteins are crucial for bacterial pathogenesis, particularly in the delivery of pathogenic and symbiotic bacteria into their hosts. Therefore, identification of bacterial secreted proteins plays an important role for the study of diseases, drug design and development of vaccines (Yu *et al*, 2010). These predicted proteins may perform a role that is critical to *Campylobacter*.

These putative secreted proteins were first analysed using Gneg-PLoc and Gneg-mPLoc for their locations. Those proteins predicted as membrane proteins were further analysed for the presence of TMH and β-barrels (BB) using TMHMM and PRED-TMBB respectively. Enzyme/protease prediction has also been performed on these proteins for possible function prediction. Finally, VirulentPred was employed to screen the putative secreted proteins for virulence factors. The final result indicates there are 9 putative hypothetical virulent classically secreted proteins (CSPs) and 40 putative hypothetical virulent NCSPs. Among them, there were a few of proteins with less than 50 AAs or located intercellularly, which left a subset of 28 putative virulent extracellular NCSPs on the top of the list to be further analysed. A brief description of each web server used together with the website address is listed in Table 2.1.

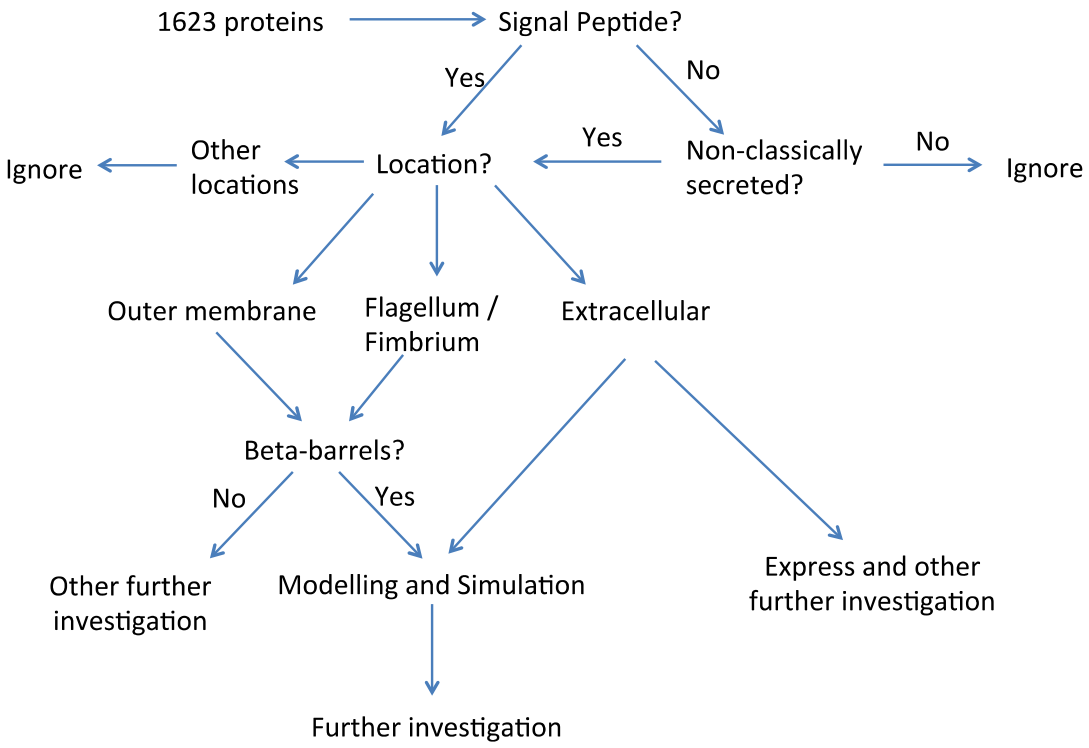

Figure 2.1: Flow chart of *Campylobacter jejuni* NCTC 11168 secretome analysis

Table 2.1: List of the webservers used in this study

No.	Name	Website address	Target
1	SignalP 3.0	http://www.cbs.dtu.dk/services/SignalP-3.0/	Protein signal peptide
2	SignalP 4.0	http://www.cbs.dtu.dk/services/SignalP/	Protein signal peptide
3	Signal-CF	http://www.csbio.sjtu.edu.cn/bioinf/Signal-CF/	Protein signal peptide
4	Signal-3L	http://www.csbio.sjtu.edu.cn/bioinf/Signal-3L/	Protein signal peptide
5	SecretomeP 2.0	http://www.cbs.dtu.dk/services/SecretomeP/	NCSPs
6	Gneg-Ploc	http://www.csbio.sjtu.edu.cn/bioinf/Gneg/	Protein subcellular localisation
7	Gneg-mPloc	http://www.csbio.sjtu.edu.cn/bioinf/Gneg-multi/	Protein subcellular localisations
8	TMHMM 2.0	http://www.cbs.dtu.dk/services/TMHMM/	Protein TMH
9	PRED-TMBB	http://biophysics.biol.uoa.gr/PRED-TMBB/	OMP beta-strand
10	MemType-2L	http://www.csbio.sjtu.edu.cn/bioinf/MemType/	Membrane protein type
11	EzyPred	http://www.csbio.sjtu.edu.cn/bioinf/EzyPred/	Enzyme functional class
12	ProtIdent	http://www.csbio.sjtu.edu.cn/bioinf/Protease/	Protease type
13	VirulentPred	http://203.92.44.117/virulent/	Virulence protein

NCSPs: non-classically secreted proteins; TMH: transmembrane helices; OMP: outer-membrane protein

2.2 Materials and Methods

The *C. jejuni* NCTC 11168 protein sequences were retrieved from the Sanger website in the FASTA format.

2.2.1 Classically Secreted Protein Prediction

To accomplish virulence mechanisms, bacteria secrete proteins into their host environment, some of which may act to subvert or down-regulate the expanding immune response (Coombes *et al*, 2004). Extracellular secretion of proteins is classified as either classically secreted or non-classically secreted based on the secretion mechanism.

In bacteria, the classical tripartite structured sec signal peptide governs most of the targeting of the secretion pathway. Besides Sec-dependent secretion, there is also a group of Sec-independent secretion pathways, such as twin-arginine translocation (Tat) secretion, which with a twin-arginine consensus motif is located within the signal peptide itself (Bendtsen *et al*, 2005). Both Sec- and Tat-dependent secretion only translocate protein across the inner membrane of the Gram-negative bacteria, while the N-terminal signal peptide plays an essential role in trans-outer membrane secretory systems as the tag signaling secretion.

CSPs are synthesized at the ribosome and transported to their site of function as directed by the targeting signals. Although many different classes of targeting signals are present, one of the commonly occurring signals is formed by short, transient peptides known as signal peptides. Signal peptides are present in both prokaryotic and eukaryotic cells and are usually found at the amino terminus of proteins destined for secretion. Signal peptides are critical for classical protein secretion and are made up of 15-40 amino acids. They are characterised by three distinct domains, a positively charged amino terminal “n” region, a central hydrophobic

"h" region, and a cleavage site of a more polar carboxy terminal "c" region which is cleaved by signal peptidases during translocation across the membrane.

In this study, five computational methods have been used to predict CSPs from *C. jejuni* NCTC 11168: SignalP 3.0 HMM, SignalP 3.0 NN (Bendtsen *et al*, 2004), SignalP 4.0 (Petersen *et al*, 2011), Signal-CF (Chou & Shen, 2007b) and Signal-3L (Shen & Chou, 2007b).

SignalP is one of the most commonly used programs which utilises artificially trained neural networks (NN) to predict N-terminal peptides. Artificial NN is inspired by the sophisticated functionality of human brains where numerous of interconnected neurons process information in parallel (Wang, 2003). An artificial NN consists of an input layer of neurons (or nodes), couple of hidden layers of neurons, and a final layer of output neurons (Wang, 2003). The formula below shows a typical architecture, where the output, h_i, of neuron i in the hidden layer is,

$$h_i = \sigma\left(\sum_{j=1}^{N} V_{ij} x_j + T_i^{hid} \right)$$

where $\sigma(\ )$ is called activation (or transfer) function, N the number of input neurons, V_{ij} the weights, x_j inputs to the input neurons, and T_i^{hid} the threshold terms of the hidden neurons (Wang, 2003). Artificial NN have been used for a great range of biological sequence analysis. In SignalP 1.0, a combined NN approach has been developed to recognise the signal peptides and their cleavage sites, which includes one network to recognize the cleavage site and another to differentiate the signal peptides and non-signal peptides (Nielsen *et al.* 1997). In version 2.0, a Hidden Markov Model (HMM) component was incorporated in its prediction strategy (Nielsen & Krogh, 1998). HMM is a popular statistical tool for modelling generative sequences (Blunsom, 2004). These sequences can be characterised by an underlying process that generating an observable sequence (Blunsom, 2004). HMM in SignalP 2.0 contains submodels for the N-terminal part, the hydrophobic

region, and the cleavage site region (Nielsen & Krogh, 1998). In the version 3.0, both NN and HMM algorithms have been updated by the motivation of the idea that the cleavage site position and the amino acid composition of the signal peptide are correlated (Bendtsen *et al*, 2004). However, SignalP 3.0 is limited in its ability to distinguish signal peptides from N-terminal TMH. In 2011, SignalP 4.0 was introduced to overcome this problem. Signal-CF and Signal-3L are similarly based on the strategy used in SignalP 3.0 and SignalP 4.0. However, Signal-CF was reported to give a better performance on signal peptide cleavage site identification and non-secreted protein identification (Chou & Shen, 2007b). It is also recognised as one of the best servers to predict long signal peptides (Chou & Shen, 2007b). Signal-3L comes with one more layer compared to Signal-CF. This 3rd-layer is used to determine the unique cleavage site through a global sequence alignment operation (Chou & Shen, 2007b).

2.2.2 Non-classically Secreted Protein Analysis

NCSPs are proteins secreted from the cytoplasm but without a classic signal peptide, which are also called leaderless secretion or the non-conventional secretory pathway. The mechanism behind this type of secretion is still unknown. For a long time, it was believed that an N-terminal signal peptide was strictly required for exporting proteins to the extracellular space until non-classical secretion was identified in eukaryotes about 25 years ago. The first published bacterial NCSP was glutamine synthetase (GlnA) in *Mycobacterium tuberculosis (M. tuberculosis)* (Harth & Horwitz, 1997). Furthermore, it is found that NCSPs such as GlnA and superoxide dismutase are secreted in pathogenic *M. tuberculosis,* but only present in the cytoplasm of the non-pathogenic mycobacterium *M. smegmatis* (Harth & Horwitz, 1999a) (Harth & Horwitz, 1999b). Experiments of *SecA2* gene deletion in *M. tuberculosis,* which is required for superoxide dismutase secretion, show the abolishment of *M. tuberculosis* virulence in mice. This suggests the new secretory pathway plays a role in the export of bacteria virulence factors (Braunstein *et al*, 2003). It is also believed that NCSPs often seem

to have a cytoplasmic function as well as an extracellular functional role (Bendtsen *et al*, 2005), which makes them more intriguing to scientists.

No signal or motif characteristic has been found in any of the majority of NCSPs. However, properties such as amino acid composition, secondary structure and disordered regions make NCSPs different from cellular proteins (Bendtsen *et al*, 2005). SecretomeP 2.0 developed artificial neural networks based on these properties for identification of NCSPs. For Gram–negative bacteria proteins, the determining score is the 'SecP score', where a value above 0.5 indicates possible secretion. NCSPs should obtain a ‘SecP score’ exceeding the normal threshold, but at the same time be predicted without a signal peptide (Bendtsen *et al*, 2005).

2.2.3 Protein Location Prediction

Determining the subcellular localisation of a protein can provide insights into how it functions and the pathways that are involved, as well as how and in what kind of cellular environments they interact with each other or other molecules (Chou & Shen, 2008a). Knowledge of the protein subcellular location can also highlight whether the protein could either provide a therapeutic target or act as a biomarker. Proteins with multiple locations or dynamic features of this kind are particularly interesting, because they may have some special biological functions (Chou & Shen, 2008a). For instance, the *E. coli* aspartate receptor, which functions in bacterial chemotaxis, is also a maltose-binding protein (MBP) receptor (Jeffery, 1999).It has different but overlapping binding sites for aspartate and MBP (Mowbray & Koshland, 1990; Wolff & Parkinson, 1988). Another example is bacterial Ftsh protein plays a role in assisting in the transport of proteins into and across membranes, and it is also an ATP-dependent metalloprotease (Jeffery, 1999). In our study, we try to predict the proteins that are totally or at one stage exposed to the host immune system.

In this study, Gneg-PLoc and Gneg-mPLoc have been chosen to predict the locations of the putative secreted proteins obtained after classical and non-classical secretion analysis. Both predictors cover eight subcellular locations of Gram-negative bacteria proteins (Figure 2.2), which are cytoplasm, extracellular space, fimbrium, flagellum, inner membrane, nucleoid, outer membrane and periplasm (Chou & Shen, 2006a). Gneg-PLoc predicts the single location of each protein, while Gneg-mPLoc is able to predict the multiple possible locations of proteins.

2.2.4 Membrane Protein Prediction

It is believed that each cell is highly organized with many functional units or organelles, and most of these units are 'enveloped' by one or more cell membranes, which are the basis for many biological functions (Chou & Shen, 2007a). Although the main content of the cell membrane is the lipid bilayer, most of the specific functions of the membrane are actually performed by the membrane proteins (Chou & Shen, 2007a). The main functions of membrane proteins include (1) transporting molecules into and out of cells by such methods as ion pumps, channel proteins and carrier proteins; (2) passing various chemical messages such as nerve impulses and hormone activity between cells; (3) attachment to parts of the cytoskeleton in order to provide shape (Chou & Shen, 2007a) and so on. It is estimated that 20-30% of all genes in most genomes encode membrane proteins (Krogh *et al*, 2001).

Membrane proteins are of different types, and the function of each membrane protein is closely correlated with the type it belongs to (Chou & Shen, 2007a). For instance, a transmembrane protein can function on both sides of the membrane or transport molecules across it, while a protein that functions on only one side of the lipid bilayer is often associated with either the lipid monolayer or a protein domain on that side (Chou & Shen, 2007a).

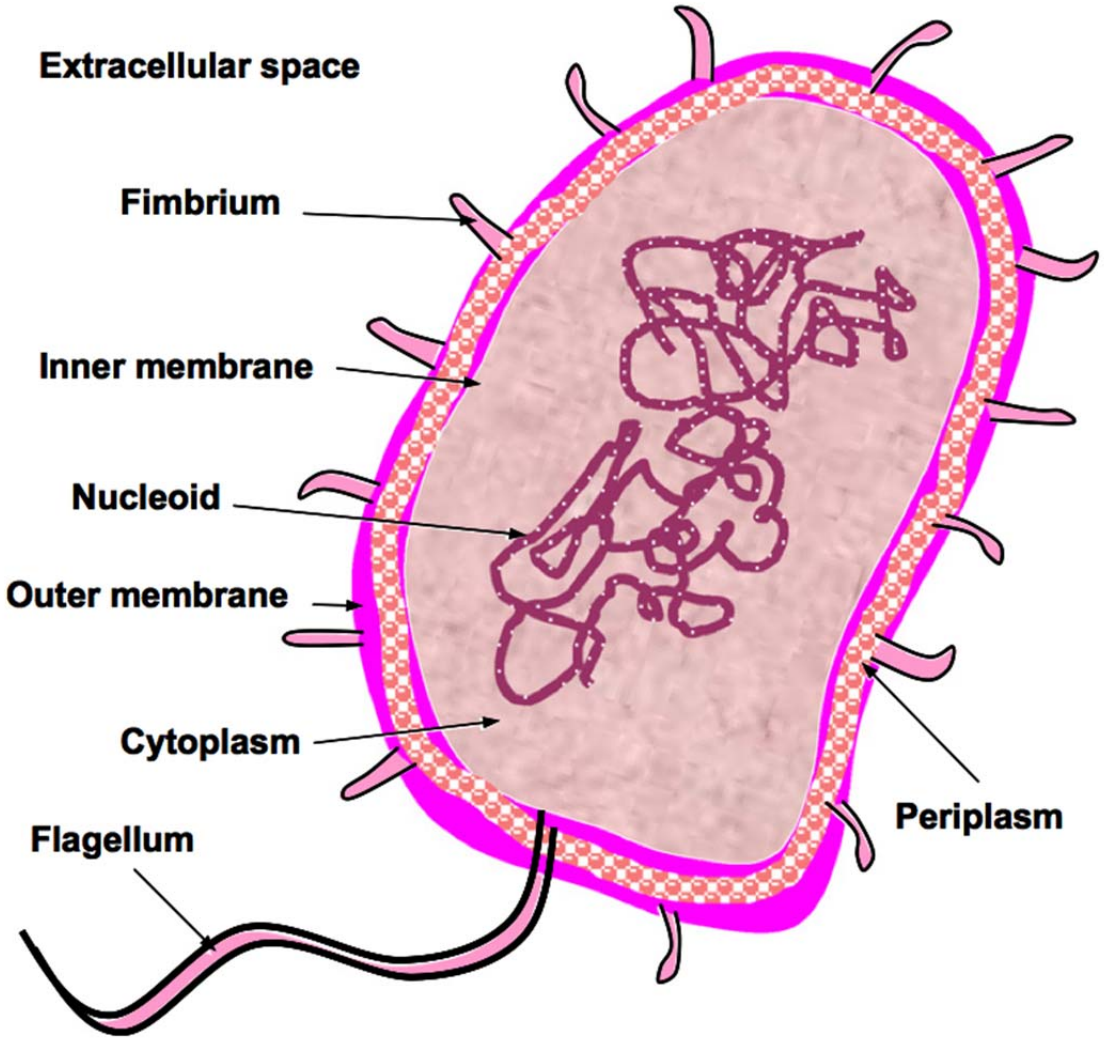

Figure 2.2: Schematic illustration of the subcellular locations of Gram-negative bacterial proteins (reproduced from Chou & Shen, 2006a).

A trans-membrane protein can be an outer membrane auto-transporter, a pore-forming toxin (PFT), an immune receptor, *etc*. Therefore, information about membrane protein types would offer important clues toward identifying the function of an uncharacterised membrane protein (Chou & Shen, 2007a). The knowledge of the type a membrane protein belongs to can provide insight into its mode of motion, which is helpful for studying its biological process at the cellular level (Chou & Shen, 2007a).

Integral membrane proteins can be divided into two distinct structural classes, the α-helical membrane proteins and the β-barrel membrane proteins (Bagos *et al*, 2004). The TMH and BBs of the putative secreted *C. jejuni* NCTC 11168 proteins have been analysed using TMHMM 2.0 (Krogh *et al*, 2001; Sonnhammer *et al*, 1998) and PRED-TMBB (Bagos *et al*, 2004) respectively. TMHMM 2.0 uses HMM based algorithms (Bagos *et al*, 2004; Krogh *et al*, 2001). One of the advantages of an HMM is that HMM is able to model helix length by setting upper and lower limits for the length of a membrane helix (Krogh *et al*, 2001). It is very well suited for TMH prediction as it can incorporate hydrophobicity, charge bias and helix length (Durbin *et al.* 1998). PRED-TMBB is capable of predicting transmembrane β-strands of the Gram-negative bacteria OMPs (Bagos *et al*, 2004).

The membrane protein types were investigated by MemType-2L (Chou & Shen, 2007a). MemType-2L is a 2-layer predictor, featured by incorporating evolution information through Pseudo Position-Specific Score Matrix vectors and Optimized Evidence-Theoretic K-Nearest Neighbour classifiers (Chou & Shen, 2007a). The concept of Pseudo Position-Specific Score Matrix used in this method was adopted from (Chou, 2001; Chou, 2005), which as given by

$$\mathbf{p}^{\xi}_{Pse-PSSM} = \left[\mathrm{E}_1 \mathrm{E}_2 \cdots \mathrm{E}_{20} G_1^{\xi} G_2^{\xi} \cdots G_{20}^{\xi} \right]^T$$

to represent the protein P, where

$$G_j^{\xi} = \frac{1}{L-\xi} \sum_{i=1}^{L-\xi} \left[\mathrm{E}_{i \to j} - \mathrm{E}_{(i+\xi) \to j} \right]^2 \ (j = 1, 2, \cdots, 20; \xi < L)$$

The Optimized Evidence-Theoretic K Nearest Neighbour classifier was employed in MemType-2L to identify the membrane proteins and their types (Chou & Shen, 2007a), which is a powerful classification engine that enhances the success rates of protein subcellular location prediction (Chou & Shen, 2006b).

In MemType-2L, the 1st layer prediction engine is to identify a query protein as membrane or non-membrane protein. If the protein is predicted as membrane protein from the 1st layer prediction, the process is automatically continued with the 2nd-layer engine to further identify its membrane type. There are eight categories included in the 2nd-layer prediction (Figure 2.3): (1) type I transmembrane, (2) type II transmembrane, (3) type III transmembrane, (4) type IV transmembrane, (5) multipass transmembrane, (6) lipid-chain-anchored membrane, (7) GPI-anchored membrane, and (8) peripheral membrane (Chou & Shen, 2007a). The classification is an extension of that by von Heijne and Gavel (1988). In the literature, type III proteins have also been defined as 'type I without cleaved signal' or type Ib. Examples of single spanning membrane proteins are the LDL receptor (type I), the transferrin receptor (type II), cytochrome *p*450 (type III) and synaptobrevin (type IV) (Spiess, 1995).

2.2.5 Enzyme Prediction

The main function of enzymes is catalysing chemical reactions, which plays a vital role in the metabolic process. In this section, there were two servers used to predict if a protein is an enzyme or more particular, a protease. Firstly, webserver EzyPred was employed to classify enzymes into six main function classes (1) Oxidoreductase, (2) Transferase, (3) Hydrolase, (4) Lyase, (5) Isomerase, and (6) Ligase, and further 49 subclasses (Shen & Chou, 2007a). EzyPred, which operates by fusing the FunD approach and Pseudo Position-Specific Score Matrix approach, is a 3-layer predictor, as the 1st layer engine identifies a query protein as enzyme or non-enzyme; the 2nd layer prediction engine is for the main functional class, and the 3rd layer predicts the sub-functional class of the query protein (Shen & Chou, 2007a).

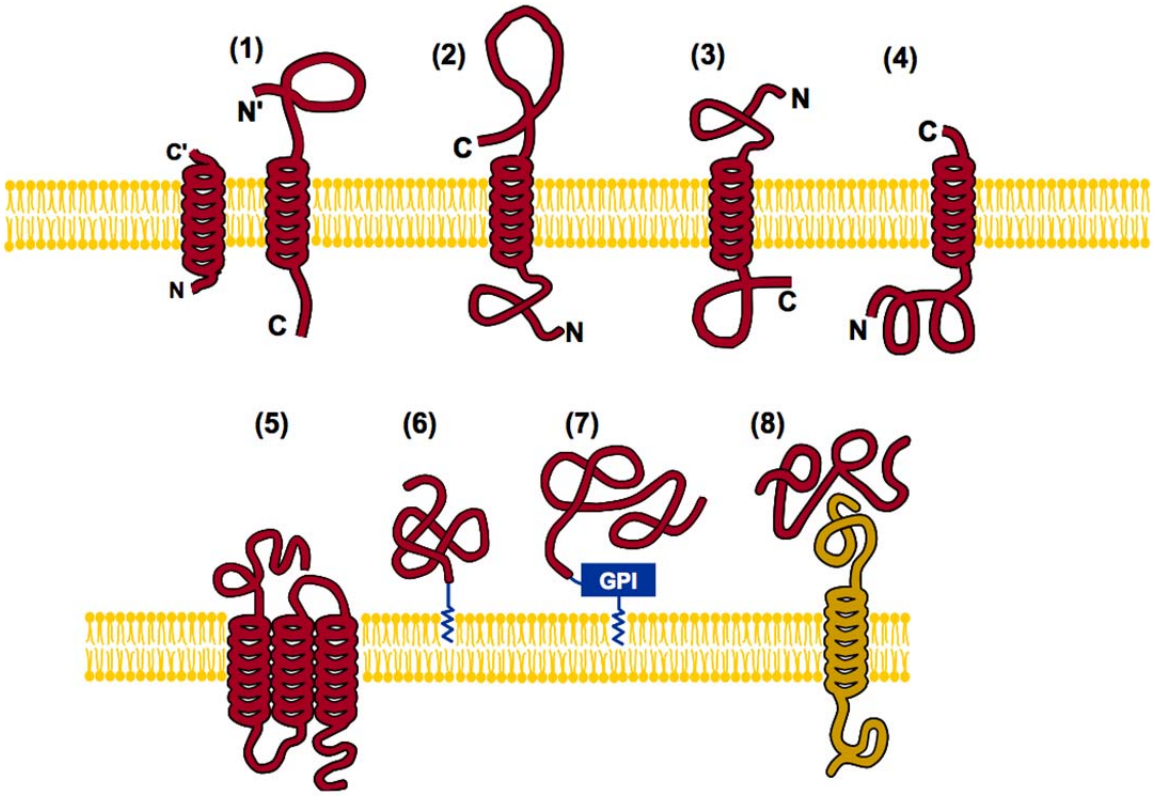

Figure 2.3: Schematic illustration of the eight types membrane proteins: (1) type I transmembrane, (2) type II transmembrane, (3) type III transmembrane, (4) type IV transmembrane, (5) multipass transmembrane, (6) lipid-chain-anchored membrane, (7) GPI-anchored membrane, and (8) peripheral membrane. As shown in the figure, type I, II, III and IV are all single-pass transmembrane proteins (reproduced from Chou & Shen, 2007a).

Then, the putative proteases were predicted by ProtIdent to be one of six classes, which include (1) aspartic, (2) cysteine, (3) glutamic, (4) metallo, (5) serine, and (6) threonine (Chou & Shen, 2008b). Proteases are also termed proteinases or peptidases, are proteolytic enzymes, which are essential for the synthesis of all proteins, controlling their size, composition, shape, turnover, and ultimate destruction (Chou & Shen, 2008b).

2.2.6 Virulent Protein Prediction

Bacterial virulence factors play important roles in bacterial pathogenesis. Prediction of bacterial virulence proteins will be helpful for the identification and characterization of virulence-associated factors, finding drug/vaccine targets against proteins indispensable for pathogenicity and understanding the complex virulence mechanism in pathogens. Virulent protein prediction was performed using the server VirulentPred (Garg & Gupta, 2008). The prediction method used in VirulentPred is based on bi-layer cascade Support Vector Machine (Garg & Gupta, 2008). Firstly, the top layer Support Vector Machine classifiers were trained and optimised with different individual protein sequence features such as amino acid composition, dipeptide composition, higher order dipeptide composition and Position Specific Iterated BLAST (PSI-BLAST) generated Position Specific Scoring Matrices (PSSM) (Garg & Gupta, 2008). Secondly, a similarity-search based module was developed using a dataset of virulent and non-virulent proteins as the BLAST database (Garg & Gupta, 2008).

2.3 Results

2.3.1 Classically Secreted Protein Prediction

All the *C. jejuni* NCTC 11168 CDS were analysed using the various webservers, and the results are shown in Table 2.2. The total CSPs numbers vary from 113 (by SignalP 4.0) (Appendix 1) up to 302 (by Signal-3L). The possible reason for the differences is that SignalP 4.0 is claimed to be the only server which claims to be able to differentiate an N-terminal transmembrane helix from a signal peptide (Petersen *et al*, 2011). The limitation of all the servers mentioned except SignalP 4.0 is that they have only limited ability to distinguish between signal peptides and N-terminal TMH (Petersen *et al*, 2011). Both signal peptides and TMH are hydrophobic, but TMH normally have longer hydrophobic regions, and without cleavage sites (Petersen *et al*, 2011). However, the cleavage-site pattern itself is not sufficient to differentiate the two kinds of sequence (Petersen *et al*, 2011). This problem causes a lot of false positive prediction of TMH from signal peptides in any complete proteome, which is most likely what happened in this case.

In training SignalP 4.0, the developers used two types of negative data. The first correspond to the negative data used in training earlier versions of SignalP, which contains cytoplasmic proteins and nuclear proteins (Petersen *et al*, 2011). The second data includes sequences that do not contain signal peptides but with transmembrane regions within the first 70 amino acids of the protein sequence (Petersen *et al*, 2011). There are two kinds of networks have been used in SignalP 4.0: transmembrane sequences as negative data to train SignalP-TM networks but trained SignalP-noTM networks without these data. These elements make SignalP 4.0 to be believed as the best signal-peptide predictor for all three Gram negative, Gram positive and Eukaryote organism types (Petersen *et al*, 2011).

Table 2.2: Total number of CSPs predicted by different servers.

	SignalP 3.0 (HMM)	SignalP 3.0 (NN)	SignalP 4.0	Signal-CF	Signal-3L
Number of predicted CSPs	295	208	113	287	302
Number of CSPs also predicted by					
SignalP 3.0 (HMM)	**20**	187	113	228	240
SignalP 3.0 (NN)	187	**6**	109	159	168
SignalP 4.0	113	109	**0**	95	98
Signal-CF	228	159	95	**3**	279
Signal-3L	240	168	98	279	**5**

CSPs: classically secreted proteins.

The numbers in red indicate the number of CSPs predicted only by that server.

It is worth mentioning that there is no SignalP 4.0 exclusive predicted sequence. All the putative CSPs picked up by SignalP 4.0 have been picked up by the SignalP 3.0 (HMM), and most of the other predictors.

2.3.2 Non-classically Secreted Protein Analysis

For the proteome of *C. jejuni* NCTC 11168, a total of 200 proteins obtained a 'SecP score' higher than 0.5, which is the threshold value to be a NCSP. However, many of these also have a predicted signal peptide, which would exclude them from the NCSP list. The final numbers of predicted NCSPs are listed in Table 2.3. As indicated in Section 2.3.1, the putative CSPs predicted results from SignalP 4.0 have been taken, which left us 140 putative NCSPs (Appendix 2) to be further analysed in the next section.

2.3.3 Protein Location Prediction

The locations indicated in red in Table 2.4 and Table 2.5 are of interest, as the proteins in these locations are the ones that have the potential to interact with chicken host molecules/cells. Sequences predicted to be less than 50 amino acids were labelled as 'Too Short', and excluded from the prediction as they might represent fragments rather than real proteins.

For the putative CSPs, 23 of which were predicted located extracellularly or surface-exposed using Gneg-PLoc. Using Gneg-mPLoc, 40 putative CSPs were predicted to be located extracellularly or on the cell surface. Among them, 17 putative CSPs were predicted by both servers (Figure 2.4). The total number of putative CSPs that possibly to interact with the chicken immune system is 46 (about 41% of the total number).

Table 2.3 Number of NCSPs predicted by SecretomeP 2.0 after excluding the ones predicted to also contain a signal peptide.

	SignalP 3.0 (HMM)	SignalP 3.0 (NN)	SignalP 4.0	Signal-CF	Signal-3L
Number of proteins with > 0.5 SecP score	200	200	200	200	200
Number of proteins with > 0.5 SecP score but also contain a signal peptide	88	86	60	105	114
Number of NCSPs	**112**	**114**	**140**	**95**	**86**

NCSPs: non-classically secreted proteins

Table 2.4: Results of subcellular location prediction of CSPs and NCSPs using Gneg-PLoc, SignalP 4.0 and SecretomeP 2.0.

Servers	**SignalP 4.0 & SecretomeP 2.0**	
Predicted protein locations	*CSPs*	*NCSPs*
Extracelluar	10	27
Flagellar	3	8
Fimbrium	0	1
Outer membrane	10	11
Periplasm	9	7
Inner membrane	7	2
Cytoplasm	73	78
Too short to be predicted	1	6
Total Number	**23/113**	**47/140**

Too short to be predicted: protein with less than 50 amino acids; CSPs: classically secreted proteins; NCSPs: non-classically secreted proteins.

The locations shaded in red indicate proteins that can interact with chicken host cells.

Table 2.5: Results of multiple locations prediction of *C. jejuni* NCTC 11168 putative secreted proteins by using the server Gneg-mPLoc.

CSPs and NCSPs prediction methods	SignalP 4.0 & SecretomeP 2.0	
Locations	**CSPs**	**NCSPs**
Extracellular.	12	25
Fimbrium.	1	2
Outer membrane.	13	9
Extracellular. Fimbrium.	0	1
Extracellular. Periplasm.	1	0
Outer membrane. Extracellular.	1	1
Inner membrane. Extracellular.	5	13
Inner membrane. Outer membrane.	4	2
Inner membrane. Extracellular. Fimbrium.	1	0
Inner membrane. Cytoplasm. Extracellular.	1	1
Inner membrane. Outer membrane. Extracellular.	0	1
Inner membrane. Outer membrane. Cytoplasm. Extracellular. Periplasm.	1	0
Cytoplasm.	3	8
Periplasm.	23	7
Inner membrane.	36	42
Inner membrane. Cytoplasm.	4	19
Inner membrane. Periplasm.	4	2
Cytoplasm. Periplasm.	2	1
Too short to be predicted.	1	6
Total	**40/113**	**55/140**

The locations shaded in red indicate proteins that can interact with chicken host cells; too short to be predicted: protein with less than 50 amino acids; CSPs: classically secreted proteins; NCSPs: non-classically secreted proteins.

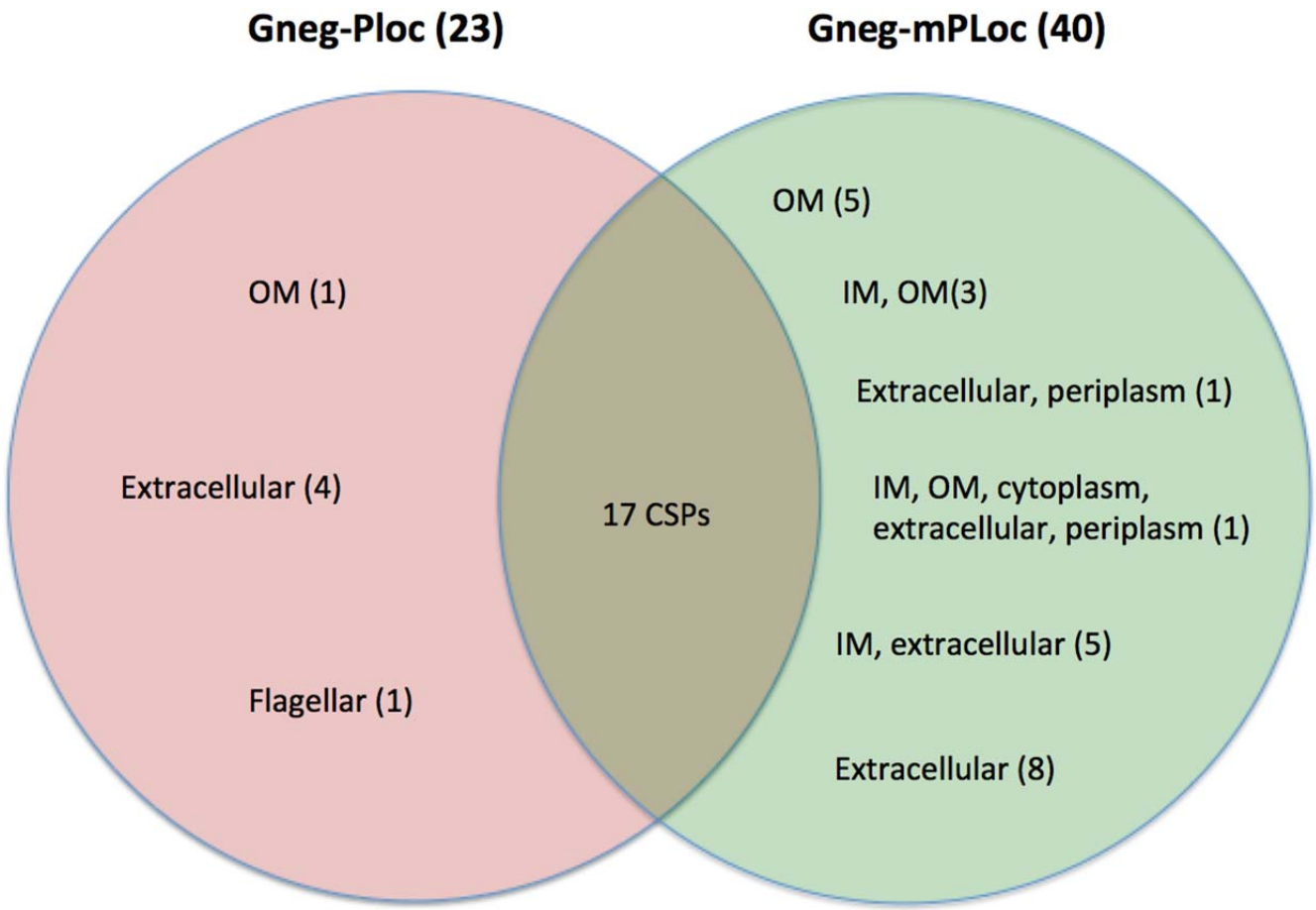

Figure 2.4: Comparison of putative CSPs location prediction by Gneg-PLoc and Gneg-mPLoc. The 17 CSPs are the ones predicted to be extracellular or surface-exposed by both Gneg-PLoc and Gneg-mPLoc.

CSPs: classically secreted proteins; OM: outer membrane; IM: inner membrane.

There are 47 putative NCSPs predicted to be located extracellularly or on the surface of the cells by Gneg-PLoc, and 55 putative NCSPs picked up by Gneg-mPLoc with at least one stage located extracellularly or exposed to the host environment. Thirty-two (32) of them were predicted extracellular or surface-exposed by both methods (Figure 2.5). The total number of putative NCSPs with the location of interest is 70 (50% of the total number).

Generally, more putative NCSPs were predicted to be located extracellular and/or on the cell surface comparing to the CSPs, even NCSPs do not predicted to contain a signal peptide. It reveals the alternative pathways could exist within Gram-negative organisms as *C. jejuni*.

2.3.4 Membrane Protein Prediction

The numbers of proteins with TMH or TMBB are listed in Tables 2.6 to 2.9 and Figure 2.6. About 78% (88 proteins) of the 113 putative CSPs were predicted without TMH, and 17% (19 proteins) were predicted contain one TMH. The 17% proteins all have their predicted TMH region located in the first 60 AAs, which indicates that the predicted TMH are most likely signal peptides (Krogh *et al*, 2001). Only about 5% putative CSPs (6 in total) were predicted containing TMH besides signal peptides. For these 6 putative CSPs, 5 of them were predicted also containing TMBBs, and the one that predicted containing 12 TMHs were predicted not an OMP by PRED-TMBB, which indicates that it is could be an inner-membrane protein. The total number of putative membrane proteins predicted with TMH or/and with TMBB is 46, which means around 40% of the putative CSPs are putative membrane proteins. Five of them were predicted as TMBB-containing OMPs with the presence of TMH(s).

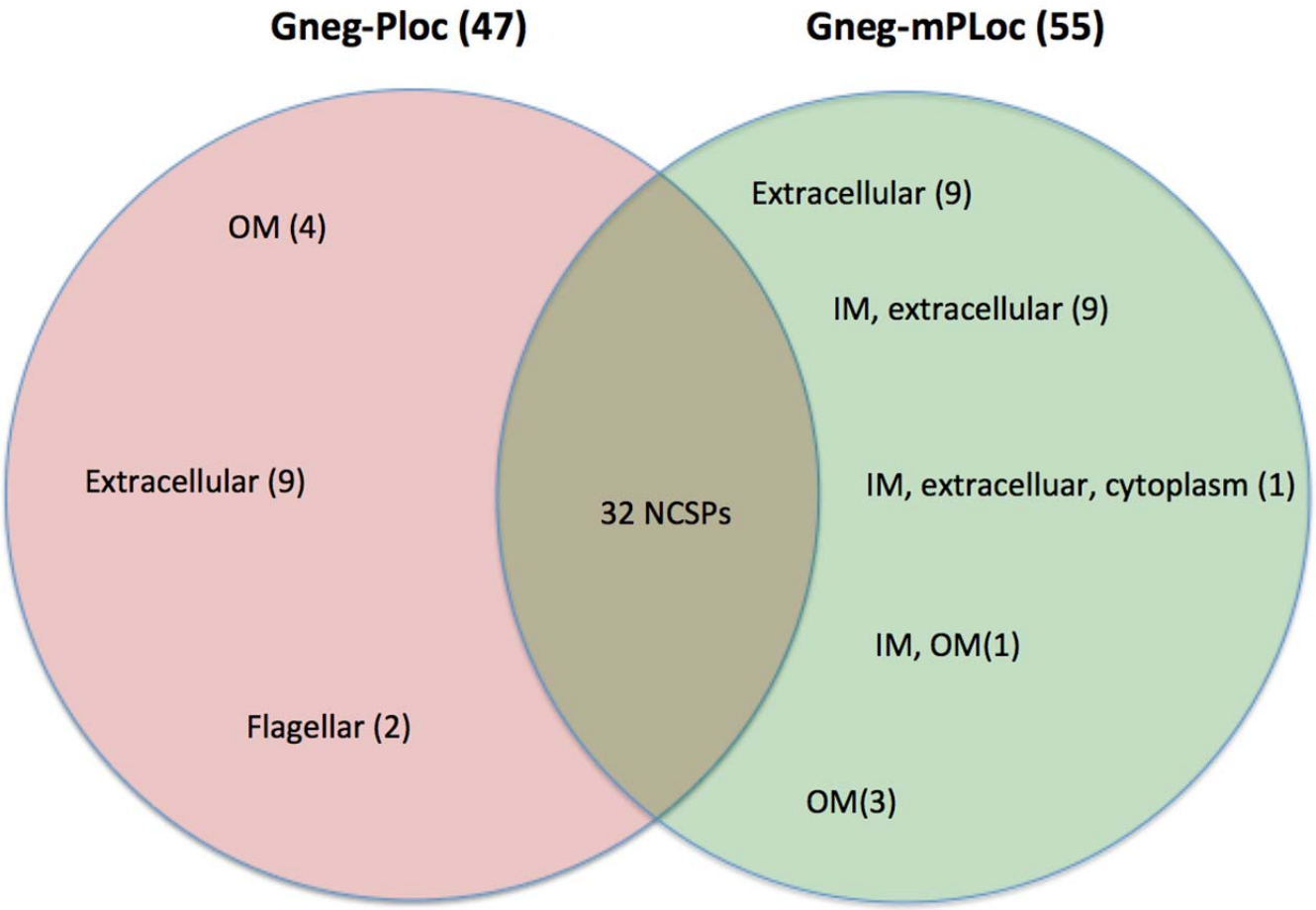

Figure 2.5: Comparison of putative NCSPs location prediction by Gneg-PLoc and Gneg-mPLoc. The 32 NCSPs are the ones predicted to be extracellular or surface-exposed by both Gneg-PLoc and Gneg-mPLoc.

NCSPs: non-classically secreted proteins OM: outer membrane; IM: inner membrane.

Table 2.6: Putative CSPs trans-membrane helices and membrane type prediction.

TMHMM 2.0		***MemType-2L***								
No. of TMH	**No. of CSPs**	**Gpi Anchor**	**Lipid Anchor**	**Multi-pass**	**Peripheral**	**Single-pass Type I**	**Single-pass Type II**	**Single-pass Type IV**	**Not a MP**	**Too short to be predicted**
0	88	1	5	12	5	1	1	0	62	1
1	19	0	2	2	0	0	0	1	14	0
3	2	0	0	2	0	0	0	0	0	0
4	1	0	0	1	0	0	0	0	0	0
7	1	0	0	0	0	0	0	0	1	0
12	1	0	0	1	0	0	0	0	0	0
13	1	0	0	1	0	0	0	0	0	0
Total	**113**	**1**	**7**	**19**	**5**	**1**	**1**	**1**	**77**	**1**

TMH: transmembrane helices; MP: membrane protein; too short to be predicted: protein with less than 50 amino acids; CSPs: classically secreted proteins.

Table 2.7: Putative NCSP trans-membrane helices and membrane type prediction.

TMHMM 2.0		***MemType-2L***								
No. of TMH	**No. of NCSPs**	**Gpi Anchor**	**Lipid Anchor**	**Multi-pass**	**Peripheral**	**Single-pass Type I**	**Single-pass Type II**	**Single-pass Type IV**	**Not a MP**	**Too short to be predicted**
0	116	1	5	3	1	2	1	0	97	6
1	22	1	1	3	1	0	3	0	13	0
2	1	0	0	1	0	0	0	0	0	0
12	1	0	0	0	0	0	0	0	1	0
Total	**140**	**2**	**6**	**7**	**2**	**2**	**4**	**0**	**111**	**6**

TMH: transmembrane helices; MP: membrane protein; too short to be predicted: protein with less than 50 amino acids; NCSPs: non-classically secreted proteins.

Table 2.8: Putative CSPs transmembrane beta-barrel and membrane type prediction.

PRED-TMBB		***MemType-2L***								
Types	**No. of CSPs**	**Gpi Anchor**	**Lipid Anchor**	**Multi-pass**	**Peripheral**	**Single-pass Type I**	**Single-pass Type II**	**Single-pass Type IV**	**Not a MP**	**Too short to be predicted**
OMP with 8 to 22 BBs	22	0	2	9	1	0	0	0	10	0
OMP with < 8 or > 22 BBs	23	0	1	6	0	0	0	0	16	0
Not an OMP	68	1	4	4	4	1	1	1	51	1
Total	**113**	**1**	**7**	**19**	**5**	**1**	**1**	**1**	**77**	**1**

OMP: outer-membrane protein; MP: membrane protein; too short to be predicted: protein with less than 50 amino acids; CSPs: classically secreted proteins; BB: beta-barrel.

Table 2.9: Putative NCSPs transmembrane beta-barrel and membrane type prediction.

PRED-TMBB		***MemType-2L***								
Types	**No. of NCSPs**	**Gpi Anchor**	**Lipid Anchor**	**Multi-pass**	**Peripheral**	**Single-pass Type I**	**Single-pass Type II**	**Single-pass Type IV**	**Not a MP**	**Too short to be predicted**
OMP with 8 to 22 BBs	19	1	2	0	0	1	1	0	14	0
OMP with < 8 or > 22 BBs	25	0	2	3	1	0	0	0	18	1
Not an OMP	96	1	2	4	1	1	3	0	79	5
Total	**140**	**2**	**6**	**7**	**2**	**2**	**4**	**0**	**111**	**6**

OMP: outer-membrane protein; MP: membrane protein; too short to be predicted: protein with less than 50 amino acids; NCSPs: non-classically secreted proteins; BB: beta-barrel.

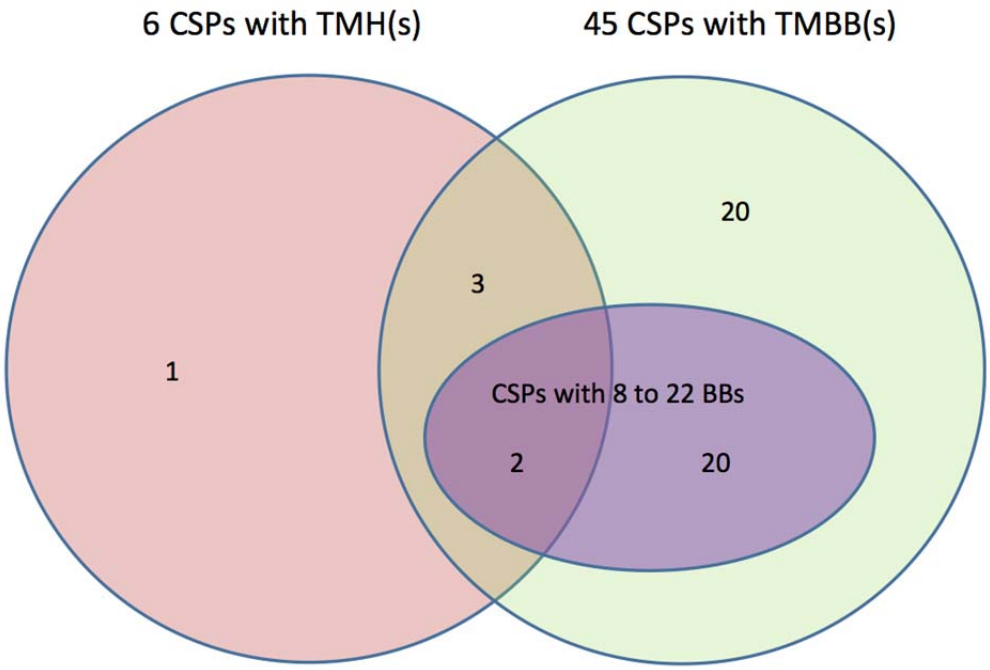

(A)

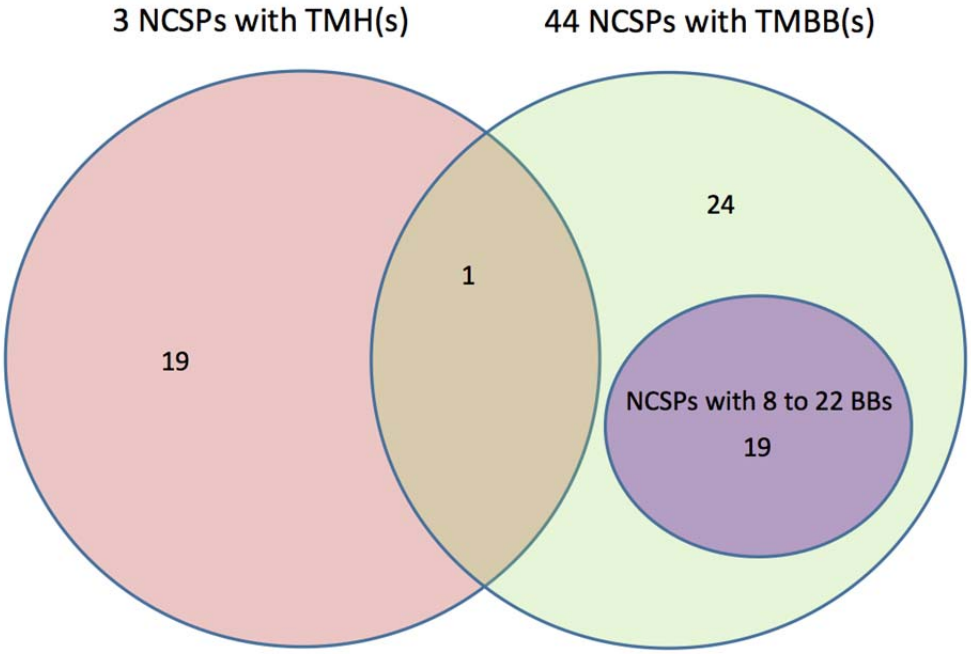

(B)

Figure 2.6: Number of putative CSPs (A) and putative NCSPs (B) predicted with TMH(s) and TMBB(s) using TMHMM 2.0 and PRED-TMBB.

TMH: transmembrane helices; TMBBs: transmembrane beta-barrels; CSPs: classically secreted proteins; NCSPs: non-classically secreted proteins.

The membrane types of the putative CSPs were predicted using Memtype-2L. Fifteen (15) of the putative CPSs without TMH or TMBB were predicted as membrane proteins using Memtype-2L. However, 13 of them were also predicted as membrane proteins using Gneg-mPLoc, which indicates these proteins might be the membrane proteins without TMH or TMBBs. For the putative 46 TMH and/or TMBB-containing CSPs, only 20 were predicted as membrane proteins by MemType-2L. As indicated in the Section 2.2.4, MemType-2L only predicts 8 types of membrane proteins. The rest putative 26 membrane proteins may belong to the other classes that are not included in MemType-2L.

Of 140 putative NCSPs, 83% of them were predicted without TMH. For the 22 putative NCSPs predicted contain one TMH, 21 of them (15%) with the predicted TMH located in the first 60 AAs, which indicates that they might be indeed signal peptides (Krogh *et al,* 2001). Only 3 putative NCSPs predicted containing TMH(s) by TMHMM 2.0, which include one with 1 TMH, one with 2 TMHs and another with 12 TMHs. The NCSP predicted contains 2 TMHs was also predicted as an OMP with 2 TMBBs, while the other two putative TMH-containing NCSPs are likely inner membrane proteins as they were predicted as non-OMP using PRED-TMBB. The total number of putative TMH and/TMBB containing NCSPs is 46, which is exactly same as the number of putative TMH and/or TMBB containing CSPs. Among them, only 10 of them were predicted as membrane proteins by MemType-2L. As discussed above, the rest of putative TMH and/or TMBB containing proteins may belong to the other types rather than the eight types predicted by MemType-2L.

2.3.5 Enzyme Prediction

For a newly found protein sequence the most interested thing scientists wish to know is about its biological function. Enzyme prediction has been performed using EzyPred and the results are shown in Table 2.10. For *C. jejuni* NCTC 11168, 22 out of 38 annotated proteins have been correctly predicted using EzyPred. Another 2 hypothetical proteins

Table 2.10: The enzyme prediction obtained from the server EzyPred based on the (A) 113 putative CSPs and (B) 140 putative NCSPs

(A)

	Annotated enzymes	Hypothetical proteins	Annotated non-enzymes or unknown function	Total
Predicted by EzyPred as an enzyme	8	0	6	**14**
Predicted by EzyPred as a non-enzyme	5	1	92	**98**
Too short for EzyPred to predict	0	0	1	**1**
Total	**13**	**1**	**99**	**113**

(B)

	Annotated enzymes	Hypothetical proteins	Annotated non-enzymes or unknown function	Total
Predicted by EzyPred as an enzyme	14	2	5	**21**
Predicted by EzyPred as a non-enzyme	10	35	68	**113**
Too short for EzyPred to predict	1	3	2	**6**
Total	**25**	**40**	**75**	**140**

and 11 annotated proteins have also been predicted as enzymes by EzyPred. For the 11 annotated proteins, some of them have been assigned with other functions and some have only been annotated with the location (such as periplasmic proteins). Therefore, they cannot be totally excluded from the enzyme class. The accuracy of EzyPred prediction for putative CSPs and NCSPs are roughly the same, around 60%. The remaining 40% have known the enzyme function, but have not been predicted.

Proteases play important roles in regulating activation, synthesis and turnover of proteins, which is essential for the bacteria and any other organisms. Protease account for about 1-5% of genomes of infectious organisms (Chou & Shen, 2008b). Actually, according to the recent inference by Rawlings et al. (Rawlings et al, 2012), the number of protease/peptidase might be as least twice as much. For the protease prediction part (results as shown in Table 2.11), there are in total 4 annotated peptidases/proteases from the 253 putative secreted proteins, which were all successfully predicted by ProtIdent. There are in total 23 putative proteases predicted from the server, besides the 4 already been identified, 19 remain to be further identified. Among the 19 putative peptidases, 11 of them are hypothetical proteins.

2.3.6 Virulent Protein Prediction

Virulence of a bacterial pathogen is its relative ability to colonise the host, potentially/actually cause disease, normally described as the number of infecting bacteria, the route of its entry into the host and its intrinsic virulence factors (Garg & Gupta, 2008). Virulence factors commonly include proteins, carbohydrates and other molecules synthesised by the bacteria (Garg & Gupta, 2008). Virulence proteins are the most important virulence factors coded in the genes present in chromosomal DNA or mobile genetic elements such as bacteriophages or plasmids (Hastings *et al*, 2004; Weiss, 2002).

Table 2.11: The protease prediction obtained from the server ProtIdent based on the (A) 113 putative CSPs and (B) 140 putative NCSPs

(A)

	Annotated protease	Annotated peptidase	Annotated enzymes other than protease/peptidase	Hypothetical proteins	Others	Total
Predicted by ProtIdent as protease	0	1	0	0	4	5
Predicted by ProtIdent as non-protease	0	0	12	1	94	107
Too short for ProtIdent to predict	0	0	0	0	1	1
Total	0	1	12	1	99	113

(B)

	Annotated protease	Annotated peptidase	Annotated enzymes other than protease/peptidase	Hypothetical proteins	Others	Total
Predicted by ProtIdent as protease	2	1	1	11	3	18
Predicted by ProtIdent as non-protease	0	0	20	26	70	116
Too short for ProtIdent to predict	0	0	1	3	2	6
Total	2	1	22	40	75	140

Five classes of virulence factors have been widely discussed: adhesins, colonisation factors, invasion factors, toxins and defensive virulence factors. According to the server VirulentPred (Garg & Gupta, 2008), 195 putative secreted virulence proteins have been predicted from the group of *C. jejuni* NCTC 11168 putative secreted proteins, which include 154 known-function/location proteins and 41 hypothetical proteins. The predicted attributes of the 41 hypothetical virulent proteins (1 putative CSPs and 40 putative NCSPs) are listed in Table 2.12 and Table 2.13.

Table 2.12: The prediction results of the 1 putative virulent hypothetical CSP from *C. jejuni* NCTC 11168

CSPs	ProtIdent	EzyPred	Gneg-PLoc	Gneg-mPLoc	MemType	TMHMM	PRED-TMBB
Cj0371	Not a protease	Not an enzyme	Cytoplasm	Cell inner membrane.	Not a MP	1	1

MP: membrane protein

Table 2.13: The prediction results of the 40 putative virulent hypothetical NCSPs from *C. jejuni* NCTC 11168

NCSPs	ProtIdent	EzyPred	Gneg-PLoc	Gneg-mPLoc	MemType	TMHMM	PRED-TMBB
Cj0055c	Not a protease	Not an enzyme	Cytoplasm	Cell inner membrane. Extracellular.	Not a MP	0	NOT an OMP
Cj0056c	Cysteine type	Not an enzyme	Cytoplasm	Cell outer membrane.	Not a MP	0	NOT an OMP
Cj0152c	Not a protease	Not an enzyme	Cytoplasm	Cell inner membrane. Extracellular.	Not a MP	1	NOT an OMP
Cj0202c	Not a protease	Not an enzyme	Cytoplasm	Extracellular.	Not a MP	0	4
Cj0243c	Not a protease	Not an enzyme	Cytoplasm	Extracellular.	Not a MP	0	NOT an OMP
Cj0391c	Serine type	Not an enzyme	Extracellular	Extracellular.	Not a MP	0	NOT an OMP
Cj0418c	Not a protease	Not an enzyme	Extracellular	Cell outer membrane.	Not a MP	0	NOT an OMP
Cj0428	Not a protease	Not an enzyme	Extracellular	Extracellular.	Not a MP	0	NOT an OMP

MP: membrane protein; OMP: outer membrane protein; too short to be predicted: protein with less than 50 amino acids.

Table 2.13: The prediction results of the 40 putative virulent hypothetical NCSPs from *C. jejuni* NCTC 11168 (cont.)

NCSPs	ProtIdent	EzyPred	Gneg-PLoc	Gneg-mPLoc	MemType	TMHMM	PRED-TMBB
Cj0700	Not a protease	Not an enzyme	Cytoplasm	Cell inner membrane. Extracellular.	Not a MP	0	NOT an OMP
Cj0736	Cysteine type	Not an enzyme	Cytoplasm	Extracellular.	Gpi anchor membrane	0	22
Cj0738	Not a protease	Not an enzyme	OM	Fimbrium.	Multi-pass membrane	0	Not an OMP
Cj0739	Serine type	Not an enzyme	Extracellular	Cell outer membrane. Extracellular.	Single-pass type I	0	NOT an OMP
Cj0740	Aspartic type	Not an enzyme	Cytoplasm	Extracellular.	Not a MP	0	NOT an OMP
Cj0741	Not a protease	Not an enzyme	Cytoplasm	Extracellular.	Not a MP	0	NOT an OMP
Cj0748	Too short to be predicted	Too short to be predicted	Too short to be predicted	Too short to be predicted	Too short to be predicted	0	NOT an OMP
Cj0794	Cysteine type	Not an enzyme	Flagellar	Extracellular.	Not a MP	0	NOT an OMP

MP: membrane protein; OMP: outer membrane protein; too short to be predicted: protein with less than 50 amino acids.

Table 2.13: The prediction results of the 40 putative virulent hypothetical NCSPs from *C. jejuni* NCTC 11168 (cont.)

NCSPs	ProtIdent	EzyPred	Gneg-PLoc	Gneg-mPLoc	MemType	TMHMM	PRED-TMBB
Cj0814	Not a protease	Not an enzyme	Extracellular	Extracellular.	Not a MP	0	NOT an OMP
Cj0815	Metallo type	Not an enzyme	Cytoplasm	Cell inner membrane. Extracellular.	Not a MP	0	NOT an OMP
Cj0816	Not a protease	Not an enzyme	Cytoplasm	Cell inner membrane.	Not a MP	0	NOT an OMP
Cj0839c	Not a protease	Not an enzyme	OM	Cell inner membrane. Extracellular.	Not a MP	0	Not an OMP
Cj0848c	Not a protease	Not an enzyme	Cytoplasm	Cell inner membrane.	Not a MP	0	3
Cj0849c	Not a protease	Not an enzyme	Cytoplasm	Cell inner membrane.	Not a MP	0	NOT an OMP
Cj0859c	Metallo type	Not an enzyme	Extracellular	Cell inner membrane.	Not a MP	0	2
Cj0873c	Not a protease	Hydrolases Acting on ester bonds	Cytoplasm	Cell inner membrane.	Not a MP	0	NOT an OMP

MP: membrane protein; OMP: outer membrane protein; too short to be predicted: protein with less than 50 amino acids.

Table 2.13: The prediction results of the 40 putative virulent hypothetical NCSPs from *C. jejuni* NCTC 11168 (cont.)

NCSPs	ProtIdent	EzyPred	Gneg-PLoc	Gneg-mPLoc	MemType	TMHMM	PRED-TMBB
Cj0878	Too short to be predicted	Too short to be predicted	Too short to be predicted	Too short to be predicted	Too short to be predicted	0	3
Cj0916c	Not a protease	Not an enzyme	Cytoplasm	Cell inner membrane.	Not a MP	0	NOT an OMP
Cj0970	Serine type	Not an enzyme	Extracellular	Extracellular.	Not a MP	0	NOT an OMP
Cj0971	Cysteine type	Not an enzyme	Extracellular	Extracellular.	Lipid anchor membrane	0	NOT an OMP
Cj0972	Serine type	Not an enzyme	Extracellular	Fimbrium.	Not a MP	0	2
Cj0974	Too short to be predicted	Too short to be predicted	Too short to be predicted	Too short to be predicted	Too short to be predicted	0	NOT an OMP
Cj1036c	Not a protease	Not an enzyme	Cytoplasm	Cell inner membrane. Extracellular.	Not a MP	0	NOT an OMP
Cj1164c	Not a protease	Hydrolases Acting on ester bonds	Cytoplasm	Cell inner membrane. Cytoplasm.	Not a MP	0	NOT an OMP

MP: membrane protein; OMP: outer membrane protein; too short to be predicted: protein with less than 50 amino acids.

Table 2.13: The prediction results of the 40 putative virulent hypothetical NCSPs from *C. jejuni* NCTC 11168 (cont.)

NCSPs	ProtIdent	EzyPred	Gneg-PLoc	Gneg-mPLoc	MemType	TMHMM	PRED-TMBB
Cj1225	Not a protease	Not an enzyme	Cytoplasm	Cell inner membrane.	Not a MP	0	NOT an OMP
Cj1232	Not a protease	Not an enzyme	Cytoplasm	Cell inner membrane.	Not a MP	0	NOT an OMP
Cj1242	Not a protease	Not an enzyme	Extracellular	Cell inner membrane. Cell outer membrane. Extracellular.	Not a MP	0	NOT an OMP
Cj1463	Not a protease	Not an enzyme	Cytoplasm	Extracellular.	Not a MP	0	NOT an OMP
Cj1464	Not a protease	Not an enzyme	Fimbrium	Cell outer membrane.	Not a MP	0	1/2
Cj1501	Not a protease	Not an enzyme	Cytoplasm	Cytoplasm.	Not a MP	0	NOT an OMP
Cj1631c	Not a protease	Not an enzyme	Flagellar	Extracellular.	Not a MP	0	NOT an OMP
Cj1656c	Not a protease	Not an enzyme	Extracellular	Extracellular. Fimbrium.	Lipid anchor membrane	0	0

MP: membrane protein; OMP: outer membrane protein; too short to be predicted: protein with less than 50 amino acids.

2.4 Discussion and Conclusion

A number of identified *C. jejuni* virulence factors are known to be involved in chicken colonisation, which is still poorly understood. Individual experimental studies for all the encoded proteins are both too time-consuming and costly to carry out. Bioinformatics tools are useful for investigating these potential virulence proteins that may be involved in chicken colonisation and evasion of the host immune response. In this study, various servers were used to identify putative virulent non-classically secreted proteins from *C. jejuni* NCTC 11168 that are fully or partially exposed extracellularly, which may be responsible for chicken immune down-regulation and/or the remarkable colonisation capability of *C. jejuni* in chickens.

After assessing the 1623 protein sequences using a variety of bioinformatics tools, 28 predicted virulent NCSPs have been identified which putatively interact with the extracelluar environment (Table 2.14). Among them, 11 of them have been predicted as a protease/peptidase. Genes *cj0243c* (σ^{54}), *cj0391c* (σ^{28}), *cj0814* (σ^{54}), *cj0859c* (σ^{28}) and *cj1656c* (σ^{28}) have been observed to be co-regulated with flagellar gene expression in Guerry-Kopecko *et al.*'s study (Guerry-Kopecko, 2012). σ^{54} promoters regulate the expression of genes required for basal body, hook and flagellar filament biosynthesis (Class II genes). σ^{28} promoters co-regulate the expression of genes required for extension and capping of the flagellum, and genes required for flagellin post-translational modification and secretion of virulence factors (Class III genes) (Carrillo *et al*, 2004). Furthermore, hypothetical protein Cj0391c and Cj1631c was overexpressed in biofilm-grown cells, along with other proteins involved in stress response, flagellar motility complex and adhesion (Kalmokoff *et al*, 2006). Protein Cj1656c have been predicted as a membrane protein using MemType. However, there is no TMH or TMBB has been bioinformatically detected.

Table 2.14 The 28 putative virulent NCS extracellular proteins

NCSPs	Size (AAs)	NCSPs	Size (AAs)
Cj0055c	274	Cj0794	426
Cj0056c	138	Cj0814	251
Cj0152c	312	Cj0815	114
Cj0202c	113	Cj0839c	65
Cj0243c	388	Cj0859c	142
Cj0391c	211	Cj0970	100
Cj0418c	234	Cj0971	130
Cj0428	127	Cj0972	107
Cj0700	231	Cj1036c	83
Cj0736	642	Cj1242	106
Cj0738	54	Cj1463	113
Cj0739	57	Cj1464	65
Cj0740	54	Cj1631c	289
Cj0741	308	Cj1656c	60

These 28 predicted virulent NCSPs have been identified which putatively interact with the extracelluar environment

Protein Cj0152c, which has been predicted locates in the cytoplasm/cell inner membrane and extracellular, has been found in the *C. jejuni* outer membrane vesicles (OMVs) (Jang *et al*, 2014). In Gram-negative bacteria, OMVs are often released extracellularly attaching to host cells through adhesive molecules then transferring compounds into the host cells (Jang *et al*, 2014). As *C. jejuni* does not have the prototypical virulence-associated secretion systems, OMV plays an important role in the coordinated delivery of virulent proteins into host cells (Elmi *et al*, 2012). Protein Cj0391c and Cj0859c were also predicted as putative protease according to server ProtIdent.

Among the listed gene candidates in Table 2.14, gene *cj0391c* has been selected for our experimental study (some others were expressed by other colleagues) and expressed as a recombinant protein in *E. coli* BL21(DE3) (Chapter 3). Protein Cj0391c was selected based on the following reasons: (1) gene *cj0391c* is σ^{28} co-regulated with flagellar gene expression (Guerry-Kopecko, 2012); (2) it was overexpressed in biofilm-grown cells, along with other proteins involved in stress response, flagellar motility complex and adhesion (Kalmokoff *et al*, 2006); (3) it predicted mainly hydrophilic (Figure 2.7); (4) none of the prediction tool indicates it is a membrane protein or contains transmembrane region (it may dissolve well and fold/function correctly in the protein storage solution and tissue culture medium); (5) it is predicted as a stable protein based on its instability index using ProtParam server (Guruprasad *et al*, 1990) (Appendix 3). This recombinant protein was then tested against chicken macrophage cells for cell proliferation and the induction of apoptosis (Chapter 3).

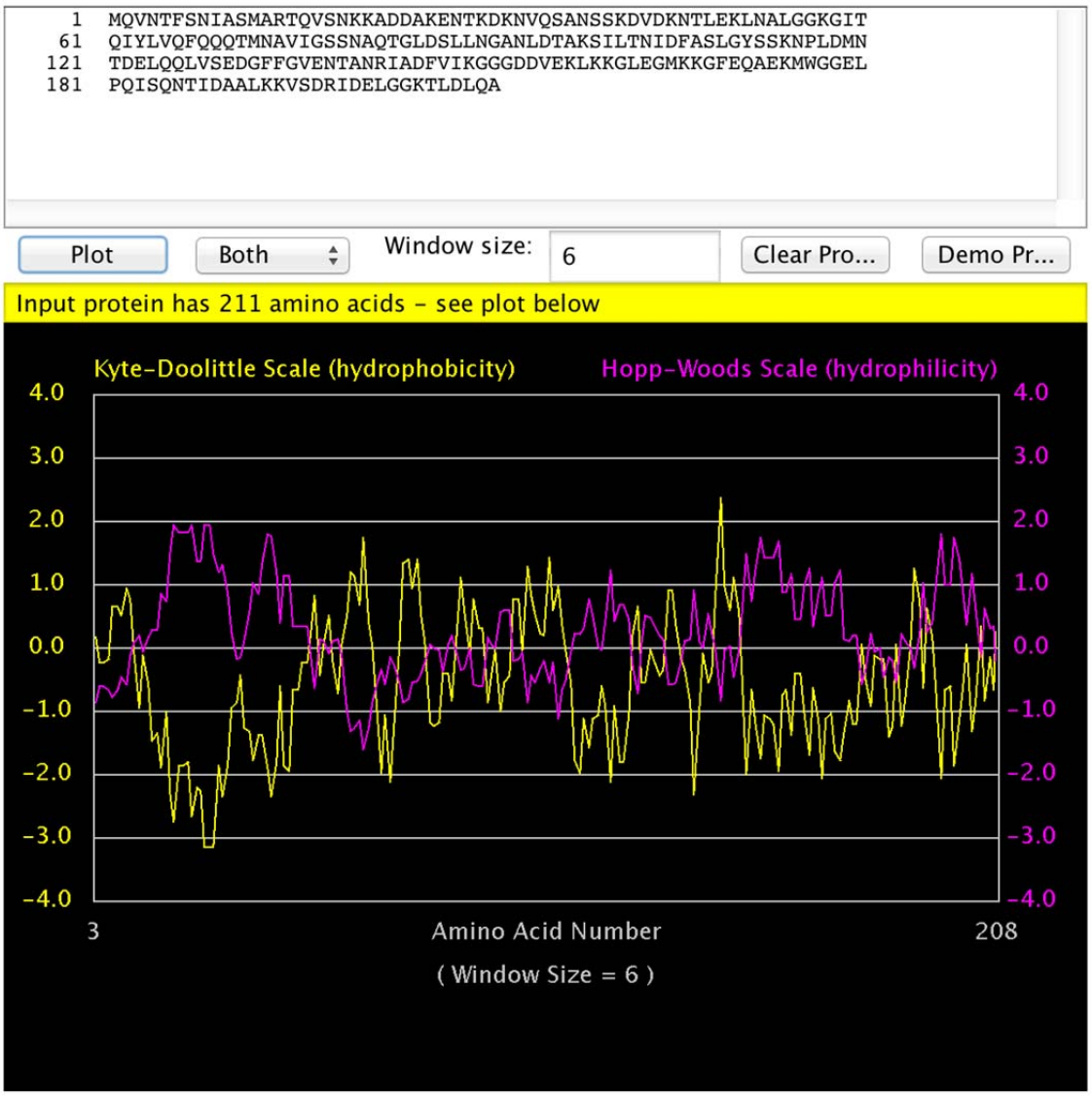

Figure 2.7: Cj0391c hydrophobicity/hydrophilicity plots prediction result using Kyte-Doolittle Scale and Hopp-Woods Scale. (Kyte-Doolittle scale: positive values indicate hydropathic regions; Hopp-Woods scale: apolar residues with negative values, while the region of maximal hydrophilicity is likely to be an antigenic site) (Hopp & Woods, 1981; Kyte & Doolittle, 1982).

CHAPTER 3. PROTEIN CJ0391C EXPRESSION AND ANALYSIS

3.1 Introduction

The *E. coli* DH5α cells containing the pREST-A/*Cj0391c* construct were obtained from a previous study. Initially, plasmid DNA from the cells was extracted and sequenced to confirm that the plasmid contained the correct sequence and the resulting protein sequence is in frame with vector-encoded sequences. Next, the plasmid was introduced into the protein expression system *E. coli* BL21(DE3)pLySs. The final steps were to express, purify and analyse the recombinant protein Cj0391c from the pRSET-A construct contained in *E. coli* BL21(DE3) cells. A pilot protein expression study was performed to determine the time required to express the maximal amount of target protein after Isopropyl-β-D-galactopyranoside (IPTG) induction.

Once optimal induction conditions for the expression of recombinant protein Cj0391c were confirmed by sodium dodecyl sulphate polyacrylamide gel electrophoresis (SDS-PAGE) and Western Blot analysis, the protein expression study was 'scaled-up', and the entire IPTG-induced culture prepared for protein purification using the sonication method. Recombinant protein from whole cell lysates (WCL) was purified using immobilised metal (nickel ion) affinity chromatography (IMAC) column, in which the nickel-bound polyHistidine tagged pRSET-A fusion protein attached to the recombinant protein was eluted with elution buffer (EB) containing increasing concentrations of imidazole.

After confirmation of the optimal elution condition for recombinant protein Cj0391c by SDS-PAGE and Western blot analysis, the pooled eluants were concentrated with Vivaspin (<5 kDa cut-off) and buffer-exchanged with Phosphate buffered saline (PBS). The amount of the purified and concentrated protein was measured by Bradford assay. MTT (3-(4,5-dimethylthiazolyl-2-yl)-2,5-diphenyltetrazolium bromide) cell proliferation assay was performed by adding filter sterilised recombinant protein Cj0391c at final concentrations of 5 ug/mL, 20 ug/mL and 40 ug/mL to chicken macrophage cell HD11 culture. Cell viability was

measured at different time points using an iMark microplate absorbance reader for the presence of intracellular purple formazan, which indicates viable cells.

An apoptosis assay was performed by using a Dead Cell Apoptosis Kit containing Annexin V Alexa Fluor® 488 and Propidium Iodide (PI) fluorescent dyes (Invitrogen Corporation, USA). The cells were incubated with 20 μg/mL of recombinant protein Cj0391c for 12 h before being subjected to CLSM.

3.2 Materials and Methods

3.2.1 General Procedures

Sterilisation of glassware, pipette tips, PCR tubes, centrifuge tubes, toothpicks, media and appropriate solutions was achieved by autoclaving at 121ºC for 20 min unless stated otherwise. All glassware was washed in pyroneg detergent and rinsed twice in distilled water. Finnpipettes® (ThermoFisher Scientific, USA) were used to dispense solutions ranging from 0.5 µL to 10 mL. Volumes above 10 mL were measured with measuring cylinders. Weighting of solids less than 2 g was done using the Mettler Toledo XS105 Dual Range top loading analytical balance, while weighting of solids greater than 2 g was performed with the ISSCO Model 300 top loading balance. Volumes of 1.5 mL or less were separated by centrifugation with the Eppendorf microcentrifuge 5415D and volumes up to 50 mL were separated by centrifugation using either the Beckman Allegra™ 21R centrifuge or the Heraeus Multifuge 1S-R centrifuge.

All media were prepared using distilled water and aseptic techniques. Media containing supplements and/or antibiotics were autoclaved and cooled to approximately 50ºC before the addition of any supplement(s) or antibiotic(s). All media and ager plates were stored at 4ºC until required.

Deionised distilled water was obtained by filtration through a Millipore Milli-Q™ water system (MQ water) (Millipore, USA) and was used to prepare all solutions unless otherwise stated. All solutions were prepared using analytical or molecular grade chemicals and stored at room temperature (RT) unless otherwise stated. Solutions that were sterilised by filtration were passed through a sterile 0.2 µm syringe filter disc.

3.2.2 General Equipments and Suppliers

96-well, colourless, flat bottom plates	Nunc, Denmark
96-Well Microplate Polystyrene Black (350µl well volume)	Chromacol, United Kingdom
Acrodisc® (0.2 µm and 0.45 µm)	Pall, USA
Balances:	
XS105 Dual Range analytical balance	Mettler Toledo, Australia
ISSCO Model 300 balance	ISSCO, Australia
Biological safety cabinet class II, BH2000 series	Clyde-Apac, Australia
BioPhotometer	Eppendorf, Germany
Centrifuge tubes:	
1.5 mL microfuge tubes	Sarstedt, Germany
10 mL centrifuge tubes	Sarstedt, Germany
15 mL centrifuge tubes	Sarstedt, Germany
50 mL centrifuge tubes	Greiner Bio-One, Germany
Centrifuges:	
Eppendorf 5414D bench top centrifuge (maximum speed 16,000 x *g*)	Eppendorf, Germany
Heraeus Multifuge 1S-R centrifuge (maximum speed 5000 x *g*)	Thermo Electron Corporation, USA
Allegra™ 21R centrifuge (maximum speed 5000 x *g*)	Beckman Coulter, USA
Cryovials (1.8 mL)	Iwaki, Japan

Dry block heater	Ratek, Australia
Electrophoresis power supply:	
EPS 3000xi	BioRad Laboratories, USA
PowerPac 300	BioRad Laboratories, USA
Electrophoresis units and components:	
DNA	
Mini gel (Mini-sub cell GT cell)	BioRad Laboratories, USA
Midi gel (Wide mini-sub cell GT cell)	BioRad Laboratories, USA
Electroporation cuvettes (0.2 cm)	Molecular Bio Products, USA
GelDoc imaging system	BioRad Laboratories, USA
FLUOstar Optima microplate reader	BMG Labtech, Germany
iBlot dry gel transfer device	Invitrogen Corporation, USA
iMark microplate absorbance reader	BioRad Laboratories, USA
Milli-Q® water filtration system	Millipore, USA
Petri dishes	BioLab, Australia
pH meter	Metrohm AG, Switzerland
Platform orbital shaker	Ratek, Australia
Polypropylene gravity flow column (1 mL)	Qiagen, Germany
Pulse controller & Gene pulser apparatus	BioRad Laboratories, USA
Px2 Thermal Cycler	Thermo Electron Corporation, USA
Syringes	
1, 3, 5, 10, 20, and 60 mL	Terumo, Australia

SGE 100 L glass syringe	SGE Analytical Science, Australia
Transilluminator (Stern *et al*)	Novex, Australia
UVette® (10 mm)	Eppendorf, Germany
Vivaspin 20 5,000 Da MWCO Diafiltration cup	Sartorius-Stedim, Germany
Water bath	Ratek, Australia

3.2.3 General Materials and Suppliers

β-mercaptoethanol

Electrophoresis purity (BioRad Laboratories, USA).

Acetic Acid (glacial)

(Merck, Germany).

Acrylamide/bisacrylamide Solution

40% acryl/bis (Amresco, USA), stored at 4ºC.

Adenosine Triphosphate (ATP)

20 mM ATP (Sigma-Aldrich, Germany), stored at -20ºC.

Agarose

1.5-2.5 % (w/v) agarose, DNA grade (Bioline, England).

Ammonium Persulphate (APS)

10% (w/v) ammonium persulphate (Sigma-Aldrich, Germany), stored at 4ºC.

Bacteriological Agar

(Oxoid, England).

Bovine Serum Albumin (BSA)

1 – 10 mg/mL BSA (Promega, USA), aliquots stored at -20ºC.

Bromophenol Blue

(BDH, USA).

Ethanol

70% (v/v), 96% (v/v), 100% (v/v) (Merck, Germany).

Ethylenediaminetetra-aetate (EDTA)

0.5 M EDTA (Merck, Germany).

Ficoll 400

(BDH, USA)

Glycerol

10% (v/v) sterile glycerol (BDH, USA).

Hydrochloric Acid (HCl)

32% (Merck, Germany).

Lambda (λ) DNA

Stored at -20ºC (Promega, USA).

Methanol

100% (Merck, Germany).

Nickel Sulfate ($NiSO_4$)

0.2 M $NiSO_4$ (BDH, USA), filtered through a 0.45 µm filter.

Orange G

Signal-Aldrich, Germany

Phosphate Buffered Saline (PBS)

Phosphate buffered saline (PBS) was prepared by dissolving 1 tablet of pre-made PBS, obtained from Oxoid, in 100 mL distilled water. It was autoclaved and stored at 4ºC.

Phosphoric Acid

85% (Chem-Supply, Australia).

Sodium Acetate (NaOAc)

3 M NaOAc (pH 5.2) (BDH, USA).

Sodium Chloride (NaCl)

0.15 M to 5 M NaCl (BDH, USA).

Sodium Dodecyl Sulphate (SDS)

10% (w/v) (Merck, Germany)

Sodium Hydroxide (NaOH)

0.1 M NaOH (Merck, Germany).

Sulphuric Acid (H_2SO_4)

1 M sulphuric acid (BDH, USA).

Tris-Acetate-EDTA (TAE) Buffer (1x)

40 mM Tris-HCl (pH 8.0) (Merck, Germany), 20 mM acetic acid (Merck, Germany), 2 mM EDTA (Merck, Germany).

Tris Buffered Saline (TBS)

25 mM Tris-HCl (pH 7.4) (Merck, Germany), 0.18 M NaCl (BDH, USA).

Tris-Base

1.5 M Tris-base (Merck, Germany), adjusted to pH 8.8 with HCl.

Tris-HCl

1.0 M Tris-base (Merck, Germany), adjusted to pH 6.8 with HCl.

Tryptone

(Oxoid, England).

Yeast Extract

(Oxoid, England).

3.2.4 Bacteriological Materials

3.2.4.1 Antibiotic Stock Solutions

Antibiotic solutions were prepared by dissolving the antibiotics in appropriate solvents to the desired concentration. These stock solutions were stored at -20ºC after being filter sterilised. Antibiotic stock concentrations were as follows:

Ampicillin

Ampicillin (CSL, Australia) was prepared as a stock at 100 mg/mL in MQ water. It was sterilized by passing the solution through a 0.2 µm filter. Working concentration of 100 µg/mL, aliquots stored at -20ºC.

Chloramphenicol

Chloramphenicol (Sigma-Aldrich, Germany) was prepared as a stock at 34 mg/mL in 96% ethanol (Merck, Germany), filtered through a 0.45 µm filter. Working concentration of 34 µg/mL, aliquots stored at -20ºC.

Skirrows Antibiotic Supplement

Skirrows supplement was supplied by Oxoid and stored at 4ºC. Two millilitres of sterile MQ water was added into one 500 mg supplement vial and mixed with the media before dispensing.

3.2.4.2 General Media

All media were prepared according to manufacturer's recommendations unless specified in the text. Sterilisation was performed at standard conditions, 121ºC for 20 min unless stated otherwise. Media was dispensed into sterile Petri dishes in a laminar flow cabinet. The media plates were dried at 37ºC for 1 h before use unless agar with a moist surface was required.

Brucella Broth

Brucella broth powder (2.8% w/v) was dissolved in distilled water and sterilised by autoclaving under standard conditions.

Horse Blood Agar (HBA) with Skirrow's Supplement (HBA-Sk)

Columbia agar base (3.9% w/v) was dissolved in distilled water and sterilised by autoclaving under standard conditions. The sterile media was cooled to approximately 50ºC before the

addition of defibrillated horse blood (5% v/v) and one vial of Skirrow's selective supplement (Oxoid, England). Each vial of Skirrow's selective supplement contained 5 mg of vancomycin, 1250 i.u. of polymixin B and 2.5 mg of trimethoprim lactate. The media was mixed thoroughly and dispensed into Petri dishes.

Luria Bertani (LB) Agar

Tryptone (1% w/v) (Oxiod, England), yeast extract (0.5% w/v) (Oxiod, England), NaCl (0.5% w/v) (BHD, USA) and bacteriological agar (1.0% w/v) (Oxiod, England) were dissolved in distilled water and sterilised by autoclaving under standard conditions. The media was mixed thoroughly and dispensed into Petri dishes.

Luria Bertani (LB) Agar with Antibiotic(s)

Tryptone (1% w/v) (Oxiod, England), yeast extract (0.5% w/v) (Oxiod, England), NaCl (0.5% w/v) (BHD, USA) and bacteriological agar (1.0% w/v) (Oxiod, England) were dissolved in distilled water and sterilised by autoclaving under standard conditions. The sterile media was cooled to approximately 50ºC before adding antibiotic(s). The media was mixed thoroughly and dispensed into Petri dishes.

Luria Bertani (LB) Broth

Tryptone (1% w/v) (Oxiod, England), yeast extract (0.5% w/v) (Oxiod, England) and NaCl (0.5% w/v) (BHD, USA) were dissolved in distilled water and sterilised by autoclaving under standard conditions.

Luria Bertani (LB) Broth with Antibiotic(s)

Tryptone (1% w/v), yeast extract (0.5% w/v) and NaCl (0.5% w/v) were dissolved in distilled water and sterilised by autoclaving under standard conditions. The sterile media was cooled to approximately 50ºC before adding antibiotic(s). The media was mixed thoroughly and dispensed into Petri dishes.

Muller Hinton Agar

Muller Hinton agar powder (3.8% w/v) was dissolved in distilled water and sterilised by autoclaving under standard conditions.

Muller Hinton Broth

Muller Hinton broth powder (2.1% w/v) was dissolved in distilled water and sterilised by autoclaving under standard conditions.

SOC Media

Tryptone (2% w/v), yeast extract (0.5% w/v), 10 mM NaCl, 2.5 mM KCl, 10 mM $MgCl_2$ and 10 mM $MgSO_4$ were dissolved in distilled water and adjusted to pH 7.0 with NaOH. The media was then sterilised by autoclaving under standard conditions. Filter-sterilised 20 mM glucose is added prior to use.

Tryptone/Skim Milk Storage Media

Skim milk powder 10% (w/v), tryptone (1% w/v) and 10 mM Tris-base were dissolved in distilled water and adjusted to pH 7.5 with HCl. It was autoclaved at 109ºC for 10 min and stored at 4ºC.

3.2.5 Bacteriological Methods

3.2.5.1 Bacterial Strains, Plasmid and Culture Conditions

The *C. jejuni* NCTC 11168 (Bolton & Coates, 1983) and *C. jejuni* 81116 (Smith & Muldoon, 1974) are the strains used throughout this study. The *C. jejuni* strains were routinely grown on HBA or HBA/Skirrow plates, and incubated at 42ºC for 48-72 h under microaerophilic conditions. Microaerobic conditions were achieved by the use of an anaerobic jar and either a Campygen gas pack, or by the addition of a microaerobic gas mixture (CO_2 10%, O_2 5%,

N_2 85%). Selected colonies were sub-cultured onto fresh plates to form pure lawn cultures and incubated under the same conditions.

The *E. coli* strains used in throughout this study are *E. coli* BL21(DE3) (Invitrogen Corporation, USA) and *E. coli* DH5α (Hanahan, 1983). All *E. coli* strains were grown on LB Agar or in LB broth at 37ºC unless stated otherwise. The cells grown in LB broth were shaken on an orbital shaker at 200 revolutions per min (rpm). Appropriate antibiotics were added to the agar plates as per requirements of the various concentrations such as ampicillin at 100 µg /mL, and chloramphenicol at 34 µg/mL.

The plasmid vector used in this project is pRSET-A (Invitrogen Corporation, USA) and the vector map is shown in Figure 3.1.

3.2.5.2 Storage of Bacterial Strains

All *Campylobacter* strains were stored at -80ºC in tryptone/skim milk freezing medium. One millilitre of sterilised tryptone/skim milk storage media was added to one lawn subculture of each strain within 48 h of incubation. The colonies were mixed with the storage media using a sterile L-shaped spreader and the bacterial culture was collected into a sterile cryogenic vial for long-term storage.

All *E. coli* strains were stored at -80ºC in glycerol freezing medium. For short-term storage of these bacterial strains, strains were stored at 4ºC on appropriate media, supplemented with the appropriate antibiotics.

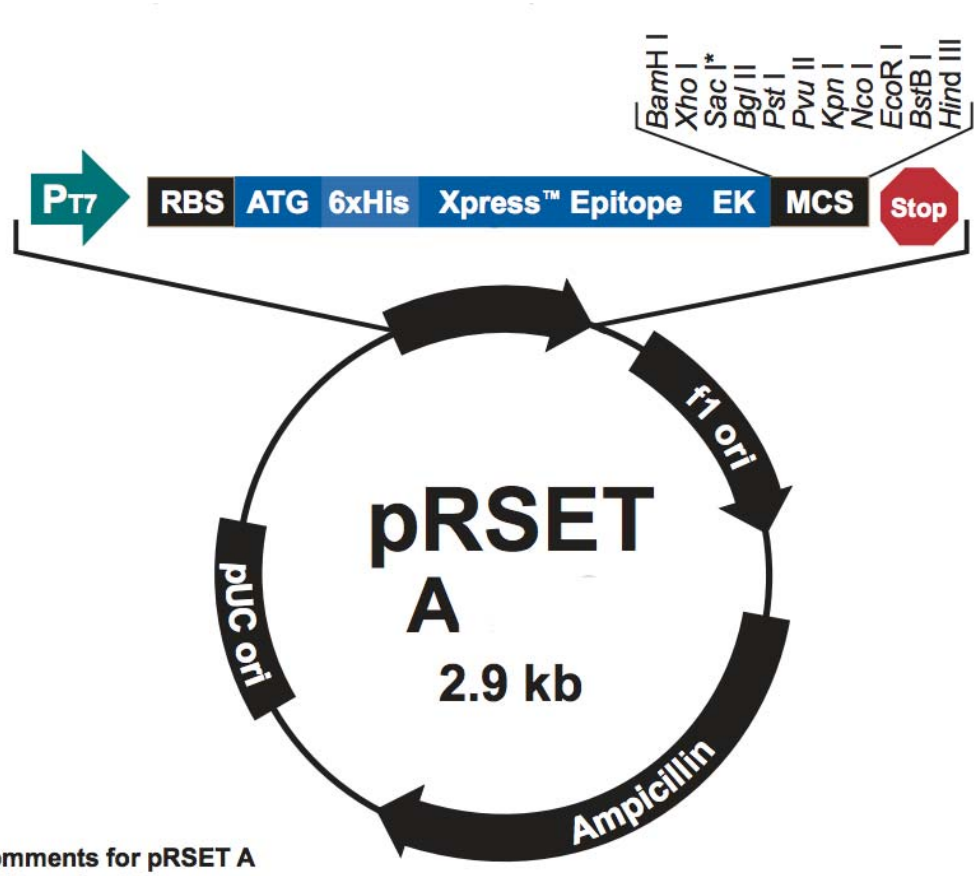

Comments for pRSET A
2897 nucleotides

T7 promoter: bases 20-39
6xHis tag: bases 112-129
T7 gene 10 leader: bases 133-162
Xpress™ epitope: bases 169-192
Multiple cloning site: bases 202-248
T7 reverse priming site: bases 295-314
T7 transcription terminator: bases 256-385
f1 origin: bases 456-911
bla promoter: bases 943-1047
Ampicillin (*bla*) resistance gene (ORF): bases 1042-1902
pUC origin: bases 2047-2720 (C)

Figure 3.1: Map of vector pRSET-A (Reproduced from Invitrogen, USA).

3.2.5.3 Preparation of Electrocompetent Cells

A single colony of *E. coli* was inoculated into 5 mL of LB broth and grown overnight at 37ºC on an orbital shaker. Two millilitres of an overnight *E. coli* culture was used to inoculate 200 mL pre-warmed LB broth and the cells were grown at 37ºC with vigorous shaking until an absorbance of 0.3 – 0.5 at 600 nm (OD_{600nm}) was achieved (early mid log phase). When the cells have reached this phase, the culture was divided into four 50 mL sterile Falcon tubes and chilled on ice for 30 min to slow down cell growth. Cells were harvested by centrifugation in a pre-chilled centrifuge for 15 min at 4,000 x *g* at 4ºC. The pellets were then resuspended in 50 mL ice-cold sterile MQ water and centrifuged at the same condition again. The cells were then resuspended in 25 mL ice-cold sterile MQ water and pelleted again. Finally, the *E. coli* cells were resuspended and combined in a total of 20 mL of ice-cold 10% sterile glycerol in MQ water and pelleted a final time. Ten per cent ice-cold sterile glycerol was added to a final volume of 50% of the cell pellet and divided into 50 µL aliquots and stored at -80°C for up to 6 months. Transformation efficiency was tested by adding 1 µg of undigested “empty” vector (miniprep sample) to a 50 µL vial of electrocompetent *E. coli* cells, and the cells were electro-transformed as described in the section below.

3.2.5.4 Electrotransformation

Briefly, 1-2 µL of purified plasmid DNA was added to 50 µL of pre-thawed electrocompetent *E. coli* cells prepared above. The cells and plasmid were transferred to an ice-cold sterile electroporation cuvette (Section 3.2.2). The cuvette was tapped lightly to settle the mixture to the bottom. Bubble present was removed before electrotansformation. The Gene Pulser setting used to deliver the DNA into the cell was set at 200 ohms, 25 µF capacitance, and 2.0-2.5 kV, with a 4-5 ms pulse. The sample was pulsed once and 1 mL of SOC medium or LB broth was immediately added to the cuvette to resuspend the cells. After transferring the medium to a 1.5 mL microfuge tube, samples were incubated on at 37ºC for 1 h with shaking. One hundred microliters of sample was plated onto LB agar containing the

appropriate antibiotics and incubated at 37ºC overnight. The remaining culture was centrifuged and the pellet was resuspended in 100 µL of SOC medium or LB broth, then spread onto LB agar containing the appropriate antibiotics and incubated at 37ºC overnight.

3.2.6 DNA Materials

3.2.6.1 General Reagents

11x DNA Loading Buffer

10% (w/v) Ficoll 400 (BDH, USA), 50% (v/v) glycerol (BDH, USA), 0.5% (w/v) Orange G (Sigma-Aldrich, Germany), 1% SDS (Merck, Germany), 10 mM EDTA (BDH, USA), 50 mM Tris-base (Merck, Germany), adjusted to pH 8.0 with HCl; stored at 4°C.

Ethanol

70 % (v/v) ethanol prepared from absolute ethanol (96%) commercial grade (Merck, Germany).

Ethidium Bromide

6 mg ethidium bromide (Sigma-Aldrich, Germany) in 2 L MQ water.

Glycerol

10-80% (v/v) glycerol, autoclaved.

Lambda(λ)-*Pst*I DNA Ladder

λ DNA (500 µg/mL) 100 µg, *Pst*I (10 U/µl) 100 U, 10x restriction enzyme Buffer H (90 µL), and MQ water were added to a final volume of 900 µL. The mixture was incubated overnight at 37ºC before the addition of 10x gel loading dye (100 µL) and stored at 4ºC. A diagram of *Pst*I digested λ-DNA is shown in Appendix 4.

MQ Water

Sterile MQ water (Millipore) or deionised water was used to prepare reagents.

Molecular Grade Water

Distilled water, DNAse-free and RNAse-free for PCR reactions and plasmid DNA methods.

Propan-2-ol (Isopropanol)

100% (v/v) Isopropanol.

Sodium Acetate (NaOAc)

3 M NaOAc (BDH, USA), adjusted to pH 4.6 with HCl, autoclaved.

Sodium Dodecyl Sulphate (SDS)

1-10% (w/v) SDS (Merck, Germany).

TAE Buffer

40 mM Tris-base, 20 mM glacial acetic acid, 2 mM EDTA.

TE Buffer, pH 8.0

10 mM Tris-base, 1 mM EDTA, adjusted to pH to 8.0 with HCl.

3.2.6.2 Commercial kits

DNA Sequencing Kit (ABI version 3.1)

Big Dye, 5x dilution buffer, stored at -20ºC (Monash University, Australia).

QIAprep Spin Miniprep Kit

(Qiagen, Germany).

Wizard® DNA Clean-up System Kit

(Promega, USA).

3.2.7 DNA Methods

3.2.7.1 Plasmid DNA Extraction (Mini Prep)

Plasmids were grown in *E. coli* DH5α and purified using the QIAprep Spin Miniprep kit (Qiagen, Germany) as per manufacturer's protocol. Briefly, template DNA was loaded and bound to a QIAquick spin column. The DNA was washed in the supplied wash buffer, eluted in MG H_2O and stored at −20ºC.

3.2.7.2 DNA Purification from PCR

Purification of DNA from PCR amplification was performed using the Wizard® DNA Clean-up System kit (Promega, USA) as per manufacturer's protocol. Briefly, PCR product was mixed with direct purification buffer and resin. The mix was then passed through a mini-column, washed in isopropanol and eluted in MG H_2O.

3.2.7.3 Agarose Gel Electrophoresis

Agarose gels (1.0%-2.0%) were used from DNA sample separation and visualisation. DNA sample (20 µL) was mixed with 2 µL of 11X DNA loading buffer before the gel electrophoresis. *λ-PstI* DNA ladder (10 µL) was loaded onto each gel. After electrophoresis, the gel was stained in a 3 mg/L ethidium bromide water bath for 5 min. The destaining process was followed as leaving under running water for 20-30 min. DNA products were visualized photographed using a BioRad GelDoc transilluminator.

3.2.7.4 Quantification of DNA Concentration

Concentration of the extracted plasmid DNA was measured by appropriate methods. The amount of plasmid DNA was either by comparing the intensity of sample DNA against the lambda *Pst*I digested molecular weight marker (50 µg/mL) (Appendix 4) on an agarose gel or by using the spectrophotometer. The purity of the sample was determined by ratio of ODs obtained at 260 nm and 280 nm (>1.8 for pure DNA) respectively.

3.2.7.5 Sequencing PCR

PCR was performed in a Px2 Thermal Cycler machine in sterile PCR tubes. Isolated plasmid DNA samples were used as templates for the PCR reaction. Sequence analysis of constructs was carried out with forward or reverse T7 promoter primers (Table 3.1). This analysis was performed to confirm the presence and orientation of inserts and to confirm all inserts were in frame with the start codon of the plasmid vector. PCR was performed using the protocol provided by Micromon DNA Sequencing Facility, Monash University, Melbourne, Australia. The details of the PCR setting and cycling conditions are stated in Table 3.2 and Table 3.3. The PCR products were sent to Monash University (Melbourne, Australia) for sequencing.

3.2.8 Protein Materials

3.2.8.1 General Materials

Ammonium Persulfate (APS)

10% (m/v) in MQ water

Blocking Buffer

5% (w/v) skim milk powder (Diploma, Australia) in TBS.

Table 3.1: Sequencing primers

Name	Sequence 5'-3'	Description
T7 Forward	TAATACGACTCACTATAGGG	Sequencing primer for pRSET-A
T7 Reverse	GCTAGTTATTGCTCAGCGG	Sequencing primer for pRSET-A

Table 3.2: Sequencing PCR setting

Sequencing reaction components	**Volume**
5 x Dilution Buffer	3 µL
T7 Forward Primer (50 ng/µL)	1 µL
T7 Reverse Primer (50 ng/µL)	1 µL
Template DNA	~ 300 ng
Big Dye	2 µL
MG H_2O	To 20 µL
Total Volume	**20 µL**

Table 3.3: Sequencing reaction cycling conditions

Stage	Details	Temperature	Time
Stage 1	Initial denaturation	96ºC	1 min
Stage 2	Denaturation	96ºC	10 sec
	Annealing	50ºC	5 sec
	Extension	60ºC	4 sec
	Number of cycles = 30		
Stage 3	Hold samples	4ºC	Indefinitely

Bradford Reagent

100 mg Coomassie Brilliant G-250 (Sigma-Aldrich, Germany) dye dissolved in 50 mL 95% (v/v) ethanol (Merck, Germany), then mixed with 100 mL 85% (v/v) phosphoric acid (Chem Supply, Australia), and brought up to 1 L with distilled water. Stored at 4°C and filtered through a 0.45 µm filter before use.

Buffer 1

0.1% sodium citrate (pH 4.5) (BDH, USA), 2.5% (w/v) Triton X-100 (Biorad Laboratories, USA).

Buffer 2

0.1% sodium citrate (pH 4.5) (BDH, USA). Dithiothreitol (DTT) (Molecular Biology Grade, Promega) was added to the concentration of 2mM just before use.

Chelating Sepharose™ Fast Flow

(GE healthcare, Sweden), charged with 0.2 M nickel sulphate ($NiSO_4$) (BDH, USA).

Coomassie Brilliant G-250

(Sigma-Aldrich, Germany).

Coomassie Blue Stain

Coomassie brilliant blue (R) powder (0.1% w/v) was dissolved in methanol (40% v/v) (BDH, USA), and glacial acetic acid (10% v/v) (Merck, Germany).

Destaining Solution

Ethanol (10% v/v) (Merck, Germany) and glacial acetic acid (10% v/v) (Merck, Germany) was prepared in MQ water.

Dithiothreitol (DTT)

1 M freshly made (Molecular Biology Grade, Promega) for every use.

Ethylenediaminetetra-aetate (EDTA)

0.5 M EDTA (Merck, Germany).

Gelatin Gel

125 mM Tris (pH 6.8) (Merck, Germany), 1% SDS (Merck, Germany), 12% bis/acrylamide (Amresco, USA), 0.1% (v/v) gelatin (Sigma-Aldrich, Germany) made up to volume with MQ water. APS 0.05% (w/v) (Sigma-Aldrich, Germany) and TEMED 0.1% (v/v) were added to polymerise.

iBlot Transfer Stacks

iBlot gel transfer stacks (nitrocellulose membrane), Regular (2 gels) or Mini (1 gel) (Invitrogen Corporation, USA).

IMAC Stripping Solution

0.5 M NaCl (BDH, USA), 50 mM EDTA (Merck, Germany).

Imidazole

5 M imidazole (Sigma-Aldrich, Germany), filtered through a 0.45 µm filter, stored at 4ºC in the dark.

IPTG Solution

Isopropylthio-β-D-galactosidase (IPTG; 24 mg/mL) was dissolved in water, filter sterilised and stored at -20ºC.

Resolving Gel

Tris-HCl pH 8.8 (375 mM) (Merck, Germany), SDS (0.1% w/v) (Merck, Germany), bis

acrylamide (12.5% v/v) (Amresco, USA) was prepared with MQ water. The setting agents ammonium persulfate (0.06% w/v) (Sigma-Aldrich, Germany) and TEMED (0.03% v/v) (BioRad Laboratories, USA) was added to the gel solution and mixed via inversion just prior to pouring.

Non-reducing Loading Buffer (5X)

60 mM Tris (pH 6.8), 25% (v/v) glycerol (BDH, USA), 2% (w/v) SDS (BDH, USA), 0.1% (w/v) bromophenol blue (Sigma-Aldrich, Germany).

Precision Plus Protein™ Kaleidoscope™ Prestained Standard

10 µL per well (BioRad Laboratories, USA), stored at -20ºC.

Precision Plus Protein™ Unstained Standards

10 µL per well (BioRad Laboratories, USA), stored at -20ºC.

Protein Binding Buffer

50 mM Tris-HCl (pH 8.0) (Merck, Germany), 150 mM NaCl (BDH, USA), 10 mM imidazole (Sigma-Aldrich, Germany), prepared before use.

Protein Elution Buffer

50 mM Tris-HCl (pH 8.0) (Merck, Germany), 150 mM NaCl (BDH, USA), 100 mM – 200 mM Imidazole (Sigma Aldrich, Germany), prepared before use.

Protein Loading Buffer (5 x)

Protein samples were loaded on to polyacrylamide gels in 1x protein loading buffer. The buffer contained 60 mM Tris-HCl (Merck, Germany), 25% (v/v) glycerol (BDH, USA), 2% (w/v) SDS (Merck, Germany), 1.4 mM 2-mercaptoethanol (BioRad Laboratories, USA), 0.1% (w/v) bromophenol blue (Sigma-Aldrich, Germany) in MQ water and stored at -20ºC.

Protein Lysis Buffer

50 mM Tris-HCl (pH 8.0) (Merck, Germany), 150 mM NaCl (BDH, USA), 20 mM imidazole (Sigma-Aldrich, Germany), 1 mg/mL lysozyme (Amresco, USA), prepared before use.

Protein Post-Sample Wash Buffer

50 mM Tris-HCl (pH 8.0) (Merck, Germany), 150 mM NaCl (BDH, USA), with 20 mM imidazole, prepared before use.

Proteinase K (100X)

300 U/mL dissolved in MQ water (Sigma-Aldrich, USA).

SDS-PAGE Running Buffer (1 x)

3% (w/v) Tris-HCl (Merck, Germany), 14.2% (w/v) glycine (Amresco, USA), 1% (w/v) SDS (Merck, Germany).

Skim Milk Powder

(Diploma, Australia).

Sodium Citrate

1% (w/v) (Merck, Germany) in distilled water and adjusted to pH 4.5.

Sodium Dodecyl Sulphate (SDS)

10% (w/v) (Merck, Germany)

Sodium Hydroxide (NaOH)

0.1 M NaOH (Merck, Germany).

Stacking Gel

The 4.5% stacking gel contained 125 mM Tris-HCl pH 6.8 (Merck, Germany), 0.1% (w/v)

SDS (Merck, Germany) and 4.5% bis-acrylamide (Amresco, USA) in MQ water. Just prior to pouring, 0.06% (w/v) ammonium persulfate (Sigma-Aldrich, Germany) and 0.03% (v/v) TEMED (BioRad Laboratories, USA) was added to the gel solution and mixed via inversion. The gel was then poured to overlay the set resolving gel.

Sulphuric Acid (H_2SO_4)

1 M sulphuric acid (BDH, USA).

TEMED (N,N,N',N'-tetramethylethylenediamine)

Electrophoresis purity (BioRad Laboratories, USA).

Whole Cell Lysis Buffer

0.1 M Tris-HCl (pH 8.0) (Merck, Germany), 2% (w/v) SDS (Merck, Germany), 15% (v/v) glycerol (BDH, USA).

3.2.8.2 Antibodies and Substrate

Chloronapthol Substrate Solution

Thirty micrograms of Chloronapthol (Sigma-Aldrich, Germany) and 10 mL methanol were mixed and made up to 50 mL with TBS. Thirty microliters of hydrogen peroxide (BDH, USA) was added just before developing. The solution was protected from light.

Primary Antibody

Monoclonal mouse anti-polyHistidine antibody IgG (GE Healthcare, Sweden) diluted 1:3000 with 1% (w/v) skim milk in TBS; stored at -20ºC.

Secondary Antibody

Goat anti-mouse IgG conjugated to horseradish peroxidase (HRP) (Abcam, England) diluted 1:5000 with 1% (w/v) skim milk in TBS; stored at -20ºC.

3.2.9 Protein Methods

3.2.9.1 Pilot Expression Study

After *E. coli* BL21(DE3) pRSET-A/*cj0391c* was grown overnight on LB agar containing ampicillin and chloramphenicol, a single colony was inoculated into 5 mL of LB broth containing the same antibiotics and incubated overnight at 37ºC with shaking at 200 rpm. Then, 0.5 mL of the overnight seed culture was inoculated into 50 mL of fresh LB broth and incubated at 37ºC with shaking until an OD of 0.4 – 0.7 at 600 nm was reached. Two millilitre volume of culture was taken before a final concentration of 1 mM IPTG was added to the remaining culture. Two millilitre aliquots were taken at 1–5 h and overnight after IPTG induction. Each cell pellet collected at the different time points were washed twice in 2 mL of 10 mM Tris-HCl (pH 8.0), resuspended in 1 mL protein lysis buffer and stored on ice until all samples were collected and prepared for sonication. All *E. coli* samples were lysed by sonication (Branson Sonic Power Co., USA) on ice at 27% for 3 cycles of 15 sec pulses with 30 sec rests between each pulse.

3.2.9.2 Protein Expression and Cell Lysate Preparation

For protein expression, fresh overnight-incubated seed culture was prepared each time for the IPTG induction on the following day. Two microlitres of seed culture was added into 200 mL of fresh LB broth in a 1 L flask containing 100 µg/mL of ampicillin and 34 µg/mL of chloramphenicol. The cells grown at 37ºC with shaking at 200 rpm until an OD of 0.4 – 0.7 at 600 nm was reached. A final concentration of 1 mM IPTG was added and protein expression was induced at 37ºC for the optimal time.

Following induction of expression, cells were harvested by centrifugation at 4,700 x *g* for 15 min at 4ºC in 50 mL Falcon tubes. The cell pellets were washed twice with 50 mL of 10 mM

Tris-HCl (pH 8.0). After washing, cells were resuspended in 5 mL of the protein lysis buffer and the sonicated (Branson Sonic Power Co., USA) on ice at 35% for 3 cycles of 15 s pulses with 30 s rest between each pulse.

3.2.9.3 Immobilised Metal Affinity Chromatography (IMAC)

(A) IMAC column preparation

Ten millilitres of thoroughly mixed Chelating Sepharose Fast Flow resin slurry (containing 20% ethanol) was added to a 5 mL gravity flow column. The resin was allowed to settle at the pre-marked 5 mL column level. The column was then washed with 10-column volume (CV) of MQ water to remove the ethanol. The gravity flow column was charged before use by passing 2.5 CV of 0.2 M nickel sulphate ($NiSO_4$) (Ni^{2+}) through the column, and then washed with at least 10 CV of MQ water to remove unbound metal ions and equilibrated with 5 CV of binding buffer just before usage.

(B) IMAC purification

The whole cell lysate was centrifuged in 1.5 mL microfuge tubes at 12,100 x *g* for 5 min at RT and the supernatant was filter sterilised before purification. Five millilitres of soluble cell lysate containing expressed recombinant protein was loaded to a pre-equilibrated IMAC column and incubated for 1 h with horizontal shaking at 4ºC to allow complete binding of the polyHistine-tagged protein to the nickel-bound resin.

The column was then returned to the vertical position and allowed to settle for 15 min before 5 mL of crude eluant was collected. The column was then washed with 5 CV of post-sample wash buffer and the flow-through eluant containing unbound protein was collected in 10 mL fractions and analysed for unbound protein via the Bradford Assay (Section 3.2.7.5). The nickel-bound polyHistidine-tagged protein was then eluted with 5 CV of EB containing

increasing concentrations of imidazole and the flow through was collected in 5 mL aliquots. Samples were analysed by SDS-PAGE (Section 3.2.7.6).

(C) IMAC column cleaning and regeneration

IMAC columns were re-used up to 4 times. Each time after usage, the column was stripped and cleaned. The column was stripped with 5 CV of IMAC stripping solution to elute the nickel. Residual EDTA from the stripping solution was then removed with 5 CV of 1 M NaOH, 5 CV of MQ water and 5 CV of 2 M NaCl. The column was finally washed with 5 CV of MQ water and stored in 20% ethanol at 4ºC. The column was recharged with nickel before usage.

3.2.9.4 Protein Concentration and Buffer Exchange

IMAC purified protein was concentrated using a centrifugal device, which concentrates the sample and removes the leftover small molecular weight un-specific proteins. Buffer exchange was performed afterwards to replace the EB with PBS. A Vivaspin 20 (5 kDa MWCO) centrifugal device was pre-conditioned twice with 10 mL MQ water. Then the EB contains protein was added into the top section of the Vivaspin 20. Centrifugation was performed at 5,000 x *g* for 10 min at 4ºC. The protein EB was allowed to filter through the device until less than 2 mL of solution remained on the top of the device. Then, 10 mL of PBS was added to the difiltration cup that has been inserted into the device. Centrifugation was repeated in 10 min intervals, until the volume of protein (in PBS) was reduced to less than 1 mL. Two times buffer exchanges were performed for each sample. The protein in PBS was then transferred from the device to a 1.5 mL microfuge tube and stored at -80ºC.

3.2.9.5 Bradford Assay

The protein concentration was determined using the Bradford method (Bradford, 1976). BSA ranging from 0 to 20 µg per 100 µL of 0.15 M NaCl was used to prepare protein standards. Ten microlitres of sample was made up to 100 µL with 0.15 M NaCl. Nine-hundreds microliters (900 µL) of Bradford reagent (Section 3.2.8.1) was added into sample and standards, which were mixed well and allowed to stand for 5 min at RT. Two hundred microlitres aliquots of each mixed sample was added to the wells of a 96-well microtitre plate in duplicate. Standards and samples absorbance were read at 600 nm with an iMark microplate absorbance reader. A standard curve, constructed by plotting the concentrations of the BSA standards (µg) versus absorbance, was used to determine the sample protein concentration.

3.2.9.6 SDS-PAGE with Coomassie Blue Stain

Proteins were separated by one-dimensional SDS-PAGE using a discontinuous buffer system. After the 12.5% resolving gel had set, the 4.5% stacking gel was then layered over the top of the resolving gel and a 12-comb cast inserted between the glass slides to form the wells. The protein gel system was assembled as per manufacturer's protocol (BioRad Laboratories, USA), and then placed within the gel tank containing 1x SDS-PAGE running buffer. Protein samples were mixed with 5x SDS sample loading buffer, heated to 100ºC in a dry heating block for 5 min, and then loaded onto the gel together with a Precision Plus Protein™ Standard (Appendix 5). The prestained Kaleidoscope™ protein standard (Appendix 5) was used if the gel was then used to do immunoblotting. Unstained Precision Plus Protein™ standard was used for gels stained by coomassie blue stain. Electrophoresis was performed at 60 V for 30 min, and then 180 V for 50 min.

On the completion of electrophoresis, the glass plates were separated and a scalpel blade was employed to cut off the stacking gel region. The gel was transferred to a square plastic container, then 25 mL of coomassie gel stain was added and the container was left overnight on a rotating shaker. After overnight staining, the coomassie was removed and replaced with 25 mL of destain solution. The destaining process was performed for 3 h with shaking and stopped by replacing the solution with distilled water.

3.2.9.7 Gelatin gel

Gelatin gels were made using gelatin gel buffer. Protein samples were mixed with non-reducing loading buffer and incubated at 37ºC for 15 min. Electrophoresis was performed at 160 V for 2 h at 4ºC, with pre-chilled SDS-PAGE running buffer. Gelatin gels were then transferred into 100 mL of buffer 1 (Section 3.2.8.1). The gels were incubated in buffer 1 for 20 min at RT with gentle shaking. The buffer was changed and incubation step repeated once. After incubated in buffer 1, the gels were then incubated in 100mL buffer 2 (Section 3.2.8.1) for 5 min with shaking at RT. The buffer was changed and the incubation repeated twice. The final incubation was performed at 37ºC for 12-24 h with gentle shaking. These gels were stained using coomassie blue staining after incubation. Unstained area indicates the presence of proteolytic activity.

3.2.9.8 Immunotransfer

Western blotting was employed to transfer proteins from a SDS-PAGE gel onto a nitrocellulose membrane. After completion of electrophoresis, the gel was removed from the glass plates and the stacking gel was discarded. The iBlot dry blotting system was used according to the manufacturer's instructions. The order of materials used to set up the iBlot system is shown below built from the anode stack at the bottom: (1) Anode stack (bottom); (2) Protein SDS-PAGE gel; (3) Filter paper (pre-soaked in distilled water); (4) Cathode stack (top); (5) Disposable sponge. The cassette was closed after air bubbles were removed from

the gel and filter paper. The transfer was performed in 7 min (Program 3). After immunotransfer was complete, the nitrocellulose membrane was maintained for immunoblotting.

3.2.9.9 Immunoblotting

The nitrocellulose membrane was firstly blocked in blocking buffer (Section 3.2.8.1) for 1 h after immunotransfered. A rotating shaker was used for all incubations and washes during immunoblotting. The membrane was then washed twice in 15 mL TBS for 2 min (each time), and then the primary antibody (Section 3.2.8.1) was added to the nitrocellulose membrane and left for 3 h at RT (or overnight at 4ºC). The membrane was then washed twice in 15 mL TBS for 5 min (each time), and the secondary antibody conjugated with HRP was added and incubated at RT for up to 2 h (or overnight at 4ºC). The membrane was washed three times in 15 mL TBS for 5 min (each time) before developing in 50 mL chloronapthol substrate solution for 30 min in dark, or until the desired resolution was achieved. The membrane was washed with distilled water to stop the reaction.

3.2.10 Tissue Culture Materials

3.2.10.1 Cell Lines

Chicken macrophage cell line HD11 was used for *in vitro* analysis, obtained from RMIT central stock stored in liquid nitrogen. Cell lines were confirmed as mycoplasma free by performing dark field microscopy and samples were prepared by the instructions provided in the RMIT tissue culture manual.

3.2.10.2 Media and Solutions

All solution and MQ water used for tissue culture have been autoclaved twice before usage unless stated otherwise.

3-(4, 5-dimethylthiazolyl-2)-2, 5-diphenyltetrazolium bromide (MTT) Solution

To 100 mL of PBS, 0.5 g of MTT (Sigma-Aldrich, USA) was added and filter sterilised though a 0.2 µm filter and store in dark at 4ºC (for use up to 3 months).

4-(2-hydroxyethyl)-1-piperazineethanesulfonic acid (HEPES)

1 M (Invitrogen Corporation, USA), stored at 4ºC.

Annexin & Propidium Iodide (PI) Master Mix

50 µL of Annexin (Invitrogen Corporation, USA) and 30 µL of PI (Invitrogen Corporation, USA) were mixed with 1.92 mL of annexin binding buffer.

Annexin Binding Buffer

400 µL of 5 X Annexin Binding Buffer (Invitrogen Corporation, USA) was mixed with 1.6 mL MQ water.

Fetal Bovine Serum (FBS)

Heat inactivated FBS was added to medium to a final concentration of 10% (v/v) (LifeTechnologies, USA).

Gentamycin

5 mg/mL filter sterilised and stored at -20ºC (Sigma-Aldrich, USA).

Roswell Park Memorial Institute (RPMI) 1640 medium, GLUTAMAX®

To 500 mL of RPMI (Invitrogen Corporation, USA), 5.81 mL of 1M HEPES buffer, 5.81 mL of

Pen/Step solution, 5.81 mL of 5 mg/mL gentamycin and 5.81 mL of 0.1 M sodium pyruvate were added by direct filter sterilisation. Aliquots were stored at 4ºC. Fresh aliquots of RPMI supplemented with 10% v/v FBS were used for cultures.

MTT Solvent

196 µL of HCl (purity 32%) was added to 50 mL DMSO.

Pen/Strep

100 U penicillin/mL and 100 µg streptomycin/mL (Sigma-Aldrich, USA).

PI Working Stock

10 µL of 1 mg/mL PI (Invitrogen Corporation, USA) was added into 90 µL of sterilised MQ water.

Trypan Blue Solution

1 % (w/v) trypan blue (Sigma-Aldrich, USA) dissolved in sterile PBS.

Trypsin Solution

Trypsin/EDTA is used to dissociate cells and stored at -20ºC (Sigma-Aldrich, USA).

3.2.11 Tissue Culture Methods

All the tissue culture steps have been carried out in a class II biohazard cabinet unless stated otherwise.

3.2.11.1 Tissue Culture Techniques

Chicken macrophage cell line HD11 was stored in liquid nitrogen and maintained in RPMI containing 10% FBS, antibiotics (100 U/mL penicillin, 100 µg/mL streptomycin and 0.05 mg/mL gentamycin), and 1 mM sodium pyruvate at 42ºC, 5% CO_2, and 95% humidity. Cultures were grown to exponential phase (~ 80% confluent) before they were passaged either transferred to a larger flask or used experimentally. The cells were passaged no more than 15 - 20 times before a fresh stock of cells were resuscitated. Cultures were passaged by removing the media and washing the cells twice in PBS. An appropriate volume of trypsin solution was added and the flask was incubated at 42ºC for 5-10 min in 5% CO_2. The dissociated cells were removed from the flask and the action of the trypsin was countered by the addition of RPMI containing 10% FBS. The cells were washed twice in media and an appropriate volume of cells were used to seed a new flask or flasks. Cells were stored in liquid nitrogen by dissociating them and washing them as described above, then resuspending them in media supplemented with 10% DMSO as a cryoprotectant. A 75 cm^2 flask of ~80% confluent cells was used to bank down 2 cryovials each containing 1 mL of cell suspension. The cells were first incubated at -80ºC for 2 days before transferring to liquid nitrogen for long term storage.

3.2.11.2 Cell Proliferation Assay

Chicken macrophage cells were cultured in 75 cm^2 tissue culture flask until 80% confluent was achieved. The cells were then seeded into a 96-well microtitre plate at the concentration of 10^5 cells/mL with the volume of 100 µL in each well. The plate was then incubated at 42ºC overnight to form a monolayer. After overnight incubation, 10 µL of filter sterilised samples in PBS were added into the wells (Figure 3.2). Controls include cells that were not exposed to any of the protein as well as positive controls (soluble fraction of *C. jejuni* 81116 cells) and

	1	2	3	4	5	6	7	8	9	10	11	12
A	Control 1	Control 2	Control 3	Sample 1	Sample 2	Sample 3	Neg. control 1	Neg. control 2	Neg. control 3)	Pos. control 1	Pos. control 2	Pos. control 3
B	Control 1	Control 2	Control 3	Sample 1	Sample 2	Sample 3	Neg. control 1	Neg. control 2	Neg. control 3	Pos. control 1	Pos. control 2	Pos. control 3
C	Control 1	Control 2	Control 3	Sample 1	Sample 2	Sample 3	Neg. control 1	Neg. control 2	Neg. control 3	Pos. control 1	Pos. control 2	Pos. control 3
D												
E	Base Line											
F	Base Line											
G	Base Line											
H												

Figure 3.2: Cell proliferation assay plate setup.

Control 1: PBS 10 µL

Control 2: PBS 10 µL

Control 3: PBS 10 µL

Sample 1: 1 µg of recombinant protein Cj0391c in 10 µL of PBS

Sample 2: 2 µg of recombinant protein Cj0391c in 10 µL of PBS

Sample 3: 4 µg of recombinant protein Cj0391c in 10 µL of PBS

Negative control 1: 1 µg of recombinant protein GFP in 10 µL of PBS

Negative control 2: 2 µg of recombinant protein GFP in 10 µL of PBS

Negative control 3: 4 µg of recombinant protein GFP in 10 µL of PBS

Positive control 1: 1 µg of soluble fraction of *C. jejuni* 81116 protein in 10 µL of PBS

Positive control 2: 2 µg of soluble fraction of *C. jejuni* 81116 protein in 10 µL of PBS

Positive control 3: 4 µg of soluble fraction of *C. jejuni* 81116 protein in 10 µL of PBS

Baseline: Chicken macrophage HD11 cells only

negative controls (GFP expressed using the same system). Each sample was tested in triplicates.

After the cells were incubated with the samples for the time required, the plate was taken out and 20 µL of MTT solution was added into each well with light protection. The plate was wrapped with foil and shaken gently on a rotating shaker for 5 min. The plate was then returned to the CO_2 incubator and processed for another 2 to 4 h. After the purple precipitate is visible, the overlaying medium was removed carefully and 100 µL of MTT solvent was added into each well to dissolve the formazan product. The plate was read by an iMark microplate absorbance reader, and OD_{600} recorded for each well.

3.2.11.3 Apoptosis Assay

Dead Cell Apoptosis Kit with Annexin V Alexa Fluor® 488 & Propidium Iodide (PI) Kit (Invitrogen Corporation, USA) has been employed for this study. Chicken macrophage cells were cultured in 75 cm^2 tissue culture flask first until 80% confluent was reached. The cells were then seeded into a 24-well microtitre plate at a concentration of 10^5 cells/mL with the volume of 500 µL in each well. The plate was then incubated at 42ºC overnight to form a monolayer.

Subsequently, 50 µL of filter sterilised samples in PBS together with negative control (green fluorescent protein/GFP expressed using the same system) were added into the wells (Figure 3.3). Every sample has been tested in triplicates. Fifty microliters of 96% ethanol was added to the positive control wells half hour before the start of the staining procedure.

The cells were first washed in pre-chilled PBS before the addition of 200 µL Annexin and PI master mix into each test well in the dark The plate then was returned to the CO_2 incubator and processed for another 15 min. The cells were washed 3 times with pre-chilled PBS with

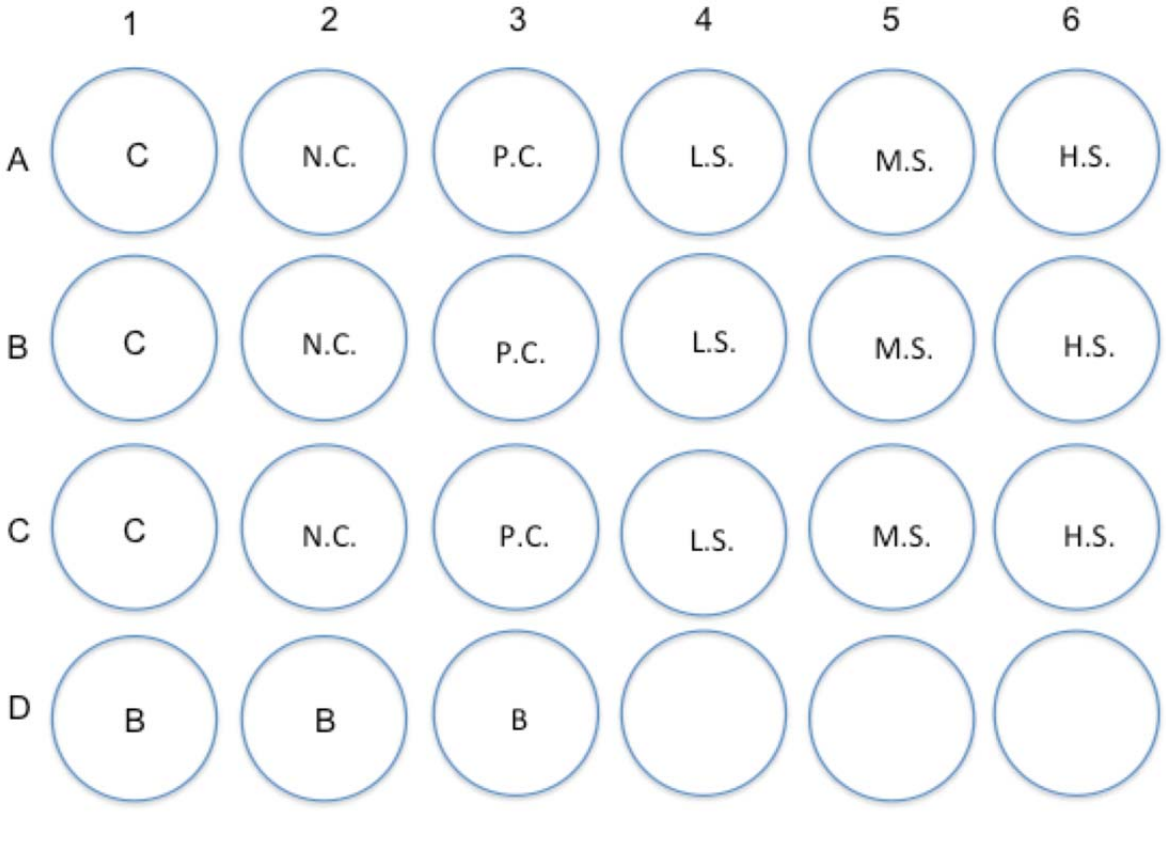

Figure 3.3: Apoptosis assay sample plate setup

B: Baseline (Chicken macrophage HD11 cells only)

C: Control (50 µL of PBS only)

N.C.: Negative Control (10 µg of recombinant GFP in 50 µL of PBS per well)

P.C.: Positive Control (50 µL of 96% Ethanol)

L: Low conc. of sample (2.5 µg of recombinant protein Cj0391c in 50 µL of PBS per well)

M: Med. conc. of sample (5 µg of recombinant protein Cj0391c in 50 µL of PBS per well)

H: High conc. of sample (10 µg of recombinant protein Cj0391c in 50 µL of PBS per well)

a final volume of 200 µL of PBS added to each well. Confocal imaging of cells was carried out with a Nikon Eclipse Ti-E A1 laser-scanning confocal system (Nikon Instrument Inc, USA), using the 100X and 200X objectives.

3.3 Results

3.3.1 Protein Expression and Purification

According to the protein pilot expression study, the optimal conditions for protein Cj0391c expression is incubation with 1mM IPTG at 37ºC for 5 h (Figure 3.4). The recombinant protein was then isolated by using nickel affinity chromatography (Section 3.2.7.3). The optimal imidazole concentration to elute the target protein Cj0391c is 140mM and the results are shown in Figure 3.5.

GFP was employed as a negative control in both the chicken macrophage cell proliferation assay and apoptosis assay. The optimisation study has also been done for *E. coli* BL21(DE3) pREST-A/GFP. For GFP expression, the cells show the best expression profile in the presence of 0.01 mM IPTG when incubated overnight at 37ºC. The GFP was also purified using the IMAC columns (Section 3.2.7.3), and the imidazole concentration required in order to elute the bound GFP was 200 mM (Figure 3.6).

For the expression of the recombinant protein Cj0391c, the target protein concentration did not increase significantly after 5 h and the yield has never reached the production level of GFP. One possible reason for this is that Cj0391c is a toxin, which may reduce the expression level in *E. coli* BL21(DE3).

3.3.2 Protease Assay

In section 2.3.5, protein Cj0391c has been predicted to be a protease by webserver EzyPred, and this was assayed by running a gelatin gel to detect gelatinase activity. Protease K was

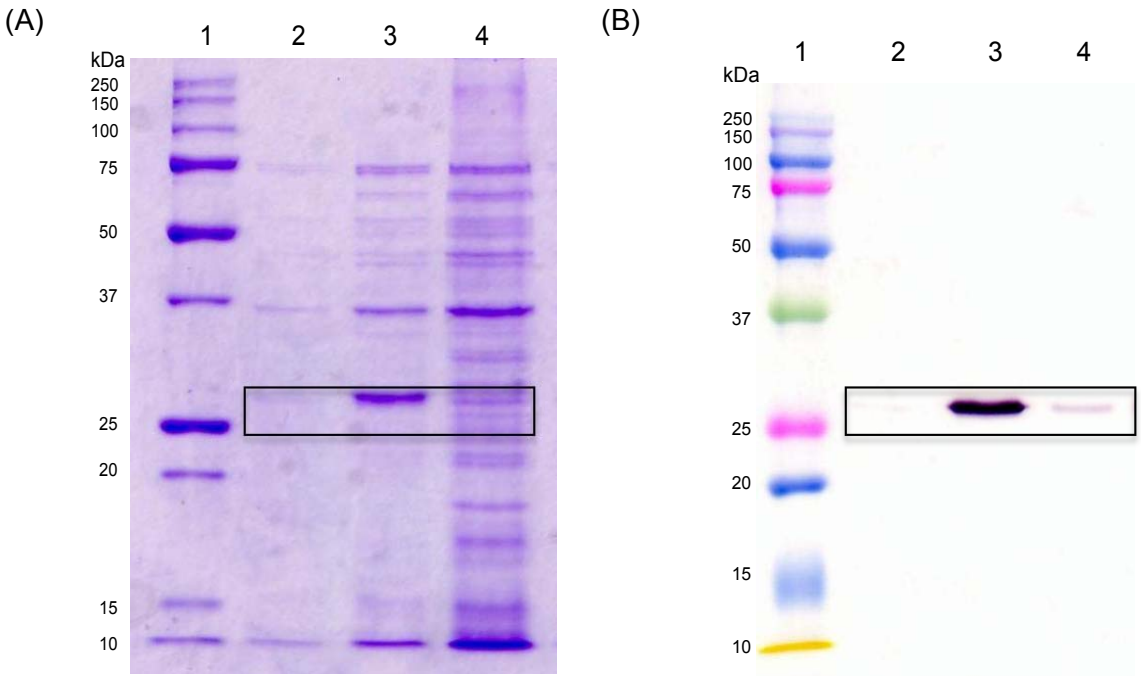

Figure 3.4: SDS-PAGE and immunoblotting analysis of soluble fractions of *E. coli* BL21(DE3) cells protein expression system containing the pRSET-A/*cj0391c* insert at different time points with 1 mM IPTG induction at 37ºC

(A) Lane 1. Precision Plus Protein™ Unstained Standard

Lane 2. Soluble fraction of pre-IPTG induction

Lane 3. Soluble fraction of 5 h 1 mM IPTG induction

Lane 4. Soluble fraction of overnight 1 mM IPTG induction

(B) Lane 1. Precision Plus Protein™ Kaleidoscope™ Standard

Lane 2. Soluble fraction of pre-IPTG induction

Lane 3. Soluble fraction of 5 h 1 mM IPTG induction

Lane 4. Soluble fraction of overnight 1 mM IPTG induction

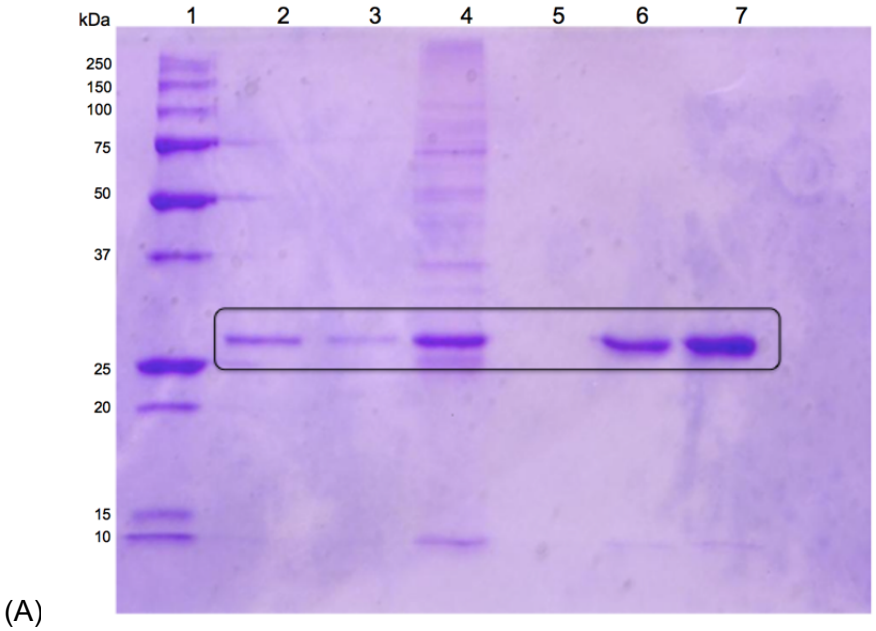

(A)

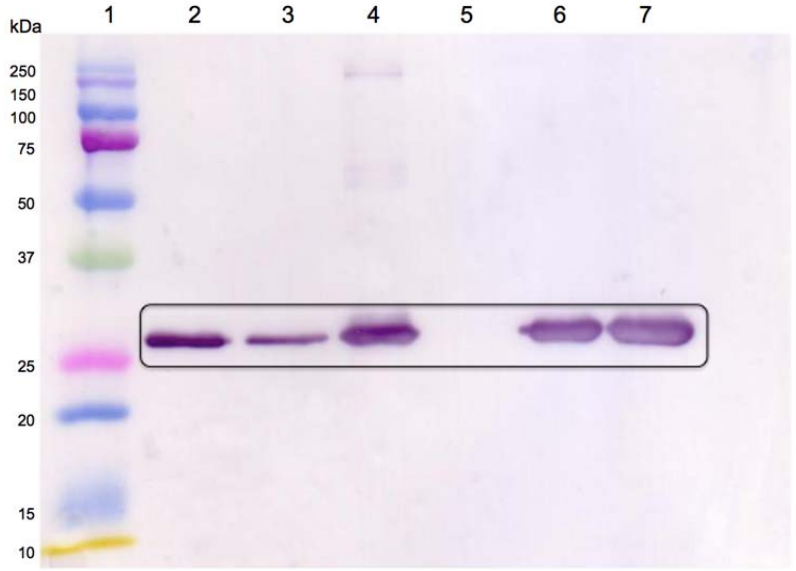

(B)

Figure 3.5: SDS-PAGE and immunoblotting analysis of recombinant protein Cj0391c post IMAC purification, concentration and buffer exchange

Lane 1 (A) Precision Plus Protein™ Unstained Standard

(B) Precision Plus Protein™ Kaleidoscope™ Standard

Lane 2 IMAC-purified bound-protein Cj0391c from the first 5 eluants

Lane 3 IMAC-purified bound-protein Cj0391c from the 6st eluant

Lane 4 Soluble fraction before IMAC-purification

Lane 5 Flow-through from Vivaspin (5 kDa cut-off)

Lane 6 Concentrated sample protein from Vivaspn

Lane 7 Concentrated and buffer exchanged protein Cj0391c in PBS

(A)

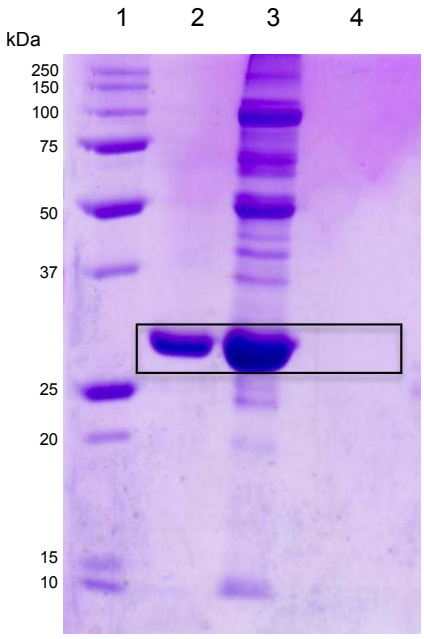

(B)

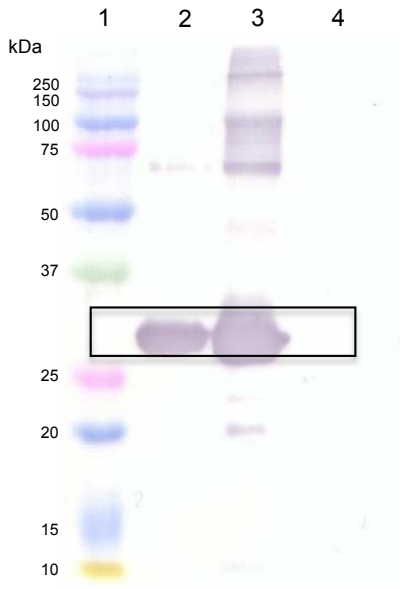

Figure 3.6: SDS-PAGE and immunoblotting analysis of recombinant protein GFP after IMAC purification, concentration and buffer exchange

Lane 1 (A) Precision Plus Protein™ Unstained Standard

(B) Precision Plus Protein™ Kaleidoscope™ Standard

Lane 2 Concentrated and buffer exchanged protein GFP in PBS

Lane 3 Total fraction of *E. coli* BL21(DE3) pREST-A/GFP overnight with 0.01 mM IPTG induction

Lane 4 Flow-through from Vivaspin (5 kDa cut-off)

used as a positive control. The gelatin gel can be seen in Figure 3.7. No discernable protease activity has been observed and from the result, it can be conclude that recombinant protein Cj0391c is most likely not a protease.

3.3.3 Cell Proliferation Assay

This assay measures the cell proliferation rate and conversely, when metabolic events lead to apoptosis, the reduction in cell viability. Measurement of cell viability and proliferation forms the basis for numerous *in vitro* assays of a cell population's response to external factors. The reduction of tetrazolium salts is now widely accepted as a reliable way to examine cell proliferation. The yellow tetrazolium MTT is reduced by metabolically active cells, in part by the action of dehydrogenase enzymes, to generate reducing equivalents such as nicotinamide adenine dinucleotide and nicotinamide adenine dinucleotide phosphate (Mosmann, 1983). The resulting intracellular purple formazan was solubilized and quantified by spectrophotometer. The chicken macrophage HD11 cells were used for the cell proliferation assay and results are shown in Figure 3.8. The HD11 cells viability was reduced after 72 h and 96 h incubation by approximately 75% and 90% respectively, which suggests the possible role of recombinant protein Cj0391c in reducing the chicken macrophage cells HD11 viability.

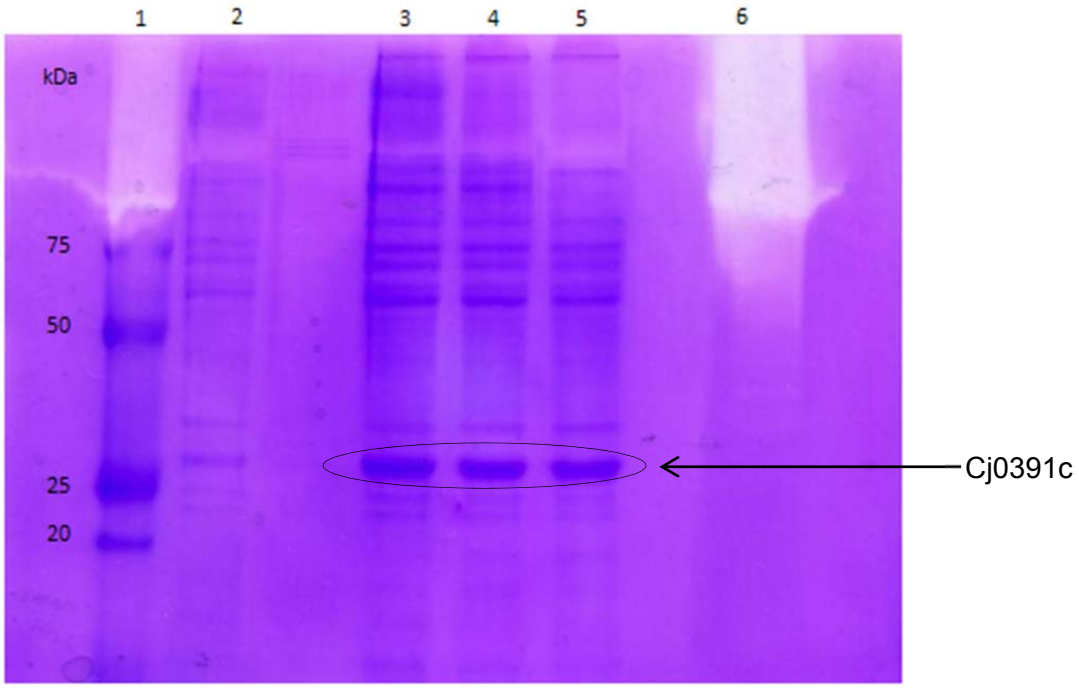

Figure 3.7: Gelatin gel of *E. coli* BL21(DE3) pRSET-A/Cj0391c expressed protein sample. Result indicates that no discernable protease activity of recombinant protein Cj0391c has been observed. Recombinant protein Cj0391c is most likely not a protease.

Lane 1: Precision Plus Protein™ Unstained Standard with molecular sizes listed.

Lane 2: Total fraction of *E. coli* BL21(DE3) pRSET-A/Cj0391c protein expression before IPTG-induction.

Lane 3: Total fraction of *E. coli* BL21(DE3) pRSETA/Cj0391c protein expression after 5 h IPTG-induction.

Lane 4: Soluble fraction of *E. coli* BL21(DE3) pRSETA/Cj0391c protein expression after 5 h IPTG-induction.

Lane 5: Filtered (0.2 µm) Soluble fraction of *E. coli* BL21(DE3) pRSETA/Cj0391c protein expression after 5 h IPTG-induction.

Lane 6: Positive control Proteinase K

(A)

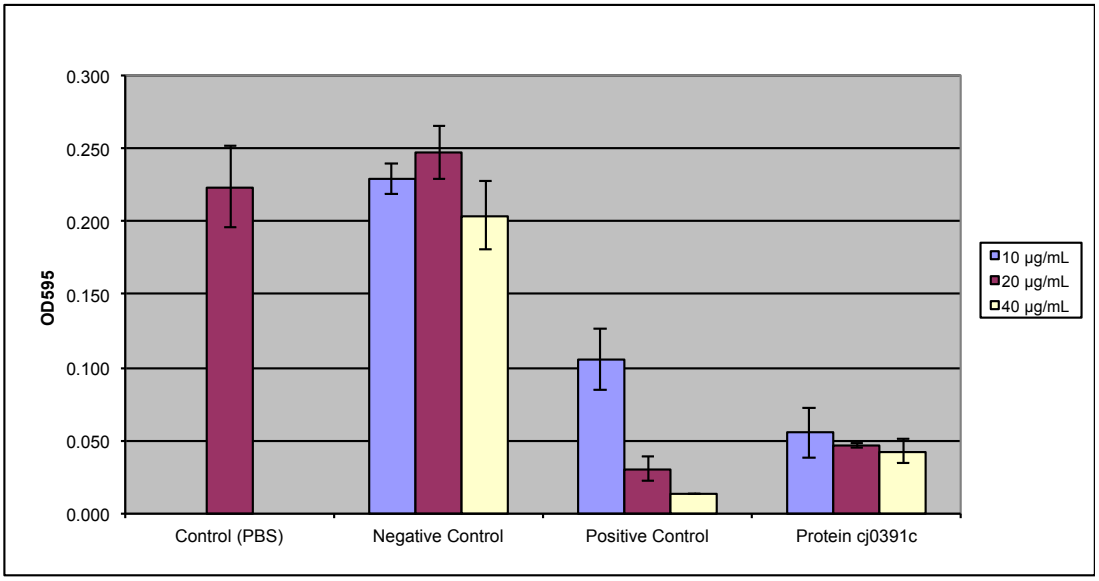

(B)

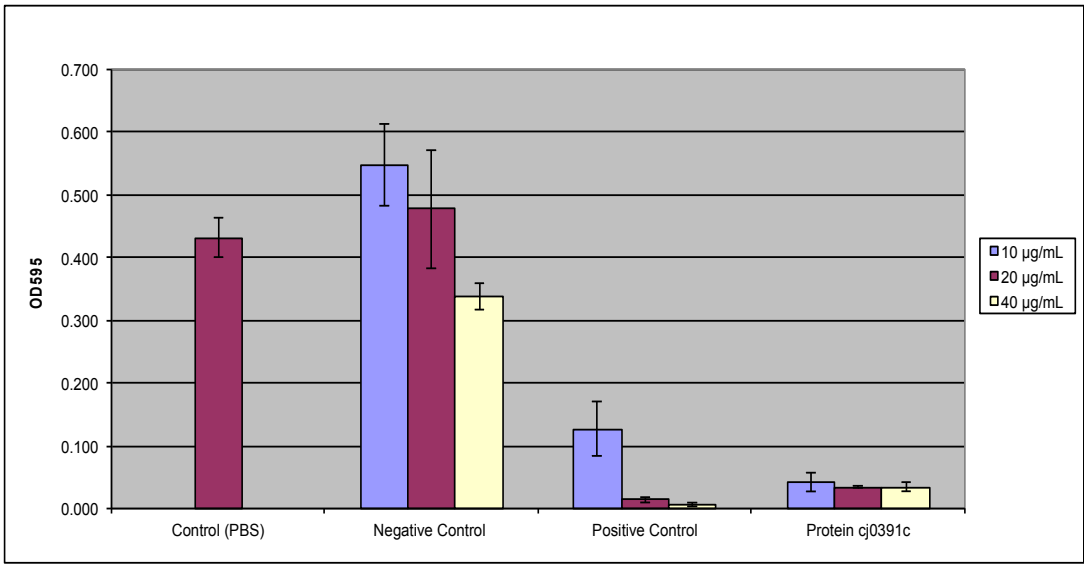

Figure 3.8: Chicken macrophage HD11 cells challenged with recombinant protein Cj0391c for 72 h (A) and 96 h (B). Each bar represents mean ± standard errors of 3 separate experiments in triplicate. The negative control used was GFP expressed by the same system. The positive control used was soluble fraction of *C. jejuni* 81116 cells. The HD11 cells viability was reduced after 72 h and 96 h incubation by approximately 75% and 90% respectively, which suggests a possible role of recombinant protein Cj0391c in reducing viability of the chicken macrophage cells HD11.

3.3.4 Apoptosis Assay

The apoptosis assay was performed using the Dead Cell Apoptosis Kit with Annexin V Alexa Fluor® 488 and Propidium Iodide (PI) Kit (Invitrogen Corporation, USA). It detects the externalization of phosphatidylserine in apoptotic cells using recombinant annexin V conjugated to green-fluorescent Alexa Fluor® 488 dye and dead cells using PI. PI stains necrotic cells with red fluorescence. After treatment with both fluorescent dyes, apoptotic cells show a green fluorescence, dead cells exhibit a combination of red and green fluorescence, and live cells show little or no fluorescence. After incubating the HD11 cells with the protein samples for 12 h, it is observed there is an apoptotic process in the chicken macrophage cells in the presence of recombinant protein Cj0391c (Figure 3.9 and 3.10). The images were taken under 100 times magnification and 200 times magnification using CLSM.

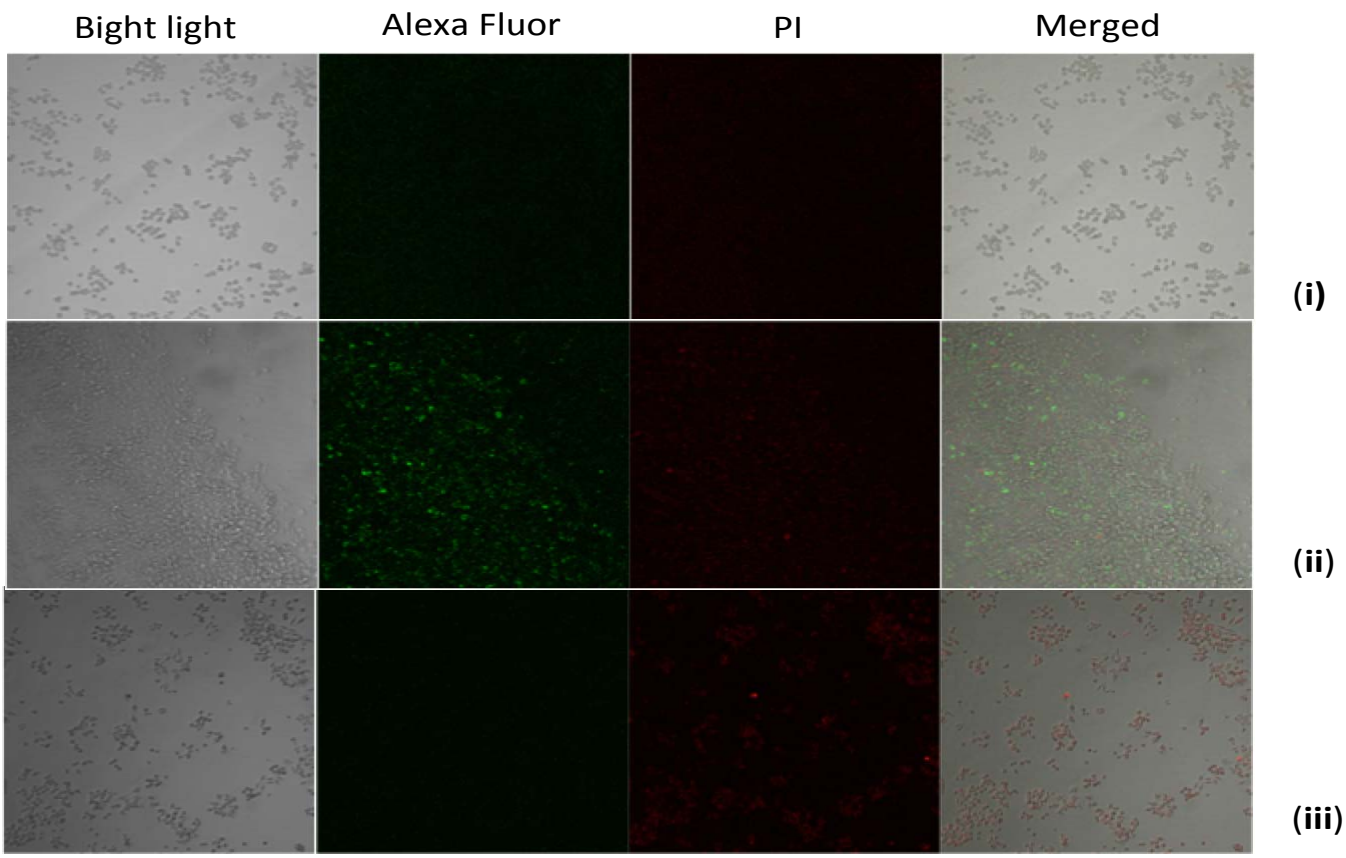

Figure 3.9: Confocal laser scanning microscopy (CLSM) micrographs for apoptosis assay with annexin V-Alexa Fluor 488 (green fluorescence) and propidium iodide (PI) (red fluorescence) in chicken macrophage cell line DH11 incubated for 12 h with 20 µg/mL of recombinant protein Cj0391c at 100x magnification. i. Negative control (GFP); ii. Recombinant protein Cj039c; iii: Positive control (Soluble fraction of *C. jejuni* 81116 cells). After incubating the HD11 cells with the protein samples for 12 h, it is observed there is an apoptotic process in the chicken macrophage cells in the presence of recombinant protein Cj0391c.

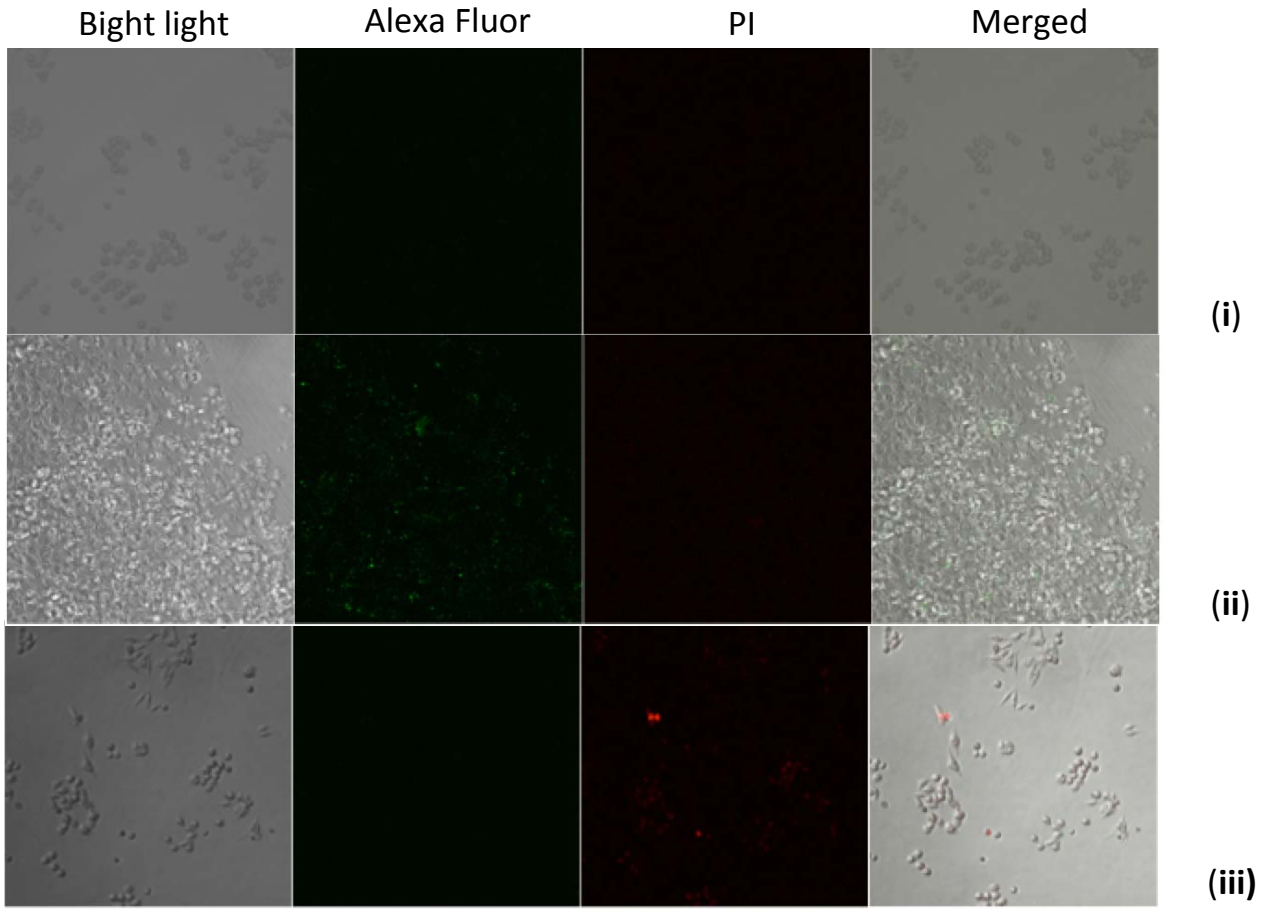

Figure 3.10: Confocal laser scanning microscopy (CLSM) micrographs for apoptosis assay with annexin V-Alexa Fluor 488 (green fluorescence) and propidium iodide (PI) (red fluorescence) in chicken macrophage cell line DH11 incubated for 12 h with 20 µg/mL of recombinant protein Cj0391c at 200x magnification. i. Negative control (GFP); ii. Recombinant protein Cj039c; iii: Positive control (Soluble fraction of *C. jejuni* 81116 cells). After incubating the HD11 cells with the protein samples for 12 h, it is observed there is an apoptotic process in the chicken macrophage cells in the presence of recombinant protein Cj0391c.

3.4 Discussion and Conclusion

As a commensal, *C. jejuni* colonises heavily onto the chicken epithelial cell layer of particularly the ceca, however no intestinal inflammation is seen (Dhillon *et al*, 2006). However, induction of immune-associated gene and protein expression after *Campylobacter* colonisation has been observed through different studies. Analysis of isolated chicken tissue displayed an increased cytokine expression (Smith *et al*, 2008) and circulating monocytes/macrophages (Meade *et al*, 2009), and several different types of chicken cells produce or upregulate cytokines during *in vitro* infection (Larson *et al*, 2008; Li *et al*, 2008; Smith *et al*, 2005).

Campylobacter activates human and chicken TLR2 and TLR4, but not TLR5. *C. jejuni* evades TLR-5 recognition through glycosylation of its flagella (Howard *et al*, 2009). *Campylobacter* initiates both MyD88 and TRIF-dependent immune responses in human through the activation of TLR2, TLR4 and TLR9 (Andersen-Nissen *et al*, 2005; Watson & Galan, 2005). Chickens lack TLR9, but have the unique DNA-sensing TLR21 (Brownlie *et al*, 2009), which can be activated by *Campylobacter* chromosomal DNA (de Zoete *et al*, 2010). However, *Campylobacter* is unable to activate MyD88-independent IFN-ß transcription via chTLR4 signaling in the chicken (de Zoete *et al*, 2010). The activation of the human and chicken TLR2 complexes indicates that *Campylobacter* lipoproteins can act as a TLR2 ligand.

Macrophages belong to the mononuclear phagocytic system lineage. This cell type is unique in that as it is a crucial player in both the innate and adaptive immune responses (Qureshi, 2003). The classic macrophage functions include chemotaxis, phagocytosis, the killing of bacteria and tumour cells, and cytokine production (Qureshi, 2003).

Chemotaxis is a function present in both monocytes and macrophages, which involves migration toward an inflammatory gradient (Qureshi, 2003). Chemotactic signals can be derived from bacterial products, certain synthetic peptides, products of the immune reaction, or certain factors released by the damaged cells and extracellular matrix (Qureshi, 2003). Macrophage cells perform phagocytic functions via several different mechanisms. Most of the phagocytic functions are mediated via target-specific receptors present on the macrophage cell surfaces. These receptors are capable of binding specific phagocytic targets (Chansiripornchai & Sasipreeyajan, 2009; Qureshi, 2003).

A study of de Zoete *et al.* (2010) demonstrateds the poor activation of chTLRs by viable *Campylobacter* compared to lysed bacteria, which indicate bacterial integrity in the intestine as a potential determinant of inflammatory pathology. This suggests that bacterial lysis may be needed to expose full TLR-stimulative potential. In a hostile environment, *Campylobacter* will likely be disrupted after phagocytosis by macrophages and dendritic cells. However, the apoptotic effect observed from our study may contribute to a reduction in phagocytosis.

Cellular assays indicate that chicken macrophage cells undergo apoptosis after 12 h incubation with recombinant protein Cj0391c. This phenomena may explain why *C. jejuni* can colonise the chicken intestine at a very high levels, as if the Cj0391c protein can kill macrophages they will be unable to (1) phagocytose and kill *C. jejuni* or (2) present processed antigen to T cells.

Based on the above observations, we explore a number of hypotheses for the mechanisms by which Cj0391c induces chicken macrophage apoptosis as well as the possible structure of Cj0391c.

(1) Protein Cj0391c may be a death receptor ligand with structure similar to protein tumour necrosis factor (TNF)-α or TNF-related apoptosis-inducing ligand (TRAIL). However, the protein sequence alignment results indicate that sequence alignment between protein

Cj0391c and these ligands is comparably poor (data not shown). Additionally, death receptor ligands are typically comprised of β-strands. None of the secondary structure and fold prediction methods employed on Cj0391c suggests that it contains any β-strand content.

(2) It may be a toxin similar to Shiga-toxin. However, Shiga-toxin and Shiga-related toxins are composed of two subunits from two different genes, an effector subunit and a membrane binding subunit. Cj0391c is a most probably a single subunit in our experiment, as it was expressed as a single chain, but still causes chicken macrophage cell apoptosis. However, we cannot exclude the possibility that Cj0391c might be a Shiga-like toxin.

(3) Cj0391c may be a toxin acting via formation of α-helical ion channel enabling the exchange of ions, causing DNA fragmentation and cell lysis (pore-forming toxin). In support of this hypothesis, a number of independent secondary structure and fold recognition methods predict that protein Cj0391c contains at least 8 helices. The lengths of the predicted helices range from 8 to 32 residues long, which is consistent with the length required to span a typical bilayer membrane.

Pore-forming toxins (PFTs) are a class of proteins that convert from a soluble form to a membrane-integrated pore (Parker & Feil, 2005). They perform their toxicity either by destruction of the membrane permeability barrier or by delivery of toxic components through the pores (Mueller *et al*, 2009). They can be divided into two classes, α-PFTs and β-PFTs, depending on the suspected mode of membrane integration, either by α-helical or β-sheet elements (Gouaux, 1997). By 2013, there are only 3 α-PFTs with known 3D structure, cytolysin A (ClyA, aka HlyE) (PDB code 2WCD), fragaceatoxin C (FraC) (PDB code 3LIM) and dermcidin (PDB code 2YMK). The C-terminal sequence of protein Cj0391c aligns well with dermcidin (discussed in Chapter 4).

Based on the bioinformatics analysis in Chapter 2 and the experimental results described in this chapter, a hypothesis has formed that Cj0391c may be an α-PFT. We further explore the

likelihood of this hypothesis by constructing a model, examining the theoretical structural stability and computationally analysed in a simple lipid bilayer under various conditions (Chapter 4).

CHAPTER 4. PROTEIN MODELLING AND MOLECULAR DYNAMICS STIMULATIONS

4.1 Introduction

In the previous chapters it was shown that Cj0391c induces apoptosis in chicken macrophages. This chapter describes attempts to model the structure of Cj0391c. Knowing the structure of the protein will lend insights into the mechanism by which Cj0391c exerts its activity against chicken macrophages.

We employ a number of prediction techniques to obtain a structure. Several structure prediction methods including secondary structure prediction were used to propose secondary structure and possible folds of Cj0391c. The results from these approaches suggest that Cj0391c is an α-helical protein. Thus, one of its mechanisms of cytotoxicity may be similar to other helical toxins, including membrane disruption by penetration of peptides; and subsequent formation of ion channels. We also used sequence alignment to find an appropriate template, focusing on known α-helical PFTs (there were only three α-helical PFTs structures available in PDB prior to 2013). Fortuitously, the structure of an α-helical toxin, dermcidin, was solved recently. The C-terminus of protein Cj0391c has sequence similarity with this PFT. After the identification, a homology model of Cj0391c was built using dermcidin as a structural template, and molecular dynamics (MD) simulation was employed to simulate the dynamics of the structure within a simple lipid bilayer environment.

There are two main reasons to perform the MD simulation. The first reason is to study the quality of the model built. We want to check if it is stable in a lipid bilayer environment at physiological temperature, thus indicating whether dermcidin is a plausible model for the C-terminus of Cj0391c. Secondly, simulation enable us to generate experimentally testable hypotheses regarding the roles of temperature and zinc on several measurable properties including pore size and hexamer structure. The pore size is related to conductance, which can be tested with single channel recording, if the pore forms.

In particular, we simulated at a range of temperature from 300 K to 314 K, to examine the possible difference in Cj0391c functional properties within its two main hosts (human and chicken), as well as to determine the limits of the protein's heat stability (to check if the structure is stable at high temperature). The effects of zinc have also been examined, as it is known to be crucial to the function of dermcidin. MD simulations were used to determine the role of zinc in the structure integrity and function of the proposed Cj0391c C-terminal hexametric transmembrane helix bundle.

4.2 Materials and Methods

4.2.1 Protein Structure Prediction

We have employed the fold prediction method, I-TASSER, to predict the 3D structure of Cj0391c as well as to predict its secondary structure. I-TASSER has been ranked as the best server for protein structure prediction according to the 2006-2012 CASP (Critical Assessment of Techniques for Protein Structure Prediction) experiment.

I-TASSER is a hierarchical protein structure modelling approach based on the secondary-structure enhanced Profile-Profile threading Alignment (Wu & Zhang, 2007) and the iterative implementation of the Threading ASSEmbly Refinement (TASSER) program (Zhang & Skolnick, 2004a). Initially, prediction of the protein Cj0391c structure had been attempted to using *ab initio* folding and threading methods, as there was no homology model available. I-TASSER is the best server to predict protein structures with no homology model and it combines both *ab initio* folding and threading methods (Roy *et al*, 2010). After submitting the protein sequence, I-TASSER first generates three-dimensional atomic models from multiple threading alignments, and also iterative structural assembly simulations (Roy *et al*, 2010). Then the function of the same protein is inferred by structurally matching the 3D models with other proteins with known function (Roy *et al*, 2010). There are four stages involved in the prediction before the models are ready for estimation of prediction accuracy: (1) threading; (2) structural assembly; (3) model selection and refinement and (4) structural-based functional annotation (Roy *et al*, 2010). Threading refers to a bioinformatics procedure for identifying a structural unknown protein from solved structure protein databases, which may contain a similar structure or similar structural motif as the query protein (Roy *et al*, 2010). In the first stage, the query protein sequence is matched against a non-redundant sequence database by PSI-BLAST, to see the evolutionary relatives (Roy *et al*, 2010). In stage 2, continuous fragments in the threading alignments from the stage 1 results are excised and

used to assemble structural conformations for the sections that are well aligned, with the unaligned regions built by *ab initio* modelling as well (Wu *et al,* 2007; Zhang *et al,* 2003). In the third stage, the system performs the fragment assembly simulation again, which starts from the selected cluster centroids (Roy *et al*, 2010). In the final stage, the function of the query protein is inferred from the PDB, by structurally matching the predicted models against the proteins of known structure and function (Roy *et al*, 2010).

The protein sequence of Cj0391c was submitted in I-TASSER for model ~~building~~ prediction. After the protein sequence submission, the following results have been obtained: (1) up to 5 predicted models ranked based on the structure density of the SPICKER clustering; (2) C-score of all the I-TASSER models; (3) estimated TM-score and RMSD (root-mean-square deviation) for the first model.

SPICKER is a clustering algorithm to identify the near-native models by clustering protein structures generated during simulations (Zhang & Skolnick, 2004c). C-score is a confidence score for estimating the quality of the predicted models, which is typically in the ranger of [-5, 2] (Roy *et al*, 2010). The C-score of the I-TASSER is defined as below,

$$C-score=\ln\left[\frac{M}{Mtot}\cdot\frac{1}{\langle RMSD\rangle}\cdot\frac{\prod_{i=1}^{4}Z(i)}{\prod_{i=1}^{4}Z_0(i)}\right]$$

where M is the multiplicity of structures in the SPICKER cluster; M_{tot} is the total number of the I-TASSER structure decoys used in the clustering (Zhang, 2008). The $\langle RMSD\rangle$ in the formula is the average RMSD of the decoys to the cluster centroid, while $Z(i)$ represents the highest Z score and $Z_0(i)$ is a program-specified Z-score cut-off for distinguishing between the good and bad models (Zhang, 2008). A higher C-score signifies a model with a higher confidence and vice-versa (Roy *et al*, 2010). Predicted TM-score and RMSD are also provided for model 1 from each job, which indicate how much the predicted models relative the native structures based on the C-score (Roy *et al*, 2010). TM-score is a scale for

measuring the structural similarity between two structures, while RMSD is an average distance of all residue pairs in two structures (Roy *et al*, 2010). The TM-score is defined to access the topological similarity of two protein structures and it is displayed as below

$$TM-score = \frac{1}{L}\sum_{i=1}^{L}\frac{1}{1+d_i^2/d_0^{2'}}$$

where d_i is the distance of the ith pair of residues between two structures after an optimal superposition (Zhang & Skolnick, 2004b). In the same formula, d_0 is equals to $1.24\sqrt[3]{L-15}-1.8$, and L is the protein length (Zhang, 2008). TM-score is introduced to solve the problem of RMSD that RMSD is sensitive to the local error (Roy *et al*, 2010). In TM-score, the small distance is weighted higher than the big distance, which makes the TM-score insensitive to the local modelling error (Roy *et al*, 2010). A higher than 0.5 TM-score indicates that the predicted model is of correct topology, while a lower than 0.17 TM-score indicates a random similarity (Roy *et al*, 2010). It should be mentioned that the estimated quality is provided only for the first model, although the C-scores of all 5 models have been given (Roy *et al*, 2010). The correlation of C-score and modelling quality for the other lower-ranked models are much weaker compared to the first model (Roy *et al*, 2010).

4.2.2 Sequence Alignment

We used Clustal-Omega (Sievers *et al*, 2011) to align the sequence of Cj0391c and human dermcidin (PDB code 2YMK). Sequence alignments are now one of the most widely used bioinformatics analyses (Larkin *et al*, 2007). Clustal is the oldest of the currently most widely used programs having been first distributed by post on floppy disks in the late 1980s (Larkin *et al*, 2007). The current Clustal programs all derive from Clustal W (Thompson *et al*, 1994). In benchmark tests, Clustal Omega shows distinctly more accurate results than most widely used, fast methods and comparable in accuracy to some of the intensive slow methods (Table 4.1) (Sievers *et al*, 2011). Clustal Omega employs seeded guide trees

Table 4.1: HomFam benchmarking results (reproduced from Sievers *et al*, 2011).

	93≤N≤2957 (41 families)	3127≤*N*≤9105 (33 families)	10099≤*N*≤50157 (18 families)
Aligner	TC/t (s)	TC/t (s)	TC/t (s)
Clustal Omega	0.708/2114.0	0.639/11719.5	0.464/27328.9
Kalign	0.569/324.9	0.563/6752.0	0.420/286711.0
MAFFT default	0.550/238.9	0.462/3115.4	-/-
MAFFT - parttree	-/-	-/-	0.253/6119.4
MUSCLE default	0.533/104587.0	-/-	-/-
MUSCLE – maxiters 2	-/-	0.416/8239.2	0.216/110292.0

The columns show total column score (TC) and total run time in seconds for groupings of small (<3000 sequences), medium (3000-10000 sequences) and large (>10000 sequence) HomFam test cases respectively. TC gives the proportion of the total alignment columns that is recovered (Sievers *et al*, 2011).

and HMM profile-profile techniques to generate alignments (Sievers *et al*, 2011). The important feature of making the progressive alignment approach scale is the method used to make the guide tree (Sievers *et al*, 2011). Generally, it involves aligning all N sequences to each other giving time and memory requirements of $\mathrm{O}\left(N^2\right)$ (Sievers *et al*, 2011). The methods which can routinely make alignments of more than about 10,000 sequences is very fast, but lead to a loss in accuracy. It has to be compensated for by iteration and other heuristics, while with Clustal Omega, a modified version of mBed (Blackshields *et* al, 2010) is used (Sievers *et al*, 2011). It has complexity of $\mathrm{O}\left(N \log N\right)$ and produces guide trees that are just as accurate as those from the other conventional means (Sievers *et al*, 2011). In Clustal Omega, the alignments are computed using a high accurate HHalign package (Soding, 2005), which aligns two profile HMM (Eddy, 1998).

4.2.3 Comparative Protein Structure Modelling

Comparative (or homology) modelling was employed to construct a 3D model of the C-terminus of Cj0391c, using human dermcidin as a template. Comparative modelling can sometimes provide a useful 3D model for a protein that is related to at least one known protein structure (Eswar *et al*, 2006). Comparative modelling predicts the target protein 3D structure based primarily on its alignment to one or more known structure protein(s) (Eswar *et al*, 2006). In our study, the 3D structure of hexamer 391 model has been built based on protein dermcidin (PDB code 2YMK) using Modeller version 9.10 (Sali & Blundell, 1993). The steps in comparative protein structure modelling have been listed in Figure 4.1. The prediction process consists of fold assignment, target-template alignment, model building, and model evaluation (Dalton & Heffernan, 1989).

Initially, the phosphatidylethanolamine-phosphatidylglycerol (POPE) bilayer was obtained from the website Lipidbook (http://lipidbook.bioch.ox.ac.uk), which contained 437 POPE

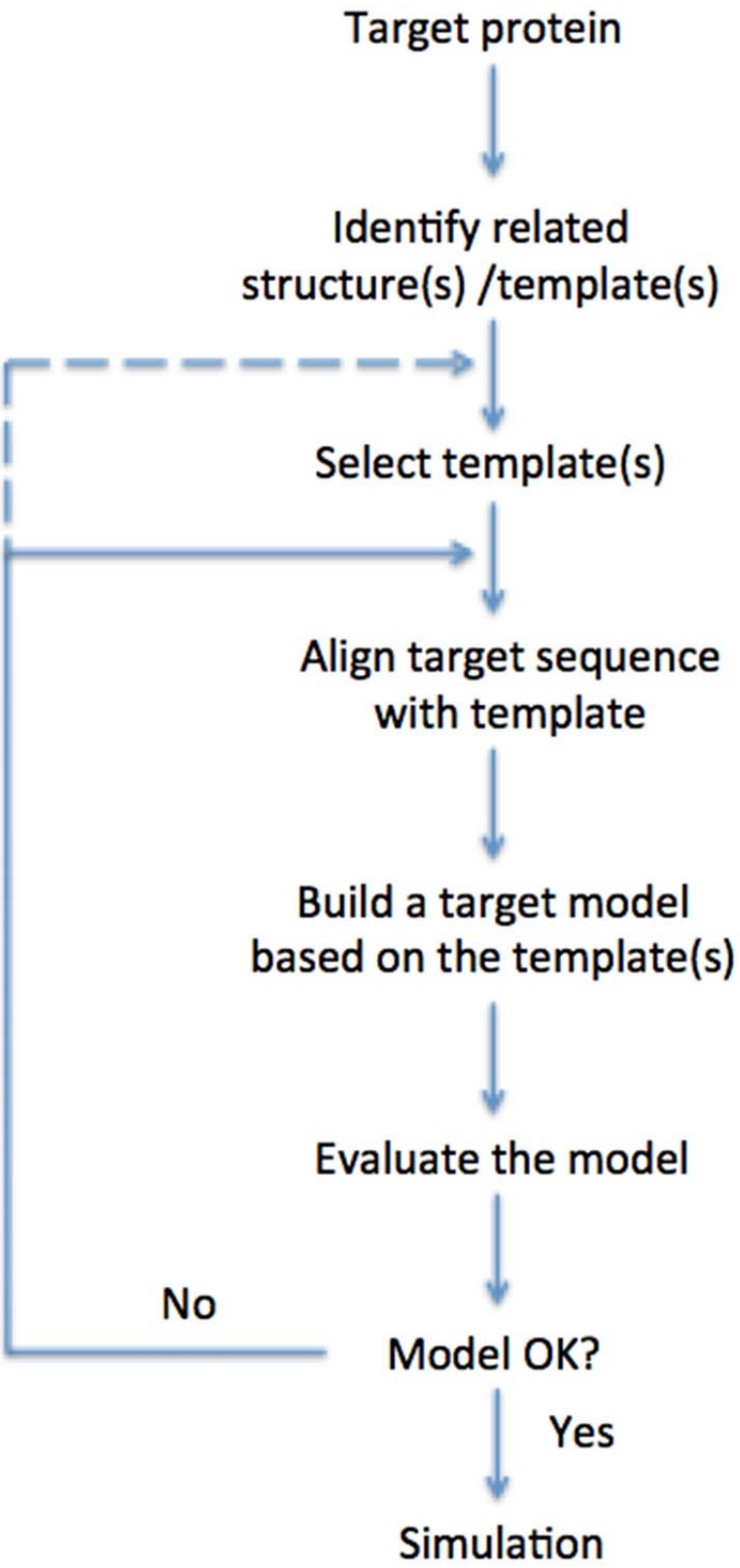

Figure 4.1: Steps in comparative protein structure modelling (adapted from Marti-Renom *et al*, 2000).

lipids. Then, the hexamer 391 was inserted into POPE bilayer. Forty-seven (47) lipids next to the protein were then removed after positing protein 391 in the middle of the bilayer (with remaining 390 POPE lipids). A total number of 23335 and 32824 water molecules have been placed in the systems with zinc and without respectively. Twelve zinc ions have been added to the protein complex to generate another system (391-ZN). The positions of Zn were based on their corresponding positions in the dermcidin structure.

4.2.4 Molecular Dynamics and Simulation

Molecular dynamics is a technique for computer simulation of complex systems, modelled at the atomic level. The equations of motion are solved numerically to follow the time evolution of the system, allowing the derivation of kinetic and thermodynamic properties of interest by means of 'computer experiments'. Biologically important macromolecules and their environments are routinely studied using molecular dynamics simulations. MD employs Newton's Second Law of motion as below

$$F = m \cdot a = m \cdot \frac{dv}{dt} = m \cdot \frac{d^2x}{dt^2}$$

where F is the force exerted on the particle, m is its mess, a is its acceleration, v is the velocity and x is the particle position. The position of each atom is updated at each time step based on numerically solving Newton's equations. Potential energy between atoms dictates motions of the atoms. This potential (force field) describes bonded (bond, angle, dihedral) and non-bonded (Lennard-Jones, electrostatic) interatomic interactions. Different force fields employ different parameters (e.g. spring constant for bonded interactions) based on experiments and high-level quantum chemistry calculations.

MD is one of the most important and widely used molecular simulation techniques. This method was created subsequent to Monte Carlo in order to study the dynamical behaviour of many-particle systems. The technique used in this project is classical MD, as implemented in the program GROningen Machine for Chemical Simulations (GROMACS), which is a MD

package primarily designed for simulation of proteins, lipids and nucleic acids. The simulation system was built and calculations were performed using the GROMACS version 4.6.3 with the CHARMM36 force field. The starting structure coordinates of 391 was built and bilayer POPE was obtained from Lipidbook as described in Section 4.2.3 (Domanski *et al*, 2010).

After the hexamer model 391 has been built by molecular modelling, it has been setup in lipid bilayer POPE (named 391-POPE in this study). Twelve zinc ions have been added in the complex (named 391-ZN-POPE in this study). Both complexes have been simulated under 3 different temperatures (300 K, 310 K and 314 K) for 100 ns. Therefore, 6 sets of MD trajectories have been obtained using GROMACS. The six protein-ion-bilayer simulation complexes are named 391-300K, 391-310K, 391-314K, 391-ZN-300K, 391-ZN-310K and 391-ZN-314K.

After the topology file for the protein and bilayer was made, a simulation box was constructed with chosen proportions. The dimensions of each box was 100 x 100 x 100 Å and was filled with explicitly represented water molecules until water density reached ~ 1.0 g/cm^3. As the solutes had a non-zero total charge, counterions (Cl^-) were incorporated in the simulation box to neutralize the system. After the construction of the system was finalized, energy minimization was applied to correct for bad van der Waals contacts or steric clashes between the protein and water molecules. The first-order minimization method of steepest descent was performed to reach the lowest local energy point.

The solvent equilibration stage consisted of constant pressure simulations at T = 300 K/310 K/314 K, P = 1 bar with protein atoms restrained to allow the solvent and bilayer to relax around the solute. Equilibration of the entire system was performed afterwards when the protein was allowed to move. At the end of the simulations, RMSD, helix bending and pore size were analysed using different tools. Visualisation and structural representation of each system were performed using Visual Molecular Dynamics (VMD) (Humphrey *et al*, 1996). Time steps of 2 ps were used to integrate the equations of motion. The neighbor list of the

simulations was updated every 10 steps. The pressure coupling used was the Parrinello-Rahman barostats (reference here). The thermostat used was Bussi's thermostat (Bussi *et al,* 2007). Particle Mesh Ewald summation was used to treat electrostatics (Essmann *et al*, 1995).

4.2.5 Helix Dynamics Analysis

Helix flexibility plays a key role in the mechanisms of channel gating, receptor activation and molecule transport for membrane proteins (Dahl *et al*, 2012). The flexibility of α-helices is important for pore-forming protein function and calls for better visualisation and analysis (Dahl *et al*, 2012). The dynamics of transmembrane α-helices can be explored by MD simulations, which is becoming an increasingly important tool to complement the protein function study and structure stability evaluation.

In this study, a plugin for VMD called Bendix was employed for helix dynamics investigation. Bendix features custom helix representation and geometry indicative graphics that assist analysis of both static structures and complex molecular dynamics simulation trajectories (Dahl *et al*, 2012). The Heatmap display of helix curvature aiding analysis of the relationship between different structures, dynamic conformational changed and structure stability.

4.2.6 Pore Size Analysis

We used PoreWalker (Pellegrini-Calace *et al*, 2009), a web-available method for the detection and characterisation of channels in our models from their 3D structure before and after MD analysis. The algorithm of PoreWalker is both heuristic and iterative, which includes the steps in Figure 4.2. In term of outputs, in addition to diameter profiles, PoreWalker describes several specific pore features, in particular the shape and the regularity of the channel cavity, and the position of pore centres along the channel. These features can be

very helpful to gain further insights into the functional and structural properties of pore-forming protein channels by triggering specific *in silico* or experimental analyses. The protein structures in PDB format were submitted on the server for analysis and the results outputs are in the following 4 sections (1) Pore shape, which shows the prediction of the shape of the pore; (2) Pore visualisation: eight pictures (four for the whole structure and four to the pore only) are provided to visualise the pore and estimated way through it; (3) Slideshows of cross sections of the pore, which contain snapshots corresponding to pore slices of X Å and taken from the lowest to the highest x-coordinates; (4) Features of the cavity, which show the centres of the pore at 1 Å slices and the smallest diameter per slice (Pellegrini-Calace *et al*, 2009).

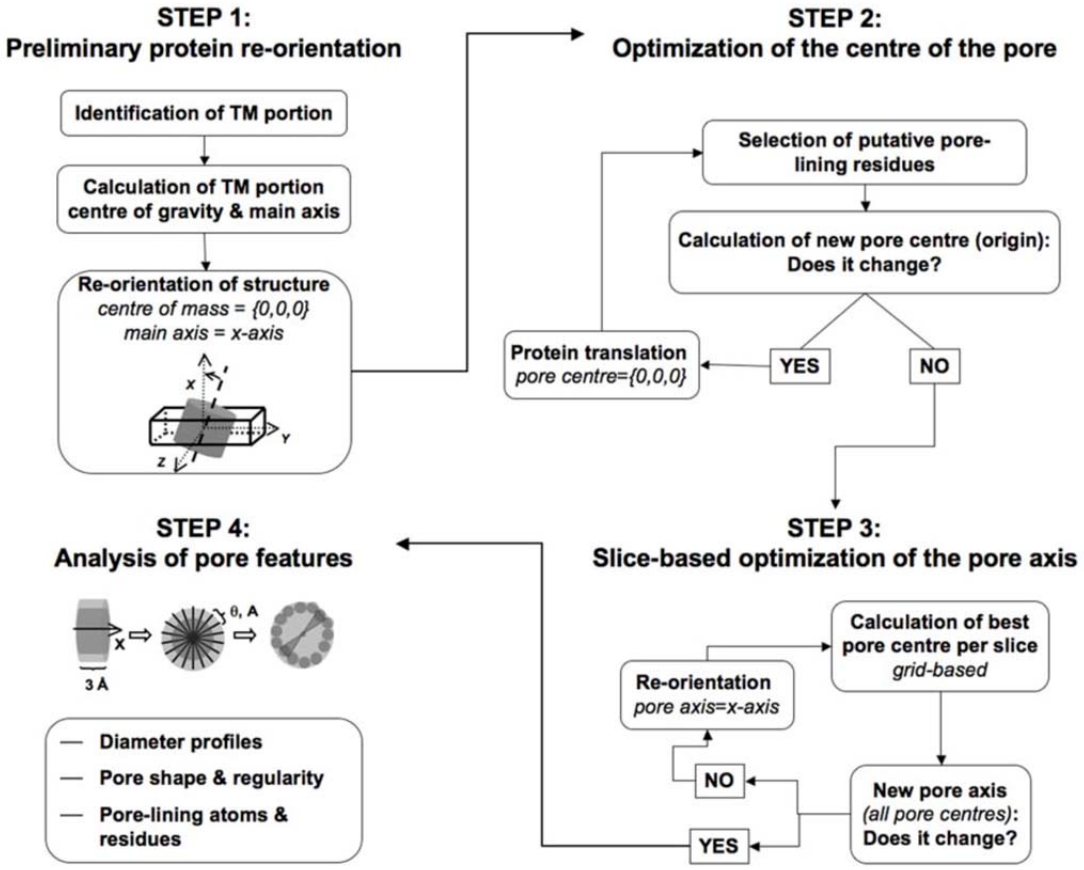

Figure 4.2: Flowchart of PoreWalker stepwise algorithm (reproduced from Pellegrini-Calace *et al*, 2009).

4.3 Results

4.3.1 Protein Structure Prediction

The first time protein Cj0391c sequence submission to the I-TASSER server was done on Aug 3rd, 2010 and the latest submission was on Jun 27th, 2014. The secondary structure prediction based on the protein sequence only is shown in Figure 4.3. The 3D structure prediction results are shown in Figure 4.4 and 4.5.

The secondary structure predictions are represented as H for helix and C for Coil, together with the confidence scores, which range from 9 (most confident) to 0 (least confident). The results obtained from two submissions are very similar, with only a few amino acids difference in some of the helix lengths.

There were also five 3D structures generated by the webserver each time, which are ranked by the C-score indicating the confidence of prediction (Roy *et al*, 2010).

The C-score of the best-predicted Cj0391c model has been improved from –3.66 to -2.12 through 4 years time, likely due to more protein structures being available from PDB for the server to use to build Cj0391c structures. The RMSD of the best model has also been improved from 14.2±3.8Å to 10.2±4.6Å. It is clear that the best predicted model obtained in the year 2014 is completely different from the model obtained from the year 2010. However, all of the predicted models indicate that Cj0391c is most likely an α -helical protein. The TM-score changed from 0.3±0.10 to 0.46±0.15, which is also a big improvement. However, it is still lower than 0.5, which is the threshold for a reasonably correct topology. Therefore, the 3D models predicted from I-TASSER were not used for the simulation. Nevertheless, the strong evidence for α-helicity of a substantial portion of the protein led us to seek α-helical structural templates.

(A)

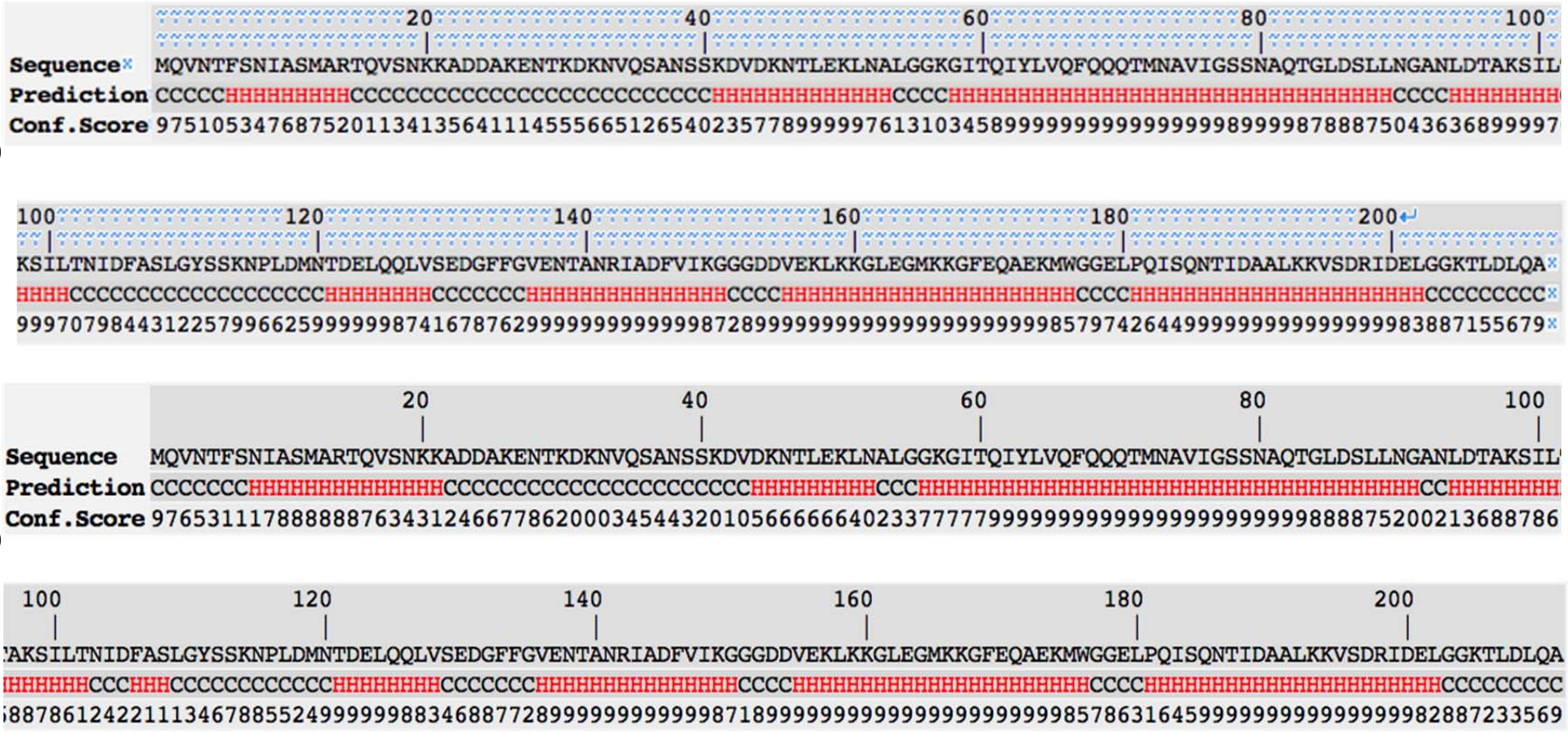

(B)

Figure 4.3: Secondary structure prediction of Cj0391c from I-TASSER on (A) Aug 3rd, 2010 and (B) Jun 27th, 2014. (Prediction: H: helix C: Coil; Confidence score range from 9-most confident to 0-least confident)

(A) 

Model 1 C-score=-3.66

Estimated TM-score = 0.3±0.10 Estimated RMSD = 14.2±3.8Å

(B) 

Model 2 C-score=-4.28

(C) 

Model 3 C-score=-4.99

(D) 

Model 4 C-score=-5

(E) 

Model 5 C-score=-4.50

Figure 4.4: Protein Cj0391c structure prediction results from I-TASSER on Aug 3rd, 2010

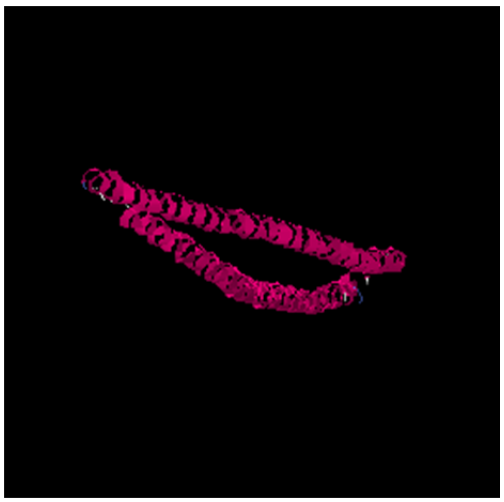

(A)

Model 1 C-score=-2.12

Estimated TM-score = 0.46±0.15 Estimated RMSD = 10.2±4.6Å

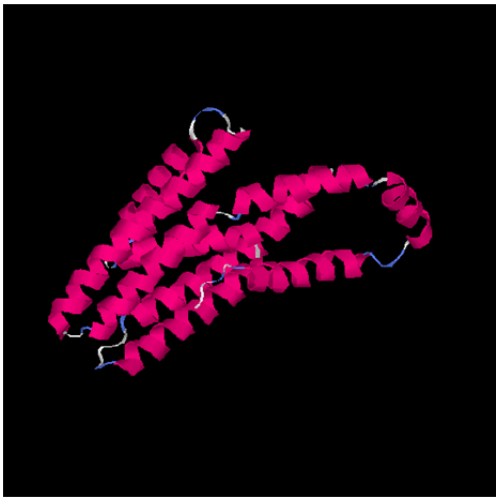

(B)

(C)

Model 2 C-score=-4.08

Model 3 C-score=-3.12

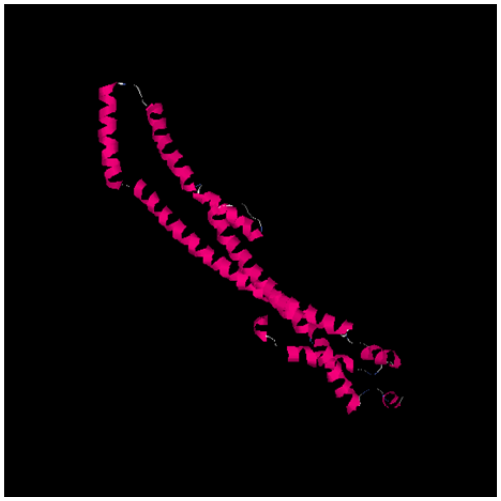

(D)

(E)

Model 4 C-score=-3.78

Model 5 C-score=-4.18

Figure 4.5: Protein Cj0391c structure prediction results from I-TASSER on Jun 27th, 2014

4.3.2 Sequence Alignment

As discussed in Chapter 3, protein Cj0391c may be a toxin acting via formation of α-helical ion channel. Additionally, as indicated by I-TASSER results, Cj0391c is most likely an α-helical protein. Prior to 2013, there was no α-helical toxin with sequence similarity with Cj0391c was identified on PDB. However, in late 2013, an α-helical toxin called dermcidin (PDB code 2YMK) was identified. This protein has some sequence similarity with Cj0391c.

The sequence alignment between dermcidin (PDB code 2YMK) and protein Cj0391c was performed using Clustal Omega, and the result is shown in Figure 4.6. The alignment score is 16.67 and the result indicates that the C-terminal of protein Cj0391c aligns well with 2YMK. The sequence alignment was used for homology modelling in section 4.3.3. Note that only the C-terminus of Cj0391c aligns well with 2YMK. This suggests that the C-terminal region may act as the membrane-permeating domain, while the N-terminal part may serve other functions, such as initial binding/anchoring to membrane, in a similar fashion to, for instance, equinatoxin-II. The binding of equinatoxin-II to lipid membranes is a two-step process, an exposed aromatic cluster mediates the initial attachment, and the N-terminal amphiphilic helix translocates into the lipid phase (Hong *et al*, 2002).

4.3.3 Model Construction

The protein model was constructed by modeller 9.10, and posited in the POPE bilayer. The systems are shown in Figure 4.7 (without zinc) and Figure 4.8 (with zinc).

```
CLUSTAL O(1.2.1) multiple sequence alignment


cj0391c      MQVNTFSNIASMARTQVSNKKADDAKENTKDKNVQSANSSKDVDKNTLEKLNALGGKGIT
2YMK         ------------------------------------------------------------


cj0391c      QIYLVQFQQQTMNAVIGSSNAQTGLDSLLNGANLDTAKSILTNIDFASLGYSSKNPLDMN
2YMK         ------------------------------------------------------------


cj0391c      TDELQQLVSEDGFFGVENTANRIADFVIKGGGDDVEKLKKGLEGMKKGFEQAEKMWGGEL
2YMK         ----------------------------------SSLLEKGLDGAKKAVGGLGKLGKDAV
                                                . *:***:* **..    *:    :

cj0391c      PQISQNTIDAALKKVSDRIDELGGKTLDLQA
2YMK         EDLES-VGKGAVHDVKDVLDSVL--------
              ::.. . ..*::.*.* :*.:
```

Figure 4.6: Sequence alignment of protein Cj0391c and dermcidin 2YMK using Clustal Omega.

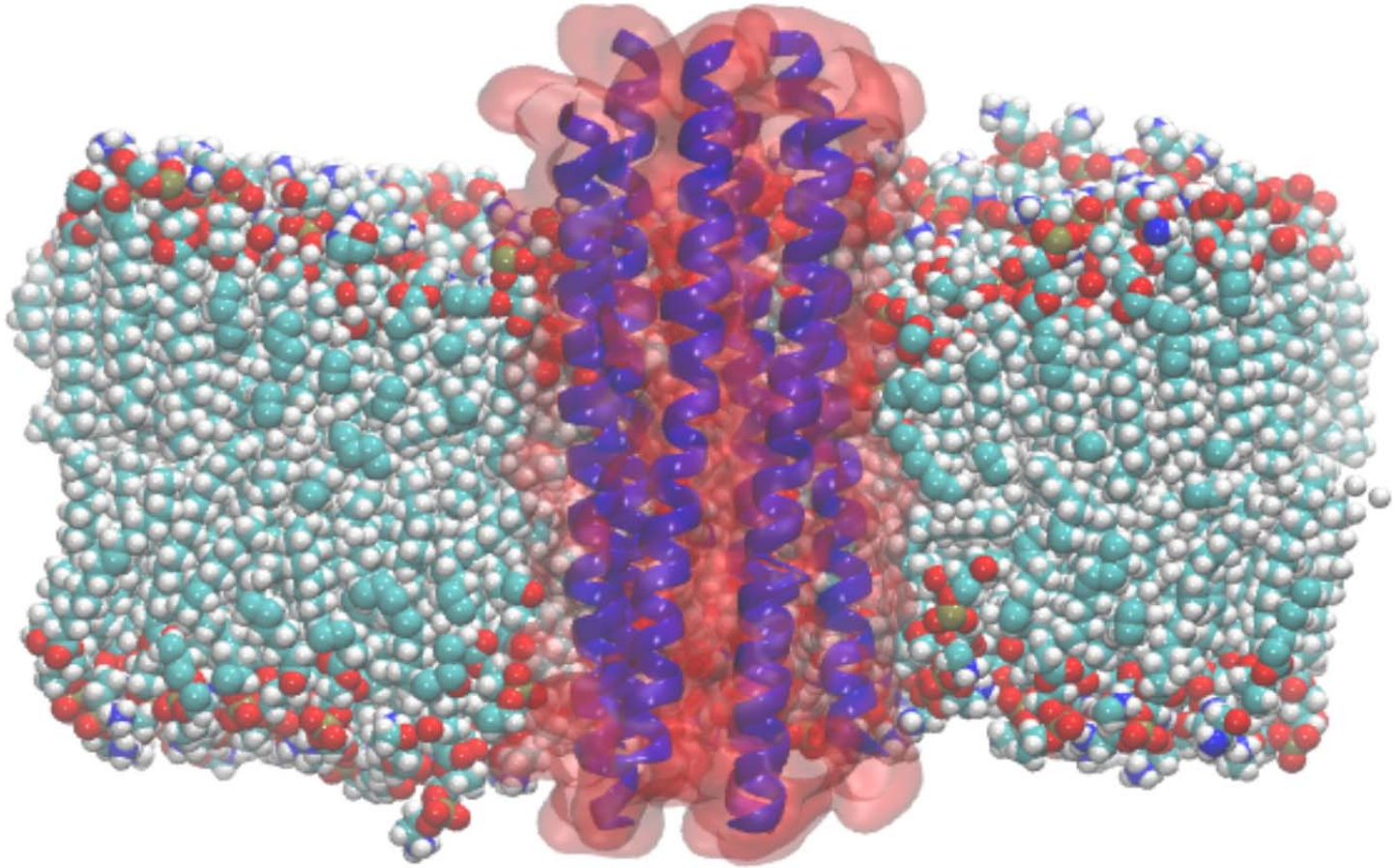

Figure 4.7: The hexamer protein model 391 inserted in bilayer POPE without the present of zinc.

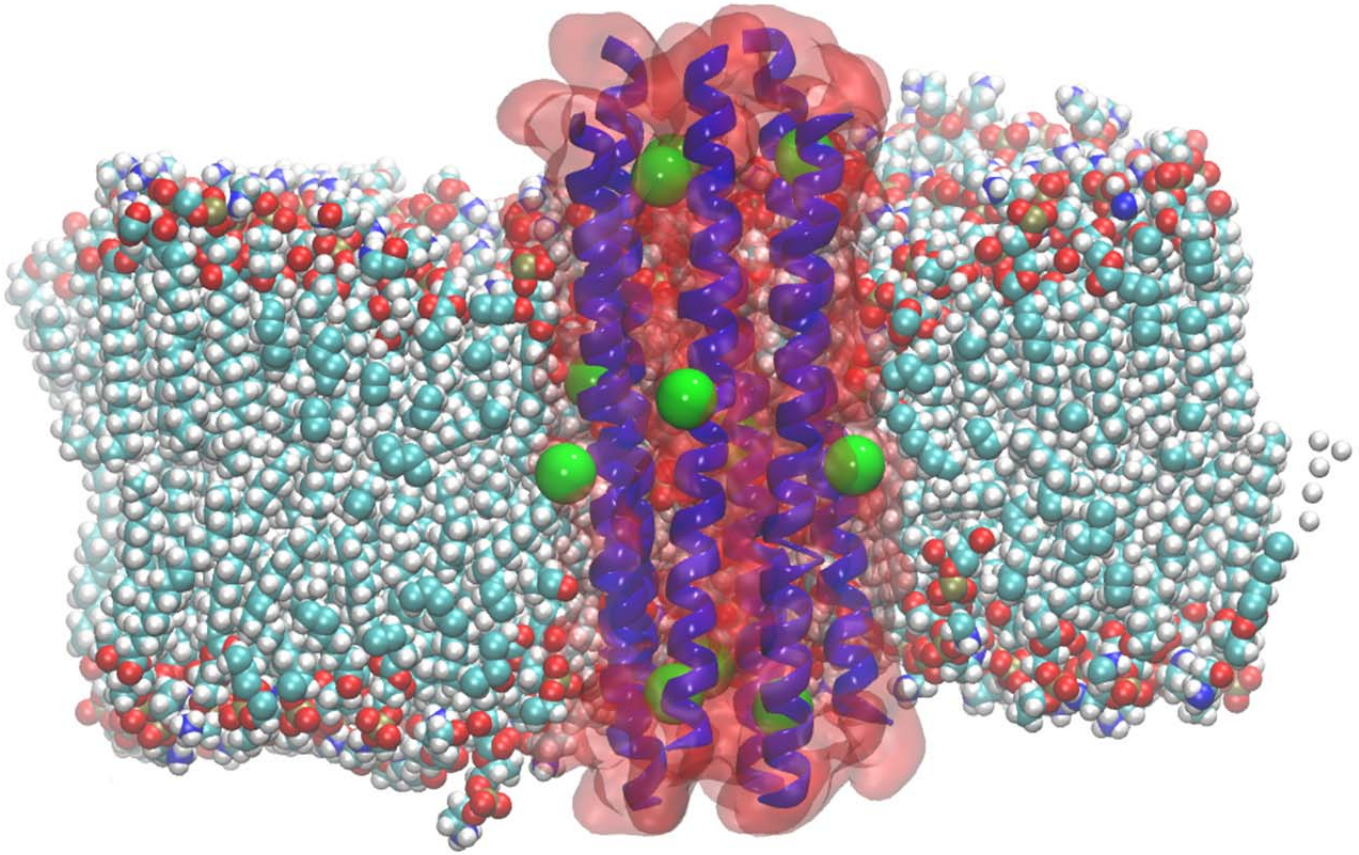

Figure 4.8: The hexamer protein model 391 inserted in bilayer POPE with the present of 12 Zn^{2+} (Green balls: Zn^{2+}).

4.3.4 RMSD Analysis

The root-mean-square deviation (RMSD) of a protein during MD simulation is a frequently used measure of the structural difference between confirmations of a protein. It can be used to examine the change of confirmation during the course of a MD simulation. To investigate the stability of protein 391 under various conditions, RMSD calculations have been performed. The plots show a moving average of 100 ps to enable effective comparison of the overall trends between the systems.

The RMSD plots of the trajectories of 391 from different systems are shown in Figure 4.9. RMSD was performed on the backbone atoms of the whole hexamer helix bundle. It can be observed that in the presence of Zn, RMSD levels out at ~4 Å at temperatures of 300 K, 310 K and 314 K, Indicating relative stability of the bundle at these temperatures. Without the presence of Zn, at 300 K, a similar RMSD value was obtained, indicating that at this temperature even without Zn the bundle structure is maintained. However, when the simulation temperature reached 310 K and 314 K, without Zn, RMSD is substantially higher and does not level out even after 100 ns of MD simulation. Results suggesting that the bundle structure is quite different from that of dermcidin. Thus, Zn appears to maintain hexamer structure at temperature > 310 K, but at low temperature 300 K, Zn is not essential for this role.

The individual helix RMSD of each model are shown in Figure 4.10 to Figure 4.15. RMSD of the 391-300K model indicates that three helices (helix 1, 5 and 6) exhibited similar RMSD at the end of the simulation. The other three helices show much higher RMSD. Therefore, without Zn, at 300 K, half of the helices maintained their structures, while the others did not. The specific details of each helix structure are discussed in the Section 4.3.3. At 310 K, the same model without Zn, substantial divergence in RMSD values are observed for all of the helices. Two helices (helix 1 and helix 6) maintained similar structures to dermcidin, while all the other helices range from 4 to 8 Å. The one with the highest RMSD value is the helix 3,

which lost helicity completely. This indicates breaking of symmetry in helix structure, which means the 6 helixes do not have the same structure anymore. For the same hexamer without Zn at 314 K (391-314K model), all of the helices except helix 4, showed very high RMSD, which indicates that all but one helix has completely diverged from the initial structure. The bundle lost helical symmetry totally.

The RMSD of 391-ZN-300K, two helices (helix 3 and 4) with slightly lower RMSD comparing to the other four. Generally, all of the helices have similar RMSD at the end of the 100ns simulation. The 391-ZN-310K model also had comparably low RMSD (all below 4 Å). Helix 6 is the one with the lowest RMSD (<2.5 Å) through the whole simulation, while helix 3 is the one with the highest. For the model 391-ZN-314K, most helices have fairly low and similar RMSD, except helix 2, which indicates the helix structure for 5 out of 6 helices was maintained.

In conclusion, after 30 ns, the RMSD from systems 391-310K and 391-314K are almost double the value of the other 4 systems, which indicates at higher temperature (>=300 K), zinc helps to keep the structure stable. For the simulation temperature at 300 K, the RMSD values are quite similar for both models (with and without zinc).

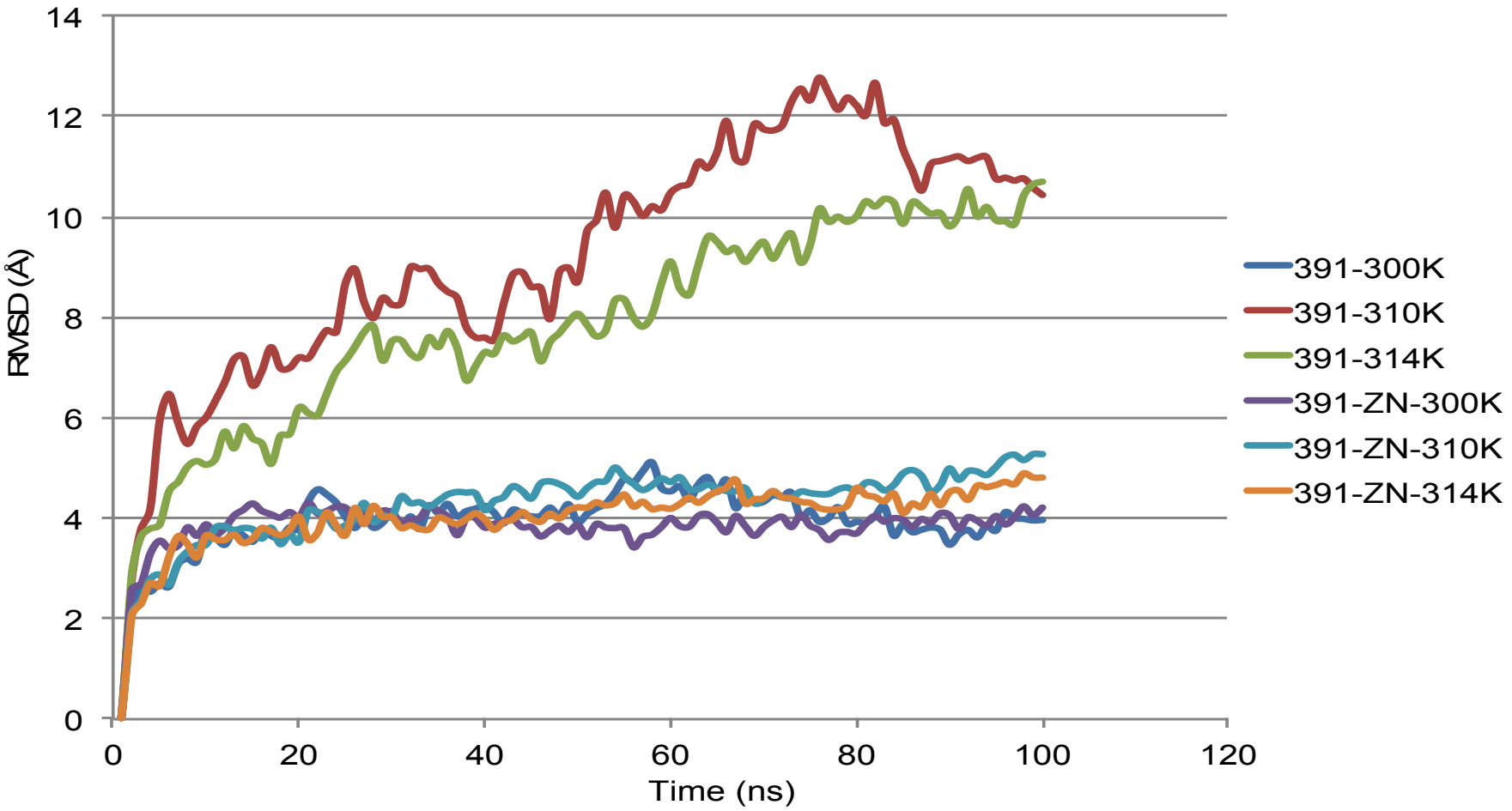

Figure 4.9: RMSD plots of the trajectories of the protein 391 from systems 391-300K, 391-310K, 391-314K, 391-ZN-300K, 391-ZN-310K and 391-ZN-314K.

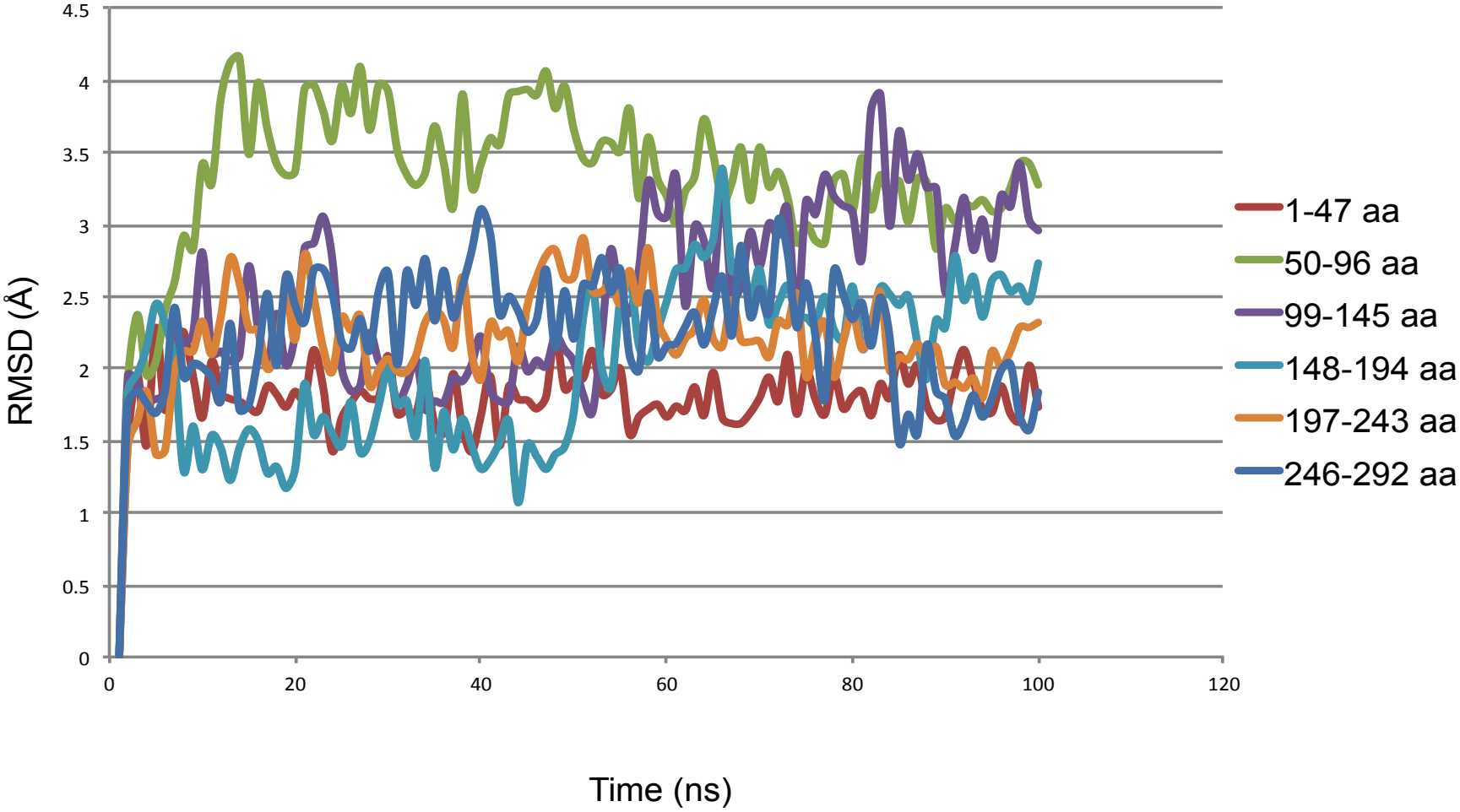

Figure 4.10: RMSD plots of the trajectories of each helix from system 391-300K.

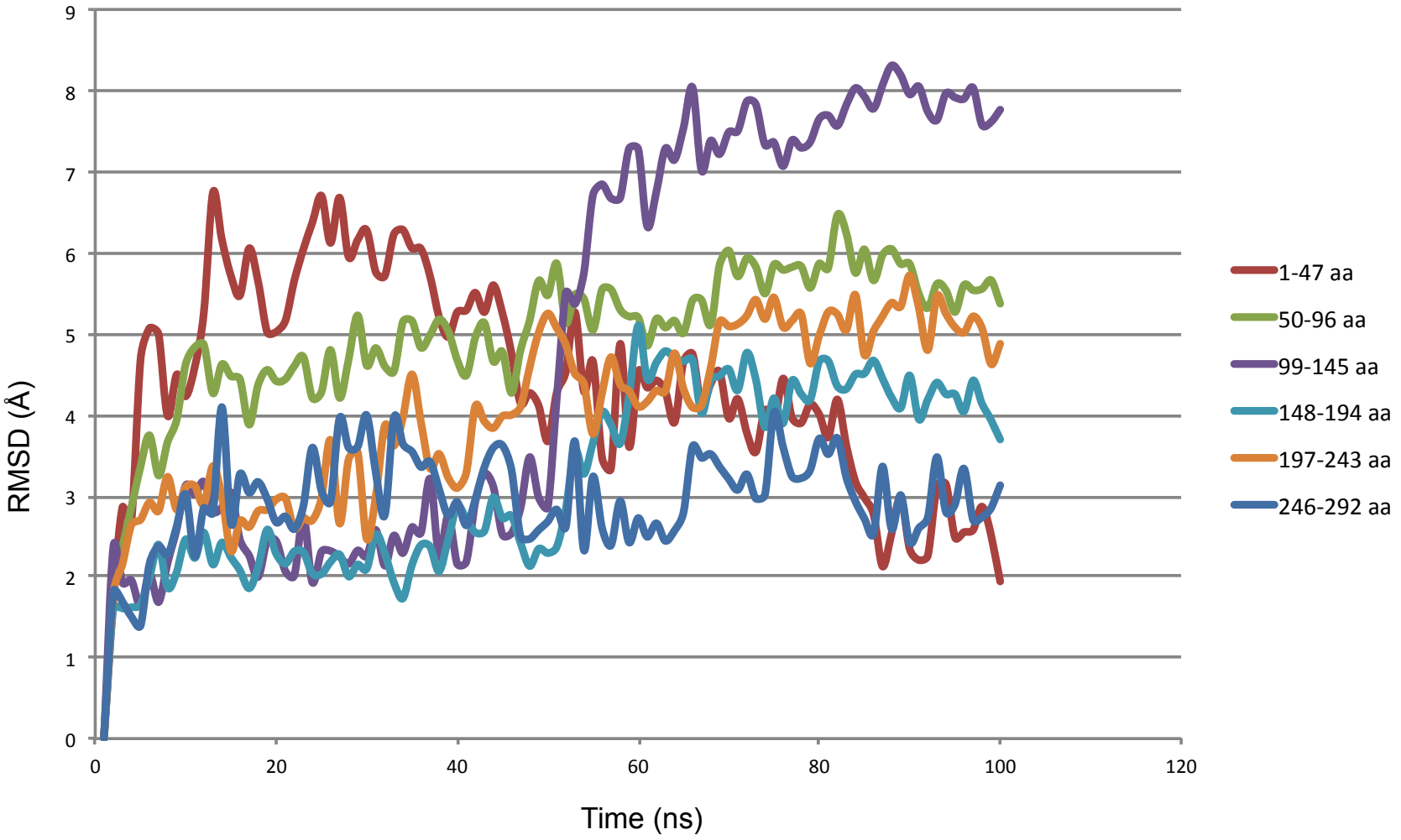

Figure 4.11: RMSD plots of the trajectories of each helix from system 391-310K.

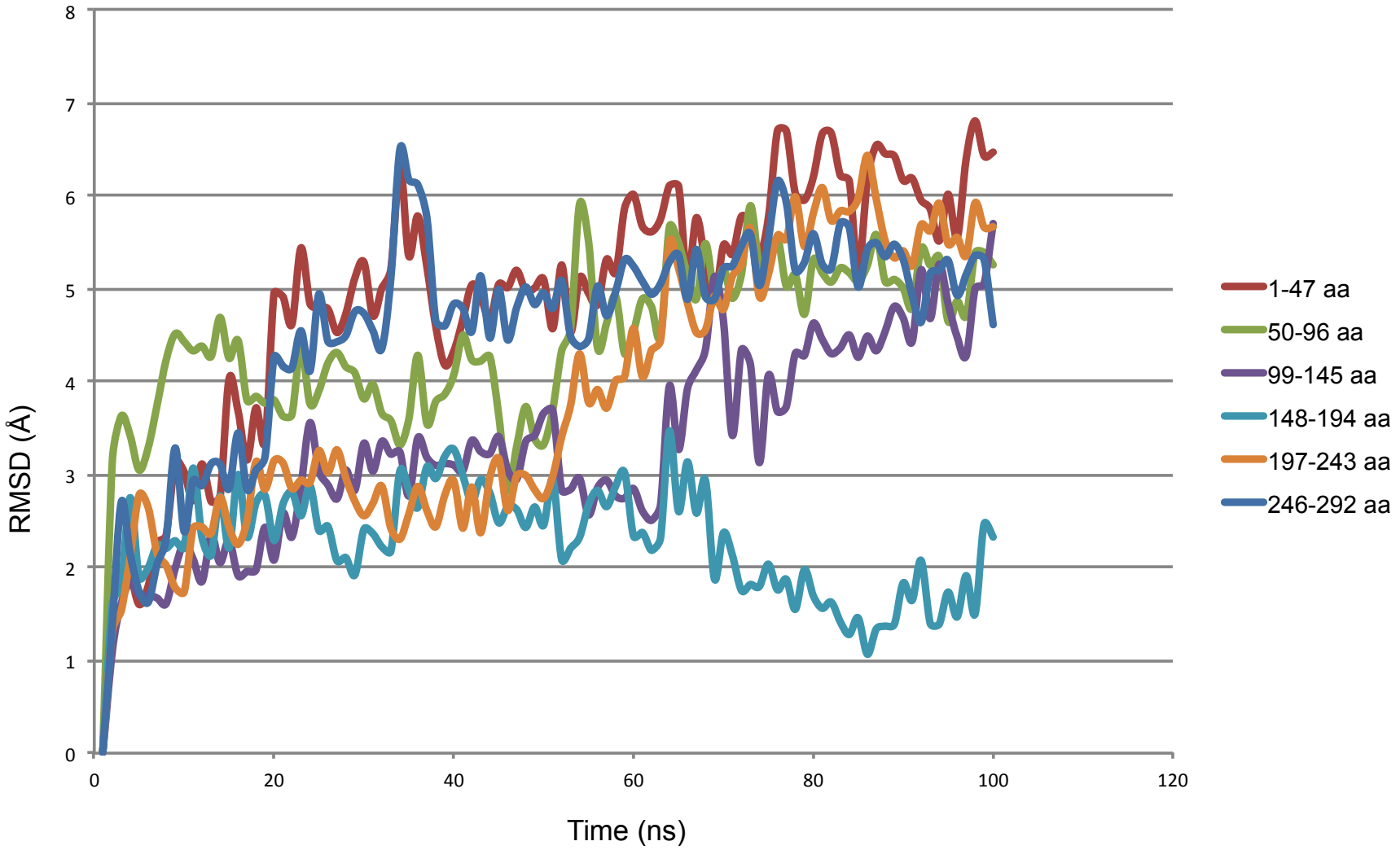

Figure 4.12: RMSD plots of the trajectories of each helix from system 391-314K.

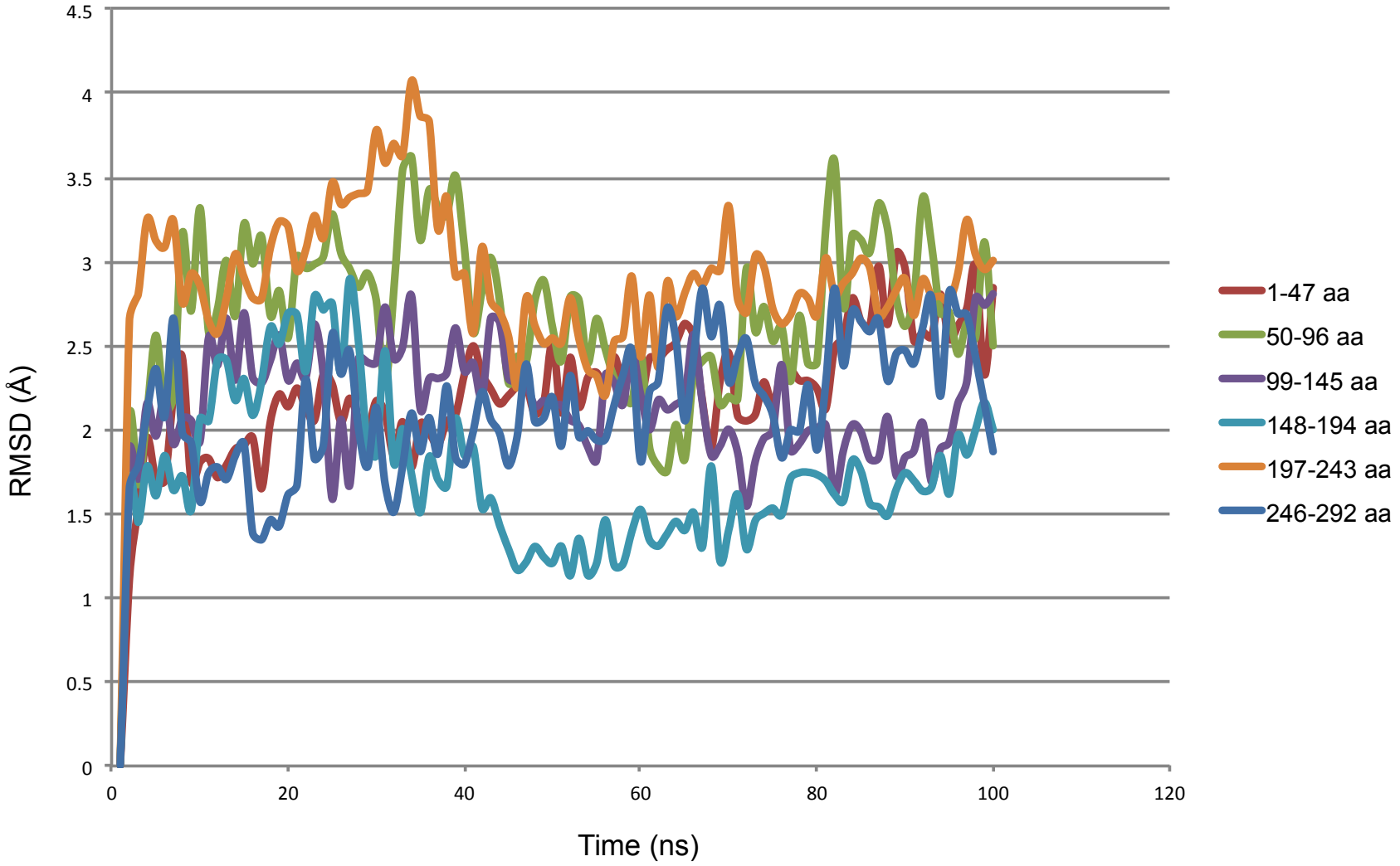

Figure 4.13: RMSD plots of the trajectories of each helix from system 391-ZN-300K.

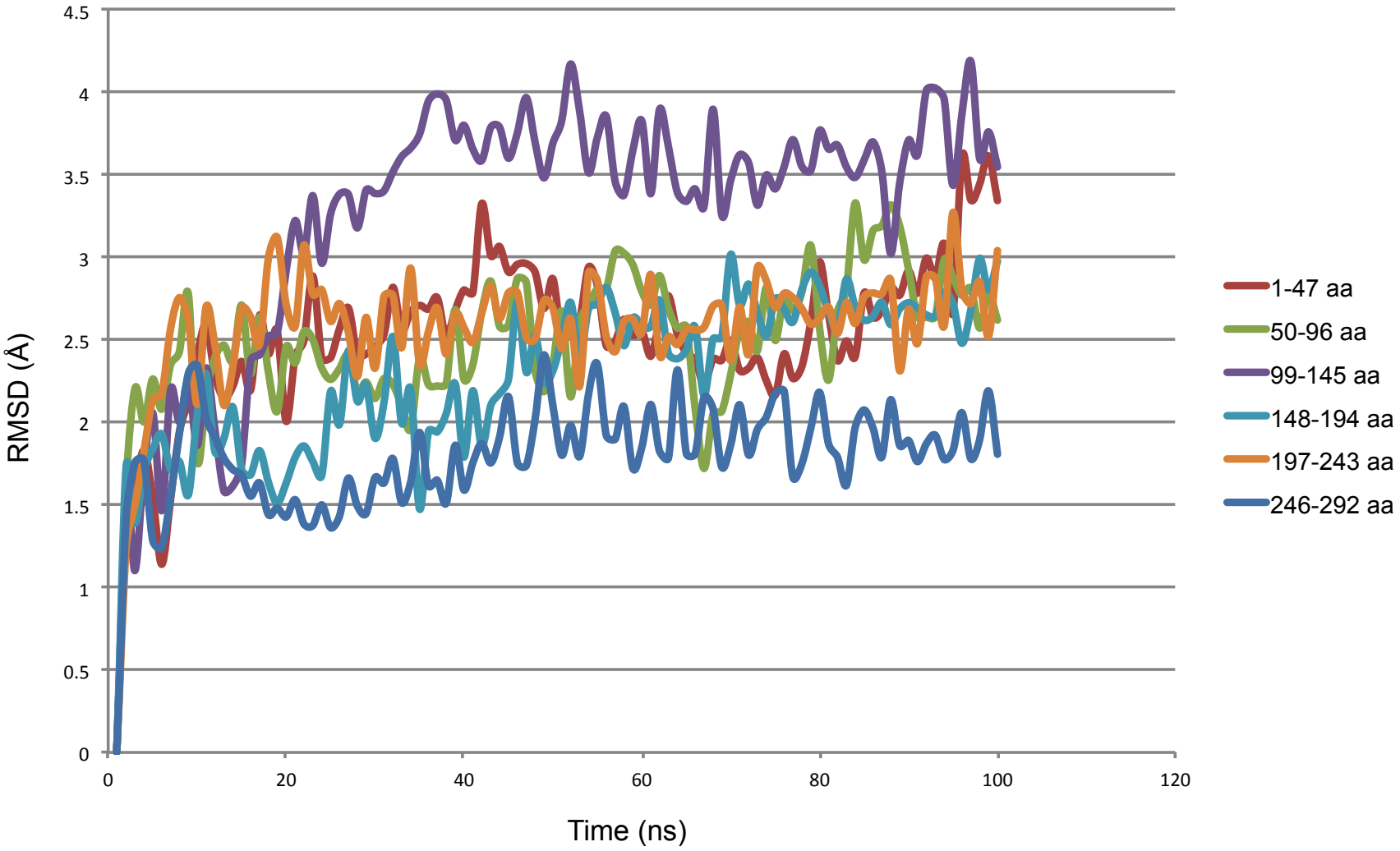

Figure 4.14: RMSD plots of the trajectories of each helix from system 391-ZN-310K.

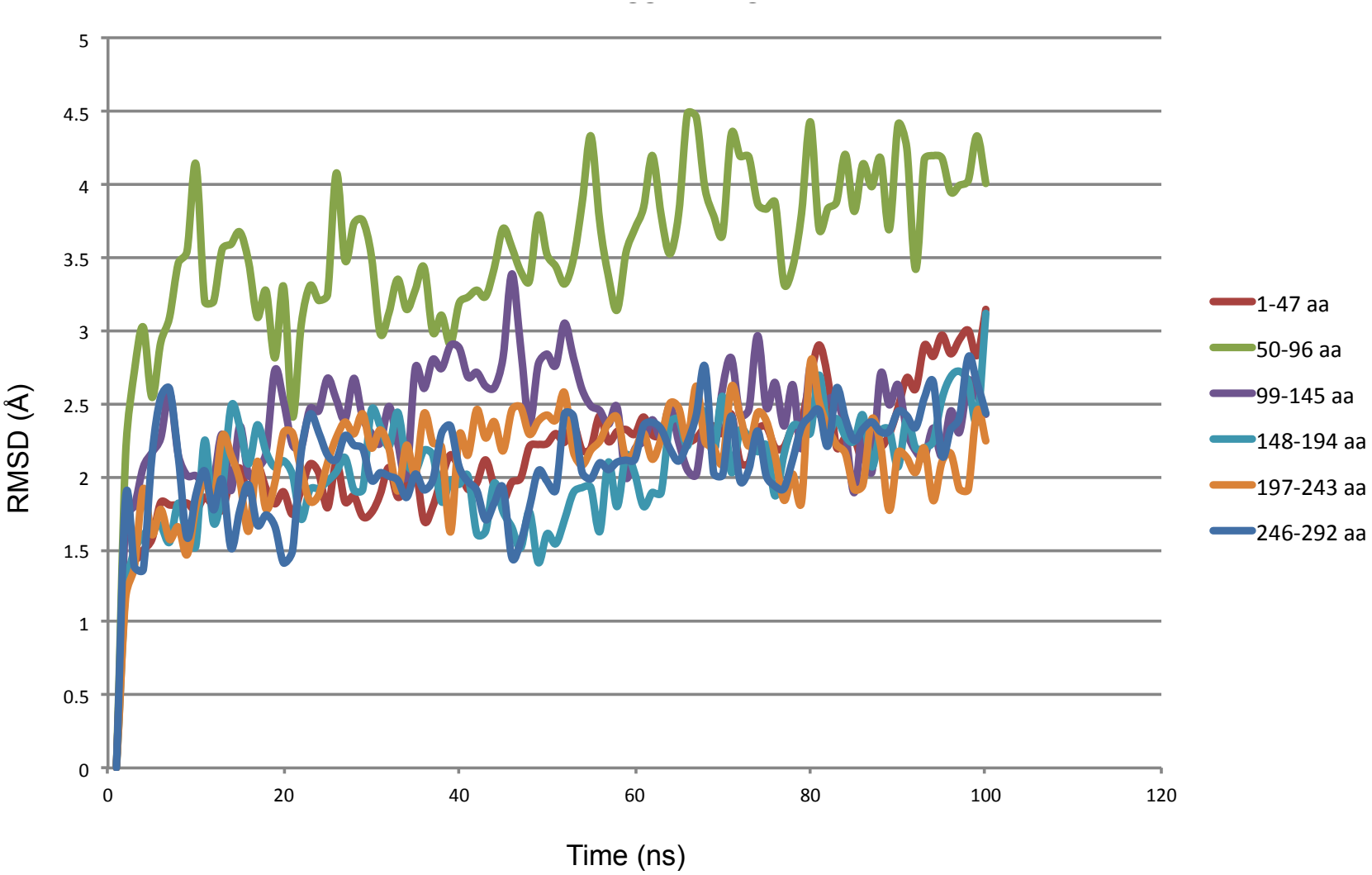

Figure 4.15: RMSD plots of the trajectories of each helix from system 391-ZN-314K.

4.3.5 Helix Dynamics Analysis

The helices with the highest RMSD value from each model was chosen for bending analysis by using the tool Bendix, providing the most extreme example of helical distortion that resulted in each simulation. The results are shown in Figure 4.16 to Figure 4.21. The angle-indicative heatmapping of each model and helix with the highest RMSD have been displayed. The colour scheme is Red-Green-Blue: red indicates the areas of highest helix axis angle; green for intermediate angle magnitudes; blue for angles closed to, or at 0 degrees (Dahl *et al*, 2012). The heatmap display of helix curvature aiding analysis of the relationship between different structures and dynamic conformational changed (Dahl *et al*, 2012). Angle data has also been displayed using a 3D landscape, where it takes into account the maximum angle computed during each trajectory and uses it as the colour threshold to scale the heatmap accordingly (Dahl *et al*, 2012).

For the low temperature model 391-300K, which is without Zn, it can be observed that the helix bundle retains its tight-packed structure, similar to the initial homology model. All helices are quite straight, which is in agreement with the RMSD results (as in Figure 4.9). It is obvious that distortive bending occurred in the mid-section, which consist of residues 185 to 190, Pro-Gln-Ile-Ser-Gln-Asn (PQISQN). Proline is a common helix-breaking residue, located at the hinge region in bent helices of many transmembrane proteins. Proline residues cause kinks in helices, and sterically prevent the (i-3)-carbonyl-(i + 1)-amino backbone hydrogen bond form forming (von Heijne, 1991). It is believed most transmembrane helix deformations (~60%) happen at proline residues (Yohannan *et al*, 2004). In the middle of a helix, proline distorts ideal α-helix geometry, due to the steric conflicts with the preceding residue and the loss of a backbone H bond (Reiersen & Rees, 2001). These distortions caused by proline might be functionally important in a helix. For instance, the distortion locations can be a weak point to facilitate movements required for the function of some transmembrane channels (Bright *et al*, 2002; Jin *et al*, 2002; Tieleman *et al*, 2001). For hexamer 391, helix kinking may

therefore also be important for its ion permeability. This may be tested experimentally by mutagenesis studies (eg. P185A mutants).

For the model 391-310K, most helices are distorted, in agreement with the obtained RMSD. The highest extent of distortion again occurs around residues 185 to 190. The whole bundle itself formed a ‘hourglass’ shape, with helices bent at the middle part of the complex. For the 391-314K model, all helices are highly distorted, and the bending region is still in the middle section. The model lost helical bundle symmetry and the ‘hourglass is more evident. In the model 391-ZN-300K, all the helices are all aligned straight in a tight-packed array, which is similar to dermcidin. Only one helix (helix 5) substantial disordered at the top section from residues 194 to 198, which are Lys-Val-Ser-Asp-Arg (KVSDR). For the model 391-ZN-310K and 391-ZN-314K, despite of the high temperatures, both model helices are still straight but exhibit more extreme bending at the end and limited bending at the middle.

In conclusion, simulation results indicate that the most bended area of the no zinc models is in the middle section of the bundles. However, for the models with the present of zinc, the most flexible areas are at the end of the helices. For the overall structures, zinc helps to keep the bundle together and stop the helix bending at the middle when the simulation temperature is 310 K or 314 K.

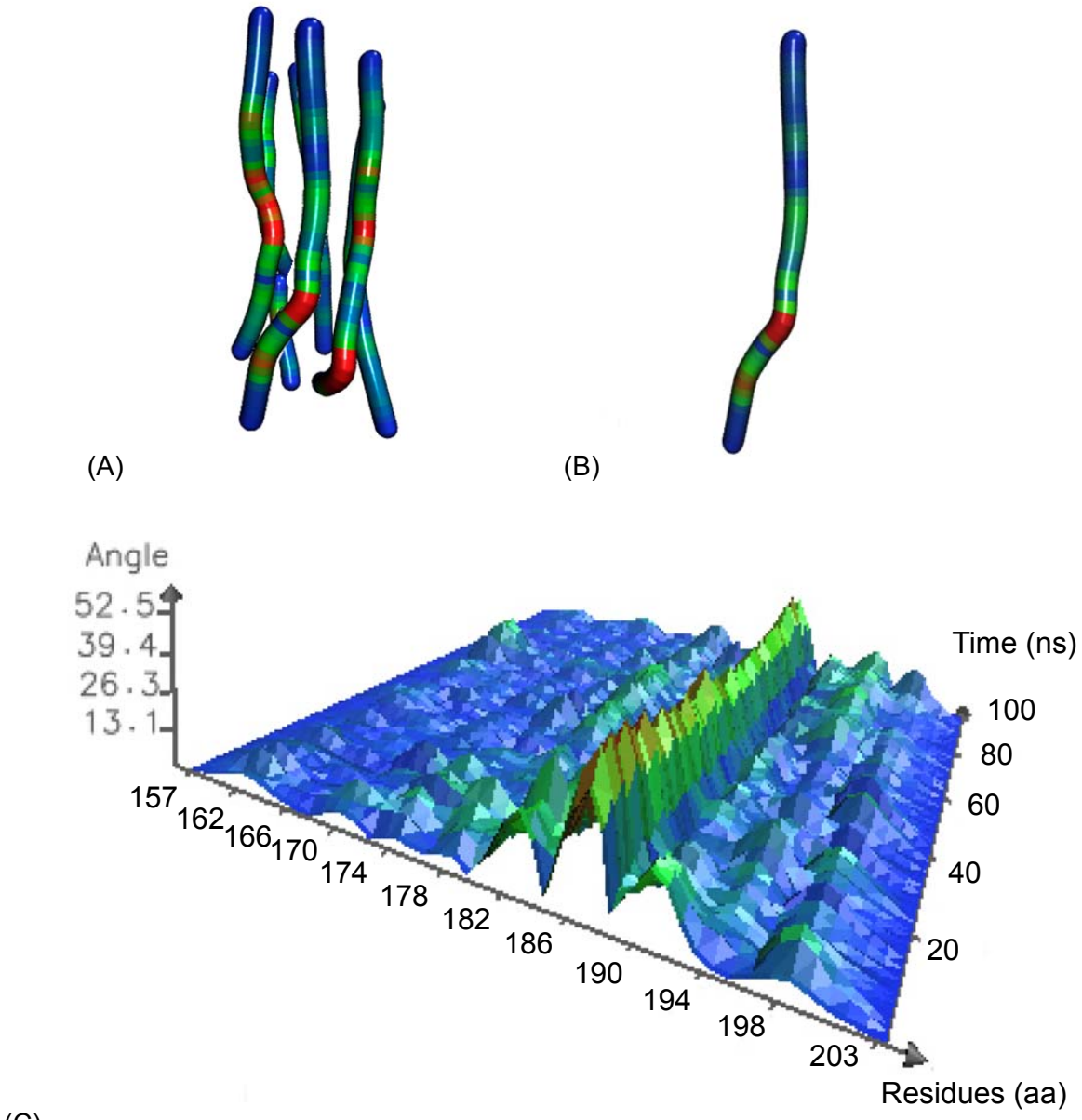

Figure 4.16: Bendix analysis of model 391-300K. (A) Angle-indicative heatmapping of model 391-300K from MD simulation. (B) Angle-indicative heatmapping of helix 2 of model 391-300K from MD simulation. (C) Heatmap surface of the helix 2 trajectory from model 391-300K MD simulation.

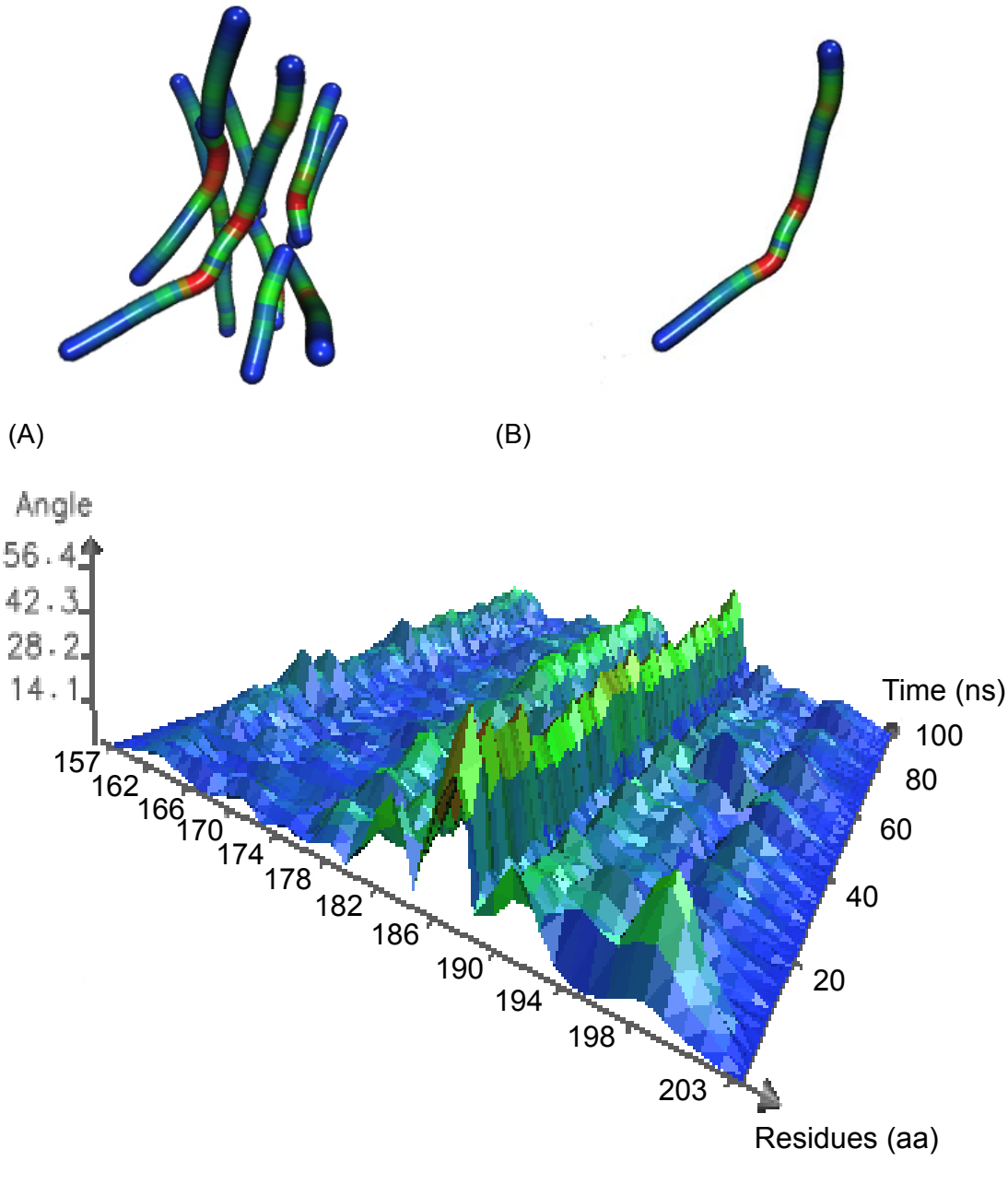

Figure 4.17: Bendix analysis of model 391-310K. (A) Angle-indicative heatmapping of model 391-310K from MD simulation. (B) Angle-indicative heatmapping of helix 2 of model 391-310K from MD simulation. (C) Heatmap surface of the helix 2 trajectory from model 391-310K MD simulation.

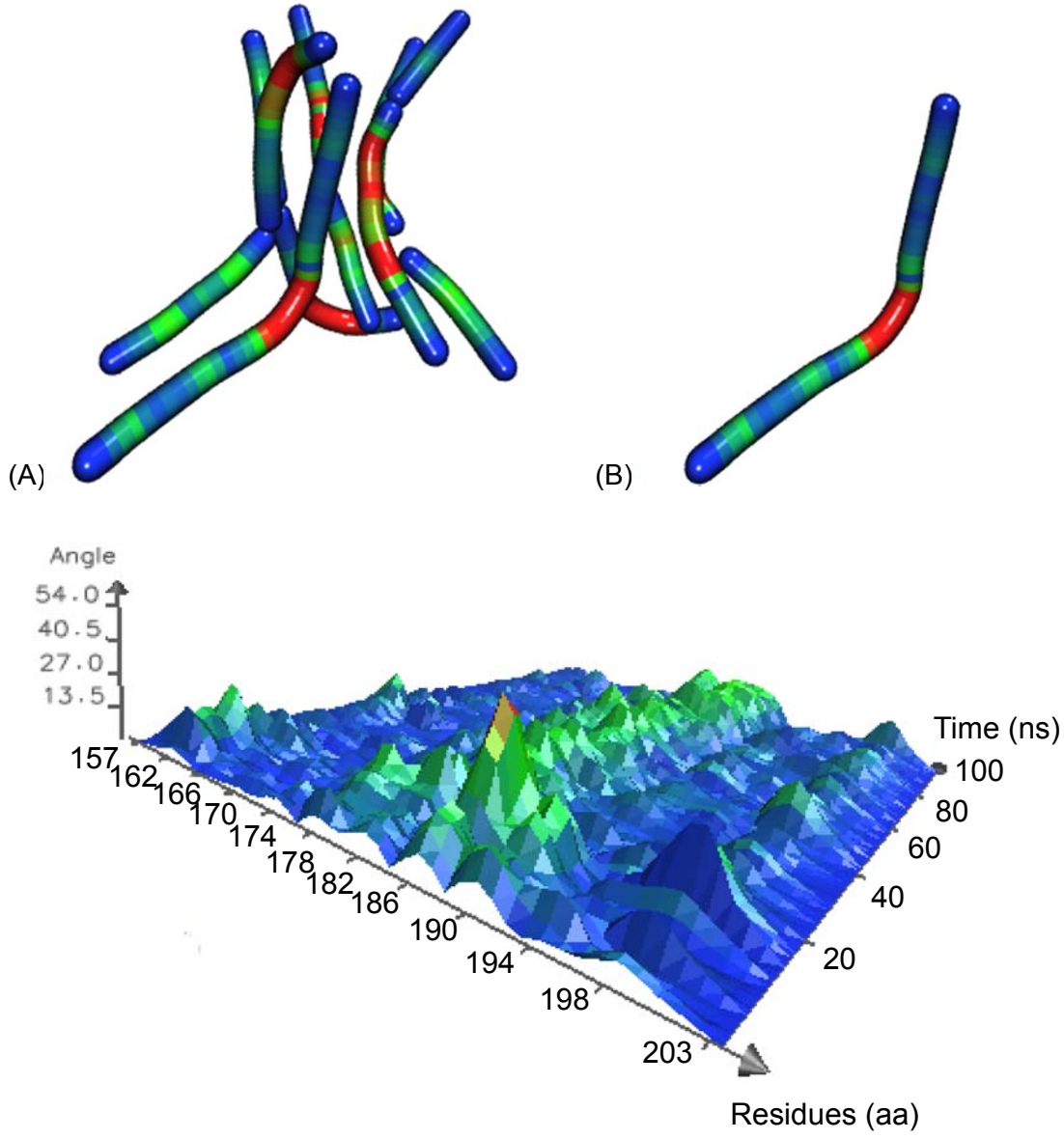

Figure 4.18: Bendix analysis of model 391-314K. (A) Angle-indicative heatmapping of model 391-314K from MD simulation. (B) Angle-indicative heatmapping of helix 1 of model 391-314K from MD simulation. (C) Heatmap surface of the helix 1 trajectory from model 391-314K MD simulation.

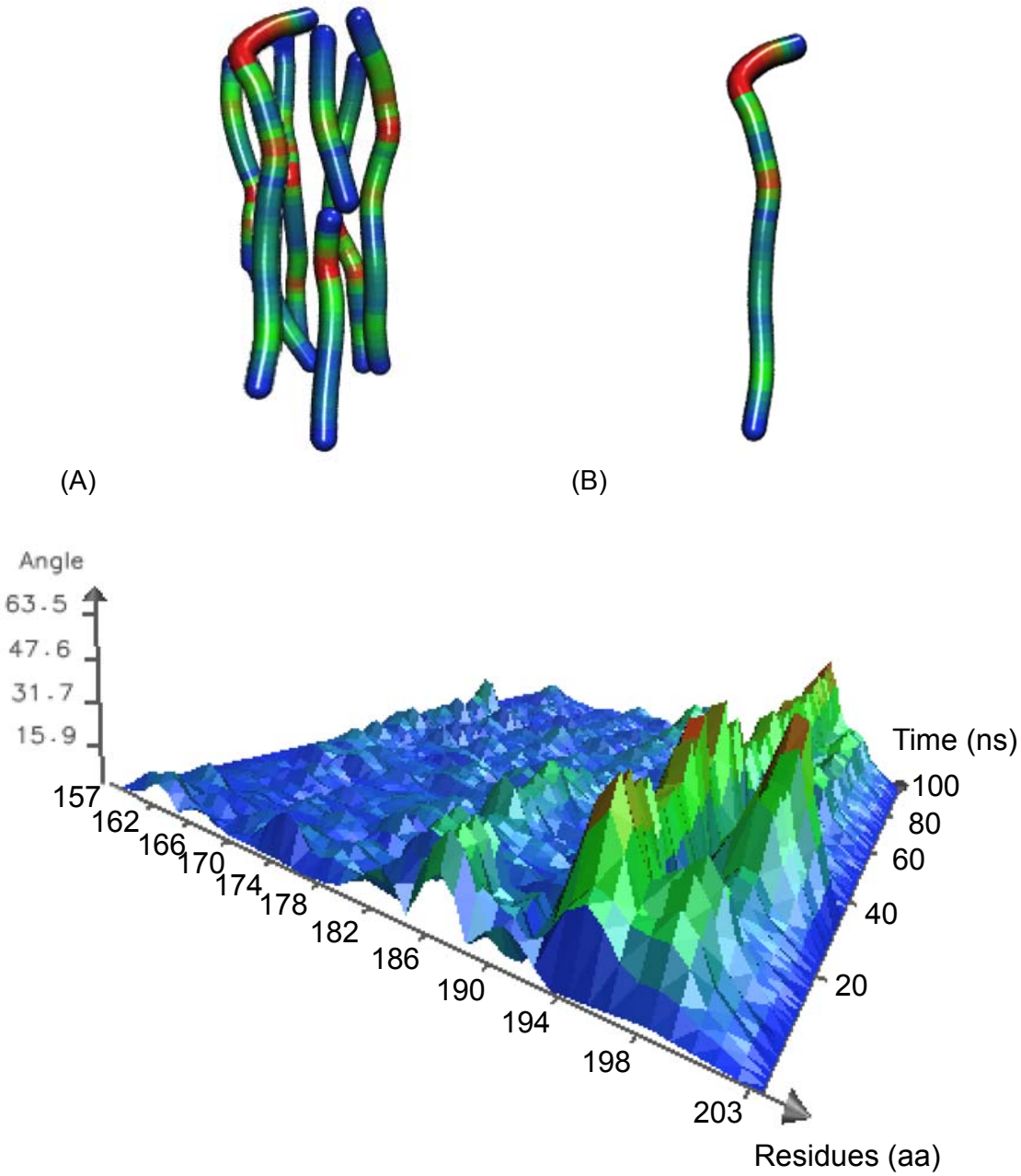

Figure 4.19: Bendix analysis of model 391-ZN-300K. (A) Angle-indicative heatmapping of model 391-ZN-300K from MD simulation. (B) Angle-indicative heatmapping of helix 5 of model 391-ZN-300K from MD simulation. (C) Heatmap surface of the helix 5 trajectory from model 391-ZN-300K MD simulation.

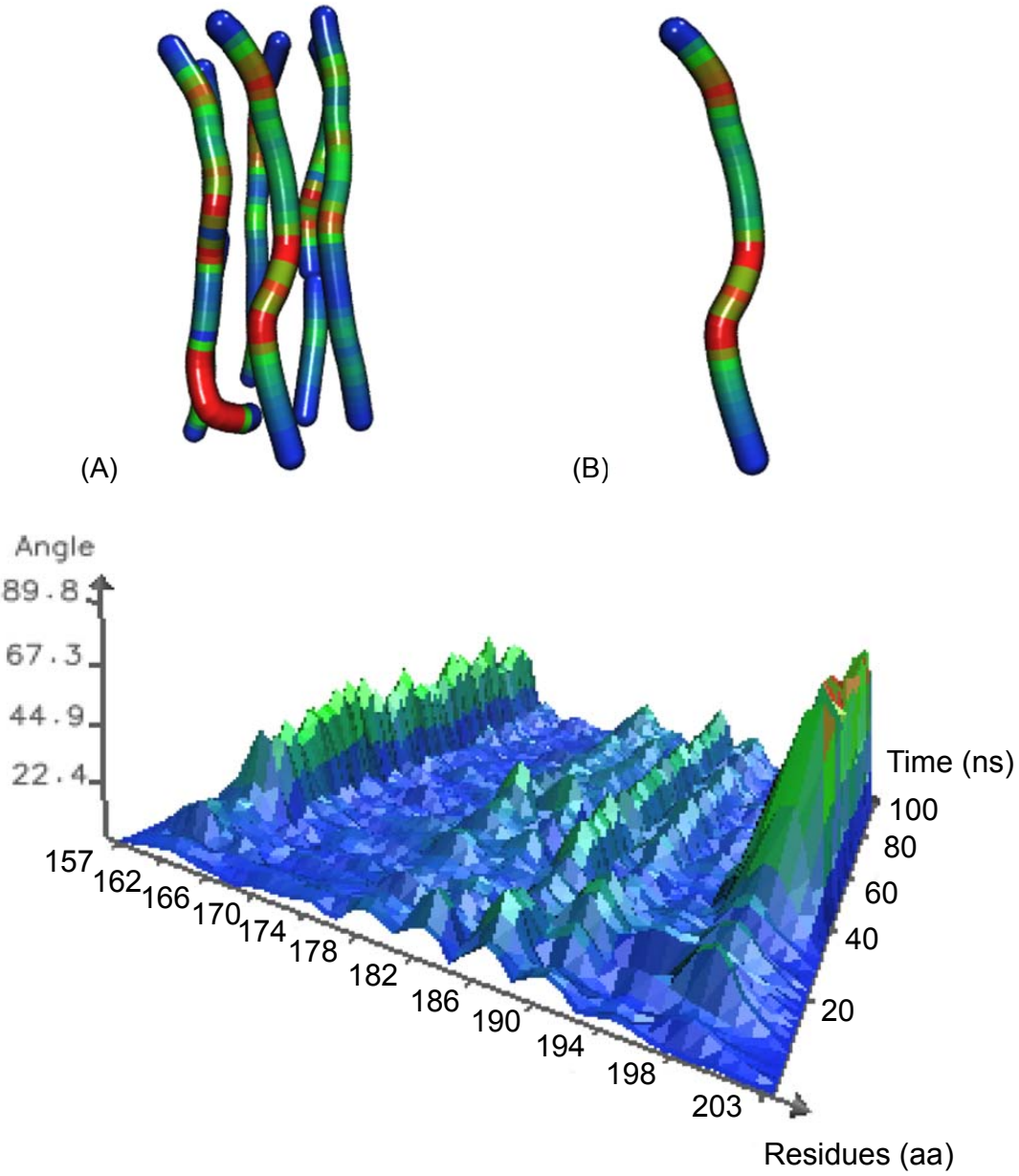

Figure 4.20: Bendix analysis of model 391-ZN-310K. (A) Angle-indicative heatmapping of model 391-ZN-310K from MD simulation. (B) Angle-indicative heatmapping of helix 3 of model 391-ZN-310K from MD simulation. (C) Heatmap surface of the helix 3 trajectory from model 391-ZN-310K MD simulation.

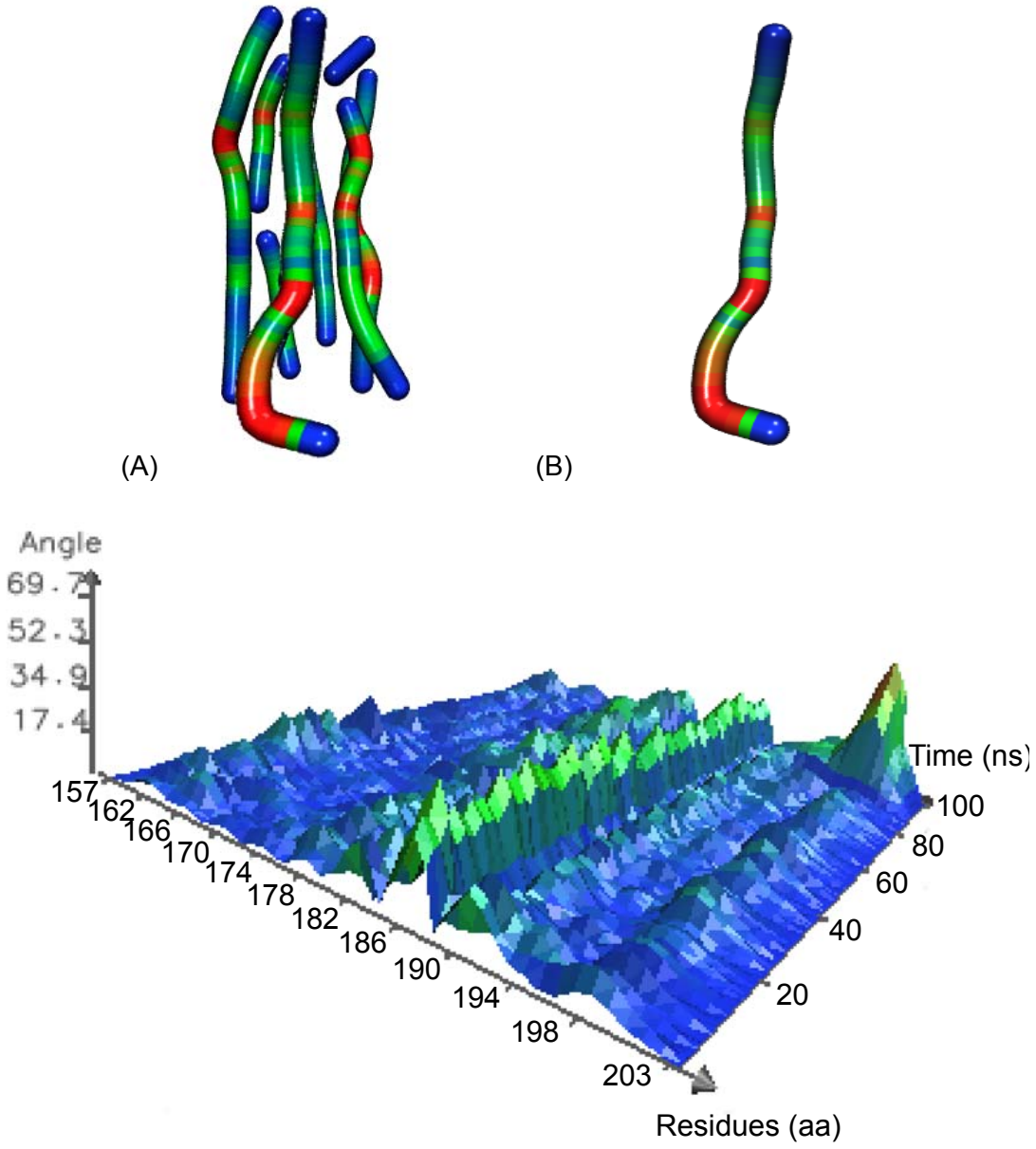

(C)

Figure 4.21: Bendix analysis of model 391-ZN-314K. (A) Angle-indicative heatmapping of model 391-ZN-314K from MD simulation. (B) Angle-indicative heatmapping of helix 2 of model 391-ZN-314K from MD simulation. (C) Heatmap surface of the helix 2 trajectory from model 391-ZN-314K MD simulation.

4.3.6 Pore Size Analysis

The initial Cj0391c homology model, as well as PDB structures obtained from the final frame of each of the MD simulation trajectories have been uploaded to PoreWalker website for pore size and features analysis. The results from PoreWalker are shown in Figure 4.22 to Figure 4.29.

Figure 4.22 shows the results from PoreWalker, which present the pore diameter profile for homology model of Cj0391c based on dermcidin. The structure submitted was the 391 hexamer model before simulation. For the model without Zn at 300 K, the pore diameter is relatively high at the two ends (5~7 Å), while low at the centre (~ 2 Å). When the temperature is at 310 K, the profile shows a more distinct shape, wide at both ends and narrow in the middle, which is consistent with the 'hourglass' shape appearance of the helix bundle. The pore size and shape is quite similar from the simulation temperature at 314 K compared with 310 K, just with even more apparent shape. The starting 391 model with the presence of Zn is similar to the starting model of 391 without Zn. For the 391-ZN-300K model, the pore is narrow at one end and wide at the other. The shape of the bundle resembles slight 'peeling off' at one end, which can be observed from Figure 4.26 (A). When the simulation temperature is increased to 310 K with Zn present, the pore structure is very similar to the model at 300 K. This trend was the same when the temperature reached 314 K. The lowest size is about 3 Å.

Results show that the pores are filled with both positively and negatively charged residues, and further work will be required to ascertain whether the pore is ion selective. Generally, for the models without zinc, the middle of the pore is narrower compare to the models with zinc, which is consistent with the results obtained from the helix dynamics analysis indicating higher degree of bending at the middle for the zinc-free structures. However, all of the model

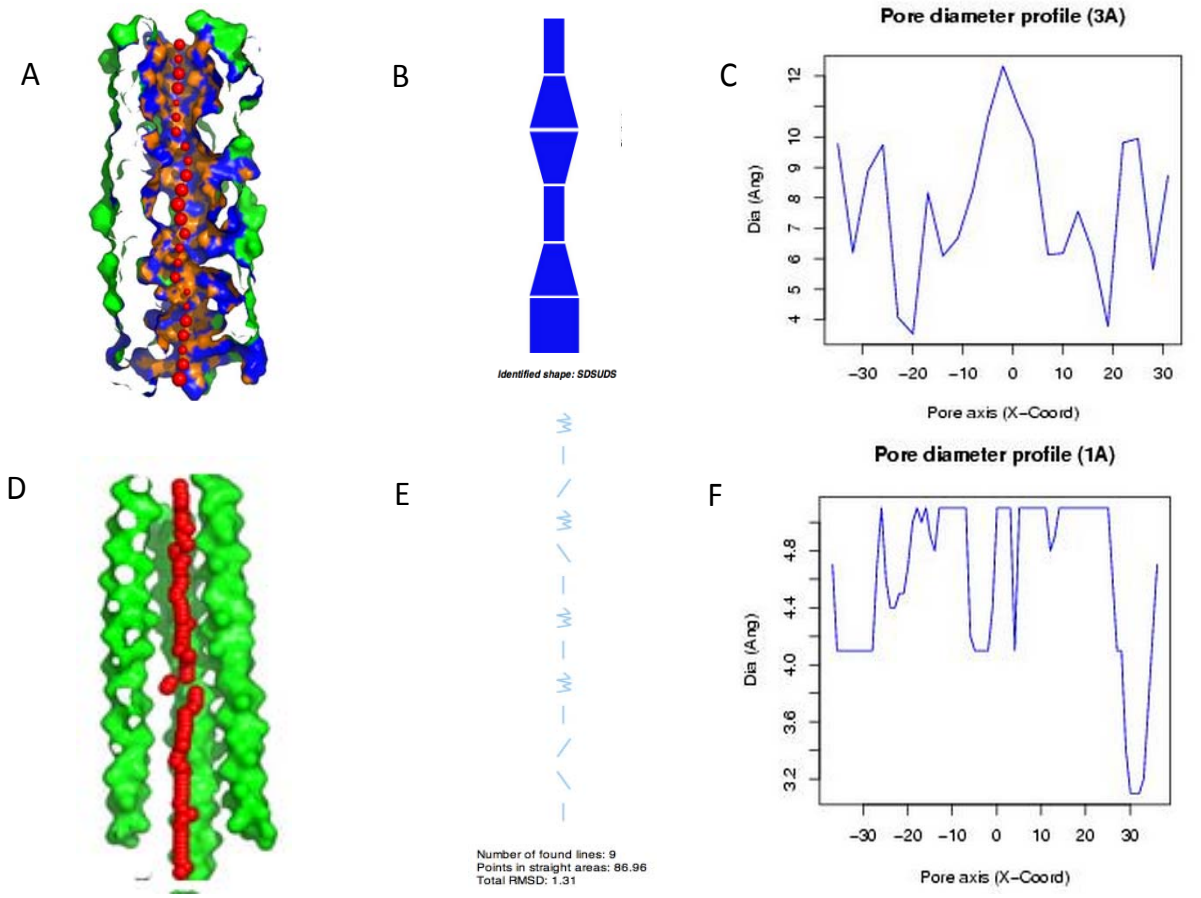

Figure 4.22: Pore size analysis of model 391 without zinc before MD simulation

(A) visualisation of a pore section showing pore-lining residues and pore centres at 3Å steps: the section of the structure was obtained by cutting the protein structure along the xy-plane, where the x-axis corresponds to the pore-axis, and y-coordinate>0 only are displayed. Pore-lining atoms and residues are coloured in orange and blue, respectively. The remaining part of the protein is shown in green. Red spheres represent pore centres at given pore heights and their diameters correspond to 1/10 of the pore diameter calculated at that point; (B) representation of the shape of the pore and shape characterization string: the pore is simplified as a stack of building blocks going from the most negative to the most positive coordinate along the pore axis (x-axis). D, U and S indicate conical frustums of decreasing diameter, conical frustums of increasing diameter and cylinders, respectively; (C) pore diameter profile at 3Å steps corresponding the pore shape in (B). Pore axis (X-Coord): the position along the pore axis is shown as x-coordinate in Å. Dia (Ang): pore diameter value in Å; (D) visualization of a pore section showing the position of the biggest spheres (pore centres) that can be built along the channel at 1Å steps: the section of the structure was obtained by cutting the protein structure along the xy-plane. The protein structure is coloured in green; (E) diagram of the regularity of the pore cavity as number of lines that can approximate the positions of the pore centres at 1Å steps (PRINCIP). The pore is represented as a series of consecutive straight and wiggly lines representing channel areas where pore centres can (straight) or cannot (wiggly) be fitted to a line, going form the most negative to the most positive coordinate along the pore axis (x-axis). Vertical lines describe either the only low-RMSD areas throughout a pore or low-RMSD areas that are co-linear. Diagonal lines represent low-RMSD areas, which are different from the low-RMSD areas other identified along the channel. Curve lines indicate areas where pore centres are highly spread; (F) pore diameter profile at 1Å steps. Pore axis (X-Coord): the position along the pore axis is shown as x-coordinate in Å. Dia (Ang): pore diameter value in Å (Figure legend reproduced from Pellegrini-Calace. *et al*, 2009).

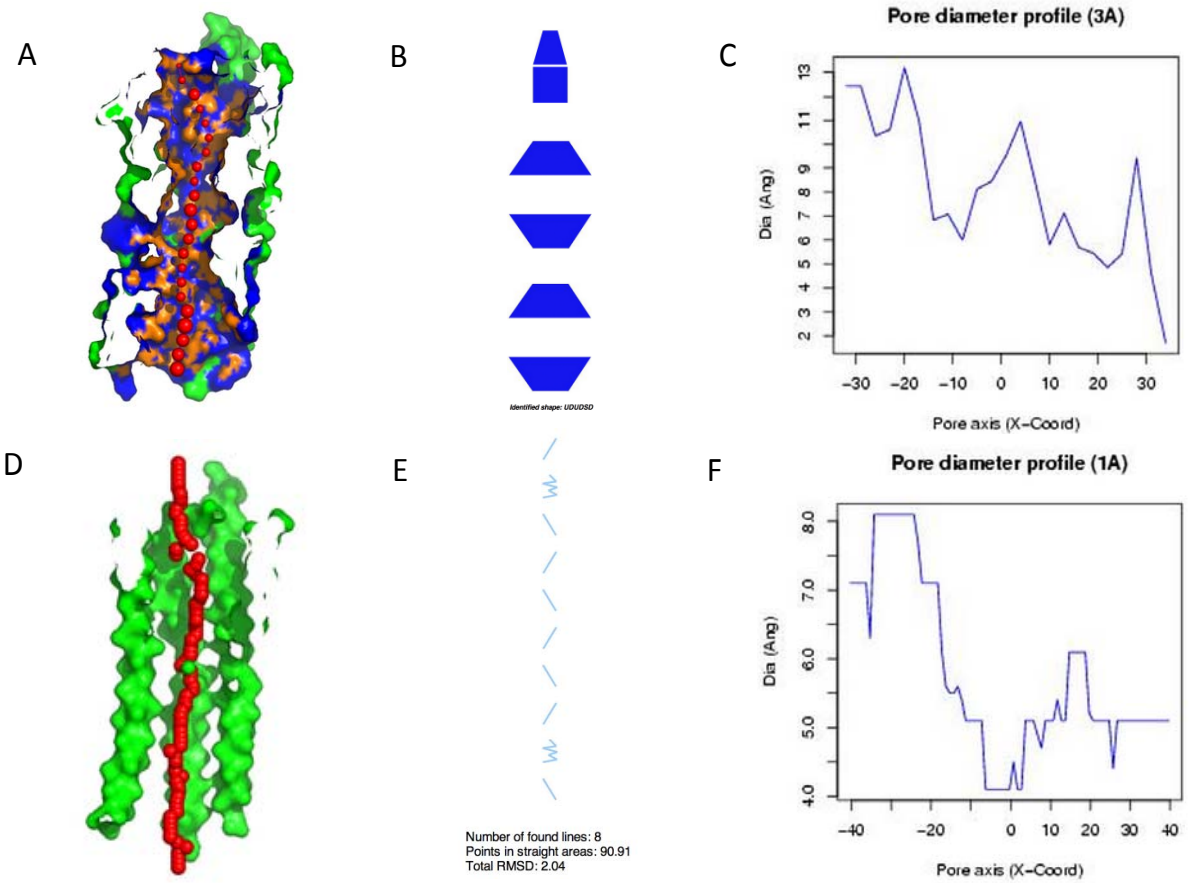

Figure 4.23: Pore size analysis of model 391 without zinc after simulating for 100 ns at 300 K (See Figure 4.21 caption for details explanation).

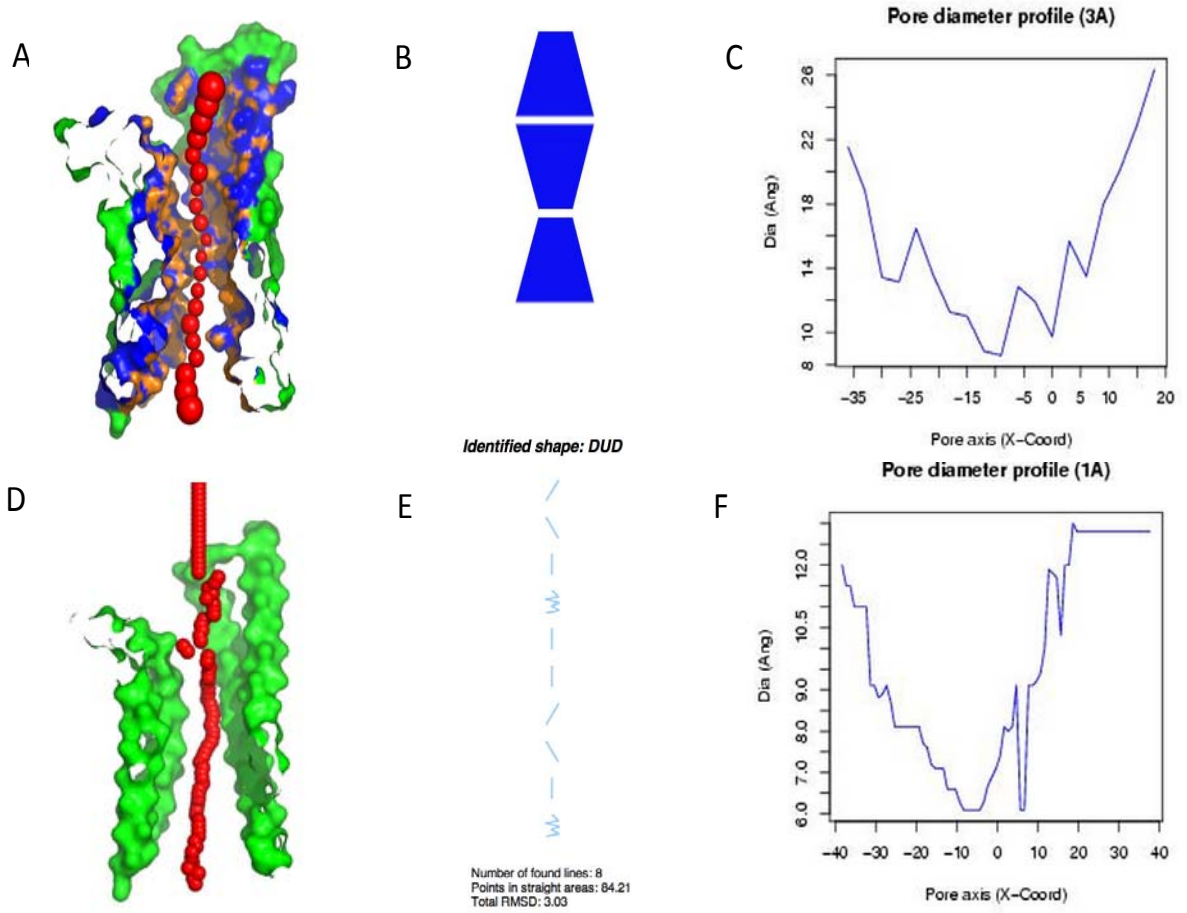

Figure 4.24: Pore size analysis of model 391 without zinc after simulating for 100 ns at 310 K (See Figure 4.21 caption for details explanation).

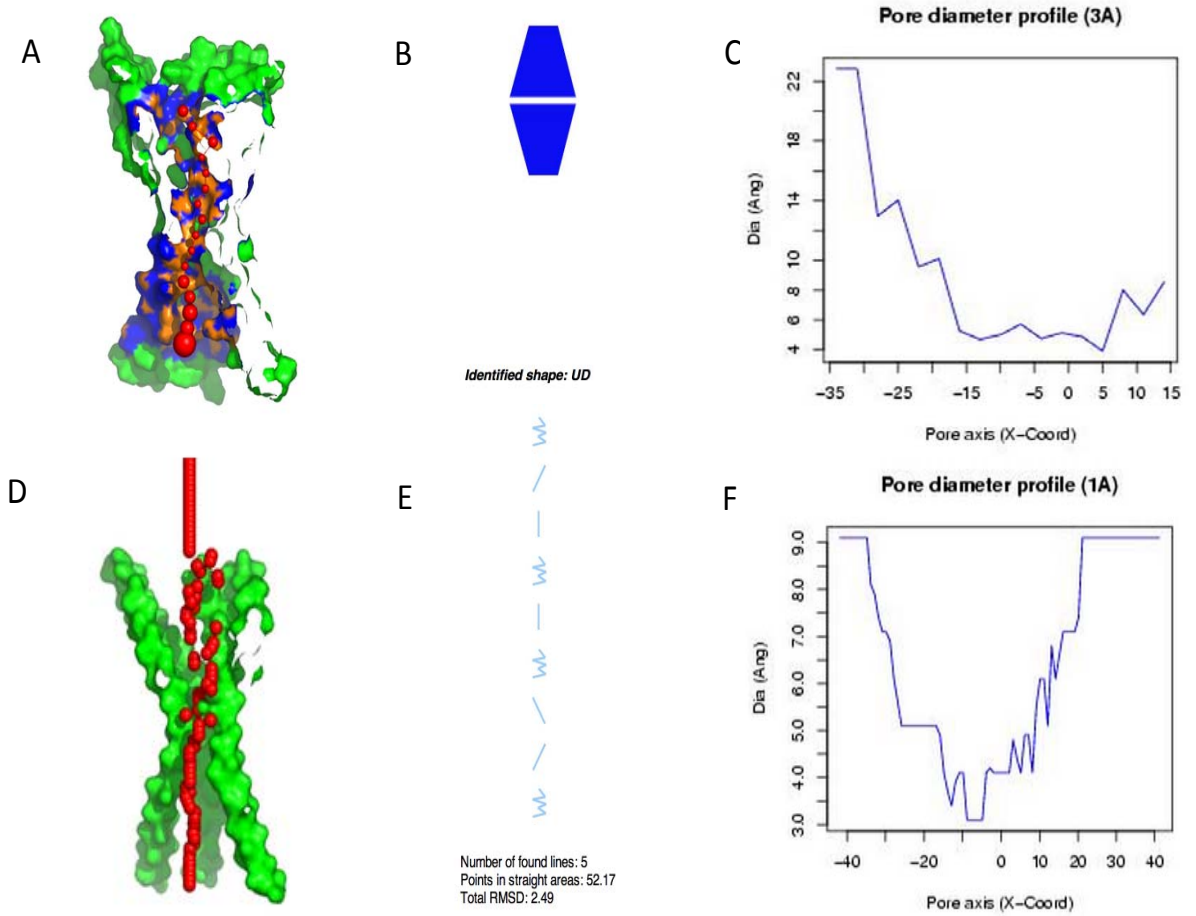

Figure 4.25: Pore size analysis of model 391 without zinc after simulating for 100 ns at 314 K (See Figure 4.21 caption for details explanation).

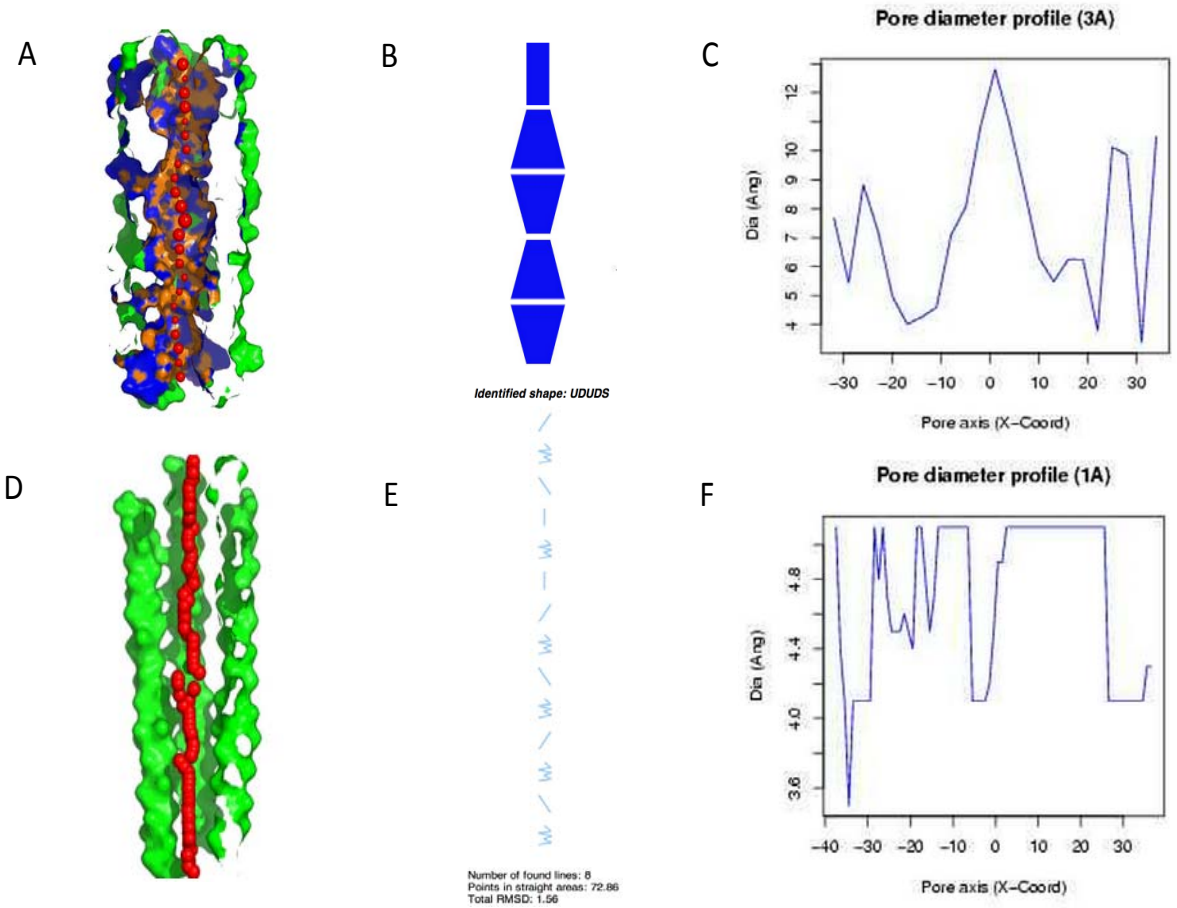

Figure 4.26: Pore size analysis of model 391 with zinc before MD simulation (See Figure 4.21 caption for details explanation).

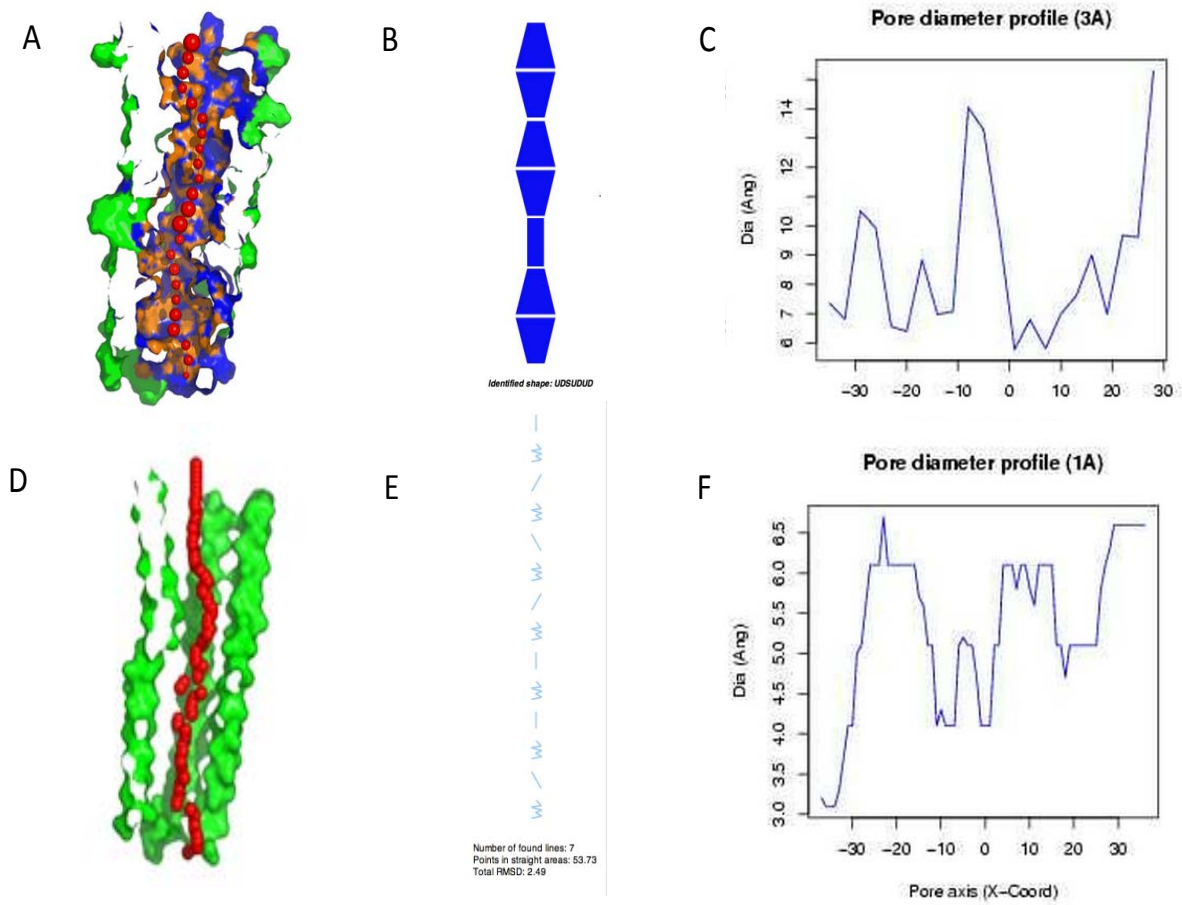

Figure 4.27: Pore size analysis of model 391 with zinc after simulating for 100 ns at 300 K (See Figure 4.21 caption for details explanation).

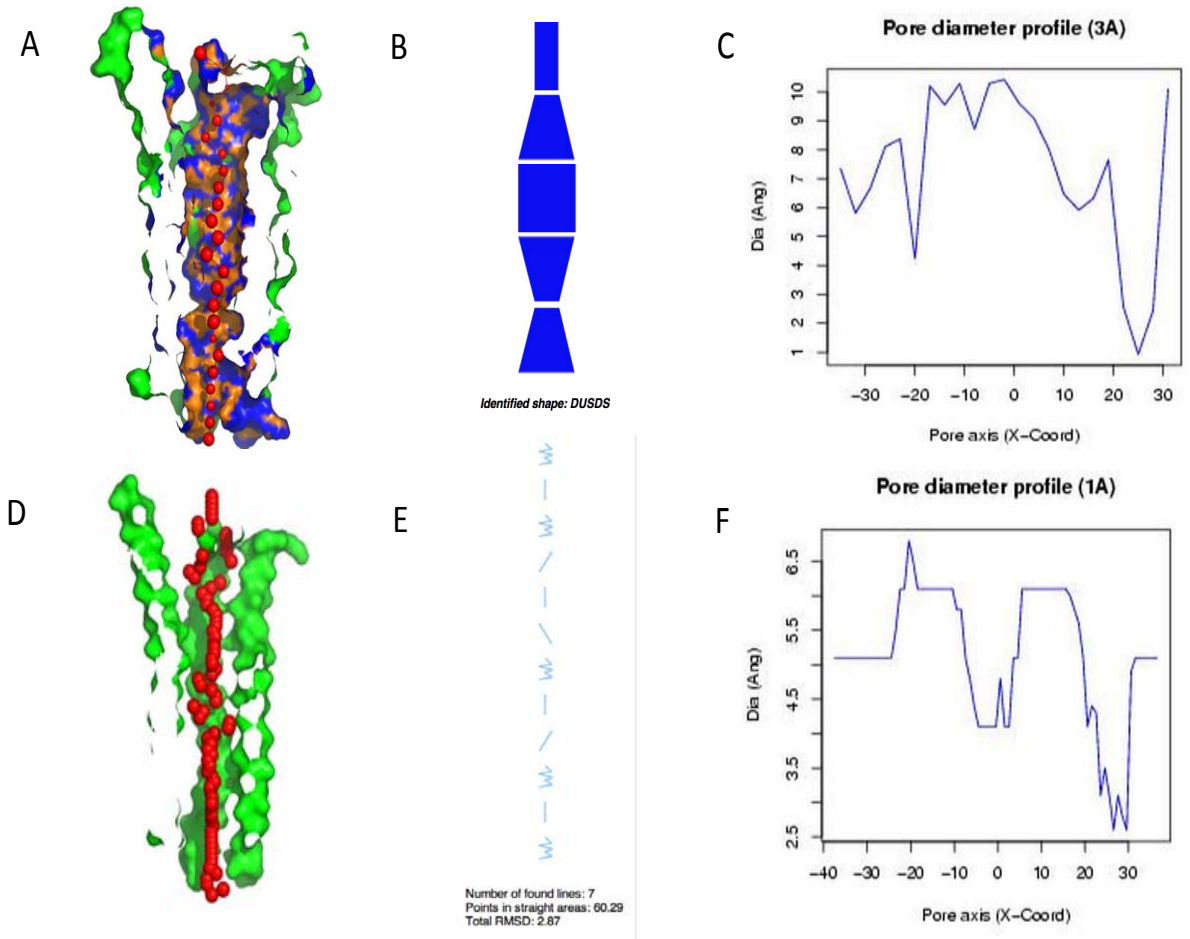

Figure 4.28: Pore size analysis of model 391 with zinc after simulating for 100 ns at 310 K (See Figure 4.21 caption for details explanation).

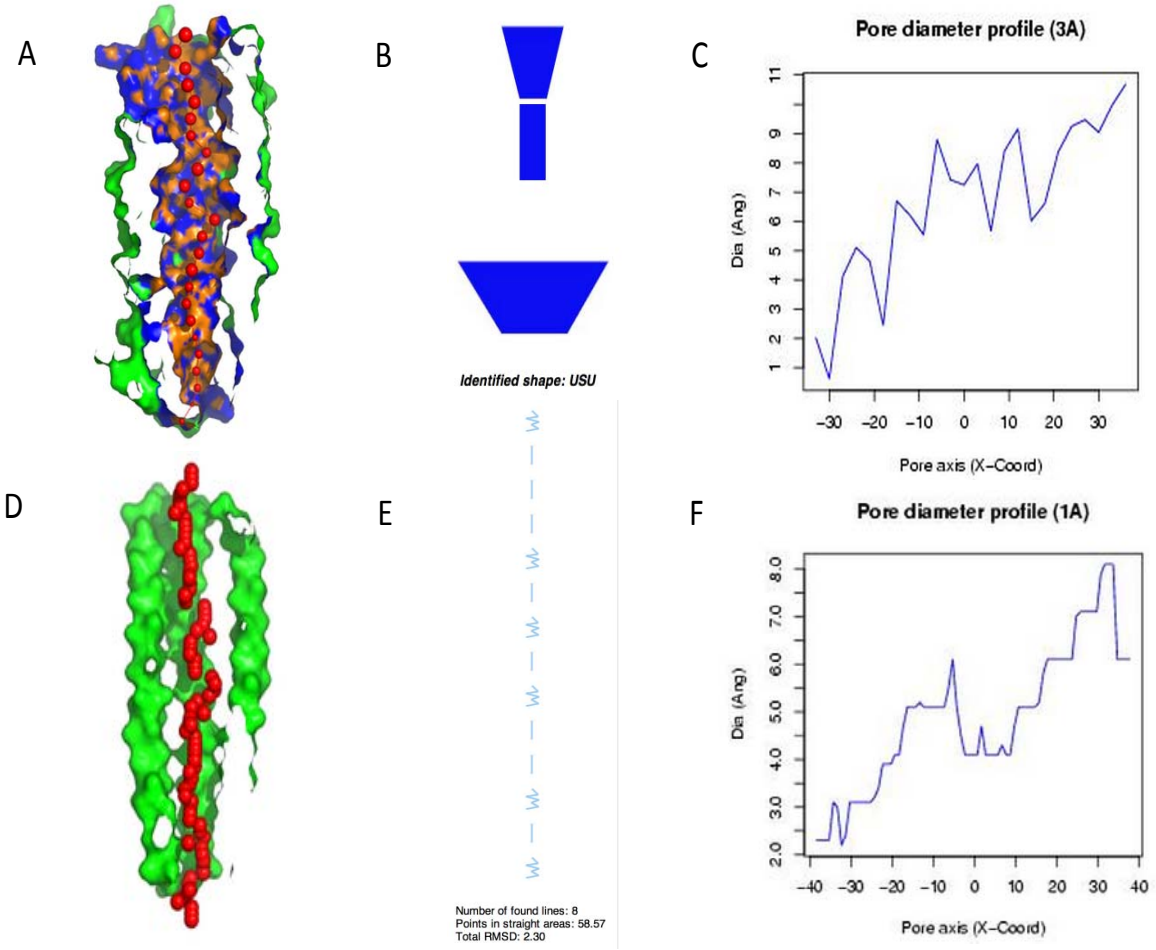

Figure 4.29: Pore size analysis of model 391 with zinc after simulating for 100 ns at 314 K (See Figure 4.21 caption for details explanation).

channels are big enough to fit at least one water molecule. The overall pore sizes are wider with the low temperature simulations, indicating that conductance might be higher at low temperature.

4.3.7 Bilayer and Water Environment Around Zinc

The Zn^{2+} were initially placed in the same positions of the dermcidin model, on the outside of the bundle in between the helices. These positions are not normally considered a favourable environment for divalent cations. However, after 100 ns simulation, the lipid bilayer adapts so that the Zn^{2+} is complexed to polar groups of lipid headgroups; and also water partially permeates the bilayer near the Zn^{2+} to form a solvent 'shell'. Figure 4.30 (A) shows the structure of the 391-ZN-300K 100 ns simulation model, while similar results are obtained in the other simulation models. Illustration of one Zn^{2+} in the 391-ZN-300K simulation after 100 ns complexed to water molecules and phosphate groups of surrounding POPE is shown in Figure 4.30 (B). Thus Zn^{2+} does not remain in an energetically unfavourable environment of the lipid tails. Instead, the bilayer structurally adapts to form a polar environment around the Zn^{2+}. Similar phenomena have been examined by previous MD simulations. For example, in the study of Wang and Larson (2014), the function of charged ions involved in facilitating water channel formation has also been discussed, involving similar distortion of bilayer structure to accommodate passage of charged ions through the membrane core region.

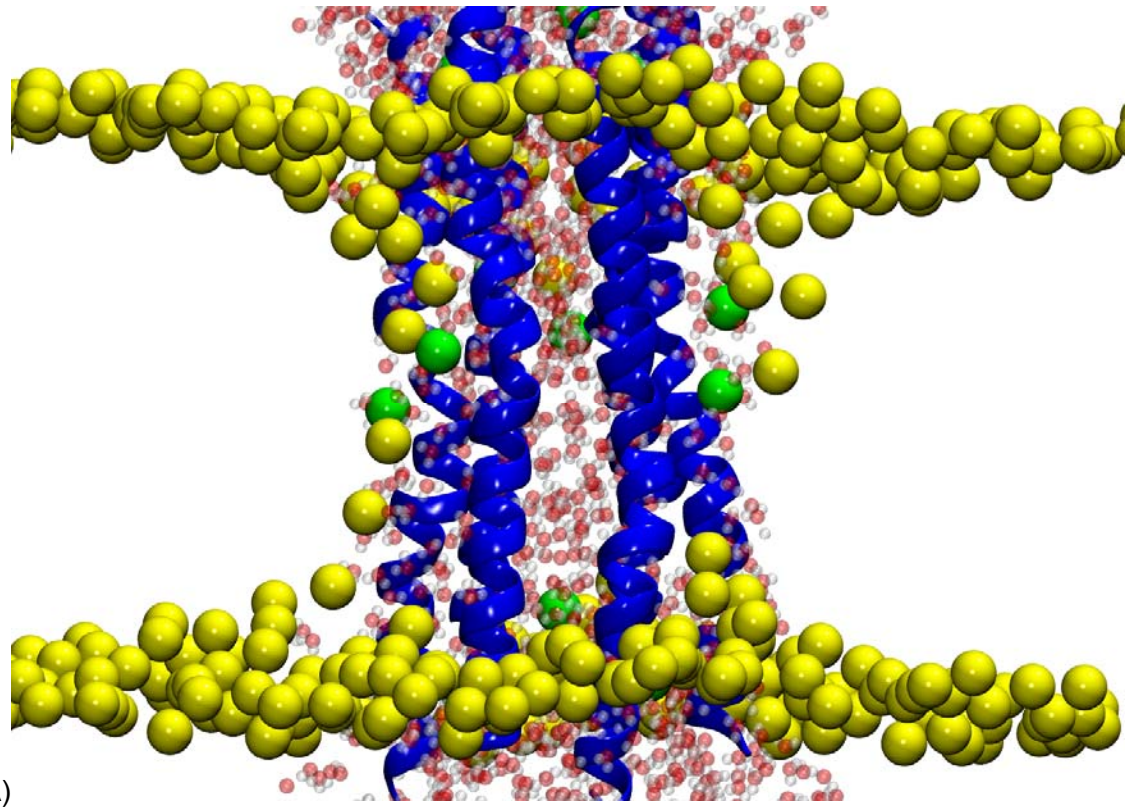

(A)

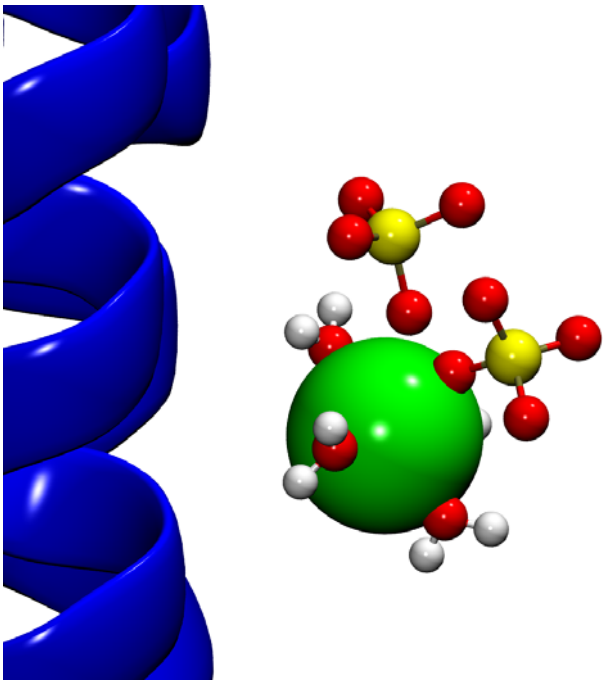

(B)

Figure 4.30: (A) The structure of model 391-ZN-300K after 100 ns simulation. (B) Illustration of one Zn^{2+} in the 391-ZN-300K simulation after 100 ns complexed to water molecules and phosphate groups of surrounding POPE (green: Zn^{2+}; red: oxygen; yellow: phosphorus; white: hydrogen).

4.4 Discussion and Conclusion

Using dermcidin as a structural template, we employed homology modelling to build the hexamer structure of Cj0391c (the hexamer is named 391 in this study), and simulated its atomic-level motions in a lipid bilayer using fully-solvated molecular dynamics. Their dynamics have been investigated by atomistic MD methods, in which the motions of the individual atoms of the proteins together with their solvent/cellular environments are explicitly computed based on Newtonian mechanics. Molecular simulation software packages GROMACS was used to obtain MD trajectories.

We examined the effects of zinc on the structure of protein 391, and propose that while zinc has comparatively little effect on hexamer symmetry at low temperature, it is crucial to maintaining symmetry and helix linearity at elevated temperatures. Simulations also elucidated the influences of zinc and temperature on pore size and shape, forming a basis for experiments to study the functional properties of this protein under various conditions.

Based on the experimental observations from Chapter 3, we explore a number of hypotheses for the mechanisms by which Cj0391c induces chicken macrophage apoptosis as well as the possible structure of Cj0391c.

The first hypothesis raised was protein Cj0391c might be a death receptor ligand with structure similar to TNF-α or TRAIL. However, the protein sequence alignment results indicate that sequence alignment between protein Cj0391c and these ligands is comparably poor (as death receptor ligands are typically comprised of β-strands). None of the secondary structure and fold prediction methods employed on Cj0391c suggests that it contains any β-strand content.

The second hypothesis was protein Cj0391c may be a toxin similar to Shiga-toxin. However, Shiga-toxin and Shiga-related toxins are composed of two subunits from two different genes,

an effector subunit and a membrane binding subunit. Cj0391c is a most probably a single subunit in our experiment (Chapter 3), as it was expressed as a single chain, but still causes chicken macrophage cell apoptosis. However, we cannot exclude the possibility that Cj0391c might be a Shiga-like toxin.

Finally, protein Cj0391c may be a toxin acting via formation of α-helical ion channel enabling the exchange of ions (pore-forming toxin), causing DNA fragmentation and cell lysis. Pore-forming toxins (PFTs) are a class of proteins that convert from a soluble form to a membrane-integrated pore (Parker & Feil, 2005). They can be divided to two main groups based on the suspected mode of membrane integration, α-PFTs and β-PFTs. Since all the secondary structure prediction utilised all indicated similar results, Cj0391c is proposed to be α-helical, and the C-terminal is also α-helical. However, it does not align well with any known helical toxin, except dermcidin (PDB code 2YMK). The sequence alignments with the only three 3D assembled structures available α-PFTs in PDB, which are cytolysinA (ClyA, aka HlyE) (PDB code 2WCD), fragaceatoxin C (FraC) (PDB code 3LIM) and dermcidin (PDB code 2YMK), are displayed in Figure 4.30. They are the only α-PFTs with assembled 3D structure available in PDB by 2013.

ClyA is a cytotoxic toxin towards cultured mammalian cells, which induces apoptosis of macrophages and promotes tissue pervasion (Fuentes *et al*, 2008; Lai *et al*, 2000; Oscarsson *et al*, 1999). FraC is an actinoporin isolated from the sea anemone *Actinia fragacea*, which consists of a crown-shaped nonamer with an external diameter of about 11.0 nm and an internal diameter of ~5.0 nm (Mechaly *et al*, 2009). Dermcidin is an antimicrobial peptide that has a broad spectrum of activity (Schittek *et al*, 2001). It is expressed in the sweat glands and secreted into the sweat and transported to the epidermal surface (Schittek *et al*, 2001). The structure of assembled dermcidin solved at 2.5-Å resolution shows a channel architecture comprising a hexameric bundle formed elongated α-helices, with overall

```
CLUSTAL O(1.1.0) multiple sequence alignment


Cj0391c                         MQVNTFSNIASMARTQVSNKKADDAKENTKDKNVQSANSSKDVDKNTLEKLNALGGKGIT
2YMK:A|PDBID|CHAIN|SEQUENCE     ------------------------------------------------------------


Cj0391c                         QIYLVQFQQQTMNAVIGSSNAQTGLDSLLNGANLDTAKSILTNIDFASLGYSSKNPLDMN
2YMK:A|PDBID|CHAIN|SEQUENCE     ------------------------------------------------------------


Cj0391c                         TDELQQLVSEDGFFGVENTANRIADFVIKGGGDDVEKLKKGLEGMKKGFEQAEKMWGGEL
2YMK:A|PDBID|CHAIN|SEQUENCE     ----------------------------------SSLLEKGLDGAKKAVGGLGKLGKDAV
                                                                   . *:***:* **..    *:    :

Cj0391c                         PQISQNTIDAALKKVSDRIDELGGKTLDLQA
2YMK:A|PDBID|CHAIN|SEQUENCE     EDLES-VGKGAVHDVKDVLDSVL--------
                                 ::.. . ..*::.*.* :*.:



CLUSTAL O(1.1.0) multiple sequence alignment


Cj0391c                         MQVNTFSNIASMARTQVSNKKADDAKENTKDKNVQSANSSKDVDKNTLEKLNALG-----
3LIM:A|PDBID|CHAIN|SEQUENCE     --------------------AD-----VAGAVIDGAGLGFDVLKTVLEALGNVKRKIAV
                                                    **     .    ::.*  . ** *..** *  :

Cj0391c                         ------GKGITQIYLVQFQQQTMNAVIGSSNAQTGLDSLLNGANLDT--AKSILTNIDFA
3LIM:A|PDBID|CHAIN|SEQUENCE     GIDNESGKTWTAM-NTYFRSGTSDIVL-PHKVAHGKALLYNGQKNRGPVATGVVGVIAY-
                                      **  * :  . *:. * : *:   :.  *   * ** :     *..::  * :

Cj0391c                         SLGYSSKNPLDMNTDELQQLVSEDGFFGVENTANRIAD----FVIKGGGDDVEKLKKGLE
3LIM:A|PDBID|CHAIN|SEQUENCE     --SMSDGNTLA-------V------LFSVPYDYNWYSNWWNVRVYKGQKRADQRMYEELY
                                  . *. * *               :*.*    *  ::     * **     ::: : *

Cj0391c                         GMKKGFEQAEKMWGGELPQISQNTIDAALKKVSDRIDELGGKTLDLQA---
3LIM:A|PDBID|CHAIN|SEQUENCE     YHRSPFR-GDNGWHSRGL-------GYGLK-SRGFMNSSGHAILEIHVTKA
                                  :. *. .:: * ..           .**     ::. *   *:::.
!



CLUSTAL O(1.1.0) multiple sequence alignment


Cj0391c                         MQVNTFSNIASMARTQVSNKKADDAKENTKDKNVQ-------SANSSKDVDKNTLEKL--
2WCD:A|PDBID|CHAIN|SEQUENCE     -----------MHHHH-------HHTEIVADKTVEVVKNAIETADGALDLYNKYLDQVIP
                                           * : :       . .* . **.*:       :*:.: *: :: *:::

Cj0391c                         ------------------------------------------------NALGG--KGITQI
2WCD:A|PDBID|CHAIN|SEQUENCE     WQTFDETIKELSRFKQEYSQAASVLVGDIKTLLMDSQDKYFEATQTVYEWCGVATQLLAA
                                                                                 *  . :

Cj0391c                         YLVQFQQQTMNAVIGSSNAQTGLDSLLNGAN-LD-TAKSILTNIDFASLGYSSKNPLDMN
2WCD:A|PDBID|CHAIN|SEQUENCE     YILLFDEYNEKKA--SAQKDILIKVLDDGITKLNEAQKSLLVS--SQSFNNASGKLLALD
                                *:: *:: . : .  *:: :  :. * :* . *: : **:*..    *:  :* : * ::

Cj0391c                         TDELQQLVSEDGFFGVENTANRIADFVIKGGGDDVEKLKKGLEGMKKGFEQAEKMWGGE-
2WCD:A|PDBID|CHAIN|SEQUENCE     SQLTNDFSEKSSYFQSQVDKIRKEAY--AGAAA---GVVAGPFGLIISYSIAAGVVEGKL
                                ::  ::: .:..:*  :    *   :   *..     :  *  *:  .:. *  :  *:

Cj0391c                         LPQIS-------------------QNTIDAALKKVSDRIDELGGKTLDLQA--------
2WCD:A|PDBID|CHAIN|SEQUENCE     IPELKNKLKSVQNFFTTLSNTVKQANKDIDAAKLKLTTEIAAIGEIKTETETTRFYVDYD
                                :*::.                   :: ****  *:: .*  :*  . : ::

Cj0391c                         -----------------------------------
2WCD:A|PDBID|CHAIN|SEQUENCE     DLMLSLLKEAAKKMINTCNEYQKRHGKKTLFEVPEV
```

Figure 4.31: Protein sequences alignments between Cj0391c and 2YMK, Cj0391c and 3LIM, & Cj0391c and 2WCD using Clustal Omega.

dimensions of ~8 X 4 nm (Song *et al*, 2013). Channel formation involves trimerization of antiparallel peptide dimers, which results in a firmly enclosed channel structure (Song *et al*, 2013).

The C-terminal sequence of protein Cj0391c aligns well with dermcidin. Thus, we further explore the likelihood of the hypothesis that Cj0391c is an α-PFT with the similar structure as dermcidin by examining the theoretical structural stability of Cj0391c in a helical pore bundle within a simple lipid bilayer under various conditions.

Generally, the 391 hexamer model is more stable with the present of zinc at temperature of 310 K and 314 K. At 300 K, there is not much total RMSD difference between the models 391-300K and 391-ZN-300K. However, the most flexible helices are different, which are helix 2 and helix 5 respectively. For the helices bending areas, there is a trend that with the present of zinc, the models bend more at the ends; while for the models without zinc, most of the bending occurs near the middle of the protein. The hexamer 391 pore channel size is also linked with the presence of the zinc, as with the presence of the zinc, the pore channel is wider in the middle. For the models without zinc, the channel is wider at the two ends. The overall pore size is bigger when simulated at lower temperature. In a dermcidin crystal structure study (Song *et al*, 2013), results show that zinc plays a crucial role to keep the dermcidin hexameric structure at the temperature of 310 K, which is consistent with the 391 MD simulation. Furthermore, simulations suggest that the bilayer can undergo deformation such that Zn^{2+} ions may reside in the membrane core region without being exposed to a hydrophobic lipid tail environment.

There are two more α-PFTs with crystal structure solved in 2014, which are Tc Toxin TcdA1 (PDB code 4O9Y/1VW1) and listeriolysin (PDB code 4CDB). The sequence alignments between Cj0391c and these two are attached in Appendix 6 and 7. After including the two new α-PFTs, dermcidin still has the best sequence alignment with Cj0391c.

CHAPTER 5. CONCLUSIONS AND FUTURE DIRECTIONS

In this study, various servers were used to identify putative virulent NCSPs from *C. jejuni* NCTC 11168 that are fully or partially exposed extracellularly. The final list of 28 putative NCSPs on the list may include proteins that are responsible for chicken immune system down-regulation and/or the remarkable colonisation capability of *C. jejuni* in chickens. Indeed, these two activities may be linked.

During the course of this study, a similar study was reported by Nielsen and co-workers, also aimed at identifying immunogenic and virulence-associated proteins from *C. jejuni* NCTC 11168 (Nielsen *et al*, 2012). They identified 25 genes that may encode potential antigens from *C. jejuni* NCTC 11168. These antigens do not overlap with the final protein list in our study, as they did not consider hypothetical proteins. Hence the current work is aimed at identifying a different cohort of potential virulence proteins.

Among them, Cj0243c (σ^{54}), Cj0391c (σ^{28}), Cj0814 (σ^{54}), Cj0859c (σ^{28}) and Cj1656c (σ^{28}) have been observed to be co-regulated with flagellar gene expression (Guerry-Kopecko, 2012). σ^{54} promoters regulate the expression of genes required for basal body, hook and flagellar filament biosynthesis, while σ^{28} promoters co-regulate the expression of genes required for extension and capping of the flagellum, and genes required for flagellin post-translational modification and secretion of virulence factors (Carrillo *et al*, 2004). This indicates that these proteins may be involved in related functions. They can be similar to the flagella related secretion protein CiaB, which shares similarity with other invasion-related proteins, such as *Salmonella* SipB (Kaniga *et al*, 1995) and *Yersinia* YopB (Hakansson *et al*, 1996). CiaB also lacks an identifiable signal sequence, and is therefore non-classically secreted (Konkel *et al*, 1999). Another flagella exporting-related protein is FlaC, which has sequence identity with the N- and C-terminal regions of proteins FlaA and FlaB (Song *et al*, 2004). FlaC is not required for the flagellum formation or motility, but it is secreted via the flagellum, and the FlaC protein seems to be involved in host cell invasion (discussed in Section1.7.3 and Section 1.9.2). The small acidic protein FspA is also secreted via the

flagella export system (Poly *et al*, 2007). Two variants of this protein are present, FspA1 and FspA2. FspA2 has been identified to rapidly induce apoptosis in INT407 cells, and thus likely to play a role in pathogenesis (Poly *et al*, 2007).

Hypothetical proteins Cj0391c and Cj1631c were overexpressed in *C. jejuni* NCTC 11168 biofilm-grown cells (pH 4-7), along with other proteins involved in stress responses, flagellar motility and adhesion (Kalmokoff *et al*, 2006). These two proteins are the only two hypothetical proteins overexpressed in Kalmokoff *et al.*'s study. Both of them are included in the 28 protein candidates identified in this study.

Protein Cj0152c, which has been predicted to be located in the cytoplasm/cell inner membrane and also extracellularly, has been found in *C. jejuni* outer membrane vesicles (OMVs) (Jang *et al*, 2014). In Gram-negative bacteria, OMVs are often released extracellularly attaching to host cells through adhesive molecules and then transferring compounds into the host cells (Jang *et al*, 2014). As *C. jejuni* does not have the prototypical virulence-associated secretion systems, OMVs play an important role in the coordinated delivery of virulence proteins into human intestinal epithelial cells (Elmi *et al*, 2012).

Based on the information as above, other protein candidates could be further analysed. One of the protein candidates Cj0428 has been expressed in the same *E. coli* BL21(DE3) pRSET-A system, but the production was very low in this system. There was not enough protein could be collected at the end of expression. Another expression system could be tested for Cj0428c expression. However, the instability index obtained for this protein from ProtParam indicates it is an unstable protein, which may be the reason that it was not successfully expressed. Finally, some of the other protein candidates have also been expressed and analysed by other colleagues (data not shown).

Protein candidate Cj0391c from *C. jejuni* NCTC 11168 has shown apoptotic effects in a chicken macrophage cell line HD11 in our study. Other cell lines have also been tried, which

include Chinese hamster ovary (CHO) cell line and human intestinal (INT 407) cell line. Interestingly, Cj0391c shows no noticeable effect on either of these (data not shown). One of the possible reasons could be that the specific surface structure of chicken macrophage cells may be required for Cj0391c to fully fold or function.

Based on experimental results and secondary structure prediction results, it is suggested that Cj0391c is an α-PFT which forms pores in chicken macrophage cells. A Cj0391c hexamer model was built based on a recently solved α-PFT structure, dermcidin.

For molecular models, there was no homology model we could use to build Cj0391c structure as no template with sufficient similarity was detected in the protein data bank. In the future, more protein sequences with/without annotated function and 3D models will be available from the database, which might lead us to find a structural homologue of Cj0391c.

Experimentally, the mechanisms of action of Cj0391c on chicken macrophage membrane could be further analysed by: (1) single channel conductance measurement (patch clamp) to test the channel conductance/pore size differences between each model (if the pore forms); (2) electron microscopy can be employed to view the pore structure in chicken macrophage membranes; (3) circular dichroism can be employed to conform the protein secondary structure; (4) the hexamer structure, such as helix bending and flexibility, could be further analysed by probing with a number of experimental techniques, including X-ray diffraction, electron microscopy, nuclear magnetic resonance, and fluorescence probe techniques (Bhunia *et al*, 2010; Dzuba & Raap, 2013; Groulx *et al*, 2010).

As mentioned in Section 3.4, there are several mechanisms that Cj0391c may induce apoptosis in chicken macrophages. This study explored one possibility. Future work would involve exploring other oligomers, arrangements, *etc*. Simulations of spontaneous oligomerisation within a membrane will also be performed in the future.

As indicated from the Section 1.11, a vaccine would help to reduce the colonisation of *C. jejuni* in chickens, thus reducing levels of transmission to people. Protein Cj0391c could be tested as a vaccine candidate in chicken, as inactivating this protein may allow chicken macrophages to phagocytose and kill the colonising bacteria.

In summary, this work has used bioinformatics techniques to mine the *Campylobacter* genome for potential virulence factors. As genome sequence analysis becomes routine, these kinds of analyses may yield potential vaccine and/or targets for a wide range of pathogens.

References

Abuoun M, Manning G, Cawthraw SA, Ridley A, Ahmed IH, Wassenaar TM, Newell DG (2005) Cytolethal distending toxin (CDT)-negative *Campylobacter jejuni* strains and anti-CDT neutralizing antibodies are induced during human infection but not during colonization in chickens. *Infect Immun* **73:** 3053-3062

Akira S (2006) TLR signaling. *Curr Top Microbiol Immunol* **311:** 1-16

Alaimo C, Catrein I, Morf L, Marolda CL, Callewaert N, Valvano MA, Feldman MF, Aebi M (2006) Two distinct but interchangeable mechanisms for flipping of lipid-linked oligosaccharides. *EMBO J* **25:** 967-976

Allos BM (2001) *Campylobacter jejuni* Infections: update on emerging issues and trends. *Clin Infect Dis* **32:** 1201-1206

Altekruse SF, Stern NJ, Fields PI, Swerdlow DL (1999) *Campylobacter jejuni*--an emerging foodborne pathogen. *Emerg Infect Dis* **5:** 28-35

Andersen-Nissen E, Smith KD, Strobe KL, Barrett SL, Cookson BT, Logan SM, Aderem A (2005) Evasion of Toll-like receptor 5 by flagellated bacteria. *Proc Natl Acad Sci U S A* **102:** 9247-9252

Asakura H, Yamasaki M, Yamamoto S, Igimi S (2007) Deletion of peb4 gene impairs cell adhesion and biofilm formation in *Campylobacter jejuni*. *FEMS Microbiol Lett* **275:** 278-285

Ashgar SS, Oldfield NJ, Wooldridge KG, Jones MA, Irving GJ, Turner DP, Ala'Aldeen DA (2007) CapA, an autotransporter protein of *Campylobacter jejuni*, mediates association with human epithelial cells and colonization of the chicken gut. *J Bacteriol* **189:** 1856-1865

Aspinall GO, Monteiro MA, Pang H, Kurjanczyk LA, Penner JL (1995) Lipo-oligosaccharide of *Campylobacter lari* strain PC 637. Structure of the liberated oligosaccharide and an associated extracellular polysaccharide. *Carbohydr Res* **279:** 227-244

Atterbury RJ, Connerton PL, Dodd CE, Rees CE, Connerton IF (2003) Isolation and characterization of *Campylobacter* bacteriophages from retail poultry. *Appl Environ Microbiol* **69:** 4511-4518

Avrain L, Vernozy-Rozand C, Kempf I (2004) Evidence for natural horizontal transfer of *tetO* gene between *Campylobacter jejuni* strains in chickens. *J Appl Microbiol* **97:** 134-140

Baar C, Eppinger M, Raddatz G, Simon J, Lanz C, Klimmek O, Nandakumar R, Gross R, Rosinus A, Keller H, Jagtap P, Linke B, Meyer F, Lederer H, Schuster SC (2003) Complete genome sequence and analysis of *Wolinella succinogenes*. *Proc Natl Acad Sci U S A* **100:** 11690-11695

Bachtiar BM, Coloe PJ, Fry BN (2007) Knockout mutagenesis of the kpsE gene of *Campylobacter jejuni* 81116 and its involvement in bacterium-host interactions. *FEMS Immunol Med Microbiol* **49:** 149-154

Backert S, Meyer TF (2006) Type IV secretion systems and their effectors in bacterial pathogenesis. *Curr Opin Microbiol* **9:** 207-217

Bacon DJ, Alm RA, Burr DH, Hu L, Kopecko DJ, Ewing CP, Trust TJ, Guerry P (2000) Involvement of a plasmid in virulence of *Campylobacter jejuni* 81-176. *Infect Immun* **68:** 4384-4390

Bacon DJ, Alm RA, Hu L, Hickey TE, Ewing CP, Batchelor RA, Trust TJ, Guerry P (2002) DNA sequence and mutational analyses of the pVir plasmid of *Campylobacter jejuni* 81-176. *Infect Immun* **70:** 6242-6250

Bacon DJ, Szymanski CM, Burr DH, Silver RP, Alm RA, Guerry P (2001) A phase-variable capsule is involved in virulence of *Campylobacter jejuni* 81-176. *Mol Microbiol* **40:** 769-777

Bagos PG, Liakopoulos TD, Spyropoulos IC, Hamodrakas SJ (2004) PRED-TMBB: a web server for predicting the topology of beta-barrel outer membrane proteins. *Nucleic Acids Res* **32:** W400-404

Baker MD, Wolanin PM, Stock JB (2006) Signal transduction in bacterial chemotaxis. *BioEssays : news and reviews in molecular, cellular and developmental biology* **28:** 9-22

Baqar S, Applebee LA, Gilliland TC, Jr., Lee LH, Porter CK, Guerry P (2008) Immunogenicity and protective efficacy of recombinant *Campylobacter jejuni* flagellum-secreted proteins in mice. *Infect Immun* **76:** 3170-3175

Bates C, Hiett KL, Stern NJ (2004) Relationship of *Campylobacter* isolated from poultry and from darkling beetles in New Zealand. *Avian Dis* **48:** 138-147

Bendtsen JD, Kiemer L, Fausboll A, Brunak S (2005) Non-classical protein secretion in bacteria. *BMC Microbiol* **5:** 58

Bendtsen JD, Nielsen H, von Heijne G, Brunak S (2004) Improved prediction of signal peptides: SignalP 3.0. *J Mol Biol* **340:** 783-795

Bendtsen JD, Wooldridge KG (2009) Non-classical Secretion. In *Bacterial Secreted Proteins*, Wooldridge KG (ed), pp 225-235. Norfolk, UK: Caister Academic Press

Berndtson E (1996) *Campylobacter* in Broiler Chickens Ph.D. Thesis, Swedish University of Agricultural Sciences, Uppsala, Swenden

Berndtson E, Danielsson-Tham ML, Engvall A (1996) *Campylobacter* incidence on a chicken farm and the spread of *Campylobacter* during the slaughter process. *Int J Food Microbiol* **32:** 35-47

Bhunia A, Domadia PN, Torres J, Hallock KJ, Ramamoorthy A, Bhattacharjya S (2010) NMR structure of pardaxin, a pore-forming antimicrobial peptide, in lipopolysaccharide micelles: mechanism of outer membrane permeabilization. *J Biol Chem* **285:** 3883-3895

Biswas D, Fernando U, Reiman C, Willson P, Potter A, Allan B (2006) Effect of cytolethal distending toxin of *Campylobacter jejuni* on adhesion and internalization in cultured cells and in colonization of the chicken gut. *Avian Dis* **50:** 586-593

Biswas D, Fernando UM, Reiman CD, Willson PJ, Townsend HG, Potter AA, Allan BJ (2007) Correlation between *in vitro* secretion of virulence-associated proteins of *Campylobacter jejuni* and colonization of chickens. *Curr Microbiol* **54:** 207-212

Biswas D, Itoh K, Sasakawa C (2003) Role of microfilaments and microtubules in the invasion of INT-407 cells by *Campylobacter jejuni*. *Microbiol Immunol* **47:** 469-473

Blackshields G, Sievers F, Shi W, Wilm A, Higgins DG (2010) Sequence emBedding for fast construction of guide trees for multiple sequence alignment. *Algorithms Mol Biol* **5:** 21

Blaser MJ, Glass RI, Huq MI, Stoll B, Kibriya GM, Alim AR (1980) Isolation of *Campylobacter fetus* subsp. *jejuni* from Bangladeshi children. *J Clin Microbiol* **12:** 744-747

Blunsom, P. (2004) Hidden markov models. *Lecture notes,* **August**: *15*, 18-19.

Bolton FJ, Coates D (1983) A study of the oxygen and carbon dioxide requirements of thermophilic campylobacters. *J Clin Pathol* **36:** 829-834

Bradford MM (1976) A rapid and sensitive method for the quantitation of microgram quantities of protein utilizing the principle of protein-dye binding. *Anal Biochem* **72:** 248-254

Bras AM, Chatterjee S, Wren BW, Newell DG, Ketley JM (1999) A novel *Campylobacter jejuni* two-component regulatory system important for temperature-dependent growth and colonization. *J Bacteriol* **181:** 3298-3302

Braunstein M, Espinosa BJ, Chan J, Belisle JT, Jacobs WR, Jr. (2003) SecA2 functions in the secretion of superoxide dismutase A and in the virulence of *Mycobacterium tuberculosis*. *Mol Microbiol* **48:** 453-464

Bright JN, Shrivastava IH, Cordes FS, Sansom MS (2002) Conformational dynamics of helix S6 from Shaker potassium channel: simulation studies. *Biopolymers* **64:** 303-313

Brogden KA, Roth, J.A., Stanton T.B., Bolin, C.A., Minion, F.C., Wannemuehler, M.J. (2000) *Virulence Mechanisms of Bacterial Pathogens* 3edn. Washington DC: ASM Press.

Brownlie R, Zhu J, Allan B, Mutwiri GK, Babiuk LA, Potter A, Griebel P (2009) Chicken TLR21 acts as a functional homologue to mammalian TLR9 in the recognition of CpG oligodeoxynucleotides. *Mol Immunol* **46:** 3163-3170

Burr DH, Rollins D, Lee LH, Pattarini DL, Walz SS, Tian JH, Pace JL, Bourgeois AL, Walker RI (2005) Prevention of disease in ferrets fed an inactivated whole cell *Campylobacter jejuni* vaccine. *Vaccine* **23:** 4315-4321

Bussi G, Donadio D, Parrinello M (2007) Canonical sampling through velocity rescaling. *J chemical physics* **126:** 014101

Buzby JC, Allos BM, Roberts T (1997) The economic burden of *Campylobacter*-associated Guillain-Barre syndrome. *J Infect Dis* **176 Suppl 2:** S192-197

Bywater R, Deluyker, H., Deroover, E., de Jong, A., Marion, H., McConville, M., Rowan, T., Shryock, T., Shuster, D., Thomac, V., *et al*. (2004) A European survey of antimicrobial susceptinility among zoonotic and commensal bacteria isolated form food-producing animals. *J Antimicrob Chemother* **54:** 744-754

Calva JJ, Ruiz-Palacios GM, Lopez-Vidal AB, Ramos A, Bojalil R (1988) Cohort study of intestinal infection with *Campylobacter* in Mexican children. *Lancet* **1:** 503-506

Carrillo CD, Taboada E, Nash JH, Lanthier P, Kelly J, Lau PC, Verhulp R, Mykytczuk O, Sy J, Findlay WA, Amoako K, Gomis S, Willson P, Austin JW, Potter A, Babiuk L, Allan B, Szymanski CM (2004) Genome-wide expression analyses of *Campylobacter jejuni* NCTC 11168 reveals coordinate regulation of motility and virulence by *flhA*. *J Biol Chem* **279:** 20327-20338

Cawthraw S, Ayling R, Nuijten P, Wassenaar T, Newell DG (1994) Isotype, specificity, and kinetics of systemic and mucosal antibodies to *Campylobacter jejuni* antigens, including flagellin, during experimental oral infections of chickens. *Avian Dis* **38:** 341-349

Cawthraw SA, Wassenaar TM, Ayling R, Newell DG (1996) Increased colonization potential of *Campylobacter jejuni* strain 81116 after passage through chickens and its implication on the rate of transmission within flocks. *Epidemiol Infect* **117:** 213-215

Chansiripornchai N, Sasipreeyajan J (2009) PCR detection of four virulence-associated genes of *Campylobacter jejuni* isolates from Thai broilers and their abilities of adhesion to and invasion of INT-407 cells. *J Vet Med Sci* **71:** 839-844

Chou KC (2001) Prediction of protein cellular attributes using pseudo amino acid composition. *Proteins: Structure., Funct., Genet* **43:** 246-255

Chou KC (2005) Using amphiphilic pseudo amino acid composition to predict enzyme subfamily classes. *Bioinformatics* **21:** 10-19

Chou KC, Shen HB (2006a) Large-scale predictions of gram-negative bacterial protein subcellular locations. *J Proteome Res* **5:** 3420-3428

Chou KC, Shen HB (2006b) Predicting enkaryotic protein subcellular location by fusing optimized evidence-theoretic K-nearest neighbour classifier. *J Proteome Res* **5:** 1888-1897

Chou KC, Shen HB (2007a) MemType-2L: a web server for predicting membrane proteins and their types by incorporating evolution information through Pse-PSSM. *Biochem Biophys Res Commun* **360:** 339-345

Chou KC, Shen HB (2007b) Signal-CF: a subsite-coupled and window-fusing approach for predicting signal peptides. *Biochem Biophys Res Commun* **357:** 633-640

Chou KC, Shen HB (2008a) Cell-PLoc: a package of Web servers for predicting subcellular localization of proteins in various organisms. *Nat Protoc* **3:** 153-162

Chou KC, Shen HB (2008b) ProtIdent: a web server for identifying proteases and their types by fusing functional domain and sequential evolution information. *Biochem Biophys Res Commun* **376:** 321-325

Chou WK, Dick S, Wakarchuk WW, Tanner ME (2005) Identification and characterization of NeuB3 from *Campylobacter jejuni* as a pseudaminic acid synthase. *J Biol Chem* **280:** 35922-35928

Coker AO, Isokpehi RD, Thomas BN, Amisu KO, Obi CL (2002) Human campylobacteriosis in developing countries. *Emerg Infect Dis* **8:** 237-244

Colegio OR, Griffin TJt, Grindley ND, Galan JE (2001) In vitro transposition system for efficient generation of random mutants of *Campylobacter jejuni*. *J Bacteriol* **183:** 2384-2388

Coombes BK, Valdez Y, Finlay BB (2004) Evasive maneuvers by secreted bacterial proteins to avoid innate immune responses. *Curr Biol : CB* **14:** R856-867

Cortes-Bratti X, Chaves-Olarte E, Lagergard T, Thelestam M (2000) Cellular internalization of cytolethal distending toxin from *Haemophilus ducreyi. Infect Immun* **68:** 6903-6911

Dahl AC, Chavent M, Sansom MS (2012) Bendix: intuitive helix geometry analysis and abstraction. *Bioinformatics* **28:** 2193-2194

Dalpke A, Frank J, Peter M, Heeg K (2006) Activation of toll-like receptor 9 by DNA from different bacterial species. *Infect Immun* **74:** 940-946

Dalton JP, Heffernan M (1989) Thiol proteases released *in vitro* by *Fasciola hepatica*. *Mol Biochem Parasitol* **35:** 161-166

Day WA, Jr., Sajecki JL, Pitts TM, Joens LA (2000) Role of catalase in *Campylobacter jejuni* intracellular survival. *Infect Immun* **68:** 6337-6345

de Boer P, Wagenaar JA, Achterberg RP, van Putten JP, Schouls LM, Duim B (2002) Generation of *Campylobacter jejuni* genetic diversity *in vivo*. *Mol Microbiol* **44:** 351-359

de Zoete MR, Keestra AM, Roszczenko P, van Putten JP (2010) Activation of human and chicken toll-like receptors by *Campylobacter* spp. *Infect Immun* **78:** 1229-1238

de Zoete MR, van Putten JP, Wagenaar JA (2007) Vaccination of chickens against *Campylobacter*. *Vaccine* **25:** 5548-5557

Dev IK, Harvey RJ, Ray PH (1985) Inhibition of prolipoprotein signal peptidase by globomycin. *J Biol Chem* **260:** 5891-5894

Dhillon AS, Shivaprasad HL, Schaberg D, Wier F, Weber S, Bandli D (2006) *Campylobacter jejuni* infection in broiler chickens. *Avian Dis* **50:** 55-58

Dingle KE, Colles FM, Wareing DR, Ure R, Fox AJ, Bolton FE, Bootsma HJ, Willems RJ, Urwin R, Maiden MC (2001) Multilocus sequence typing system for *Campylobacter jejuni*. *J Clin Microbiol* **39:** 14-23

Domanski J, Stansfeld PJ, Sansom MS, Beckstein O (2010) Lipidbook: a public repository for force-field parameters used in membrane simulations. *J Membr Biol* **236:** 255-258

Dunlop SP, Jenkins D, Neal KR, Spiller RC (2003) Relative importance of enterochromaffin cell hyperplasia, anxiety, and depression in postinfectious IBS. *Gastroenterology* **125:** 1651-1659

Dzuba SA, Raap J (2013) Spin-echo electron paramagnetic resonance (EPR) spectroscopy of a pore-forming (Lipo)peptaibol in model and bacterial membranes. *Chem Biodiver* **10:** 864-875

Eddy SR (2004) What is a hidden markov model? *Nat Biotechnol* **22:** 1315-1316

EFSA (2010) EFSA scientific opinion on quantification of the risk posed by broiler meat to human campylobacteriosis in the EU. *EFSA Journal* **8**(1): 1437

Ekdahl K, Andersson Y (2004) Regional risks and seasonality in travel-associated campylobacteriosis. *BMC Infect Dis* **4:** 54

Ekdahl K, Normann B, Andersson Y (2005) Could flies explain the elusive epidemiology of campylobacteriosis? *BMC Infect Dis* **5:** 11

El-Shibiny A, Connerton PL, Connerton IF (2005) Enumeration and diversity of campylobacters and bacteriophages isolated during the rearing cycles of free-range and organic chickens. *Appl Environ Microbiol* **71:** 1259-1266

Elliott KT, Dirita VJ (2008) Characterization of CetA and CetB, a bipartite energy taxis system in *Campylobacter jejuni*. *Mol Microbiol* **69:** 1091-1103

Elmi A, Watson E, Sandu P, Gundogdu O, Mills DC, Inglis NF, Manson E, Imrie L, Bajaj-Elliott M, Wren BW, Smith DG, Dorrell N (2012) *Campylobacter jejuni* outer membrane vesicles play an important role in bacterial interactions with human intestinal epithelial cells. *Infect Immun* **80:** 4089-4098

Erf GF. (1997) Immune System Function and Development in Broilers. In Sci. CoEfP (ed.). Univ. Arkansas., Fayetteville.

Essmann U, Lee H, Berkowitz ML, Darden T, Lee H, Pedersen LG (1995) A smooth particle mesh Ewald method. *The Journal of chemical physics* **103(19)**: 8577-8593.

Eswar N, Webb B, Marti-Renom MA, Madhusudhan MS, Eramian D, Shen MY, Pieper U, Sali A (2006) Comparative protein structure modeling using Modeller. *Current protocols in bioinformatics / editoral board, Andreas D Baxevanis [et al]* **Chapter 5:** Unit 5 6

Evans SA (1997) Epidemiological studies of *Salmonella* and *Campylobacter* in poultry. Ph.D. Thesis Thesis, University of London, London, Untied Kingdom

Faruque AS, Mahalanabis D, Islam A, Hoque SS, Hasnat A (1993) Common diarrhea pathogens and the risk of dehydration in young children with acute watery diarrhea: a case-control study. *Am J Tro Med Hyg* **49:** 93-100

Fosse J, Seegers H, Magras C (2008) Foodborne zoonoses due to meat: a quantitative approach for a comparative risk assessment applied to pig slaughtering in Europe. *Veterinary research* **39:** 1

Fouts DE, Mongodin EF, Mandrell RE, Miller WG, Rasko DA, Ravel J, Brinkac LM, DeBoy RT, Parker CT, Daugherty SC, Dodson RJ, Durkin AS, Madupu R, Sullivan SA, Shetty JU, Ayodeji MA, Shvartsbeyn A, Schatz MC, Badger JH, Fraser CM, Nelson KE (2005) Major structural differences and novel potential virulence mechanisms from the genomes of multiple *Campylobacter* species. *PLoS Biol* **3:** e15

Fox JG, Rogers AB, Whary MT, Ge Z, Taylor NS, Xu S, Horwitz BH, Erdman SE (2004) Gastroenteritis in NF-kappaB-deficient mice is produced with wild-type Camplyobacter jejuni but not with *C. jejuni* lacking cytolethal distending toxin despite persistent colonization with both strains. *Infect Immun* **72:** 1116-1125

Freedman DO, Weld LH, Kozarsky PE, Fisk T, Robins R, von Sonnenburg F, Keystone JS, Pandey P, Cetron MS, GeoSentinel Surveillance N (2006) Spectrum of disease and relation to place of exposure among ill returned travelers. *N Engl J Med* **354:** 119-130

French NP, the Molecular Epidemiology and Veterinary Public Health Group HRI (2008) Enhancing Surveillance of Potentially Foodborne Enteric Diseases in New Zealand: Human Campylobacteriosis in the Manawatu. *Final report: FDI* **236:** 2005

Friedman CR, Neimann, J., Wegener, H. C. & Tauxe, R. V. (ed) (2000) *Epidemiology of Campylobacter jejuni infections in the United States and other industrialized Nations*. Washington D. C. : ASM Press, 121-138pp

Fry BN, Feng S, Chen YY, Newell DG, Coloe PJ, Korolik V (2000a) The galE gene of *Campylobacter jejuni* is involved in lipopolysaccharide synthesis and virulence. *Infect Immun* **68:** 2594-2601

Fry BN, Feng S, Chen YY, Newell DG, Coloe PJ, Korolik V (2000b) The galE gene of *Campylobacter jejuni* is involved in lipopolysaccharide synthesis and virulence. *Infect Immun* **68:** 2594-2601

Fuentes JA, Villagra N, Castillo-Ruiz M, Mora GC (2008) The *Salmonella* Typhi hlyE gene plays a role in invasion of cultured epithelial cells and its functional transfer to S. Typhimurium promotes deep organ infection in mice. *Res Microbiol* **159:** 279-287

Fujimura H (2013) The Guillain-Barre syndrome. *Handbook of clinical neurology* **115:** 383-402

Funke G, Baumann R, Penner JL, Altwegg M (1994) Development of resistance to macrolide antibiotics in an AIDS patient treated with clarithromycin for *Campylobacter jejuni* diarrhea. *Eur J Clin Microbiol Infect Dis* **13:** 612-615

Garg A, Gupta D (2008) VirulentPred: a SVM based prediction method for virulent proteins in bacterial pathogens. *BMC Bioinformatics* **9:** 62

Garmory HS, Brown KA, Titball RW (2002) *Salmonella* vaccines for use in humans: present and future perspectives. *FEMS Microbiol Rev* **26:** 339-353

Gasteiger E, Hoogland C, Gattiker A, Duvaud S, Wilkins MR, Appel RD, Bairoch A (2005) Protein Identification and Analysis Tools on the ExPASy Server. In *The Proteomics Protocols Handbook*, Walker JM (ed), pp 571-607.: Humana Press

Gaynor EC, Cawthraw S, Manning G, MacKichan JK, Falkow S, Newell DG (2004) The genome-sequenced variant of *Campylobacter jejuni* NCTC 11168 and the original clonal clinical isolate differ markedly in colonization, gene expression, and virulence-associated phenotypes. *J Bacteriol* **186:** 503-517

Ge B, Girard W, Zhao S, Friedman S, Gaines SA, Meng J (2006) Genotyping of *Campylobacter* spp. from retail meats by pulsed-field gel electrophoresis and ribotyping. *J Appl Microbiol* **100:** 175-184

Gilbert M, Karwaski MF, Bernatchez S, Young NM, Taboada E, Michniewicz J, Cunningham AM, Wakarchuk WW (2002) The genetic bases for the variation in the lipo-oligosaccharide of the mucosal pathogen, *Campylobacter jejuni*. Biosynthesis of sialylated ganglioside mimics in the core oligosaccharide. *J Biol Chem* **277:** 327-337

Golden NJ, Acheson DW (2002) Identification of motility and autoagglutination *Campylobacter jejuni* mutants by random transposon mutagenesis. *Infect Immun* **70:** 1761-1771

Goodman SN, Sladky JT (2005) A Bayesian approach to randomized controlled trials in children utilizing information from adults: the case of Guillain-Barre syndrome. *Clinical trials* **2:** 305-310; discussion 364-378

Goon S, Kelly JF, Logan SM, Ewing CP, Guerry P (2003) Pseudaminic acid, the major modification on *Campylobacter* flagellin, is synthesized via the Cj1293 gene. *Mol Microbiol* **50:** 659-671

Gouaux E (1997) Channel-forming toxins: tales of transformation. *Curr Opin Struct Biol* **7:** 566-573

Gradel KO, Nielsen HL, Schonheyder HC, Ejlertsen T, Kristensen B, Nielsen H (2009) Increased short- and long-term risk of inflammatory bowel disease after salmonella or *Campylobacter* gastroenteritis. *Gastroenterology* **137:** 495-501

Grant CC, Konkel ME, Cieplak W, Jr., Tompkins LS (1993) Role of flagella in adherence, internalization, and translocation of *Campylobacter jejuni* in nonpolarized and polarized epithelial cell cultures. *Infect Immun* **61:** 1764-1771

Grant KA, Belandia IU, Dekker N, Richardson PT, Park SF (1997) Molecular characterization of pldA, the structural gene for a phospholipase A from *Campylobacter coli*, and its contribution to cell-associated hemolysis. *Infect Immun* **65:** 1172-1180

Griffiths PL, Park RW (1990) Campylobacters associated with human diarrhoeal disease. *J Appl Bacteriol* **69:** 281-301

Groulx N, Juteau M, Blunck R (2010) Rapid topology probing using fluorescence spectroscopy in planar lipid bilayer: the pore-forming mechanism of the toxin Cry1Aa of Bacillus thuringiensis. *J Gen Physiol* **136:** 497-513

Guerin MT, Martin W, Reiersen J, Berke O, McEwen SA, Bisaillon JR, Lowman R (2007) A farm-level study of risk factors associated with the colonization of broiler flocks with *Campylobacter* spp. in Iceland, 2001-2004. *Acta Vet Scandinavica* **49:** 18

Guerry P (2007) *Campylobacter* flagella: not just for motility. *TIM* **15:** 456-461

Guerry P, Alm, R.A., Power, M.E. Trust, T.J. (ed) (1992) *Molecular and structural analysis of Campylobatcter flagellin* Washington ASM Press, 267-281pp

Guerry P, Ewing CP, Hickey TE, Prendergast MM, Moran AP (2000) Sialylation of lipooligosaccharide cores affects immunogenicity and serum resistance of *Campylobacter jejuni*. *Infect Immun* **68:** 6656-6662

Guerry P, Ewing CP, Schirm M, Lorenzo M, Kelly J, Pattarini D, Majam G, Thibault P, Logan S (2006) Changes in flagellin glycosylation affect *Campylobacter* autoagglutination and virulence. *Mol Microbiol* **60:** 299-311

Guerry P, Poly F, Riddle M, Maue AC, Chen YH, Monteiro MA (2012) *Campylobacter* polysaccharide capsules: virulence and vaccines. *Frontiers in cellular and infection microbiology* **2:** 7

Guerry P, Pope PM, Burr DH, Leifer J, Joseph SW, Bourgeois AL (1994) Development and characterization of recA mutants of *Campylobacter jejuni* for inclusion in attenuated vaccines. *Infect Immun* **62:** 426-432

Guerry P, Szymanski CM, Prendergast MM, Hickey TE, Ewing CP, Pattarini DL, Moran AP (2002) Phase variation of *Campylobacter jejuni* 81-176 lipooligosaccharide affects ganglioside mimicry and invasiveness *in vitro*. *Infect Immun* **70:** 787-793

Guerry-Kopecko PSS, MD; Shahida Baqar, Olney, MD. (2012) Secreted Campylobacter flagella coregulated proteins as immunogens. *United States Patent* USA, Vol. US 8221764 B2.

Gundogdu O, Bentley SD, Holden MT, Parkhill J, Dorrell N, Wren BW (2007) Re-annotation and re-analysis of the *Campylobacter jejuni* NCTC 11168 genome sequence. *BMC Genomics* **8:** 162

Guruprasad K, Reddy BV, Pandit MW (1990) Correlation between stability of a protein and its dipeptide composition: a novel approach for predicting *in vivo* stability of a protein from its primary sequence. *Protein Eng* **4:** 155-161

Haddad N, Marce C, Magras C, Cappelier JM (2010) An overview of methods used to clarify pathogenesis mechanisms of *Campylobacter jejuni*. *J Food Prot* **73:** 786-802

Hakansson S, Schesser K, Persson C, Galyov EE, Rosqvist R, Homble F, Wolf-Watz H (1996) The YopB protein of Yersinia pseudotuberculosis is essential for the translocation of Yop effector proteins across the target cell plasma membrane and displays a contact-dependent membrane disrupting activity. *EMBO J* **15:** 5812-5823

Hald B, Skovgard H, Bang DD, Pedersen K, Dybdahl J, Jespersen JB, Madsen M (2004) Flies and *Campylobacter* infection of broiler flocks. *Emerg Infect Dis* **10:** 1490-1492

Hald T, H. C., Wegener, and B. B. Jorgensen. (1999) Annual Report on Zoonoses in Denmark 1998. In Ministry of Food AaF (ed.), Copenhagen, Denmak.

Hanahan D (1983) Studies on transformation of Escherichia coli with plasmids. *J Mol Biol* **166:** 557-580

Harris NV, Weiss NS, Nolan CM (1986) The role of poultry and meats in the etiology of *Campylobacter jejuni*/coli enteritis. *Am J Public Health* **76:** 407-411

Harth G, Horwitz MA (1997) Expression and efficient export of enzymatically active Mycobacterium tuberculosis glutamine synthetase in Mycobacterium smegmatis and evidence that the information for export is contained within the protein. *J Biol Chem* **272:** 22728-22735

Harth G, Horwitz MA (1999a) Export of recombinant Mycobacterium tuberculosis superoxide dismutase is dependent upon both information in the protein and mycobacterial export machinery. A model for studying export of leaderless proteins by pathogenic mycobacteria. *J Biol Chem* **274:** 4281-4292

Harth G, Horwitz MA (1999b) An inhibitor of exported Mycobacterium tuberculosis glutamine synthetase selectively blocks the growth of pathogenic mycobacteria in axenic culture and in human monocytes: extracellular proteins as potential novel drug targets. *J Exp Med* **189:** 1425-1436

Hartley-Tassell LE, Shewell LK, Day CJ, Wilson JC, Sandhu R, Ketley JM, Korolik V (2010) Identification and characterization of the aspartate chemosensory receptor of *Campylobacter jejuni*. *Mol Microbiol* **75:** 710-730

Hassane DC, Lee RB, Mendenhall MD, Pickett CL (2001) Cytolethal distending toxin demonstrates genotoxic activity in a yeast model. *Infect Immun* **69:** 5752-5759

Hassane DC, Lee RB, Pickett CL (2003) *Campylobacter jejuni* cytolethal distending toxin promotes DNA repair responses in normal human cells. *Infect Immun* **71:** 541-545

Hastings IM, Paget-McNicol S, Saul A (2004) Can mutation and selection explain virulence in human P. falciparum infections? *Malaria J* **3:** 2

Hastings R, Colles FM, McCarthy ND, Maiden MC, Sheppard SK (2011) *Campylobacter* genotypes from poultry transportation crates indicate a source of contamination and transmission. *J Appl Microbiol* **110:** 266-276

He H, Genovese KJ, Nisbet DJ, Kogut MH (2006) Profile of Toll-like receptor expressions and induction of nitric oxide synthesis by Toll-like receptor agonists in chicken monocytes. *Mol Immunol* **43:** 783-789

Henderson IR, Navarro-Garcia F, Desvaux M, Fernandez RC, Ala'Aldeen D (2004) Type V protein secretion pathway: the autotransporter story. *Microbiology and molecular biology reviews : MMBR* **68:** 692-744

Hendrixson DR (2006) A phase-variable mechanism controlling the *Campylobacter jejuni* FlgR response regulator influences commensalism. *Mol Microbiol* **61:** 1646-1659

Hendrixson DR, Akerley BJ, DiRita VJ (2001) Transposon mutagenesis of *Campylobacter jejuni* identifies a bipartite energy taxis system required for motility. *Mol Microbiol* **40:** 214-224

Hendrixson DR, DiRita VJ (2003) Transcription of sigma54-dependent but not sigma28-dependent flagellar genes in *Campylobacter jejuni* is associated with formation of the flagellar secretory apparatus. *Mol Microbiol* **50:** 687-702

Hendrixson DR, DiRita VJ (2004) Identification of *Campylobacter jejuni* genes involved in commensal colonization of the chick gastrointestinal tract. *Mol Microbiol* **52:** 471-484

Hermans D, Pasmans F, Heyndrickx M, Van Immerseel F, Martel A, Van Deun K, Haesebrouck F (2012) A tolerogenic mucosal immune response leads to persistent *Campylobacter jejuni* colonization in the chicken gut. *Crit Rev Microbiol* **38:** 17-29

Hickey TE, Baqar S, Bourgeois AL, Ewing CP, Guerry P (1999) *Campylobacter jejuni*-stimulated secretion of interleukin-8 by INT407 cells. *Infect Immun* **67:** 88-93

Hickey TE, Majam G, Guerry P (2005) Intracellular survival of *Campylobacter jejuni* in human monocytic cells and induction of apoptotic death by cytholethal distending toxin. *Infect Immun* **73:** 5194-5197

Hickey TE, McVeigh AL, Scott DA, Michielutti RE, Bixby A, Carroll SA, Bourgeois AL, Guerry P (2000) *Campylobacter jejuni* cytolethal distending toxin mediates release of interleukin-8 from intestinal epithelial cells. *Infect Immun* **68:** 6535-6541

Hofreuter D, Novik V, Galan JE (2008) Metabolic diversity in *Campylobacter jejuni* enhances specific tissue colonization. *Cell Host Microbe* **4:** 425-433

Hong Q, Gutierrez-Aguirre I, Barlic A, Malovrh P, Kristan K, Podlesek Z, Macek P, Turk D, Gonzalez-Manas JM, Lakey JH, Anderluh G (2002) Two-step membrane binding by Equinatoxin II, a pore-forming toxin from the sea anemone, involves an exposed aromatic cluster and a flexible helix. *J Biol Chem* **277:** 41916-41924

Hopp TP, Woods KR (1981) Prediction of protein antigenic determinants from amino acid sequences. *Proc Natl Acad Sci U S A* **78:** 3824-3828

Howard SL, Jagannathan A, Soo EC, Hui JP, Aubry AJ, Ahmed I, Karlyshev A, Kelly JF, Jones MA, Stevens MP, Logan SM, Wren BW (2009) *Campylobacter jejuni* glycosylation island important in cell charge, legionaminic acid biosynthesis, and colonization of chickens. *Infect Immun* **77:** 2544-2556

Hu L, Bray MD, Osorio M, Kopecko DJ (2006a) *Campylobacter jejuni* induces maturation and cytokine production in human dendritic cells. *Infect Immun* **74:** 2697-2705

Hu L, Kopecko DJ (1999) *Campylobacter jejuni* 81-176 associates with microtubules and dynein during invasion of human intestinal cells. *Infect Immun* **67:** 4171-4182

Hu L, McDaniel JP, Kopecko DJ (2006b) Signal transduction events involved in human epithelial cell invasion by *Campylobacter jejuni* 81-176. *Microb Pathog* **40:** 91-100

Hugdahl MB, Beery JT, Doyle MP (1988) Chemotactic behavior of *Campylobacter jejuni*. *Infect Immun* **56:** 1560-1566

Humphrey T, O'Brien S, Madsen M (2007) Campylobacters as zoonotic pathogens: a food production perspective. *Int J Food Microbiol* **117:** 237-257

Humphrey TJ, Martin KW, Slader J, Durham K (2001) *Campylobacter* spp. in the kitchen: spread and persistence. *Symp Ser Soc Appl Microbiol***:** 115S-120S

Humphrey W, Dalke A, Schulten K (1996) VMD: visual molecular dynamics. *J Mol Graph* **14:** 33-38, 27-38

Jacobs-Reitsma WF, Bolder NM, Mulder RW (1994) Cecal carriage of *Campylobacter* and *Salmonella* in Dutch broiler flocks at slaughter: a one-year study. *Poult Sci* **73:** 1260-1266

Jagannathan A, Constantinidou C, Penn CW (2001) Roles of rpoN, fliA, and flgR in expression of flagella in *Campylobacter jejuni*. *J Bacteriol* **183:** 2937-2942

Jagusztyn-Krynicka EK, Laniewski P, Wyszynska A (2009) Update on *Campylobacter jejuni* vaccine development for preventing human campylobacteriosis. *Expert Rev Vaccines* **8:** 625-645

Jang KS, Sweredoski MJ, Graham RL, Hess S, Clemons WM, Jr. (2014) Comprehensive proteomic profiling of outer membrane vesicles from *Campylobacter jejuni*. *J Proteomics* **98:** 90-98

Janssen R, Krogfelt KA, Cawthraw SA, Van Pelt W, Wagenaar JA, Owen RJ (2008) Host-pathogen interactions in *Campylobacter* infections: The host perspective. *Clin Microbiol Rev* **21:** 505-518

Jeffery CJ (1999) Moonlighting proteins. *Trends Biochem Sci* **24:** 8-11

Jess T, Simonsen J, Nielsen NM, Jorgensen KT, Bager P, Ethelberg S, Frisch M (2011) Enteric *Salmonella* or *Campylobacter* infections and the risk of inflammatory bowel disease. *Gut* **60:** 318-324

Jeurissen SH, Janse EM, van Rooijen N, Claassen E (1998) Inadequate anti-polysaccharide antibody responses in the chicken. *Immunobiology* **198:** 385-395

Jin S, Joe A, Lynett J, Hani EK, Sherman P, Chan VL (2001) JlpA, a novel surface-exposed lipoprotein specific to *Campylobacter jejuni*, mediates adherence to host epithelial cells. *Mol Microbiol* **39:** 1225-1236

Jin S, Song YC, Emili A, Sherman PM, Loong Chan V (2003) JlpA of *Campylobacter jejuni* interacts with surface-exposed heat shock protein 90Î± and triggers signalling pathways leading to the activation of NF-ÎºB and p38 MAP kinase in epithelial cells. *Cell Microbiol* **5:** 165-174

Jin T, Peng L, Mirshahi T, Rohacs T, Chan KW, Sanchez R, Logothetis DE (2002) The (beta)gamma subunits of G proteins gate a K(+) channel by pivoted bending of a transmembrane segment. *Mol Cell* **10:** 469-481

Jones MA, Marston KL, Woodall CA, Maskell DJ, Linton D, Karlyshev AV, Dorrell N, Wren BW, Barrow PA (2004) Adaptation of *Campylobacter jejuni* NCTC 11168 to high-level colonization of the avian gastrointestinal tract. *Infect Immun* **72:** 3769-3776

Justice SS, Lauer SR, Hultgren SJ, Hunstad DA (2006) Maturation of intracellular Escherichia coli communities requires SurA. *Infect Immun* **74:** 4793-4800

Kakuda T, DiRita VJ (2006) Cj1496c encodes a *Campylobacter jejuni* glycoprotein that influences invasion of human epithelial cells and colonization of the chick gastrointestinal tract. *Infect Immun* **74:** 4715-4723

Kaldor J, Pritchard H, Serpell A, Metcalf W (1983) Serum antibodies in *Campylobacter enteritis*. *J Clin Microbiol* **18:** 1-4

Kalischuk LD, Inglis GD, Buret AG (2009) *Campylobacter jejuni* induces transcellular translocation of commensal bacteria via lipid rafts. *Gut pathogens* **1:** 2

Kalmokoff M, Lanthier P, Tremblay TL, Foss M, Lau PC, Sanders G, Austin J, Kelly J, Szymanski CM (2006) Proteomic analysis of *Campylobacter jejuni* 11168 biofilms reveals a role for the motility complex in biofilm formation. *J Bacteriol* **188:** 4312-4320

Kaniga K, Tucker S, Trollinger D, Galan JE (1995) Homologs of the Shigella IpaB and IpaC invasins are required for *Salmonella typhimurium* entry into cultured epithelial cells. *J Bacteriol* **177:** 3965-3971

Kapperud G, Aasen S (1992) Descriptive epidemiology of infections due to thermotolerant *Campylobacter* spp. in Norway, 1979-1988. *APMIS : acta pathologica, microbiologica, et immunologica Scandinavica* **100:** 883-890

Kapperud G, Skjerve E, Vik L, Hauge K, Lysaker A, Aalmen I, Ostroff SM, Potter M (1993) Epidemiological investigation of risk factors for *Campylobacter* colonization in Norwegian broiler flocks. *Epidemiol Infect* **111:** 245-255

Karlyshev AV, Champion OL, Churcher C, Brisson JR, Jarrell HC, Gilbert M, Brochu D, St Michael F, Li J, Wakarchuk WW, Goodhead I, Sanders M, Stevens K, White B, Parkhill J, Wren BW, Szymanski CM (2005a) Analysis of *Campylobacter jejuni* capsular loci reveals multiple mechanisms for the generation of structural diversity and the ability to form complex heptoses. *Mol Microbiol* **55:** 90-103

Karlyshev AV, Everest P, Linton D, Cawthraw S, Newell DG, Wren BW (2004) The *Campylobacter jejuni* general glycosylation system is important for attachment to human epithelial cells and in the colonization of chicks. *Microbiology* **150:** 1957-1964

Karlyshev AV, Ketley JM, Wren BW (2005b) The *Campylobacter jejuni* glycome. *FEMS Microbiol Rev* **29:** 377-390

Karlyshev AV, Linton D, Gregson NA, Lastovica AJ, Wren BW (2000) Genetic and biochemical evidence of a *Campylobacter jejuni* capsular polysaccharide that accounts for Penner serotype specificity. *Mol Microbiol* **35:** 529-541

Karlyshev AV, Linton D, Gregson NA, Wren BW (2002) A novel paralogous gene family involved in phase-variable flagella-mediated motility in *Campylobacter jejuni*. *Microbiology* **148:** 473-480

Karlyshev AV, Wren BW (2001) Detection and initial characterization of novel capsular polysaccharide among diverse *Campylobacter jejuni* strains using alcian blue dye. *J Clin Microbiol* **39:** 279-284

Katarzyna E, Jagusztyn K, Å aniewski P, WyszyÅ„ska A (2009) Update on *Campylobacter jejuni* vaccine development for preventing human campylobacteriosis. *Exp Rev Vaccines* **8:** 625-645

Keestra AM, de Zoete MR, Bouwman LI, van Putten JP (2010) Chicken TLR21 is an innate CpG DNA receptor distinct from mammalian TLR9. *J Immunol* **185:** 460-467

Kelle K, Pages JM, Bolla JM (1998) A putative adhesin gene cloned from *Campylobacter jejuni*. *Res Microbiol* **149:** 723-733

Kelly J, Jarrell H, Millar L, Tessier L, Fiori LM, Lau PC, Allan B, Szymanski CM (2006) Biosynthesis of the *N*-linked glycan in *Campylobacter jejuni* and addition onto protein through block transfer. *J Bacteriol* **188:** 2427-2434

Kemp R, Leatherbarrow AJ, Williams NJ, Hart CA, Clough HE, Turner J, Wright EJ, French NP (2005) Prevalence and genetic diversity of *Campylobacter* spp. in environmental water samples from a 100-square-kilometer predominantly dairy farming area. *Appl Environ Microbiol* **71:** 1876-1882

Kervella M, Pages JM, Pei Z, Grollier G, Blaser MJ, Fauchere JL (1993) Isolation and characterization of two *Campylobacter* glycine-extracted proteins that bind to HeLa cell membranes. *Infect Immun* **61:** 3440-3448

Ketley JM (1997a) Pathogeneis of enteric infection by *Campylobacter. Microbiology* **143:** 5-21

Ketley JM (1997b) Pathogenesis of enteric infection by *Campylobacter*. *Microbiology* **143 (Pt 1):** 5-21

Kiehlbauch JA, Albach RA, Baum LL, Chang KP (1985) Phagocytosis of *Campylobacter jejuni* and its intracellular survival in mononuclear phagocytes. *Infect Immun* **48:** 446-451

Kist M, Bereswill S (2001) *Campylobacter jejuni*. *Contrib Microbiol* **8:** 150-165

Konkel ME, Christensen JE, Keech AM, Monteville MR, Klena JD, Garvis SG (2005) Identification of a fibronectin-binding domain within the *Campylobacter jejuni* CadF protein. *Mol Microbiol* **57:** 1022-1035

Konkel ME, Cieplak W, Jr. (1992) Altered synthetic response of *Campylobacter jejuni* to cocultivation with human epithelial cells is associated with enhanced internalization. *Infect Immun* **60:** 4945-4949

Konkel ME, Garvis SG, Tipton SL, Anderson DE, Jr., Cieplak W, Jr. (1997) Identification and molecular cloning of a gene encoding a fibronectin-binding protein (CadF) from *Campylobacter jejuni*. *Mol Microbiol* **24:** 953-963

Konkel ME, Kim BJ, Klena JD, Young CR, Ziprin R (1998) Characterization of the thermal stress response of *Campylobacter jejuni*. *Infect Immun* **66:** 3666-3672

Konkel ME, Kim BJ, Rivera-Amill V, Garvis SG (1999) Bacterial secreted proteins are required for the internaliztion of *Campylobacter jejuni* into cultured mammalian cells. *Mol Microbiol* **32:** 691-701

Konkel ME, Klena JD, Rivera-Amill V, Monteville MR, Biswas D, Raphael B, Mickelson J (2004) Secretion of virulence proteins from *Campylobacter jejuni* is dependent on a functional flagellar export apparatus. *J Bacteriol* **186:** 3296-3303

Kopp E, Medzhitov R (2003) Recognition of microbial infection by Toll-like receptors. *Curr Opin Immunol* **15:** 396-401

Kosunen TU (1986) Serotyping of *Campylobacter* fetus subsp. fetus and C. fetus subsp. venerealis by passive hemagglutination technique based on soluble autoclaved antigens. *Acta pathologica, microbiologica, et immunologica Scandinavica Section B, Microbiology* **94:** 245-249

Kowarik M, Young NM, Numao S, Schulz BL, Hug I, Callewaert N, Mills DC, Watson DC, Hernandez M, Kelly JF, Wacker M, Aebi M (2006) Definition of the bacterial *N*-glycosylation site consensus sequence. *EMBO J* **25:** 1957-1966

Krause-Gruszczynska M, Rohde M, Hartig R, Genth H, Schmidt G, Keo T, Konig W, Miller WG, Konkel ME, Backert S (2007a) Role of the small Rho GTPases Rac1 and Cdc42 in host cell invasion of *Campylobacter jejuni*. *Cell Microbiol* **9:** 2431-2444

Krause-Gruszczynska M, van Alphen LB, Oyarzabal OA, Alter T, Hanel I, Schliephake A, Konig W, van Putten JP, Konkel ME, Backert S (2007b) Expression patterns and role of the CadF protein in *Campylobacter jejuni* and *Campylobacter coli*. *FEMS Microbiol Lett* **274:** 9-16

Krogh A, Larsson B, von Heijne G, Sonnhammer EL (2001) Predicting transmembrane protein topology with a hidden Markov model: application to complete genomes. *J Mol Biol* **305:** 567-580

Kuroki S, Saida T, Nukina M, Haruta T, Yoshioka M, Kobayashi Y, Nakanishi H (1993) *Campylobacter jejuni* strains from patients with Guillain-Barre syndrome belong mostly to Penner serogroup 19 and contain beta-*N*-acetylglucosamine residues. *Ann Neurol* **33:** 243-247

Kyte J, Doolittle RF (1982) A simple method for displaying the hydropathic character of a protein. *J Mol Biol* **157:** 105-132

Lai XH, Arencibia I, Johansson A, Wai SN, Oscarsson J, Kalfas S, Sundqvist KG, Mizunoe Y, Sjostedt A, Uhlin BE (2000) Cytocidal and apoptotic effects of the ClyA protein from Escherichia coli on primary and cultured monocytes and macrophages. *Infect Immun* **68:** 4363-4367

Lara-Tejero M, Galan JE (2000) A bacterial toxin that controls cell cycle progression as a deoxyribonuclease I-like protein. *Science* **290:** 354-357

Lara-Tejero M, Galan JE (2001) CdtA, CdtB, and CdtC form a tripartite complex that is required for cytolethal distending toxin activity. *Infect Immun* **69:** 4358-4365

Larkin MA, Blackshields G, Brown NP, Chenna R, McGettigan PA, McWilliam H, Valentin F, Wallace IM, Wilm A, Lopez R, Thompson JD, Gibson TJ, Higgins DG (2007) Clustal W and Clustal X version 2.0. *Bioinformatics* **23:** 2947-2948

Larsen JC, Szymanski C, Guerry P (2004) *N*-linked protein glycosylation is required for full competence in *Campylobacter jejuni* 81-176. *J Bacteriol* **186:** 6508-6514

Larson CL, Shah DH, Dhillon AS, Call DR, Ahn S, Haldorson GJ, Davitt C, Konkel ME (2008) *Campylobacter jejuni* invade chicken LMH cells inefficiently and stimulate differential expression of the chicken CXCLi1 and CXCLi2 cytokines. *Microbiology* **154:** 3835-3847

Lee LH, Burg E, 3rd, Baqar S, Bourgeois AL, Burr DH, Ewing CP, Trust TJ, Guerry P (1999) Evaluation of a truncated recombinant flagellin subunit vaccine against *Campylobacter jejuni*. *Infect Immun* **67:** 5799-5805

Lee MD, Newell DG (2006) *Campylobacter* in poultry: filling an ecological niche. *Avian Dis* **50:** 1-9

Lee RB, Hassane DC, Cottle DL, Pickett CL (2003) Interactions of *Campylobacter jejuni* cytolethal distending toxin subunits CdtA and CdtC with HeLa cells. *Infect Immun* **71:** 4883-4890

Leon-Kempis Mdel R, Guccione E, Mulholland F, Williamson MP, Kelly DJ (2006) The *Campylobacter jejuni* PEB1a adhesin is an aspartate/glutamate-binding protein of an ABC transporter essential for microaerobic growth on dicarboxylic amino acids. *Mol Microbiol* **60:** 1262-1275

Levine MM, Kotloff KL, Barry EM, Pasetti MF, Sztein MB (2007) Clinical trials of Shigella vaccines: two steps forward and one step back on a long, hard road. *Nat Rev Microbiol* **5:** 540-553

Li L, Sharipo A, Chaves-Olarte E, Masucci MG, Levitsky V, Thelestam M, Frisan T (2002) The Haemophilus ducreyi cytolethal distending toxin activates sensors of DNA damage and repair complexes in proliferating and non-proliferating cells. *Cell Microbiol* **4:** 87-99

Li YP, Ingmer H, Madsen M, Bang DD (2008) Cytokine responses in primary chicken embryo intestinal cells infected with *Campylobacter jejuni* strains of human and chicken origin and the expression of bacterial virulence-associated genes. *BMC Microbiol* **8:** 107

Li Z, Lou H, Ojcius DM, Sun A, Sun D, Zhao J, Lin X, Yan J (2014) Methyl-accepting chemotaxis proteins 3 and 4 are responsible for *Campylobacter jejuni* chemotaxis and jejuna colonization in mice in response to sodium deoxycholate. *J Med Microbiol* **63:** 343-354

Lin J, Sahin O, Michel LO, Zhang Q (2003) Critical role of multidrug efflux pump CmeABC in bile resistance and *in vivo* colonization of *Campylobacter jejuni*. *Infect Immun* **71:** 4250-4259

Linton D, Dorrell N, Hitchen PG, Amber S, Karlyshev AV, Morris HR, Dell A, Valvano MA, Aebi M, Wren BW (2005) Functional analysis of the *Campylobacter jejuni N*-linked protein glycosylation pathway. *Mol Microbiol* **55:** 1695-1703

Linton D, Gilbert M, Hitchen PG, Dell A, Morris HR, Wakarchuk WW, Gregson NA, Wren BW (2000) Phase variation of a beta-1,3 galactosyltransferase involved in generation of the ganglioside GM1-like lipo-oligosaccharide of *Campylobacter jejuni*. *Mol Microbiol* **37:** 501-514

Logan SM, Trust TJ (1982) Outer membrane characteristics of *Campylobacter jejuni*. *Infect Immun* **38:** 898-906

Louis VR, Gillespie IA, O'Brien SJ, Russek-Cohen E, Pearson AD, Colwell RR (2005) Temperature-driven *Campylobacter* seasonality in England and Wales. *Appl Environ Microbiol* **71:** 85-92

Louwen R, Heikema A, van Belkum A, Ott A, Gilbert M, Ang W, Endtz HP, Bergman MP, Nieuwenhuis EE (2008) The sialylated lipooligosaccharide outer core in *Campylobacter jejuni* is an important determinant for epithelial cell invasion. *Infect Immun* **76:** 4431-4438

Louwen RP, van Belkum A, Wagenaar JA, Doorduyn Y, Achterberg R, Endtz HP (2006) Lack of association between the presence of the pVir plasmid and bloody diarrhea in *Campylobacter jejuni* enteritis. *J Clin Microbiol* **44:** 1867-1868

Luo N, Sahin O, Lin J, Michel LO, Zhang Q (2003) In vivo selection of *Campylobacter* isolates with high levels of fluoroquinolone resistance associated with gyrA mutations and the function of the CmeABC efflux pump. *Antimicro Agents Chemother* **47:** 390-394

MacCallum A, Haddock G, Everest PH (2005a) *Campylobacter jejuni* activates mitogen-activated protein kinases in Caco-2 cell monolayers and *in vitro* infected primary human colonic tissue. *Microbiology* **151:** 2765-2772

MacCallum A, Hardy SP, Everest PH (2005b) *Campylobacter jejuni* inhibits the absorptive transport functions of Caco-2 cells and disrupts cellular tight junctions. *Microbiology* **151:** 2451-2458

Mackenzie A, Barnes G (1988) Oral rehydration in infantile diarrhoea in the developed world. *Drugs* **36 Suppl 4:** 48-60

Macnab RM (2003) How bacteria assemble flagella. *Annu Rev Microbiol* **57:** 77-100

Mamelli L, Amoros JP, Pages JM, Bolla JM (2003) A phenylalanine-arginine beta-naphthylamide sensitive multidrug efflux pump involved in intrinsic and acquired resistance of *Campylobacter* to macrolides. *Int J Antimicrob Agents* **22:** 237-241

Mamelli L, Pages JM, Konkel ME, Bolla JM (2006) Expression and purification of native and truncated forms of CadF, an outer membrane protein of *Campylobacter*. *Int J Biol Macromol* **39:** 135-140

Man SM (2011) The clinical importance of emerging *Campylobacter* species. *Nat Rev Gastroenterol Hepatol* **8:** 669-685

Mao X, DiRienzo JM (2002) Functional studies of the recombinant subunits of a cytolethal distending holotoxin. *Cell Microbiol* **4:** 245-255

Marchant J, Wren B, Ketley J (2002) Exploiting genome sequence: predictions for mechanisms of *Campylobacter* chemotaxis. *Trends Microbiol* **10:** 155-159

Marshall JK, Thabane M, Garg AX, Clark WF, Salvadori M, Collins SM, Walkerton Health Study I (2006) Incidence and epidemiology of irritable bowel syndrome after a large waterborne outbreak of bacterial dysentery. *Gastroenterology* **131:** 445-450; quiz 660

McNally DJ, Hui JP, Aubry AJ, Mui KK, Guerry P, Brisson JR, Logan SM, Soo EC (2006) Functional characterization of the flagellar glycosylation locus in *Campylobacter jejuni* 81-176 using a focused metabolomics approach. *J Biol Chem* **281:** 18489-18498

McSweegan E, Walker RI (1986) Identification and characterization of two *Campylobacter jejuni* adhesins for cellular and mucous substrates. *Infect Immun* **53:** 141-148

McSweeney LA, Dreyfus LA (2004) Nuclear localization of the Escherichia coli cytolethal distending toxin CdtB subunit. *Cell Microbiol* **6:** 447-458

Meade KG, Narciandi F, Cahalane S, Reiman C, Allan B, O'Farrelly C (2009) Comparative *in vivo* infection models yield insights on early host immune response to *Campylobacter* in chickens. *Immunogenetics* **61:** 101-110

Mechaly AE, Bellomio A, Morante K, Gonzalez-Manas JM, Guerin DM (2009) Crystallization and preliminary crystallographic analysis of fragaceatoxin C, a pore-forming toxin from the sea anemone Actinia fragacea. *Acta Crystallogr Sect F Struct Biol Cryst Commun* **65:** 357-360

Meldrum RJ, Griffiths JK, Smith RM, Evans MR (2005) The seasonality of human *Campylobacter* infection and *Campylobacter* isolates from fresh, retail chicken in Wales. *Epidemiol Infect* **133:** 49-52

Miller G, Dunn GM, Smith-Palmer A, Ogden ID, Strachan NJ (2004) Human campylobacteriosis in Scotland: seasonality, regional trends and bursts of infection. *Epidemiol Infect* **132:** 585-593

Mishu B, Blaser MJ (1993) Role of infection due to *Campylobacter jejuni* in the initiation of Guillain-Barre syndrome. *Clin Infect Dis* **17:** 104-108

Molina J, Casin I, Hausfater P, Giretti E, Welker Y, Decazes J, Garrait V, Lagrange P, Modai J (1995) *Campylobacter* infections in HIV-infected patients: clinical and bacteriological features. *Aids* **9:** 881-885

Monteiro MA, Baqar S, Hall ER, Chen YH, Porter CK, Bentzel DE, Applebee L, Guerry P (2009) Capsule polysaccharide conjugate vaccine against diarrheal disease caused by *Campylobacter jejuni*. *Infect Immun* **77:** 1128-1136

Monteville MR, Konkel ME (2002) Fibronectin-facilitated invasion of T84 eukaryotic cells by *Campylobacter jejuni* occurs preferentially at the basolateral cell surface. *Infect Immun* **70:** 6665-6671

Monteville MR, Yoon JE, Konkel ME (2003) Maximal adherence and invasion of INT 407 cells by *Campylobacter jejuni* requires the CadF outermembrane protein and microfilament reorganization. *Microbiology* **149:** 153-165

Montville TJ, Matthews KR (eds) (2008) *Food Microbiology: An Introduction*. Washington, D.C.: ASM Press

Moore JE, Corcoran D, Dooley JS, Fanning S, Lucey B, Matsuda M, McDowell DA, Megraud F, Millar BC, O'Mahony R, O'Riordan L, O'Rourke M, Rao JR, Rooney PJ, Sails A, Whyte P (2005) *Campylobacter*. *Vet Res* **36:** 351-382

Moran AP, Penner JL, Aspinall GO (2000) *Campylobacter* Lipopolysaccharides. In *Campylobacter*, Nachamkin I, Blaser MJ (eds), pp 241-257. Washington DC, USA: ASM Press

Moran AP, Prendergast MM, Appelmelk BJ (1996) Molecular mimicry of host structures by bacterial lipopolysaccharides and its contribution to disease. *FEMS Immunol Med Microbiol* **16:** 105-115

Moran AP, Zahringer U, Seydel U, Scholz D, Stutz P, Rietschel ET (1991) Structural analysis of the lipid A component of *Campylobacter jejuni* CCUG 10936 (serotype O:2) lipopolysaccharide. Description of a lipid A containing a hybrid backbone of 2-amino-2-deoxy-D-glucose and 2,3-diamino-2,3-dideoxy-D-glucose. *Eur J Biochem* **198:** 459-469

Morgan DG, Baumgartner JW, Hazelbauer GL (1993) Proteins antigenically related to methyl-accepting chemotaxis proteins of Escherichia coli detected in a wide range of bacterial species. *J Bacteriol* **175:** 133-140

Morooka T, Umeda A, Amako K (1985) Motility as an intestinal colonization factor for *Campylobacter jejuni*. *J Gen Microbiol* **131:** 1973-1980

Mosmann T (1983) Rapid colorimetric assay for cellular growth and survival: application to proliferation and cytotoxicity assays. *J Immunol Methods* **65:** 55-63

Mowbray SL, Koshland DE, Jr. (1990) Mutations in the aspartate receptor of Escherichia coli which affect aspartate binding. *J Biol Chem* **265:** 15638-15643

Mueller M, Grauschopf U, Maier T, Glockshuber R, Ban N (2009) The structure of a cytolytic alpha-helical toxin pore reveals its assembly mechanism. *Nature* **459:** 726-730

Mullner P, Jone G, Noble A, Spencer SEF, Hathaway S, French NP (2009) Source Attribution of Food-Borne Zoonoses In New Zealand: A Modified Hald Model. *Risk Analysis* **29:** 970-984

Nachamkin I, Blaser MJ (eds) (2000) *Campylobacter*. Washington, D.C.: ASM Presss

Nachamkin I, Blaser, M. J. (ed) (2008) *Campylobacter*. Washington, DC: ASM press, 498pp

Nachamkin I, Fischer SH, Yang XH, Benitez O, Cravioto A (1994) Immunoglobulin A antibodies directed against *Campylobacter jejuni* flagellin present in breast-milk. *Epidemiol Infect* **112:** 359-365

Nachamkin I, Yang XH (1989) Human antibody response to *Campylobacter jejuni* flagellin protein and a synthetic N-terminal flagellin peptide. *J Clin Microbiol* **27:** 2195-2198

Nachamkin I, Yang XH, Stern NJ (1993) Role of *Campylobacter jejuni* flagella as colonization factors for three-day-old chicks: analysis with flagellar mutants. *Appl Environ Microbiol* **59:** 1269-1273

Newell DG, Fearnley C (2003) Sources of *Campylobacter* colonization in broiler chickens. *Appl Environ Microbiol* **69:** 4343-4351

Nielsen H, Engelbrecht J, Brunak S, Heijne GV (1997) Identification of prokaryotic and enkaryotic signal peptides and prediction of their cleavage sites. *Protein Eng* **10:** 1-6

Nielsen H, Krogh A (1998) Prediction of signal peptides and signal anchors by a Hidden Markov model . *Proc Int Conf Intell Syst Mol Biol* **6:** 122-130

Nielsen LN, Luijkx TA, Vegge CS, Johnsen CK, Nuijten P, Wren BW, Ingmer H, Krogfelt KA (2012) Identification of immunogenic and virulence-associated *Campylobacter jejuni* proteins. *Clinical and vaccine immunology : CVI* **19:** 113-119

Nishikubo S, Ohara M, Ueno Y, Ikura M, Kurihara H, Komatsuzawa H, Oswald E, Sugai M (2003) An N-terminal segment of the active component of the bacterial genotoxin cytolethal distending toxin B (CDTB) directs CDTB into the nucleus. *J Biol Chem* **278:** 50671-50681

Nita-Lazar M, Wacker M, Schegg B, Amber S, Aebi M (2005) The N-X-S/T consensus sequence is required but not sufficient for bacterial *N*-linked protein glycosylation. *Glycobiology* **15:** 361-367

Nothaft H, Szymanski CM (2010) Protein glycosylation in bacteria: sweeter than ever. *Nat Rev Microbiol* **8:** 765-778

Nuijten PJ, van den Berg AJ, Formentini I, van der Zeijst BA, Jacobs AA (2000) DNA rearrangements in the flagellin locus of an flaA mutant of *Campylobacter jejuni* during colonization of chicken ceca. *Infect Immun* **68:** 7137-7140

Nylen G, Dunstan F, Palmer SR, Andersson Y, Bager F, Cowden J, Feierl G, Galloway Y, Kapperud G, Megraud F, Molbak K, Petersen LR, Ruutu P (2002) The seasonal distribution of *Campylobacter* infection in nine European countries and New Zealand. *Epidemiol Infect* **128:** 383-390

O'Ryan M, Prado V, Pickering LK (2005) A millennium update on pediatric diarrheal illness in the developing world. *Seminars in pediatric infectious diseases* **16:** 125-136

Oberhelman RA, Gilman RH, Sheen P, Taylor DN, Black RE, Cabrera L, Lescano AG, Meza R, Madico G (1999) A placebo-controlled trial of Lactobacillus GG to prevent diarrhea in undernourished Peruvian children. *J Pediatr* **134:** 15-20

Oelschlaeger TA, Guerry P, Kopecko DJ (1993) Unusual microtubule-dependent endocytosis mechanisms triggered by *Campylobacter jejuni* and Citrobacter freundii. *Proc Natl Acad Sci U S A* **90:** 6884-6888

Oldfield NJ, Wooldridge KG (2009) Protein Secretion and the Pathogenesis of Campylobatcer jejuni. In *Bacterial Secretion Proteins*, Wooldridge KG (ed), pp 299-311. Norfolk, UK: Caister Academic Press

Oscarsson J, Mizunoe Y, Li L, Lai XH, Wieslander A, Uhlin BE (1999) Molecular analysis of the cytolytic protein ClyA (SheA) from Escherichia coli. *Mol Microbiol* **32:** 1226-1238

Palyada K, Threadgill D, Stintzi A (2004) Iron acquisition and regulation in *Campylobacter jejuni*. *J Bacteriol* **186:** 4714-4729

Panigrahi P, Losonsky G, DeTolla LJ, Morris JG, Jr. (1992) Human immune response to *Campylobacter jejuni* proteins expressed *in vivo*. *Infect Immun* **60:** 4938-4944

Parker MW, Feil SC (2005) Pore-forming protein toxins: from structure to function. *Progress in biophysics and molecular biology* **88:** 91-142

Parkhill J, Wren BW, Mungall K, Ketley JM, Churcher C, Basham D, Chillingworth T, Davies RM, Feltwell T, Holroyd S, Jagels K, Karlyshev AV, Moule S, Pallen MJ, Penn CW, Quail MA, Rajandream MA, Rutherford KM, van Vliet AH, Whitehead S, Barrell BG (2000) The genome sequence of the food-borne pathogen *Campylobacter jejuni* reveals hypervariable sequences. *Nature* **403:** 665-668

Pavlovskis OR, Rollins DM, Haberberger RL, Jr., Green AE, Habash L, Strocko S, Walker RI (1991) Significance of flagella in colonization resistance of rabbits immunized with *Campylobacter* spp. *Infect Immun* **59:** 2259-2264

Pearson AD, Greenwood MH, Feltham RK, Healing TD, Donaldson J, Jones DM, Colwell RR (1996) Microbial ecology of *Campylobacter jejuni* in a United Kingdom chicken supply chain: intermittent common source, vertical transmission, and amplification by flock propagation. *Appl Environ Microbiol* **62:** 4614-4620

Pei Z, Blaser MJ (1993) PEB1, the major cell-binding factor of *Campylobacter jejuni*, is a homolog of the binding component in gram-negative nutrient transport systems. *J Biol Chem* **268:** 18717-18725

Pei Z, Burucoa C, Grignon B, Baqar S, Huang XZ, Kopecko DJ, Bourgeois AL, Fauchere JL, Blaser MJ (1998) Mutation in the peb1A locus of *Campylobacter jejuni* reduces interactions with epithelial cells and intestinal colonization of mice. *Infect Immun* **66:** 938-943

Pei ZH, Ellison RT, 3rd, Blaser MJ (1991) Identification, purification, and characterization of major antigenic proteins of *Campylobacter jejuni*. *J Biol Chem* **266:** 16363-16369

Pellegrini-Calace M, Maiwald T, Thornton JM (2009) PoreWalker: a novel tool for the identification and characterization of channels in transmembrane proteins from their three-dimensional structure. *PLoS Comput Biol* **5:** e1000440

Penner JL, Hennessy JN (1980) Passive hemagglutination technique for serotyping *Campylobacter fetus* subsp. jejuni on the basis of soluble heat-stable antigens. *J Clin Microbiol* **12:** 732-737

Penner JL, Hennessy JN, Congi RV (1983) Serotyping of *Campylobacter jejuni* and *Campylobacter coli* on the basis of thermostable antigens. *Eur J Clin Microbiol* **2:** 378-383

Perez-Perez GI, Blaser MJ, Bryner JH (1986) Lipopolysaccharide structures of *Campylobacter fetus* are related to heat-stable serogroups. *Infect Immun* **51:** 209-212

Petersen TN, Brunak S, von Heijne G, Nielsen H (2011) SignalP 4.0: discriminating signal peptides from transmembrane regions. *Nat Methods* **8:** 785-786

Phalipon A, Mulard LA, Sansonetti PJ (2008) Vaccination against shigellosis: is it the path that is difficult or is it the difficult that is the path? *Microbes and infection / Institut Pasteur* **10:** 1057-1062

Pickett CL, Whitehouse CA (1999) The cytolethal distending toxin family. *Trends Microbiol* **7:** 292-297

Pielsticker C, Glunder G, Rautenschlein S (2012) Colonization properties of *Campylobacter jejuni* in chickens. *European journal of microbiology & immunology* **2:** 61-65

Poly F, Ewing C, Goon S, Hickey TE, Rockabrand D, Majam G, Lee L, Phan J, Savarino NJ, Guerry P (2007) Heterogeneity of a *Campylobacter jejuni* protein that is secreted through the flagellar filament. *Infect Immun* **75:** 3859-3867

Pope JE, Krizova A, Garg AX, Thiessen-Philbrook H, Ouimet JM (2007) *Campylobacter* reactive arthritis: a systematic review. *Seminars in arthritis and rheumatism* **37:** 48-55

Prokhorova TA, Nielsen PN, Petersen J, Kofoed T, Crawford JS, Morsczeck C, Boysen A, Schrotz-King P (2006) Novel surface polypeptides of *Campylobacter jejuni* as traveller's diarrhoea vaccine candidates discovered by proteomics. *Vaccine* **24:** 6446-6455

Purdy D, Cawthraw S, Dickinson JH, Newell DG, Park SF (1999) Generation of a superoxide dismutase (SOD)-deficient mutant of *Campylobacter coli*: evidence for the significance of SOD in *Campylobacter* survival and colonization. *Appl Environ Microbiol* **65:** 2540-2546

Qureshi MA (2003) Avian macrophage and immune response: an overview. *Poult Sci* **82:** 691-698

Raphael BH, Pereira S, Flom GA, Zhang Q, Ketley JM, Konkel ME (2005) The *Campylobacter jejuni* response regulator, CbrR, modulates sodium deoxycholate resistance and chicken colonization. *J Bacteriol* **187:** 3662-3670

Ravel A, Nesbitt A, Marshall B, Sittler N, Pollari F (2011) Description and burden of travel-related cases caused by enteropathogens reported in a Canadian community. *J Travel Med* **18:** 8-19

Rawlings ND, Barrett AJ, Bateman A (2012) MEROPS: the database of proteolytic enzymes, their substrates and inhibitors. *Nucleic Acids Res* **40:** D343-350

Reid CW, Stupak J, Chen MM, Imperiali B, Li J, Szymanski CM (2008) Affinity-capture tandem mass spectrometric characterization of polyprenyl-linked oligosaccharides: tool to study protein N-glycosylation pathways. *Anal Chem* **80:** 5468-5475

Reid CW, Stupak J, Szymanski CM, Li J (2009) Analysis of bacterial lipid-linked oligosaccharide intermediates using porous graphitic carbon liquid chromatography-electrospray ionization mass spectrometry: heterogeneity in the polyisoprenyl carrier revealed. *Anal Chem* **81:** 8472-8478

Reiersen H, Rees AR (2001) The hunchback and its neighbours: proline as an environmental modulator. *TIBS* **26:** 679-684

Riddle MS, Sanders JW, Putnam SD, Tribble DR (2006) Incidence, etiology, and impact of diarrhea among long-term travelers (US military and similar populations): a systematic review. *Am J Trop Med Hyg* **74:** 891-900

Rietschel ET, Brade L, Holst O, Kulshin VA, Lindner B, Moran AP, Schade UF, Zahringer U, Brade H (1990) Molecular structure of bacterial endotoxin in relation to bioactivity. In *Endotoxin Research Series*, Nowotny A, Spitzer JJ, Ziegler EJ (eds), Vol. 1, pp 15-32. Amsterdam, The Netherlands: Elsevier Science Publishers B. V.

Rivera-Amill V, Kim BJ, Seshu J, Konkel ME (2001) Secretion of the virulence-associated *Campylobacter* invasion antigens from *Campylobacter jejuni* requires a stimulatory signal. *J Infect Dis* **183:** 1607-1616

Robinson DA (1981) Infective dose of *Campylobacter jejuni* in milk. *Br Med J (Clinical research ed)* **282:** 1584

Rodriguez LA, Ruigomez A (1999) Increased risk of irritable bowel syndrome after bacterial gastroenteritis: cohort study. *BMJ* **318:** 565-566

Rodriguez LA, Ruigomez A, Panes J (2006) Acute gastroenteritis is followed by an increasd risk of inflammatory bowel disease. *Gastroenterology* **130:** 1588-1594

Roy A, Kucukural A, Zhang Y (2010) I-TASSER: a unified platform for automated protein structure and function prediction. *Nat Protoc* **5:** 725-738

Sahin O, Luo N, Huang S, Zhang Q (2003) Effect of *Campylobacter*-specific maternal antibodies on *Campylobacter jejuni* colonization in young chickens. *Appl Environ Microbiol* **69:** 5372-5379

Sahin O, Morishita TY, Zhang Q (2002) *Campylobacter* colonization in poultry: sources of infection and modes of transmission. *Animal health research reviews / Conference of Research Workers in Animal Diseases* **3:** 95-105

Sahin O, Zhang Q, Meitzler JC, Harr BS, Morishita TY, Mohan R (2001) Prevalence, antigenic specificity, and bactericidal activity of poultry anti-*Campylobacter* maternal antibodies. *Appl Environ Microbiol* **67:** 3951-3957

Sali A, Blundell TL (1993) Comparative protein modelling by satisfaction of spatial restraints. *J Mol Biol* **234:** 779-815

Samuel MC, Vugia DJ, Shallow S, Marcus R, Segler S, McGivern T, Kassenborg H, Reilly K, Kennedy M, Angulo F, Tauxe RV, Emerging Infections Program FoodNet Working G (2004) Epidemiology of sporadic *Campylobacter* infection in the United States and declining trend in incidence, FoodNet 1996-1999. *Clin Infect Dis* **38 Suppl 3:** S165-174

Schittek B, Hipfel R, Sauer B, Bauer J, Kalbacher H, Stevanovic S, Schirle M, Schroeder K, Blin N, Meier F, Rassner G, Garbe C (2001) Dermcidin: a novel human antibiotic peptide secreted by sweat glands. *Nature Immuno* **2:** 1133-1137

Schmidt-Ott R, Pohl S, Burghard S, Weig M, Gross U (2005) Identification and characterization of a major subgroup of conjugative *Campylobacter jejuni* plasmids. *J Infect* **50:** 12-21

Scott AE, Timms AR, Connerton PL, Loc Carrillo C, Adzfa Radzum K, Connerton IF (2007) Genome dynamics of *Campylobacter jejuni* in response to bacteriophage predation. *PLoS Pathogens* **3:** e119

Scott-Tucher A, Henderson IR (2009) Type V Secretion. In *Bacterial Secreted Proteins*, Wooldridge KG (ed), 7, pp 139-157. Norfolk, UK: Caister Academic Press

Sebald M, Veron M (1963) [Base DNA Content and Classification of Vibrios]. *Annales de l'Institut Pasteur* **105:** 897-910

Sert V, Cans C, Tasca C, Bret-Bennis L, Oswald E, Ducommun B, De Rycke J (1999) The bacterial cytolethal distending toxin (CDT) triggers a G2 cell cycle checkpoint in mammalian cells without preliminary induction of DNA strand breaks. *Oncogene* **18:** 6296-6304

Shah N, DuPont HL, Ramsey DJ (2009) Global etiology of travelers' diarrhea: systematic review from 1973 to the present. *Am J Trop Med Hyg* **80:** 609-614

Sharma JM (1991) Overview of the avian immune system. *Vet Immunol Immunopathol* **30:** 13-17

Shen HB, Chou KC (2007a) EzyPred: a top-down approach for predicting enzyme functional classes and subclasses. *Biochem Biophys Res Commun* **364:** 53-59

Shen HB, Chou KC (2007b) Signal-3L: A 3-layer approach for predicting signal peptides. *Biochem Biophys Res Commun* **363:** 297-303

Sheppard SK, Dallas JF, Strachan NJC, MacRae M, MaCarthy ND, Wilson DJ, Gormley FJ, Falush D, Ogden ID, Maiden MCJ, Forbes KJ (2009) *Campylobacter* Genotyping to Determine the Source of Human Infection. *Clinical Infect Dis* **48:** 1072-1078

Shoaf-Sweeney KD, Larson CL, Tang X, Konkel ME (2008) Identification of *Campylobacter jejuni* proteins recognized by maternal antibodies of chickens. *Appl Environ Microbiol* **74:** 6867-6875

Siegesmund AM, Konkel ME, Klena JD, Mixter PF (2004) *Campylobacter jejuni* infection of differentiated THP-1 macrophages results in interleukin 1 beta release and caspase-1-independent apoptosis. *Microbiology* **150:** 561-569

Sievers F, Wilm A, Dineen D, Gibson TJ, Karplus K, Li W, Lopez R, McWilliam H, Remmert M, Soding J, Thompson JD, Higgins DG (2011) Fast, scalable generation of high-quality protein multiple sequence alignments using Clustal Omega. *Mol Syst Biol* **7:** 539

Sizemore DR, Warner B, Lawrence J, Jones A, Killeen KP (2006) Live, attenuated *Salmonella typhimurium* vectoring *Campylobacter* antigens. *Vaccine* **24:** 3793-3803

Skirrow MB (1977) *Campylobacter* enteritis: a "new" disease. *Br Med J* **2:** 9-11

Skirrow MB (1987) A demographic survey of campylobacter, salmonella and shigella infections in England. A Public Health Laboratory Service Survey. *Epidemiol Infect* **99:** 647-657

Skirrow MB, M. J. (ed) (2000) *Clinical Aspects of Campylobacter Infection*. Washington D. C. : ASM Press, 69-88pp

Smith CK, Abuoun M, Cawthraw SA, Humphrey TJ, Rothwell L, Kaiser P, Barrow PA, Jones MA (2008) *Campylobacter* colonization of the chicken induces a proinflammatory response in mucosal tissues. *FEMS Immunol Med Microbiol* **54:** 114-121

Smith CK, Kaiser P, Rothwell L, Humphrey T, Barrow PA, Jones MA (2005) *Campylobacter jejuni*-induced cytokine responses in avian cells. *Infect Immun* **73:** 2094-2100

Smith MV, 2nd, Muldoon PJ (1974) *Campylobacter fetus* subspecies jejuni (*Vibrio fetus*) from commercially processed poultry. *Appl Microbiol* **27:** 995-996

Smith T, Taylor MS (1919) Some Morphological and Biological Characters of the *Spirilla* (*Vibrio* Fetus, *N. Sp*.) Associated with Disease of the Fetal Membranes in Cattle. *J Exp Med* **30:** 299-311

Soding J (2005) Protein homology detection by HMM–HMM comparison. *Bioinformatics* **21:** 951–960

Sommerlad SM, Hendrixson DR (2007) Analysis of the roles of FlgP and FlgQ in flagellar motility of *Campylobacter jejuni*. *J Bacteriol* **189:** 179-186

Song C, Weichbrodt C, Salnikov ES, Dynowski M, Forsberg BO, Bechinger B, Steinem C, de Groot BL, Zachariae U, Zeth K (2013) Crystal structure and functional mechanism of a human antimicrobial membrane channel. *Proc Natl Acad Sci U S A* **110:** 4586-4591

Song YC, Jin S, Louie H, Ng D, Lau R, Zhang Y, Weerasekera R, Al Rashid S, Ward LA, Der SD, Chan VL (2004) FlaC, a protein of *Campylobacter jejuni* TGH9011 (ATCC43431) secreted through the flagellar apparatus, binds epithelial cells and influences cell invasion. *Mol Microbiol* **53:** 541-553

Sonnhammer EL, von Heijne G, Krogh A (1998) A hidden Markov model for predicting transmembrane helices in protein sequences. *Proceedings / International Conference on Intelligent Systems for Molecular Biology ; ISMB International Conference on Intelligent Systems for Molecular Biology* **6:** 175-182

Soofi SB, Habib MA, von Seidlein L, Khan MJ, Muhammad S, Bhutto N, Khan MI, Rasool S, Zafar A, Clemens JD, Nizami Q, Bhutta ZA (2011) A comparison of disease caused by Shigella and *Campylobacter* species: 24 months community based surveillance in 4 slums of Karachi, Pakistan. *J Infect Public Health* **4:** 12-21

Sorvillo FJ, Lieb LE, Waterman SH (1991) Incidence of campylobacteriosis among patients with AIDS in Los Angeles County. *J Acquir Immune Defic Syndr* **4:** 598-602

Spiess M (1995) Heads or tails--what determines the orientation of proteins in the membrane. *FEBS Lett* **369:** 76-79

St Michael F, Szymanski CM, Li J, Chan KH, Khieu NH, Larocque S, Wakarchuk WW, Brisson JR, Monteiro MA (2002) The structures of the lipooligosaccharide and capsule polysaccharide of *Campylobacter jejuni* genome sequenced strain NCTC 11168. *Eur J Biochem* **269:** 5119-5136

Stanley K, Cunningham R, Jones K (1998) Isolation of *Campylobacter jejuni* from groundwater. *J Appl Microbiol* **85:** 187-191

Stern NJ, Kazmi SU, Roberson BS, Ono K, Juven BJ (1988) Response of *Campylobacter jejuni* to combinations of ferrous sulphate and cadmium chloride. *J Appl Bacteriol* **64:** 247-255

Stintzi A (2003) Gene expression profile of *Campylobacter jejuni* in response to growth temperature variation. *J Bacteriol* **185:** 2009-2016

Strachan NJC, Gormley FJ, Rotariu O, Ogden ID, Miller G, Dunn GM, Sheppard SK, Dallas JF, Reid TMS, Howie H, Maiden MCJ, Forbes KJ (2009) Attibution of *Campylobacter* Infections in Northeast Scotland to Specific Sources by Use of Multilous Sequence Typing. *J Infect Dis* **199:** 1205-1208

Szymanski CM, Burr DH, Guerry P (2002) *Campylobacter* protein glycosylation affects host cell interactions. *Infect Immun* **70:** 2242-2244

Szymanski CM, King M, Haardt M, Armstrong GD (1995) *Campylobacter jejuni* motility and invasion of Caco-2 cells. *Infect Immun* **63:** 4295-4300

Szymanski CM, Michael FS, Jarrell HC, Li J, Gilbert M, Larocque S, Vinogradov E, Brisson JR (2003) Detection of conserved *N*-linked glycans and phase-variable lipooligosaccharides and capsules from *Campylobacter* cells by mass spectrometry and high resolution magic angle spinning NMR spectroscopy. *J Biol Chem* **278:** 24509-24520

Szymanski CM, Yao R, Ewing CP, Trust TJ, Guerry P (1999) Evidence for a system of general protein glycosylation in *Campylobacter jejuni*. *Mol Microbiol* **32:** 1022-1030

Takata T, Ando T, Israel DA, Wassenaar TM, Blaser MJ (2005) Role of dprA in transformation of *Campylobacter jejuni*. *FEMS Microbiol Lett* **252:** 161-168

Tareen AM, Dasti JI, Zautner AE, Gross U, Lugert R (2010) *Campylobacter jejuni* proteins Cj0952c and Cj0951c affect chemotactic behaviour towards formic acid and are important for invasion of host cells. *Microbiology* **156:** 3123-3135

Taylor DN, Echeverria P, Pitarangsi C, Seriwatana J, Bodhidatta L, Blaser MJ (1988) Influence of strain characteristics and immunity on the epidemiology of *Campylobacter* infections in Thailand. *J Clin Microbiol* **26:** 863-868

Tee W, Mijch A (1998) *Campylobacter jejuni* bacteremia in human immunodeficiency virus (HIV)-infected and non-HIV-infected patients: comparison of clinical features and review. *Clin Infect Dis* **26:** 91-96

Thibault P, Logan SM, Kelly JF, Brisson JR, Ewing CP, Trust TJ, Guerry P (2001) Identification of the carbohydrate moieties and glycosylation motifs in *Campylobacter jejuni* flagellin. *J Biol Chem* **276:** 34862-34870

Thies FL, Weishaupt A, Karch H, Hartung HP, Giegerich G (1999) Cloning, sequencing and molecular analysis of the *Campylobacter jejuni* groESL bicistronic operon. *Microbiology* **145 (Pt 1):** 89-98

Thompson JD, Higgins DG, Gibson TJ (1994) CLUSTAL W: improving the sensitivity of progressive multiple sequence alignment through sequence weighting, position-specific gap penalties and weight matrix choice. *Nucleic Acids Res* **22:** 4673-4680

Thornley JP, Jenkins D, Neal K, Wright T, Brough J, Spiller RC (2001) Relationship of *Campylobacter* toxigenicity *in vitro* to the development of postinfectious irritable bowel syndrome. *J Infect Dis* **184:** 606-609

Tieleman DP, Shrivastava IH, Ulmschneider MR, Sansom MS (2001) Proline-induced hinges in transmembrane helices: possible roles in ion channel gating. *Proteins* **44:** 63-72

Tracz DM, Keelan M, Ahmed-Bentley J, Gibreel A, Kowalewska-Grochowska K, Taylor DE (2005) pVir and bloody diarrhea in *Campylobacter jejuni* enteritis. *Emerg Infect Dis* **11:** 838-843

Tribble DR, Bager S, Thompson A (2008a) Developemtn of a human vaccine. In *Campylobatcer*, Nachamkin I, Szymanski CM, Blaser MJ (eds), 3rd edn, pp 429-444. Washington, DC, USA: ASM Press

Tribble DR, Baqar S, Thompson A (2008b) Development of a human vaccine. In *campylobacter*, Nachamkin I, Szymanski CM, Blaser MJ (eds), 3rd Edition edn, pp 429-444. Washington, DC ASM Press

van de Giessen AW, Bloemberg BP, Ritmeester WS, Tilburg JJ (1996) Epidemiological study on risk factors and risk reducing measures for *Campylobacter* infections in Dutch broiler flocks. *Epidemiol Infect* **117:** 245-250

van Mourik A, Bleumink-Pluym NM, van Dijk L, van Putten JP, Wosten MM (2008) Functional analysis of a *Campylobacter jejuni* alkaline phosphatase secreted via the Tat export machinery. *Microbiology* **154:** 584-592

van Spreeuwel JP, Duursma GC, Meijer CJ, Bax R, Rosekrans PC, Lindeman J (1985) *Campylobacter coli*tis: histological immunohistochemical and ultrastructural findings. *Gut* **26:** 945-951

Vegge CS, Brondsted L, Li YP, Bang DD, Ingmer H (2009) Energy taxis drives *Campylobacter jejuni* toward the most favorable conditions for growth. *Appl Environ Microbiol* **75:** 5308-5314

Velayudhan J, Jones MA, Barrow PA, Kelly DJ (2004) L-serine catabolism via an oxygen-labile L-serine dehydratase is essential for colonization of the avian gut by *Campylobacter jejuni*. *Infect Immun* **72:** 260-268

Venkatesan MM, Ranallo RT (2006) Live-attenuated Shigella vaccines. *Expert Rev Vaccines* **5:** 669-686

von Heijne G (1991) Proline kinks in transmembrane alpha-helices. *J Mol Biol* **218:** 499-503

Wacker M, Linton D, Hitchen PG, Nita-Lazar M, Haslam SM, North SJ, Panico M, Morris HR, Dell A, Wren BW, Aebi M (2002) *N*-linked glycosylation in *Campylobacter jejuni* and its functional transfer into *E. coli*. *Science* **298:** 1790-1793

Wadhams GH, Armitage JP (2004) Making sense of it all: bacterial chemotaxis. *Nature reviews Mol Cell Biol* **5:** 1024-1037

Wai SN, Lindmark B, Soderblom T, Takade A, Westermark M, Oscarsson J, Jass J, Richter-Dahlfors A, Mizunoe Y, Uhlin BE (2003) Vesicle-mediated export and assembly of pore-forming oligomers of the enterobacterial ClyA cytotoxin. *Cell* **115:** 25-35

Walker RI (2005) Considerations for development of whole cell bacterial vaccines to prevent diarrheal diseases in children in developing countries. *Vaccine* **23:** 3369-3385

Wallis MR (1994) The pathogenesis of *Campylobacter jejuni*. *Br J Biomed Sci* **51:** 57-64

Wang SC (2003) Artificial neural network. In *Interdisciplinary Computing in Java Programming*, pp. 81-100. Springer US.

Wassenaar TM, Blaser MJ (1999) Pathophysiology of *Campylobacter jejuni* infections of humans. *Microbes and infection / Institut Pasteur* **1:** 1023-1033

Wassenaar TM, Engelskirchen M, Park S, Lastovica A (1997) Differential uptake and killing potential of *Campylobacter jejuni* by human peripheral monocytes/macrophages. *Med Microbiol Immun***186:** 139-144

Watson RO, Galan JE (2005) Signal transduction in *Campylobacter jejuni*-induced cytokine production. *Cell Microbiol* **7:** 655-665

Weiss RA (2002) Virulence and pathogenesis. *Trends Microbiol* **10:** 314-317

Whitehouse CA, Balbo PB, Pesci EC, Cottle DL, Mirabito PM, Pickett CL (1998) *Campylobacter jejuni* cytolethal distending toxin causes a G2-phase cell cycle block. *Infect Immun* **66:** 1934-1940

Widders PR, Perry R, Muir WI, Husband AJ, Long KA (1996) Immunisation of chickens to reduce intestinal colonisation with *Campylobacter jejuni*. *Br Poult Sci* **37:** 765-778

Wiesner RS, Hendrixson DR, DiRita VJ (2003) Natural transformation of *Campylobacter jejuni* requires components of a type II secretion system. *J Bacteriol* **185:** 5408-5418

Wigley P (2013) Immunity to bacterial infection in the chicken. *Dev Comp Immun* **41:** 413-417

Wilson DL, Bell JA, Young VB, Wilder SR, Mansfield LS, Linz JE (2003) Variation of the natural transformation frequency of *Campylobacter jejuni* in liquid shake culture. *Microbiology* **149:** 3603-3615

Wilson DJ, Gabriel E, Leatherbarrow AJ, Cheesbrough J, Gee S, Bolton E, Fox A, Fearnhead P, Hart CA, Diggle PJ (2008) Tracing the source of campylobacteriosis. *PLoS Genet* **4:** 1000203

Withington SG, Chambers ST (1997) The cost of campylobacteriosis in New Zealand in 1995. *N Z Med J* **110:** 222-224

Wolff C, Parkinson JS (1988) Aspartate taxis mutants of the *Escherichia coli* tar chemoreceptor. *J Bacteriol* **170:** 4509-4515

Woodall CA, Jones MA, Barrow PA, Hinds J, Marsden GL, Kelly DJ, Dorrell N, Wren BW, Maskell DJ (2005) *Campylobacter jejuni* gene expression in the chick cecum: evidence for adaptation to a low-oxygen environment. *Infect Immun* **73:** 5278-5285

Wooldridge KG, Ketley JM (1997) *Campylobacter*-host cell interactions. *Trends Microbiol* **5:** 96-102

Wooldridge KG, Williams PH, Ketley JM (1996) Host signal transduction and endocytosis of *Campylobacter jejuni*. *Microb Pathog* **21:** 299-305

Wosten MM, Wagenaar JA, van Putten JP (2004) The FlgS/FlgR two-component signal transduction system regulates the fla regulon in *Campylobacter jejuni*. *J Biol Chem* **279:** 16214-16222

Wu S, Skolnick J, Zhang Y (2007) Ab initio modeling of small proteins by iterative TASSER simulations. *BMC Biol* **5:**17

Wu S, Zhang Y (2007) LOMETS: a local meta-threading-server for protein structure prediction. *Nucleic Acids Res* **35:** 3375-3382

Wyszynska A, Raczko A, Lis M, Jagusztyn-Krynicka EK (2004) Oral immunization of chickens with avirulent *Salmonella* vaccine strain carrying *C. jejuni* 72Dz/92 cjaA gene elicits specific humoral immune response associated with protection against challenge with wild-type *Campylobacter*. *Vaccine* **22:** 1379-1389

Yamamoto M, Sato S, Hemmi H, Uematsu S, Hoshino K, Kaisho T, Takeuchi O, Takeda K, Akira S (2003) TRAM is specifically involved in the Toll-like receptor 4-mediated MyD88-independent signaling pathway. *Nature Immunol* **4:** 1144-1150

Yao R, Burr DH, Doig P, Trust TJ, Niu H, Guerry P (1994) Isolation of motile and non-motile insertional mutants of *Campylobacter jejuni*: the role of motility in adherence and invasion of eukaryotic cells. *Mol Microbiol* **14:** 883-893

Yao R, Burr DH, Guerry P (1997) CheY-mediated modulation of *Campylobacter jejuni* virulence. *Mol Microbiol* **23:** 1021-1031

Yohannan S, Faham S, Yang D, Whitelegge JP, Bowie JU (2004) The evolution of transmembrane helix kinks and the structural diversity of G protein-coupled receptors. *Proc Natl Acad Sci U S A* **101:** 959-963

Young KT, Davis LM, DiRita VJ (2007) *Campylobacter jejuni*: Molecular biology and pathogenesis. *Nature Rev Microbiol* **5:** 665-679

Young NM, Brisson JR, Kelly J, Watson DC, Tessier L, Lanthier PH, Jarrell HC, Cadotte N, St Michael F, Aberg E, Szymanski CM (2002) Structure of the *N*-linked glycan present on multiple glycoproteins in the Gram-negative bacterium, *Campylobacter jejuni*. *J Biol Chem* **277:** 42530-42539

Yu L, Guo Y, Li Y, Li G, Li M, Luo J, Xiong W, Qin W (2010) SecretP: identifying bacterial secreted proteins by fusing new features into Chou's pseudo-amino acid composition. *J Theor Biol* **267:** 1-6

Zautner AE, Tareen AM, Gross U, Lugert R (2012) Chemotaxis in *Campylobacter jejuni*. *Eur J Microbiol Immunol* **2:** 24-31

Zhang W, Brooun A, McCandless J, Banda P, Alam M (1996) Signal transduction in the archaeon Halobacterium salinarium is processed through three subfamilies of 13 soluble and membrane-bound transducer proteins. *Proc Natl Acad Sci U S A* **93:** 4649-4654

Zhang Y (2008) I-TASSER server for protein 3D structure prediction. *BMC Bioinformatics* **9:** 40

Zhang Y, Kolinski A, Skolnick J (2003) TOUCHSTONE II: A new approach to ab initio protein structure prediction. *Biophys J* **85:** 1145–1164

Zhang Y, Skolnick J (2004a) Automated structure prediction of weakly homologous proteins on a genomic scale. *Proc Natl Acad Sci U S A* **101:** 7594-7599

Zhang Y, Skolnick J (2004b) Scoring function for automated assessment of protein structure template quality. *Proteins* **57:** 702-710

Zhang Y, Skolnick J (2004c) SPICKER: a clustering approach to identify near-native protein folds. *J Comput* Chem **25:** 865–71

Zhao C, Ge B, De Villena J, Sudler R, Yeh E, Zhao S, White DG, Wagner D, Meng J (2001) Prevalence of *Campylobacter* spp., Escherichia coli, and *Salmonella* serovars in retail chicken, turkey, pork, and beef from the Greater Washington, D.C., area. *Appl Environ Microbiol* **67:** 5431-5436

Zilbauer M, Dorrell N, Elmi A, Lindley KJ, Schuller S, Jones HE, Klein NJ, Nunez G, Wren BW, Bajaj-Elliott M (2007) A major role for intestinal epithelial nucleotide oligomerization domain 1 (NOD1) in eliciting host bactericidal immune responses to *Campylobacter jejuni*. *Cell Microbiol* **9:** 2404-2416

Ziprin RL, Young CR, Byrd JA, Stanker LH, Hume ME, Gray SA, Kim BJ, Konkel ME (2001) Role of *Campylobacter jejuni* potential virulence genes in cecal colonization. *Avian Dis* **45:** 549-557

Ziprin RL, Young CR, Stanker LH, Hume ME, Konkel ME (1999) The absence of cecal colonization of chicks by a mutant of *Campylobacter jejuni* not expressing bacterial fibronectin-binding protein. *Avian Dis* **43:** 586-589

Appendices

Appendix 1: Predicted *C. jejuni* NCTC 11168 Classically Secreted Proteins using SignalP 4.0

periplasmic protein Accession: YP_002345089.1 GI: 218563309
outer membrane protein Accession: YP_002345087.1 GI: 218563307
periplasmic protein Accession: YP_002345047.1 GI: 218563267
periplasmic protein Accession: YP_002345038.1 GI: 218563258
DNA ligase Accession: YP_002345037.1 GI: 218563257
periplasmic protein Accession: YP_002345036.1 GI: 218563256
periplasmic thiredoxin Accession: YP_002345032.1 GI: 218563252
periplasmic protein p19 Accession: YP_002345027.1 GI: 218563247
iron permease Accession: YP_002345026.1 GI: 218563246
periplasmic protein Accession: YP_002345001.1 GI: 218563221
periplasmic protein Accession: YP_002344995.1 GI: 218563215
haemin uptake system outer membrane receptor Accession: YP_002344983.1 GI: 218563203
periplasmic protein Accession: YP_002344912.1 GI: 218563133
periplasmic oxidoreductase Accession: YP_002344894.1 GI: 218563115
periplasmic protein Accession: YP_002344891.1 GI: 218563112
flagellar basal body P-ring protein Accession: YP_002344844.1 GI: 218563065
capsule polysaccharide export system periplasmic protein Accession: YP_002344827.1 GI: 218563048
lipoprotein Accession: YP_002344769.1 GI:218562990
periplasmic protein Accession: YP_002344768.1 GI:218562989
periplasmic protein Accession: YP_002344764.1 GI:218562985
periplasmic protein Accession: YP_002344760.1 GI:218562981
periplasmic protein Accession: YP_002344759.1 GI:218562980
enterochelin uptake periplasmic binding protein Accession: YP_002344743.1 GI: 218562964
periplasmic protein Accession: YP_002344679.1 GI:218562900

fibronectin domain-containing lipoprotein Accession: YP_002344670.1 GI:218562891
major outer membrane protein Accession: YP_002344650.1 GI: 218562871
MFS transport protein Accession: YP_002344632.1 GI:218562853
periplasmic protein Accession: YP_002344631.1 GI:218562852
peptidase M23 family protein Accession: YP_002344606.1 GI:218562827
exporting protein Accession: YP_002344605.1 GI:218562826
lipoprotein thiredoxin Accession: YP_002344598.1 GI: 218562819
NLPA family lipoprotein Accession: YP_002344591.1 GI: 218562812
50 kda outer membrane protein precursor Accession: YP_002344561.1 GI: 218562782
periplasmic protein Accession: YP_002344560.1 GI: 218562781
periplasmic cytochrome C Accession: YP_002344544.1 GI: 218562765
periplasmic thioredoxin Accession: YP_002344499.1 GI: 218562720
liproprotein Accession: YP_002344424.1 GI: 218562645
lipoprotein Accession: YP_002344421.1 GI: 218562642
periplasmic protein Accession: YP_002344416.1 GI: 218562637
branched-chain amino-acid ABC transporter periplasmic binding protein Accession: YP_002344414.1 GI: 218562635
branched-chain amino-acid ABC transporter periplasmic binding protein Accession: YP_002344413.1 GI: 218562634
periplasmic protein Accession: YP_002344393.1 GI: 218562614
amino-acid transporter periplasmic solute-binding protein Accession: YP_002344377.1 GI: 218562598
periplasmic protein Accession: YP_002344364.1 GI: 218562585
lipoprotein Accession: YP_002344348.1 GI: 218562569
F0F1 ATP synthase subunit C Accession: YP_002344334.1 GI: 218562555
bifunctional adhesin/ABC transporter aspartate/glutamate-binding protein Accession: YP_002344319.1 GI: 218562540
periplasmic protein Accession: YP_002344307.1 GI: 218562528
periplasmic protein Accession: YP_002344305.1 GI: 218562526
periplasmic protein Accession: YP_002344276.1 GI: 218562497
protein disulphide isomerase Accession: YP_002344273.1 GI: 218562494

periplasmic protein Accession: YP_002344271.1 GI: 218562492
ankyrin repeat-containing periplasmic protein Accession: YP_002344241.1 GI: 218562462
Na+/H+ antiporter family protein Accession: YP_002344239.1 GI: 218562460
flagellar biosynthesis protein FliP Accession: YP_002344227.1 GI: 218562448
lipoprotein Accession: YP_002344225.1 GI: 218562446
periplasmic protein Accession: YP_002344191.1 GI: 218562412
periplasmic nitrate reductase small subunit Accession: YP_002344190.1 GI: 218562411
NLPA family lipoprotein Accession: YP_002344179.1 GI: 218562400
NLPA family lipoprotein Accession: YP_002344178.1 GI: 218562399
NLPA family lipoprotein Accession: YP_002344177.1 GI: 218562398
ferric enterobactin uptake receptor Accession: YP_002344163.1 GI: 218562384
hemagglutination activity domain-containing protein Accession: YP_002344155.1 GI: 218562376
periplasmic protein Accession: YP_002344153.1 GI: 218562374
histidine-binding protein precursor Accession: YP_002344152.1 GI: 218562373
periplasmic solute-binding protein Accession: YP_002344145.1 GI: 218562366
transthyretin-like periplasmic protein Accession: YP_002344133.1 GI: 218562354
lipoprotein Accession: YP_002344075.1 GI: 218562296
secreted transglycosylase Accession: YP_002344074.1 GI: 218562295
periplasmic phosphate binding protein Accession: YP_002344043.1 GI: 218562264
periplasmic protein Accession: YP_002344039.1 GI: 218562260
major antigenic peptide PEB-cell binding factor Accession: YP_002344026.1 GI: 218562247
DNA/RNA non-specific endonuclease Accession: YP_002344024.1 GI: 218562245
periplasmic protein Accession: YP_002344022.1 GI: 218562243
lipoprotein Accession: YP_002344021.1 GI: 218562242
periplasmic protein Accession: YP_002343992.1 GI: 218562213
exporting protein Accession: YP_002343971.1 GI: 218562192
lipoprotein Accession: YP_002343931.1 GI: 218562152

succinate dehydrogenase flavoprotein subunit Accession: YP_002343874.1 GI: 218562095
periplasmic protein Accession: YP_002343862.1 GI: 218562083
acidic periplasmic protein Accession: YP_002343861.1 GI: 218562082
periplasmic protein Accession: YP_002343857.1 GI: 218562078
lipoprotein Accession: YP_002343843.1 GI: 218562064
sulfite oxidase subunit YedY Accession: YP_002343816.1 GI: 218562037
lipoprotein Accession: YP_002343812.1 GI: 218562033
hypothetical protein Cj0371 Accession: YP_002343808.1 GI: 218562029
outer membrane channel protein CmeC Accession: YP_002343802.1 GI: 218562023
cytochrome C551 peroxidase Accession: YP_002343796.1 GI: 218562017
molybdate-binding lipoprotein Accession: YP_002343741.1 GI: 218561962
major antigenic peptide PEB3 Accession: YP_002343730.1 GI: 218561951
periplasmic protein Accession: YP_002343658.1 GI: 218561879
biopolymer transport protein Accession: YP_002343637.1 GI: 218561858
TonB-denpendent outer membrane receptor Accession: YP_002343636.1 GI: 218561857
iron transport protein Accession: YP_002343635.1 GI: 218561856
lipoprotein Accession: YP_002343634.1 GI: 218561855
periplasmic protein Accession: YP_002343627.1 GI: 218561848
heme-binding lipoprotein Accession: YP_002343618.1 GI: 218561839
TAT (Twin-Arginine Translocation) pathway signal sequence domain protein Accession: YP_002343605.1 GI: 218561826
periplasmic solute binding protein Accession: YP_002343603.1 GI: 218561824
periplasmic protein Accession: YP_002343574.1 GI: 218561795
translocation protein TolB Accession: YP_002343572.1 GI: 218561793
periplasmic protein Accession: YP_002343553.1 GI: 218561774
periplasmic protein Accession: YP_002343552.1 GI: 218561773
lipoprotein Accession: YP_002343551.1 GI: 218561772
lipoprotein Accession: YP_002343550.1 GI: 218561771

lipoprotein Accession: YP_002343549.1 GI: 218561770
cytolethal distending toxin B Accession: YP_002343540.1 GI: 218561761
cytolethal distending toxin C Accession: YP_002343539.1 GI: 218561760
periplasmic protein Accession: YP_002343521.1 GI: 218561742
cytochrome C Accession: YP_002343508.1 GI: 218561729
cytochrome C551 peroxidase Accession: YP_002343492.1 GI: 218561713
non-specific DNA binding protein Accession: YP_002343483.1 GI: 218561704
monohaem cytochrome C Accession: YP_002343476.1 GI: 218561697

Appendix 2: Predicted *C. jejuni* NCTC 11168 Non-classically Secreted Proteins using SecretomeP 2.0 and SignalP 4.0

flagellar hook protein FlgE Accession: YP_002345095.1 GI:218563315
50S ribosomal protein L3 Accession: YP_002345073.1 GI: 218563293
50S ribosomal protein L4 Accession: YP_002345072.1 GI: 218563292
50S ribosomal protein L23 Accession: YP_002345071.1 GI: 218563291
50S ribosomal protein L2 Accession: YP_002345070.1 GI: 218563290
30S ribosomal protein S19 Accession: YP_002345069.1 GI: 218563289
50S ribosomal protein L22 Accession: YP_002345068.1 GI: 218563288
50S ribosomal protein L24 Accession: YP_002345062.1 GI: 218563282
50S ribosomal protein L6 Accession: YP_002345058.1 GI: 218563278
50S ribosomal protein L15 Accession: YP_002345055.1 GI: 218563275
lipoprotein Accession: YP_002345045.1 GI: 218563265
hypothetical protein Cj1656c Accession: YP_002345025.1 GI: 218563245
lipoprotein Accession: YP_002345022.1 GI: 218563242
hypothetical protein Cj1631c Accession: YP_002345000.1 GI: 218563220
TonB transport protein Accession: YP_002344999.1 GI: 218563219
periplasmic protein Accession: YP_002344990.1 GI: 218563210
30S ribosomal protein S20 Accession: YP_002344980.1 GI: 218563200
30S ribosomal protein S11 Accession: YP_002344962.1 GI: 218563182
hypothetical protein Cj1501 Accession: YP_002344880.1 GI: 218563101
cbb3-type cytochrome c oxidase subunit II Accession: YP_002344869.1 GI: 218563090
30S ribosomal protein S9 Accession: YP_002344859.1 GI: 218563080
flagellar hook-associated protein FlgK Accession: YP_002344848.1 GI: 218563069
hypothetical protein Cj1464 Accession: YP_002344846.1 GI: 218563067
hypothetical protein Cj1463 Accession: YP_002344845.1 GI: 218563066
periplasmic protein Accession: YP_002344838.1 GI: 218563059

ATP/GTP-binding protein Accession: YP_002344832.1 GI: 218563053
cystathionine beta-lyase, N-terminus Accession:YP_002344777.1 GI:218562998
catalase Accession: YP_002344773.1 GI: 218562994
flavodoxin FldA Accession: YP_002344770.1 GI: 218562991
secreted serine protease Accession: YP_002344753.1 GI: 218562974
periplasmic cytochrome C Accession:YP_002344746.1 GI:218562967
periplasmic cytochrome C Accession:YP_002344745.1 GI:218562966
coiled-coil protein Accession:YP_002344736.1 GI:218562957
flagellin Accession: YP_002344727.1 GI: 218562948
flagellin Accession: YP_002344726.1 GI: 218562947
N-acetylmuramoyl-L-alanine amidase Accession: YP_002344660.1 GI: 218562881
chaperone protein DnaJ Accession: YP_002344651.1 GI: 218562872
phosphotyrosine protein phosphatase Accession:YP_002344649.1 GI:218562870
isomerase Accession:YP_002344646.1 GI:218562867
periplasmic protein Accession:YP_002344643.1 GI:218562864
hypothetical protein Cj1242 Accession: YP_002344633.1 GI: 218562854
peptidase M23 family protein Accession:YP_002344626.1 GI:218562847
hypothetical protein Cj1232 Accession: YP_002344623.1 GI: 218562844
serine protease Accession: YP_002344619.1 GI: 218562840
hypothetical protein Cj1225 Accession: YP_002344616.1 GI: 218562837
periplasmic protein Accession:YP_002344610.1 GI:218562831
periplasmic protein Accession: YP_002344584.1 GI: 218562805
bipartate energy taxis response protein CetB Accession: YP_002344580.1 GI: 218562801
ubiquinol-cytochrome C reductase iron-sulfur subunit Accession: YP_002344577.1 GI: 218562798
Sec-independent protein translocase Accession: YP_002344567.1 GI: 218562788
hypothetical protein Cj1164c Accession: YP_002344555.1 GI: 218562776
S-adenosylmethionine synthetase Accession: YP_002344489.1 GI: 218562710

single-stranded DNA-binding protein Accession: YP_002344464.1 GI: 218562685
aspartyl/glutamyl-tRNA amidotransferase subunit A Accession: YP_002344454.1 GI: 218562675
hypothetical protein Cj1036c Accession: YP_002344431.1 GI: 218562652
lipoprotein Accession: YP_002344378.1 GI: 218562599
outer-membrane protein Accession: YP_002344370.1 GI: 218562591
hypothetical protein Cj0974 Accession: YP_002344369.1 GI: 218562590
hypothetical protein Cj0972 Accession: YP_002344367.1 GI: 218562588
hypothetical protein Cj0971 Accession: YP_002344366.1 GI: 218562587
hypothetical protein Cj0970 Accession: YP_002344365.1 GI: 218562586
50S ribosomal protein L34 Accession: YP_002344359.1 GI: 218562580
periplasmic protein Accession: YP_002344342.1 GI: 218562563
hypothetical protein Cj0916c Accession: YP_002344314.1 GI: 218562535
DNA-binding protein HU Accession: YP_002344311.1 GI: 218562532
lagellar hook-associated protein FlgL Accession: YP_002344286.1 GI: 218562507
hypothetical protein Cj0878 Accession: YP_002344278.1 GI: 218562499
cytochrome C Accession: YP_002344275.1 GI: 218562496
hypothetical protein Cj0873c Accession: YP_002344274.1 GI: 218562495
hypothetical protein Cj0859c Accession: YP_002344266.1 GI: 218562487
hypothetical protein Cj0849c Accession: YP_002344256.1 GI: 218562477
hypothetical protein Cj0848c Accession: YP_002344255.1 GI: 218562476
secreted transglycosylase Accession: YP_002344250.1 GI: 218562471
hypothetical protein Cj0839c Accession: YP_002344246.1 GI: 218562467
hypothetical protein Cj0816 Accession: YP_002344223.1 GI: 218562444
hypothetical protein Cj0815 Accession: YP_002344222.1 GI: 218562443
hypothetical protein Cj0814 Accession: YP_002344221.1 GI: 218562442
hypothetical protein Cj0794 Accession: YP_002344201.1 GI: 218562422
nitrate reductase catalytic subunit Accession: YP_002344187.1 GI: 218562408

periplasmic protein Accession: YP_002344183.1 GI: 218562404
TonB transport protein Accession: YP_002344162.1 GI: 218562383
hypothetical protein Cj0748 Accession: YP_002344161.1 GI: 218562382
hypothetical protein Cj0741 Accession: YP_002344159.1 GI: 218562380
hypothetical protein Cj0740 Accession: YP_002344158.1 GI: 218562379
hypothetical protein Cj0739 Accession: YP_002344157.1 GI: 218562378
hypothetical protein Cj0738 Accession: YP_002344156.1 GI: 218562377
hypothetical protein Cj0736 Accession: YP_002344154.1 GI: 218562375
periplasmic protein Accession: YP_002344146.1 GI: 218562367
flagellin Accession: YP_002344138.1 GI: 218562359
hypothetical protein Cj0700 Accession: YP_002344118.1 GI: 218562339
flagellar basal body rod protein FlgG Accession: YP_002344116.1 GI: 218562337
flagellar basal-body rod protein Accession: YP_002344115.1 GI: 218562336
periplasmic protein Accession: YP_002344112.1 GI: 218562333
flagellar basal body L-ring protein Accession: YP_002344105.1 GI: 218562326
lipoprotein Accession: YP_002344058.1 GI: 218562279
secretion protein HlyD Accession: YP_002344036.1 GI: 218562257
pyridine nucleotide-disulphide oxidoreductase Accession: YP_002343990.1 GI: 218562211
flagellar capping protein Accession: YP_002343979.1 GI: 218562200
flagellar basal body rod protein FlgB Accession: YP_002343959.1 GI: 218562180
flagellar basal body rod protein FlgC Accession: YP_002343958.1 GI: 218562179
flagellar hook-basal body protein FliE Accession: YP_002343957.1 GI: 218562178
30S ribosomal protein S12 Accession: YP_002343925.1 GI: 218562146
50S ribosomal protein L1 Accession: YP_002343909.1 GI: 218562130
50S ribosomal protein L11 Accession: YP_002343908.1 GI: 218562129
50S ribosomal protein L33 Accession: YP_002343905.1 GI: 218562126
50S ribosomal protein L28 Accession: YP_002343884.1 GI: 218562105

succinate dehydrogenase subunit C Accession: YP_002343876.1 GI: 218562097
3-ketoacyl-(acyl-carrier-protein) reductase Accession: YP_002343872.1 GI: 218562093
hypothetical protein Cj0428 Accession: YP_002343865.1 GI: 218562086
hypothetical protein Cj0418c Accession: YP_002343855.1 GI: 218562076
GMC oxidoreductase subunit Accession: YP_002343852.1 GI: 218562073
oxidoreductase subunit Accession: YP_002343851.1 GI: 218562072
transmembrane protein Accession: YP_002343841.1 GI: 218562062
hypothetical protein Cj0391c Accession: YP_002343828.1 GI: 218562049
periplasmic fusion protein CmeA Accession: YP_002343804.1 GI: 218562025
flagellar motor protein MotB Accession: YP_002343774.1 GI: 218561995
ferredoxin Accession: YP_002343771.1 GI: 218561992
50S ribosomal protein L32 Accession: YP_002343768.1 GI: 218561989
transmembrane protein Accession: YP_002343710.1 GI: 218561931
molybdopterin containing oxidoreductase Accession: YP_002343706.1 GI: 218561927
highly acidic protein Accession: YP_002343693.1 GI: 218561914
50S ribosomal protein L35 Accession: YP_002343686.1 GI: 218561907
hypothetical protein Cj0243c Accession: YP_002343685.1 GI: 218561906
preprotein translocase subunit SecG Accession: YP_002343678.1 GI: 218561899
ribosome recycling factor Accession: YP_002343677.1 GI: 218561898
hypothetical protein Cj0202c Accession: YP_002343660.1 GI: 218561881
TonB transport protein Accession: YP_002343639.1 GI: 218561860
superoxide dismutase Accession: YP_002343628.1 GI: 218561849
50S ribosomal protein L31 Accession: YP_002343615.1 GI: 218561836
hypothetical protein Cj0152c Accession: YP_002343612.1 GI: 218561833
peptidoglycan associated lipoprotein Accession: YP_002343573.1 GI: 218561794
periplasmic protein Accession: YP_002343571.1 GI: 218561792
cytolethal distending toxin A Accession: YP_002343541.1 GI: 218561762

hypothetical protein Cj0056c Accession: YP_002343520.1 GI: 218561741
hypothetical protein Cj0055c Accession: YP_002343519.1 GI: 218561740
flagellar hook protein Accession: YP_002343514.1 GI: 218561735
flagellar basal body rod modification protein Accession: YP_002343513.1 GI: 218561734
flagellar hook-length control protein Accession: YP_002343512.1 GI: 218561733
cytoplasmic L-asparaginase Accession: YP_002343501.1 GI: 218561722
molydopterin containing oxidoreductase Accession: YP_002343477.1 GI: 218561698

Appendix 3: Estimated half-life and Instability index of Cj0391c using ProtParam (Gasteiger *et al,* 2005).

Estimated half-life:

The N-terminal of the sequence considered is M (Met).

The estimated half-life is: 30 hours (mammalian reticulocytes, in vitro).
>20 hours (yeast, in vivo).
>10 hours (Escherichia coli, in vivo).

Instability index:

The instability index (II) is computed to be 21.32
This classifies the protein as stable.

Appendix 4: *PstI* digested λDNA

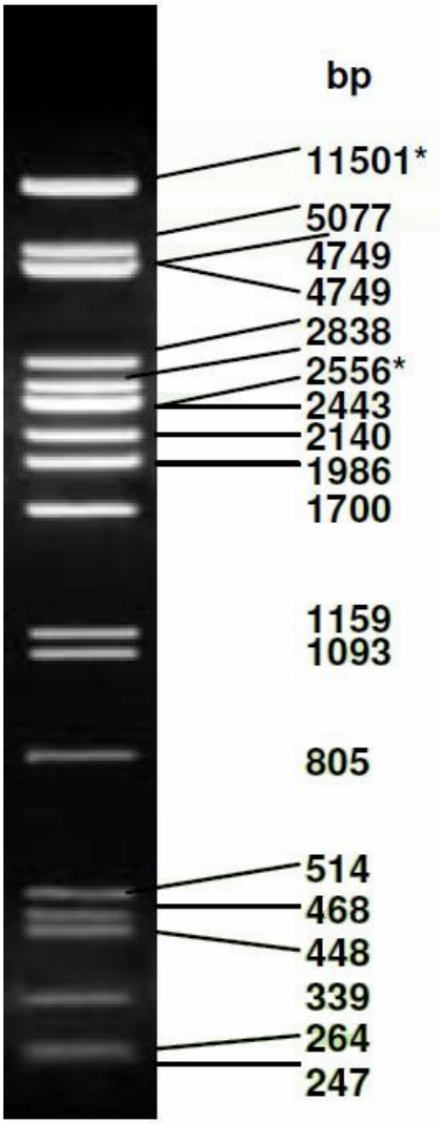

Appendix 5: Protein Standards

A. Precision Plus Protein™ Unstained Standard

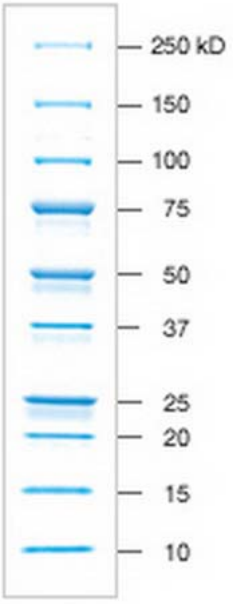

B. Precision Plus Protein™ Kaleidoscope™ Standard

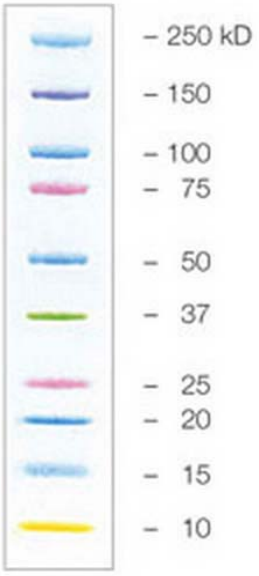

Appendix 6: Sequence alignment of Cj0391c and TcdA1 (PDB code 4O9Y/1VW1) by Clustal Omega

```
CLUSTAL O(1.2.1) multiple sequence alignment


Cj0391c         ------------------------------------------------------------
4O9Y/1VW1       MNESVKEIPDVLKSQCGFNCLTDISHSSFNEFRQQVSEHLSWSETHDLYHDAQQAQKDNR

Cj0391c         ------------------------------------------------------------
4O9Y/1VW1       LYEARILKRANPQLQNAVHLAILAPNAELIGYNNQFSGRASQYVAPGTVSSMFSPAAYLT

Cj0391c         ------------------------------------------------------------
4O9Y/1VW1       ELYREARNLHASDSVYYLDTRRPDLKSMALSQQNMDIELSTLSLSNELLLESIKTESKLE

Cj0391c         ------------------------------------------------------------
4O9Y/1VW1       NYTKVMEMLSTFRPSGATPYHDAYENVREVIQLQDPGLEQLNASPAIAGLMHQASLLGIN

Cj0391c         ------------------------------------------------------------
4O9Y/1VW1       ASISPELFNILTEEITEGNAEELYKKNFGNIEPASLAMPEYLKRYYNLSDEELSQFIGKA

Cj0391c         ------------------------------------------------------------
4O9Y/1VW1       SNFGQQEYSNNQLITPVVNSSDGTVKVYRITREYTTNAYQMDVELFPFGGENYRLDYKFK

Cj0391c         ------------------------------------------------------------
4O9Y/1VW1       NFYNASYLSIKLNDKRELVRTEGAPQVNIEYSANITLNTADISQPFEIGLTRVLPSGSWA

Cj0391c         ------------------------------------------------------------
4O9Y/1VW1       YAAAKFTVEEYNQYSFLLKLNKAIRLSRATELSPTILEGIVRSVNLQLDINTDVLGKVFL

Cj0391c         ------------------------------------------------------------
4O9Y/1VW1       TKYYMQRYAIHAETALILCNAPISQRSYDNQPSQFDRLFNTPLLNGQYFSTGDEEIDLNS

Cj0391c         ------------------------------------------------------------
4O9Y/1VW1       GSTGDWRKTILKRAFNIDDVSLFRLLKITDHDNKDGKIKNNLKNLSNLYIGKLLADIHQL

Cj0391c         ------------------------------------------------------------
4O9Y/1VW1       TIDELDLLLIAVGEGKTNLSAISDKQLATLIRKLNTITSWLHTQKWSVFQLFIMTSTSYN

Cj0391c         ------------------------------------------------------------
4O9Y/1VW1       KTLTPEIKNLLDTVYHGLQGFDKDKADLLHVMAPYIAATLQLSSENVAHSVLLWADKLQP

Cj0391c         ------------------------------------------------------------
4O9Y/1VW1       GDGAMTAEKFWDWLNTKYTPGSSEAVETQEHIVQYCQALAQLEMVYHSTGINENAFRLFV

Cj0391c         ------------------------------------------------------------
4O9Y/1VW1       TKPEMFGAATGAAPAHDALSLIMLTRFADWVNALGEKASSVLAAFEANSLTAEQLADAMN

Cj0391c         ------------------------------------------------------------
4O9Y/1VW1       LDANLLLQASIQAQNHQHLPPVTPENAFSCWTSINTILQWVNVAQQLNVAPQGVSALVGL

Cj0391c         ------------------------------------------------------------
4O9Y/1VW1       DYIQSMKETPTYAQWENAAGVLTAGLNSQQANTLHAFLDESRSAALSTYYIRQVAKAAAA

Cj0391c         ------------------------------------------------------------
4O9Y/1VW1       IKSRDDLYQYLLIDNQVSAAIKTTRIAEAIASIQLYVNRALENVEENANSGVISRQFFID

Cj0391c         ------------------------------------------------------------
4O9Y/1VW1       WDKYNKRYSTWAGVSQLVYYPENYIDPTMRIGQTKMMDALLQSVSQSQLNADTVEDAFMS
```

Appendix 6: Sequence alignment of Cj0391c and TcdA1 (PDB code 4O9Y/1VW1) by Clustal Omega (cont.)

```
Cj0391c         ------------------------------------------------------------
4O9Y/1VW1       YLTSFEQVANLKVISAYHDNINNDQGLTYFIGLSETDAGEYYWRSVDHSKFNDGKFAANA

Cj0391c         ------------------------------------------------------------
4O9Y/1VW1       WSEWHKIDCPINPYKSTIRPVIYKSRLYLLWLEQKEITKQTGNSKDGYQTETDYRYELKL

Cj0391c         ------------------------------------------------------------
4O9Y/1VW1       AHIRYDGTWNTPITFDVNKKISELKLEKNRAPGLYCAGYQGEDTLLVMFYNQQDTLDSYK

Cj0391c         ------------------------------------------------------------
4O9Y/1VW1       NASMQGLYIFADMASKDMTPEQSNVYRDNSYQQFDTNNVRRVNNRYAEDYEIPSSVSSRK

Cj0391c         ------------------------------------------------------------
4O9Y/1VW1       DYGWGDYYLSMVYNGDIPTINYKAASSDLKIYISPKLRIIHNGYEGQKRNQCNLMNKYGK

Cj0391c         ------------------------------------------------------------
4O9Y/1VW1       LGDKFIVYTSLGVNPNNSSNKLMFYPVYQYSGNTSGLNQGRLLFHRDTTYPSKVEAWIPG

Cj0391c         ------------------------------------------------------------
4O9Y/1VW1       AKRSLTNQNAAIGDDYATDSLNKPDDLKQYIFMTDSKGTATDVSGPVEINTAISPAKVQI

Cj0391c         ------------------------------------------------------------
4O9Y/1VW1       IVKAGGKEQTFTADKDVSIQPSPSFDEMNYQFNALEIDGSGLNFINNSASIDVTFTAFAE

Cj0391c         ------------------------------------------------------------
4O9Y/1VW1       DGRKLGYESFSIPVTLKVSTDNALTLHHNENGAQYMQWQSYRTRLNTLFARQLVARATTG

Cj0391c         ------------------------------------------------------------
4O9Y/1VW1       IDTILSMETQNIQEPQLGKGFYATFVIPPYNLSTHGDERWFKLYIKHVVDNNSHIIYSGQ

Cj0391c         ------------------------------------------------------------
4O9Y/1VW1       LTDTNINITLFIPLDDVPLNQDYHAKVYMTFKKSPSDGTWWGPHFVRDDKGIVTINPKSI

Cj0391c         ------------------------------------------------------------
4O9Y/1VW1       LTHFESVNVLNNISSEPMDFSGANSLYFWELFYYTPMLVAQRLLHEQNFDEANRWLKYVW

Cj0391c         ------------------------------------------------------------
4O9Y/1VW1       SPSGYIVHGQIQNYQWNVRPLLEDTSWNSDPLDSVDPDAVAQHDPMHYKVSTFMRTLDLL

Cj0391c         ------------------------------------------------------------
4O9Y/1VW1       IARGDHAYRQLERDTLNEAKMWYMQALHLLGDKPYLPLSTTWSDPRLDRAADITTQNAHD

Cj0391c         ------------------------------------------------------------
4O9Y/1VW1       SAIVALRQNIPTPAPLSLRSANTLTDLFLPQINEVMMNYWQTLAQRVYNLRHNLSIDGQP

Cj0391c         --------------------------------MQVNTFSNIASMARTQVSNK-------
4O9Y/1VW1       LYLPIYATPADPKALLSAAVATSQGGGKLPESFMSLWRFPHMLENARGMVSQLTQFGSTL
                                                *.:  * .: . **  **:

Cj0391c         -------KADDAKE--------------NTKDKNVQSANSSKDVDKNTLEKLN-------
4O9Y/1VW1       QNIIERQDAEALNALLQNQAAELILTNLSIQDKTIEEL----DAEKTVLEKSKAGAQSRF
                       .*:  :               . :**.::.     *.:*..*** :
```

Appendix 6: Sequence alignment of Cj0391c and TcdA1 (PDB code 4O9Y/1VW1) by Clustal Omega (cont.)

```
Cj0391c         ------------------------------------------------------------
4O9Y/1VW1       DSYGKLYDENINAGENQAMTLRASAAGLTTAVQASRLAGAAADLVPNIFGFAGGGSRWGA

Cj0391c         ------------------------------------------------------------
4O9Y/1VW1       IAEATGYVMEFSANVMNTEADKISQSETYRRRRQEWEIQRNNAEAELKQIDAQLKSLAVR

Cj0391c         ----------------------------------ALGGKGITQIYLVQFQQQTM----
4O9Y/1VW1       REAAVLQKTSLKTQQEQTQSQLAFLQRKFSNQALYNWLRG-RLAAIYFQFYDLAVARCLM
                                                   * *  :: **:  ::  .

Cj0391c         ------------------------------------------------------------
4O9Y/1VW1       AEQAYRWELNDDSARFIKPGAWQGTYAGLLAGETLMLSLAQMEDAHLKRDKRALEVERTV

Cj0391c         ------------------------NAVIGSSNAQTGLDSLLNGANLDTAKSILTNIDFAS
4O9Y/1VW1       SLAEVYAGLPKDNGPFSLAQEIDKLVSQGSGSAGSGNNNLAFGAGTDTKTSLQASVSFAD
                                       .  **..* :* :.*  **  ** .*: :.:.**.

Cj0391c         LGYSSKNPLDMNTDELQ-Q-LVSEDGFFGVENTANRIADFVIKGGGDDVEKLKKGLEGMK
4O9Y/1VW1       LKIREDYPASLGKIRRIKQISVTLPALLGPYQDVQAILSYGDKA------GLANGCEALA
                *   .. * .: . .   *  *:  .::*  : .: * .:  *.       * :* *.:

Cj0391c         --KGFEQA----EKMWGGELPQ-----ISQNTIDAALKKVSDRIDELGGKTLDLQA----
4O9Y/1VW1       VSHGMNDSGQFQLDFNDGKFLPFEGIAIDQGTLTLSFPN--ASMPEKGKQATMLKTLNDI
                  :*::::     .:  *::       *.* *:  :: :    : * * ::  *::

Cj0391c         ---------
4O9Y/1VW1       ILHIRYTIK
```

Appendix 7: Sequence alignment of Cj0391c and listeriolysin (PDB code 4CDB) by Clustal Omega

```
CLUSTAL O(1.2.1) multiple sequence alignment


cj0391c                         ------------------------------------------------------------
4CDB:A|PDBID|CHAIN|SEQUENCE     MAPPASPPASPKTPIEKKHADEIDKYIQGLDYNKNNVLVYHGDAVTNVPPRKGYKDGNEY

cj0391c                         -----------------MQVNTFSNI--------------------ASMART--------
4CDB:A|PDBID|CHAIN|SEQUENCE     IVVEKKKKSINQNNADIQVVNAISSLTYPGALVKANSELVENQPDVLPVKRDSLTLSIDL
                                          **::*.:                       : *

cj0391c                         -QVSNKKADDAKENTKDKNVQSA-----------------NSSKDVD--K----------
4CDB:A|PDBID|CHAIN|SEQUENCE     PGMTNQDNKIVVKNATKSNVNNAVNTLVERWNEKYAQAYPNVSAKIDYDDEMAYSESQLI
                                  ::*:. . . :*:...**:.*                * * .:*  .

cj0391c                         -----------NTLE-KLNALGGKGITQIYLVQFQQQTMNAVI----------GSS----
4CDB:A|PDBID|CHAIN|SEQUENCE     AKFGTAFKAVNNSLNVNFGAI-SEGKMQEEVISFKQIYYNVNVNEPTRPSRFFGKAVTKE
                                           *:*: :: *: .:*  *  ::.*:*   *. :          *.:

cj0391c                         ------------------------------------NAQTGLDSLLNGANLDTA---KSI
4CDB:A|PDBID|CHAIN|SEQUENCE     QLQALGVNAENPPAYISSVAYGRQVYLKLSTNSHSTKVKAAFDAAVSGKSVSGDVELTNI
                                                                  :.::.:*: :.* .:.     ..*

cj0391c                         LTNIDFASLGYSS--KNP---LDMNTDELQQLVSEDGFFG--------------------
4CDB:A|PDBID|CHAIN|SEQUENCE     IKNSSFKAVIYGGSAKDEVQIIDGNLGDLRDILKKGATFNRETPGVPIAYTTNFLKDNEL
                                :.* .* :: *..  *:    :* *  :*::::.: . *

cj0391c                         ----------------------VENTANRIADFVI-----------------------
4CDB:A|PDBID|CHAIN|SEQUENCE     AVIKNNSEYIETTSKAYTDGKINIDHSGGYVAQFNISWDEVNYDPEGNEIVQHKNWSENN
                                              ::.:.  :*:* *

cj0391c                         -------------KGGGDDVEKLKKGLEGMKKG--------------FEQAEKMWGGELP
4CDB:A|PDBID|CHAIN|SEQUENCE     KSKLAHFTSSIYLPGNARNINVYAKECTGLAWEWWRTVIDDRNLPLVKNRNISIWGTTLY
                                         * . :::   *   *:                  ::  .:**  *

cj0391c                         QISQNTIDAALKKVSDRIDELGGKTLDLQA
4CDB:A|PDBID|CHAIN|SEQUENCE     PKYSNKVDN----------------------
                                   .*.:*
```

Appendix 8: Protein 391 molecular dynamics simulation files (please see DVD attached)